Role of ARF6 in breast cancer cell invasion

Valentina Marchesin

Université Pierre et Marie Curie

Ecole doctorale 515 Complexité du Vivant

Laboratoire Dynamique de la membrane et du cytosquelette

Institut Curie, CNRS/UMR144

Role of ARF6 in breast cancer cell invasion

Par Valentina Marchesin

Thèse de doctorat en Biologie Cellulaire du Cancer

Dirigée par Dr. Philippe Chavrier

Présentée et soutenue publiquement le 18 Septembre 2014

Devant un jury composé de :

Rapporteurs: Dr. Cathy Jackson
Dr. Giorgio Scita

Examinateurs: Prof. Germain Trugnan
Dr. Alexis Gautreau
Dr. Sandrine Etienne-Manneville

Directeur de thèse: Dr. Philippe Chavrier

CONTENTS:

Résumé:

L'invasion tumorale nécessite le franchissement de la membrane basale et la migration des cellules tumorales à travers la matrice extracellulaire. Ce processus dépend de l'activité d'une métalloprotéase matricielle, MT1-MMP, ancrée à la membrane plasmique. MT1-MMP a récemment émergé comme une des principales protéases impliquées dans le remodelage de la matrice au cours de l'invasion tumorale. MT1-MMP est internalisée à partir de la surface et s'accumule dans des compartiments endosomaux, puis recycle vers les invadopodes, des protrusions membranaires à base d'actine responsables de la dégradation de la matrice. L'étude de la machinerie cellulaire qui contrôle le ciblage de MT1-MMP aux invadopodes est essentielle pour une meilleure compréhension du processus d'invasion des cellules cancéreuses. La petite protéine G ARF6 joue un rôle important dans la régulation du trafic membranaire dans la voie de l'endocytose et dans le remodelage du cytosquelette d'actine ; ARF6 est impliquée dans de nombreux évènements cellulaires qui nécessitent la polarisation cellulaire comme la migration et l'invasion des cellules tumorales. Des études récentes ont suggéré un lien entre la surexpression d'ARF6 et la capacité invasive des cellules cancéreuses du sein. Mon travail de thèse apporte un nouvel éclairage du rôle pro-invasif d'ARF6 dans le cancer du sein. Dans une étude principale, j'ai montré qu'ARF6 et deux de ses protéines effectrices JIP3 et JIP4 (protéines cytosoliques impliquées dans le transport de vésicules dépendant des microtubules), sont nécessaires au positionnement intracellulaire des endosomes contenant MT1-MMP et à son exocytose au niveau des invadopodes. La déplétion des protéines ARF6 et JIP3/4 cause une réduction de la capacité des cellules tumorales à remodeler la matrice extracellulaire et migrer à travers un environnement matriciel tridimensionnel. Nous avons également identifié un mécanisme par lequel ARF6, à travers son interaction avec JIP3/4, contrôle négativement l'activité du complexe dynactine/dynéine, un moteur moléculaire qui se déplace en direction du bout (-) des microtubules. Ce mécanisme contrôle donc négativement la clairance des endosomes MT1-MMP à partir de la périphérie cellulaire. Par ailleurs, nos analyses immuno-histochimiques d'échantillons de tumeurs mammaires ont montré qu'ARF6 est surexprimée dans les cellules tumorales par rapport aux tissus péritumoraux ; de plus ARF6 est accumulée au niveau de la membrane plasmique, avec MT1-MMP, dans un sous-groupe de carcinomes mammaires agressifs. Ces données confirment donc l'implication d'un axe ARF6-JIP3/JIP4-MT1-MMP dans le processus invasif du cancer du sein.

Dans une deuxième étude, j'ai montré que l'hyperactivation d'ARF6 induit un réarrangement important du cytosquelette d'actine à la surface ventrale des cellules tumorales mammaires avec des conséquences possibles dans la formation du lamellipode et la motilité cellulaire. J'ai montré qu'ARF6, en aval du récepteur du facteur de croissance épidermique (EGF-R), contribue à

l'activation et au ciblage de la protéine Rho, Rac1 au front cellulaire ; Rac1 active le complexe SCAR/WAVE et régule la polymérisation de l'actine ventrale lors de l'extension des lamellipodes. Mon travail a permis d'identifier de nouveaux mécanismes moléculaires par lesquels ARF6 contribue au programme invasif des cellules tumorales mammaires et apporte de nouvelles perspectives dans la compréhension de l'invasion et de la progession tumorale.

ABSTRACT

Cancer invasion occurs when tumor cells breach the basement membrane and then traffic through stromal extracellular matrix (ECM). This process relies on the action of the membrane-anchored matrix metalloprotease MT1-MMP, which has recently emerged as the major protease for matrix remodeling during tumor invasion. Recent findings showed that MT1-MMP is stored in endosomal compartments and exocytosed back to invadopodia, the actin-based membrane protrusions responsible for matrix degradation. Studying proteins that regulate targeting of MT1-MMP to invadopodia is important for a better understanding of the invasion process of breast cancer cells. The small GTP-binding protein ARF6 is known to coordinate post-endocytic recycling and actin cytoskeletal organization at the plasma membrane. Hence, ARF6 is involved in several cell events requiring cell polarization including cell migration and tumor cell invasion. Recent studies for instance suggested a link between up-regulation of ARF6 expression and activity and the invasive capacity of breast cancer cells. My PhD work has provided novel insights into how ARF6 exerts its pro-invasive role in breast cancer. In my main study I showed that ARF6 and two of its effectors JIP3 and JIP4 are required for MT1-MMP endosomes intracellular positioning and exocytosis at invadopodia and consequently for tumor cells ability to remodel the ECM and invade through a three-dimensional matrix environment. I identified a possible mechanism in which ARF6, through the interaction with JIP3/4, negatively controls the activity of the minus-end-directed microtubule motor dynactin/dynein, thus negatively regulating the clearance and inward movement of MT1-MMP endosomes from the cell periphery. Moreover by immunohistochemistry analysis in human samples I showed that ARF6 is up-regulated in carcinoma cells as compared to peritumoral tissues and is accumulated at the plasma membrane, together with MT1-MMP, in a subset of highly agressive breast carcinomas, thus corroborating the implication of an ARF6-JIP3/JIP4-MT1-MMP axis in breast cancer invasion. In a second study I addressed the contribution of ARF6 activation on actin cytoskeleton remodeling in breast cancer cells with possible implications for cell motility. I showed that ARF6 links epidermal growth factor receptor signaling to Rac1 activation and targeting to the leading edge where it activates the SCAR/WAVE complex and regulates ventral actin polymerization during lamellipodia extension. Collectively my work identifies novel molecular mechanisms through which ARF6 contributes to the invasive program of breast tumor cells and could bring new insights in the understanding of cancer invasion.

ABBREVIATIONS (other than explained in the test)

ADP: adenosine diphosphate

ACAP1: ArfGAP with coiled-coil, ankyrin repeat and PH domains 1

AMAP1: AMY-1 (associate of Myc1) associating protein

ARF: ADP-ribosylation factor *

ARNO: ARF nucleotide-binding site opener

ATP: adenosine triphosphate

EFA6: Exchange Factor for ARF6

ERBB2: v-erb-b2 avian erythroblastic leukemia viral oncogene homolog 2

FITC: Fluorescein isothiocyanate

GDP: guanosie diphosphate

GEP100: guanine nucleotide-exchange protein 100

GTP: guanosine triphosphate

HER2: Human epidermal Growth Factor Receptor-2

SCAR/WAVE: suppressor of cAMP receptor/ WASP family verprolin homology proteins

SCID: severe combined immunodeficiency

Rac1: Ras-related C3 botulinum toxin substrate 1

shRNA: small hairpin RNA

siRNA: small interferring RNA

SRC: Sarcoma tyrosine-protein kinase

TKS5: Tyrosine kinase substrate with five SH3 domains

VAMP: vesicle-associated membrane protein

WASH: WAS protein family homolog

* In capital letters for human proteins

Chapter 1: MT1-MMP regulation in cancer cell invasion

1.4 Cancer cell dissemination: general mechanism

The broad subject of interest of this study is to understand how cancer cells from the primary tumor activate the invasive programs that allow them to disseminate through the surrounding tissues and metastasize to distant organs.

Cancer invasion and metastasis are critical events that transform a locally growing tumor into a systemic and life-threatening disease. In fact while surgical resection and adjuvant therapy can cure well-confined primary tumors, metastatic disease is largely incurable because of its systemic nature and the resistance of disseminated tumor cells to existing therapeutic agents. This explains why metastasis is the first cause of death in patients with cancer (>90% of mortality) (Friedl and Alexander, 2011; Valastyan and Weinberg, 2011).

The invasive metastatic process consists of a series of steps, all of which must be successfully completed to give rise to a metastatic tumour. Cancer cell invasion starts when tumor cells that have resided within a well-confined primary tumor infiltrate into the surrounding tumor-associated stroma and thereafter into the adjacent normal tissue parenchyma. Eventually, metastasis occurs when invading tumor cells engage with blood and lymph vessels, disseminate away and colonize distant organs (Chambers et al., 2002) (Fig.1).

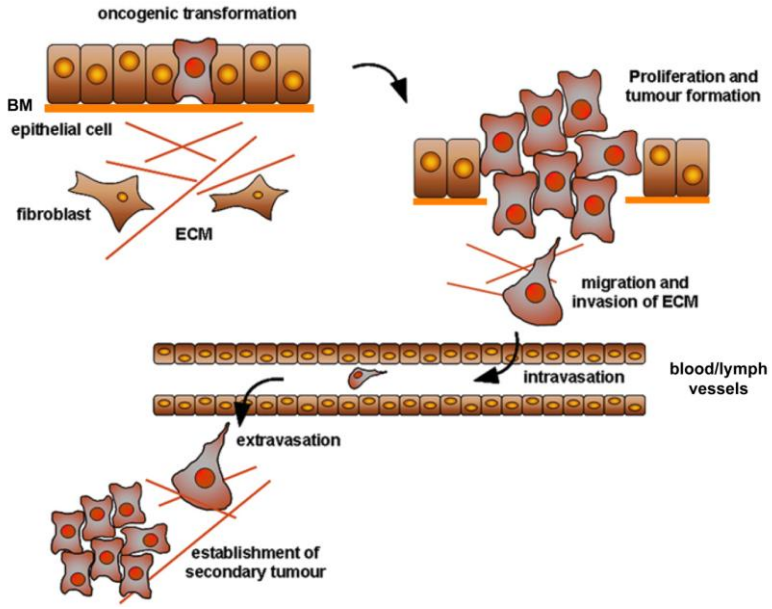

Figure1: **Scheme depicting the different steps of the metastatic cascade**. Carcinomas are tumors of epithelial origin that begins with oncogenic transformation, and progress with aberrant cell growth and proliferation to give rise to a primary tumor. Then tumor cells acquire a migratory phenotype and invade their surrounding extracellular matrix (ECM). Metastasis occurs when cancer cells enter blood or lymphatic vessels by intravasation. Metastatic cells will then attach and extravasate, establishing a secondary site on another organ/tissue. Figure from (Whale et al., 2011).

From the primary tumor in order to invade the stroma, carcinoma cells must first breach the basement membrane (BM), a specialized extracellular matrix (ECM) that separates epithelial cells from connective tissues and therefore plays vital roles in organizing epithelial tissues and providing structural support (Fig.2-1). BM is a highly cross-linked meshwork composed mainly of type-IV collagen, laminin and heparan-sulphate proteoglycans (Kalluri, 2003; Poincloux et al., 2009). The BM represents a mechanical barrier to cancer cell migration and cancer cells dissolve it through the action of specific enzymes, the matrix metalloproteinases (MMPs), which are designed to digest different components of the ECM (Hotary et al., 2006). In normal tissues, the activity of MMPs is carefully controlled via transcriptional and post-translational mechanisms. Carcinoma cells bypass these means of regulation and are instead characterized by enhanced MMP function (Kessenbrock et al., 2010). After breaching the BM, cancer cells face the interstitial stroma that is mainly constituted of a three-dimensional (3D) fibrillar network of type I collagen (Fig2-2). Here cells can migrate either individually or collectively in a mesenchymal mode (Fig2-3-4) consisting in prominent protrusions and spindle-shaped morphology, strong adhesion to ECM, and proteolytic tissue remodeling (Friedl and Alexander, 2011; Friedl and Gilmour, 2009; Friedl and Wolf, 2009). Several studies have also reported a protease-independent and acto-myosin-based, ameboid-like type of migration similar to the that observed in myeloid cell populations such as leucocytes (Friedl and Wolf, 2003; Wolf et al., 2003; Wolf et al., 2007) (Fig2-5).

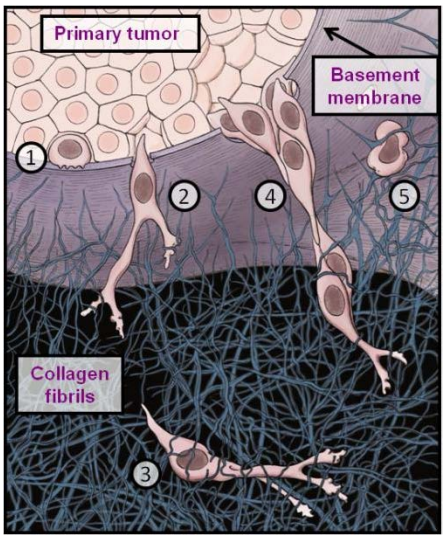

Figure 2: Scheme depicting the different steps of cancer cell invasion. From the primary tumor, cells breach the BM (1) and once they dissolve it, they infiltrate the interstitial tissues made of a three-dimensional (3D) fibrous collagen network (2). Here they can adopt a mesenchymal mode of migration either as a single-cell (3) or collectively (4). Cancer cells can also adopt a rounded-shape and migrate though a protease-independent ameboydal mode of migration (5). Figure from Poincloux et al., 2009.

The mesenchymal mode of migration through the pores of the collagen network can be considered as a cyclic multi-step process: first tumor cell remodel their actin cytoskeleton to extend protrusions at the leading edge; second they adhere to the ECM by the action of the adhesion receptors integrins; then cancer cells cleave collagen fibrils; finally the last steps of 3D migration consist of acto-myosin-mediated contraction of the cell body and of the retraction of the rear of

the cell with consequent translocation of the cell body (Friedl and Alexander, 2011; Friedl and Wolf, 2009; Ridley et al., 2003). Mesenchymal 3D migration is controlled by MMPs, in particular the membrane-tethered MT1-MMP/MMP-14, a key enzyme known to accumulate at the contact sites of the cell surface with the collagen fibrils and to cleave those fibrils that act as barriers for cell migration (Sabeh et al., 2004; Sabeh et al., 2009; Wolf et al., 2007). The capacity of tumor cells to migrate through the ECM and to switch from a protease-dependent to an –independent mode of migration depends on many factors. These factors include the geometry and physicochemical characteristics of the collagen ECM network, which *in vivo* is composed by fibrils of different caliber, orientation and density and parameters such as collagen fibrils rigidity or the pore sizes are limiting factors for cell migration (Friedl and Alexander, 2011; Friedl and Wolf, 2009; Friedl and Wolf, 2010; Sabeh et al., 2009; Wolf et al., 2013). For instance migration speed diminishes with decreasing pore size as a consequence of increased confinement for cells and MT1-MMP activity accelerates migration assuring slow but nonetheless persistent migration even in very dense matrix. Conversely, with porosity high enough to accommodate the deforming cell body, pericellular proteolysis is dispensable and migration persists despite pharmacological inhibition of MMP activity or silencing of MT1-MMP (Wolf et al., 2013). Another important emerging factor for cell migration is the deformability of the cell body in particular of the nucleus, which is the largest and most rigid organelle and therefore nucleus size, rigidity and shape seem to be critical parameters for the migration rate (Wolf et al., 2013). The current view is that cancer cell invasion is a plastic process in which tumor cells can adapt their adhesion and mechanotrasduction abilities, cytoskeleton dynamics and MMPs production and regulation to perpetuate migration and dissemination under different ECM microenvironment (Friedl and Alexander, 2011; Friedl and Wolf, 2010).

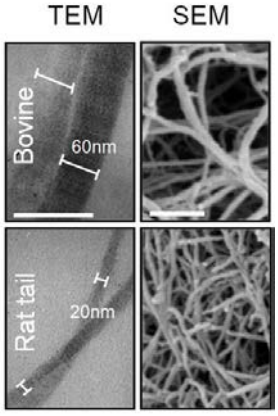

Figure 3: **Different examples of *in vitro* matrices mimicking the complexity of the 3D collagen ECM in *vivo*.** For instance bovine dermis–derived collagen matrices are characterized by fibrils with a diameter of 60 nm and pore cross sections ranging from 6–30 μm^2, while rat tendon–derived collagen, which differently from the previous one is acid-extracted and therefore maintains the intramolecular cross-links, forms thin fibrils with a 20-nm diameter and a narrow pore size range of 2–5 μm^2 (1–2 μm pore diameters). Figure showing transmission and scanning electron microscopy (TEM and SEM) pictures from Wolf et al., 2013.

1.5 Cancer cell dissemination: breast cancer model

In the case of breast adenocarcinoma, our model of study, the disease originates from the epithelial cells of the milk ducts or lobuli of the mammary gland and first progress as ductal

carcinoma in situ (DCIS), that is defined as a pre-malignant proliferation of tumor cells confined within the lumen of the ductal-lobular system (Fig4A-4B) (Cowell et al., 2013). DCIS still maintains an intact BM and an intact layer of myoepithelial cells, that are contractile cells containing α-smooth muscular actin (αSMA) and separating the epithelial cells from the BM (Pandey et al., 2010) (Fig.4B). The transition from a DCIS to an invasive ductal carcinoma (IDC) occurs when tumor cells cross the myoepithelium and perforate the BM and then invade through the stroma (Cowell et al., 2013) (Fig.4C). DCIS is found adjacent to invasive lesions in the vast majority of IDCs at the time of diagnosis and is considered the precursor of IDC as confirmed by several clinical and pathological evidences such as histological continuity and genetic signature similarities (Cowell et al., 2013).

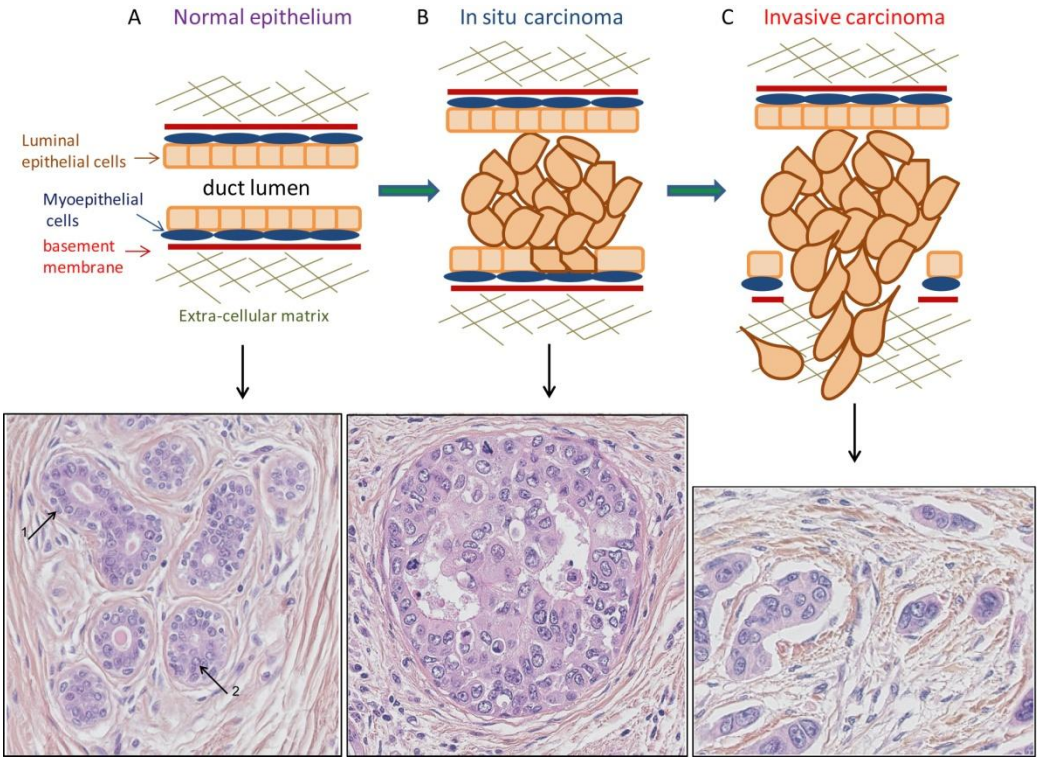

Figure 4: Scheme depicting a normal breast epithelium (A) and the transition from an *in situ* carcinoma (B) to an invasive carcinomatous lesion (C) with the correspondent pictures of human breast samples section stained for hematoxilin/eosin (H/E). (A) Normal human breast lobules and their epithelial bilayer: 1- external layer of myoepithelial (basal) cells; 2- internal layer of luminal cells. (B) In the *in situ* carcinoma malignant cells remain confined within the distended duct; myoepithelial cells are less conspicuous, because of duct distention by the tumour. (C) Invasive ductal carcinoma: the stroma is invaded by groups of malignant cells. Images: courtesy from Laetitia Fuhrmann, pathology department, Institut Curie Hospital, Paris.

Breast tumors are routinely classified according to several parameters like tumor size, histological grade (based on the size of carcinoma cell nuclei, number of mitosis and differentiation) and the presence of tumor cells in axillary lymph nodes and lymphatic vessels considered as a sign of metastasis. For what about the gene expression profile, both DCIS and IDC are classified into

four major molecular types: 1) luminal A characterized by high expression of estrogen and progesterone receptors (ER, PR) and low expression of proliferation genes; 2) luminal B characterized by low expression of ER/PR and high expression of proliferation genes; 3) ERBB2-positive subtype characterized by loss of ER/PR and amplification and/or overexpression of the epidermal growth factor (EGF) receptor ERBB2; 4) triple-negative subtype characterized by lack of expression of the ER/PR and ERBB2. These last two molecular subtypes are associated with poorest outcome (Sorlie et al., 2001; Sorlie et al., 2003).

1.6 Role of the actin cytoskeleton remodeling during cancer cell invasion

As said above, cancer cells migrating through the ECM extend cellular protrusions, such as lamellipodia or pseudopods, which allow them to adhere to the ECM and to generate forces for movement (Yamaguchi and Condeelis, 2007). The formation of these cellular protrusions strongly relies on assembly and polymerization of the actin cytoskeleton. Monomeric actin is a globular 42 kDa ATP–ADP binding protein (G actin) that is abundantly expressed in all eukaryotic cells. *In vitro*, ATP actin polymerizes into structurally polarized filaments (F actin) which are composed of two twisted helices. Once an unstable actin trimer, known as the nucleus, is formed, actin polymerization proceeds quickly at the fast growing plus end (also called barbed end) and more slowly at the minus end (also called pointed ends) (Fig.5). It is the incorporation of new actin subunits at the plus end that provides mechanical force for the generation of membrane protrusions in migrating cells (Nurnberg et al., 2011). Actin assembly inside cells is directly regulated and enhanced by various proteins that mediate *de novo* nucleation of filaments by generating actin-free barbed ends. Migrating cancer cells and in particular mammary carcinoma cells use two dominant mechanisms to generate free barbed ends at protrusive leading edges: (1) actin filament severing by cofilin, and (2) dendritic nucleation by the actin related protein 2 (ARP2) and ARP3 (Arp2/3) complex; these mechanisms synergize to amplify barbed end production (Bravo-Cordero et al., 2013). Cofilin produces free barbed ends by severing existing filaments, and new ends can serve as template to nucleate actin polymerization (Bravo-Cordero et al., 2013). In this way, by creating new actin filaments through severing, cofilin supports Arp2/3 complex-mediated actin branching (Ichetovkin et al., 2002).

The Arp2/3 complex was the first actin nucleation factor to be identified. It is an eptameric complex comprising ARP2 and ARP3, and the five actin-related protein complexes 1-5 (ARPC1-5). The complex has little nucleation activity on its own, but once activated by nucleation promoting factors (NPFs), it initiates the formation of a new (daughter) actin filament that emerges from an existing (mother) filament with an angle of 70° in a y-branch configuration (Fig.5). Briefly ARP1 and ARP2 mimics an actin dimer and an NPF protein binds to Arp2/3 through a verprolin homology central acidic (VCA) domain and to an actin monomer through the

Wiskott–Aldrich syndrome protein (WASP)-homology-2 (WH2) domain. Following the binding with NPF, ARP2 and ARP3 undergo a conformational change that stabilizes the Arp2/3 complex and allows the formation of an actin nucleation core (Goley and Welch, 2006). Well known NPFs are the ubiquitously expressed neural WASP (N-WASP) and the WASP family verprolin homology proteins (WAVE1–3) that is part of a pentameric complex (Nurnberg et al., 2011).

Another protein involved in Arp2/3-dependent actin nucleation is cortactin, which was initially identified as a phosphorylation target of SRC (Wu et al., 1991) and lacks the VCA domain. Cortactin binds to F-actin through its central repeat region (Weed et al., 2000) and to the Arp2/3 complex through its N-terminal acidic region even though it activates Arp2/3 only very weakly (Uruno et al., 2001). However, cortactin also binds to N-WASP through its carboxyl-terminal SH3 domain and leads to N-WASP activation and increased cell migration (Kowalski et al., 2005). Thus, cortactin could act as activator of Arp2/3 by synergizing with N-WASP. Cortactin also stabilizes the F-actin network and inhibits de-branching, most probably by strengthening the interactions between the Arp2/3 complex and F-actin (Weaver et al., 2001).

In addition to Arp2/3, other nucleation factors are the formins, a family of proteins responsible for elongation of unbranched actin filaments at the plus ends. Formins are defined by the presence of a highly conserved formin homology 2 (FH2) domain, which is necessary and sufficient to promote actin nucleation (Campellone and Welch, 2010). In contrast to Arp2/3 which caps pointed ends, FH2 domains bind to barbed ends actin as processive caps and preventing other capping proteins to terminate the elongation. Biochemical and structural studies with yeast and mammalian formins indicate that a dimer of FH2 domains stabilizes an actin dimer or trimer to facilitate the nucleation event. Although the nucleation mechanism is not clear yet, formins remain associated with the growing barbed ends of filaments, and sequential binding and release interactions might allow formins to 'walk' with the polymerizing barbed end, giving rise to straight bundled actin filaments(Campellone and Welch, 2010) (Fig.5). The existence of different classes of nucleator gives the cell the flexibility to assemble distinct populations of actin filaments with particular geometries and polymerization characteristics and to extend different types of protrusions in response to diverse signals (Campellone and Welch, 2010).

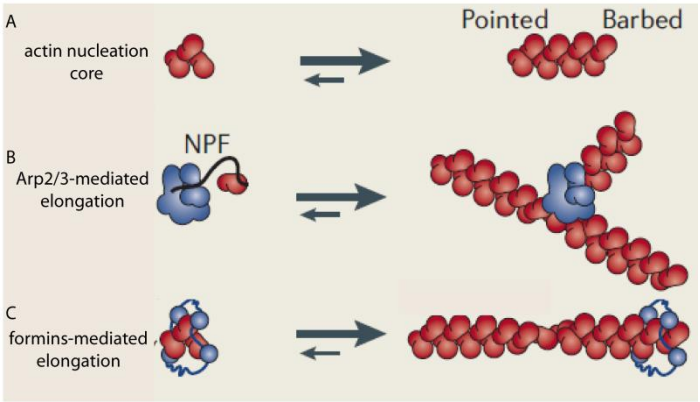

Fig.5: **Scheme depicting different mechanisms of actin nucleation.** Nucleation is the spontaneous initiation of actin-filament assembly that requires the formation of a trimeric actin nucleus (**a**). Spontaneous nucleation is kinetically unfavorable and is the rate-limiting step in polymerization, because the actin dimer intermediate is very unstable. The ARP2/3 complex is thought to mimic an actin dimer or trimer and to function as a template for the initiation of a new actin filament that branches off of an existing filament, generating y-branched actin networks (**b**). Formins instead promote the nucleation of unbranched filaments. (**c**). Formins remain associated with the growing barbed ends of filaments, and sequential binding and release interactions might allow formins to 'walk' with the polymerizing barbed end. Picture adapted from Goley and Welch, 2006.

The protrusive structures formed by migrating and invading cells plated on a 2D substratum, are termed filopodia, lamellipodia, and invadopodia, depending on their morphological, structural and functional characters. Formation of these structures is driven by spatially- and temporally-regulated actin polymerization at the leading edge (Yamaguchi and Condeelis, 2007).

Lamellipodia are the thin sheet-like protruding leading edges of cells. In lamellipodia actin organizes into a network of dendritic-branched filaments, which depends on the branching activity of the Arp2/3 complex activated by WAVE. The dendritic network in a lamellipodium produces a force that is sufficient to drive membrane protrusion and cell crawling on a planar substrate (Ridley, 2011). Filopodia are finger-like projections that form at the leading edge and are probably used by the cell to explore its environment. Filopodia comprise parallel bundles of actin filaments whose assembly depends mainly on formins such as mDia2 (Campellone and Welch, 2010). Fascin is the major actin-bundling protein that localizes to filopodia and is important for filopodium stability (Machesky and Li, 2010). One model for filopodia assembly is that they emerge from the lamellipodial F-actin network nucleated by the Arp2/3 complex through the binding of proteins such as fascin and the anticapping protein VASP (Vasodilator-stimulated phosphoprotein) (Gupton and Gertler, 2007).

1.4. Invadopodia

Invadopodia are actin-rich protrusions that form at the ventral surface of invasive cells grown on beds of ECM such as a thin layer of cross-linked gelatin, as a mimic of the BM. Invadopodia are often located underneath the nucleus and generally protrude vertically away from the cell body (Schoumacher et al., 2010). The main characteristic that distinguishes invadopodia from the other types of cellular protrusions such as lamellipodia or filopodia, is their capacity to focally degrade the ECM, as demonstrated for the first time by Chen and colleagues with the typical gelatin degradation assay (Chen et al., 1985). This assay involves plating cells on a thin layer of fluorescent ECM, such as cross-linked fluorescently-labelled gelatin. Invadopodia-associated ECM digestion leads to removal of the fluorescent ECM such that degraded areas are evident as dark spots in the fluorescent background. By immunofluorescence microscopy,

invadopodia protrusions appear as puncta that can be labelled with the F-actin-specific probe phalloidin or antibodies directed to cortactin, two major invodopodia components (Fig.6).

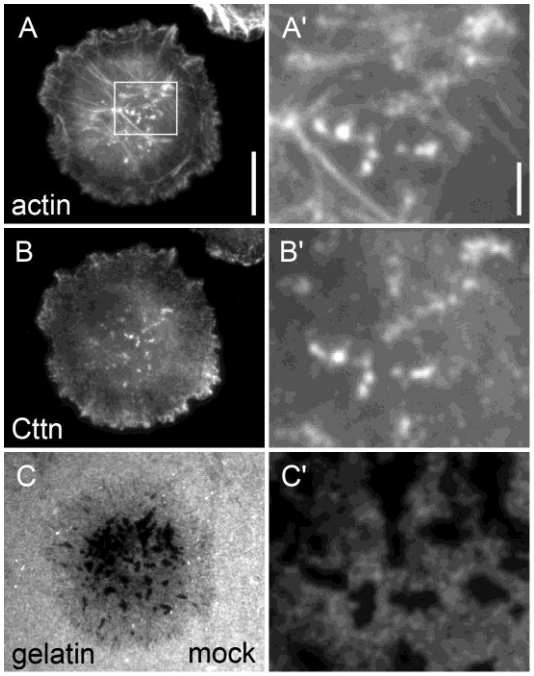

Figure 6: A typical invadopodia assay in which breast adenocarcinoma-derived cells, MDA-MB-231, were cultured for five hours on coverslips coated with crosslinked FITC–gelatin (C, C'), followed by fixation and staining with two molecular markers of invadopodia, actin filaments (A, A') and cortactin (B, B') and imaging by confocal microscopy. A', B' and C' are enlargements of the boxed region in A, B and C. Both invadopodia markers colocalize with a dark patch of degraded ECM. Scale bar for A, B, C = 10 µm, for A', B', C'= 2 µm. Picture from Steffen et al., 2008.

Invadopodia were found in cells derived from several invasive tumors, including breast carcinoma, melanoma, glioma and head and neck squamous cell carcinoma (Stylli et al., 2008). Invadopodia share similarities with podosomes, which are found in osteoclasts, monocyte-derived cells (macrophages and dendritic cells), endothelial cells and smooth muscle cells. Podosomes and invadopodia were first described in the 1980s as structures containing actin, SRC and phosphotyrosine proteins and associated with ECM degradation, which formed in chicken or mouse fibroblasts upon transformation with Rous sarcoma virus (RSV)(Chen, 1989; Chen et al., 1985; Tarone et al., 1985). The two terms have been often overlapped but nowadays podosomes are tendentially referred to degradative structures in normal cells and involved in physiological processes such as tissue remodelling and immune surveillance, while invadopodia are referred to degradative structures in cancer cells involved in the pathological processes of invasion and metastasis (Murphy and Courtneidge, 2011). The two structures also display some morphological differences: invadopodia are generally less abundant and protrude further into the ECM showing deeper and more focused degradation, while degradation by podosomes is rather shallow and widespread (Linder, 2009). Moreover invadopodia are stable for hours compared with the rapid turn-over of podosomes, these observations accounting for the higher degradative ability of cancer cells (Linder, 2009). Invadopodia and podosomes recently started to be more and more referred as invadosomes, a term that generally describe all adhesive structures that are involved in ECM degradation and invasion (Murphy and Courtneidge, 2011). The current model for

invadopodia formation implies a three-step process (Artym et al., 2006; Clark et al., 2007; Mader et al., 2011; Murphy and Courtneidge, 2011; Oser et al., 2009):

1) an initiation phase where interaction of matrix receptors on the tumor cell surface with components of the ECM and activation of growth factor receptors leads to activation of SRC and different signaling kinases such as focal adhesion kinase (FAK) and protein kinase C (PKC) and to the assembly of nascent invadopodia containing F-actin and cortactin;
2) an elongation phase which is mediated mainly by the protrusive force of the actin polymerization and requires actin regulatory proteins such as cortactin, Arp2/3, N-WASP and formins;
3) a maturation phase where invadopodia are endowed with matrix metallo-proteases (MMPs), the major enzymes involved in proteolytic remodeling of the ECM; in particular invadopodia promote ECM degradation by regulating the secretion of MMP2 and MMP-9 and above all the delivery of the membrane type-1 MMP (MT1-MMP) to ensure focalized degradation.

1.4.1. Invadopodial cytoskeleton machinery

The actin assembly machinery is critical in all the phases of invadopodia formation. Actin polymerization at invadopodia occurs both as branched filaments like for lamellipodia and as parallel filament bundles like for filopodia (Schoumacher et al., 2010). For instance the protein composition of invadopodia comprises markers typical of the dendritic branched actin network such as the Arp2/3 complex and its activators. As shown by Yamaguchi *et al.* the Arp2/3 complex and its activator N-WASP are required for invadopodia formation in highly metastatic mammary carcinoma cells as well as their upstream regulators Nck1, the Rho GTP-binding protein Cdc42 and WASP interacting protein (WIP) (Yamaguchi et al., 2005). A previous study with an N-WASP biosensor demonstrated that N-WASP is activated at the cell membrane during the initiation of invadopodium formation, thereby implicating N-WASP activity in the initiation of invasion (Lorenz et al., 2004). Cortactin is also present at invadopodia (Bowden et al., 1999) and and it is thought to form the actin core at nascent invadopodia (Artym et al., 2006; Clark et al., 2007). Indeed cortactin is strictly required for invadopodia formation in breast cancer-derived cell lines (Artym et al., 2006) and the binding of cortactin to Arp2/3 and N-WASP was shown to be important for invadopodium biogenesis in melanoma cells (Ayala et al., 2008).

Then invadopodia formation seems to be dependent also by protein involved in generation of bundled unbranched actin filaments. For example a study from my host lab showed that three members of the formin family (mDia 1-2-3) are also required for invadopodia formation and ECM degradation (Lizarraga et al., 2009). VASP is also accumulated at degradation sites

(Philippar et al., 2008) and the filopodia-specific markers the actin bundler fascin and myosin X are also required for invadopodia formation (Li et al., 2010; Schoumacher et al., 2010).

Schoumacher *et al.* showed that formation of invadopodia depends on both the dendritic and bundled actin machinery while elongation of invadopodia mostly depends on the bundled machinery, therefore suggesting a model in which invadopodia form by assembly of dendritic/diagonal and bundled actin networks and then mature by elongation of actin bundles (Fig.7) (Schoumacher et al., 2010). Moreover microtubules and intermediate filaments are required for invadopodia elongation and further growth in the ECM. Microtubules likely provide tracks for delivery of MMPs and membranes in order to allow invadopodia to further grow and penetrate the membrane (Schoumacher et al., 2010). Intermediate filaments also follow during elongation of invadopodia and likely play a role in their stabilization and maturation (Schoumacher et al., 2010).

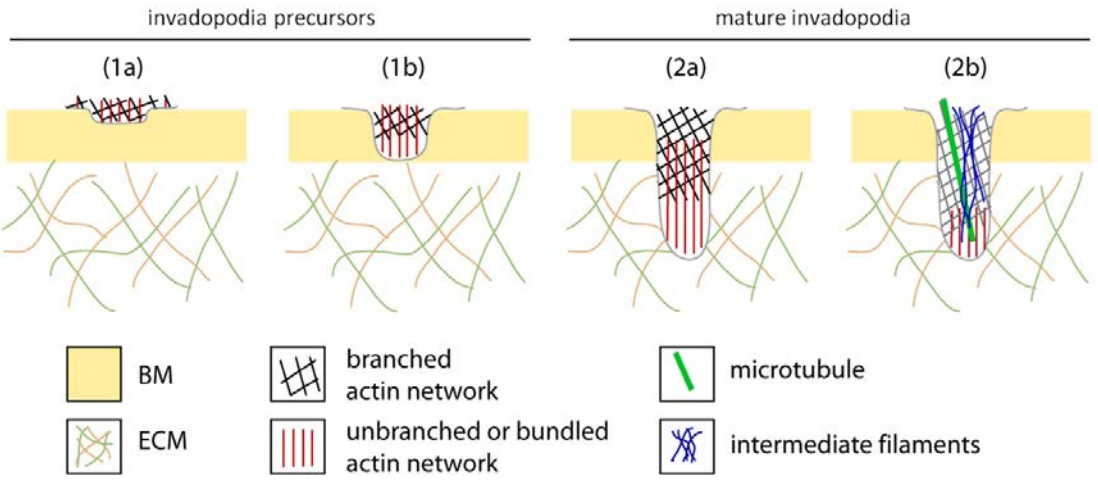

Figure 7: Scheme depicting the actin assembly in invadopodia formation (1a-1b) **and elongation** (1b-2a-2b). Invadopodia form by assembly of dendritic/diagonal and bundled actin networks and then mature by elongation of actin bundles. Microtubules and intermediate filaments are required for invadopodia maturation. Picture adapted from Schoumacher et al., 2010.

1.4.2. Invadopodia signaling

There are evidence that integrins and growth factor receptors play important roles in invadopodia formation and function. αvβ3 and β1 integrins have been found in invadopodia (Mueller and Chen, 1991; Zambonin-Zallone et al., 1989), and antibody-induced activation of β1 integrin increases degradation of the ECM (Nakahara et al., 1998). Loss of β1 integrin inhibited the formation of invadopodia in SRC-transformed fibroblasts (Destaing et al., 2010). A recent study showed that β1 integrin is required for the formation of mature, degradation-competent invadopodia in both two- and three-dimensional matrices but is dispensable for invadopodium precursor formation in metastatic human breast cancer cells. β1 integrin is indeed activated during invadopodium precursor maturation, and forced β1 integrin activation enhances the rate of

invadopodial matrix proteolysis (Beaty et al., 2013). Thus, it has been proposed that integrins contribute to invadopodia structure and function.

Invadopodia formation is also stimulated by receptors tyrosine kinase (RTKs) such as epidermal growth factor receptor (EGFR) and platelet-derived growth factor receptor (PDGFR) (Eckert et al., 2011; Mader et al., 2011; Yamaguchi et al., 2005). Activation of TKRs leads to SRC activation (Bromann et al., 2004), which is absolutely necessary for invadopodia formation and function, and the level of tyrosine phosphorylation at invadopodia positively correlates with the degree of ECM degradation (Bowden et al., 2006; Spinardi et al., 2004). Activation of integrins by ECM engagement also leads to SRC activation through the activation of focal adhesion kinase (FAK). FAK is a non-receptor protein tyrosine kinase mainly localized in focal adhesions (FAs). FAK is activated and tyrosine-phosphorylated in response to cell adhesion to the ECM mainly by binding to the cytoplasmic tail of activated β1 integrin. Activated FAK undergoes autophosphorylation at Tyr-397 and associates with SRC, leading to enhancement of its tyrosine phosphorylation and kinase activity (Mitra and Schlaepfer, 2006). FAK is also present in invadopodia and increased FAK expression promotes invadopodia formation (Hauck et al., 2002).

SRC kinase has been shown to regulate cytoskeletal remodeling during invadopodia formation through phosphorylation of cortactin and TKS5 (tyrosine kinase substrate with five SH3 domains), and these substrates have established roles in invadopodia formation. Although its role is not completely clear, TKS5 is essential for invadopodia formation since its loss causes a decrease in invadopodia formation and ECM degradation in SRC-transformed fibroblasts and in human breast tumor-derived cell lines, while TKS5 expression promotes invadopodia formation in non-invasive epithelial cells (Seals et al., 2005). TKS5 can also bind directly or indirectly to key Arp2/3 complex activators such as N-WASP and its upstream activators growth factor receptor-bound protein 2 (GRB2) (Oikawa et al., 2008) and NCK1-2 (Stylli et al., 2009). Moreover, TKS5 colocalizes with cortactin at invadopodia precursors of breast cancer cells (Oser et al., 2009).

Following its recruitment at invadopodia precursors, cortactin gets tyrosine phosphorylated either by SRC (Wu et al., 1991) or by Arg, a kinase of the Abelson (Abl) non-receptor kinase family, which is activated by SRC in response to binding of EGF to its receptor (Mader et al., 2011). Arg phosphorylates cortactin on tyrosine 421 (Y421) and the EGFR-SRC-Arg pathway has been shown to mediate functional maturation of invadopodia in breast cancer cells (Mader et al., 2011). At a mechanistic level, phosphorylation of cortactin at Y421 and Y466 is required for Nck1 binding to cortactin and recruitment at invadopodia (Oser et al., 2010). Along this line, SRC phosphorylation of cortactin *in vitro* facilitates the assembly of an Nck1–N-WASP-WIP–Arp2/3 signaling complex (Tehrani et al., 2007). In addition it was shown that cortactin phosphorylation regulates cofilin activity (Oser et al., 2009). Cofilin was previously shown to be required for invadopodium maturation and degradation activity (Desmarais et al., 2009; Yamaguchi et al.,

2005). As shown by Oser *et al.*, tyrosine phosphorylation of cortactin in response to EGF causes its dissociation from cofilin enabling cofilin to severe actin filaments to create barbed-ends at invadopodia to support Arp2/3-dependent actin polymerization. After barbed end formation, cortactin is dephosphorylated, which blocks cofilin severing activity thereby stabilizing actin at invadopodia (Oser et al., 2009).

In conclusion although cortactin tyrosine phosphorylation and cofilin severing activity are not required for initial invadopodium precursor formation, they are critical for induction of actin polymerization and matrix degradation during invadopodial maturation (Yamaguchi et al., 2005; Artym et al., 2006; Oser et al., 2009). All these studies suggested a role for cortactin in coordinating the activities of cofilin and N-WASP to spatially and temporally control activation of actin polymerization and invadopodium maturation (Fig.8).

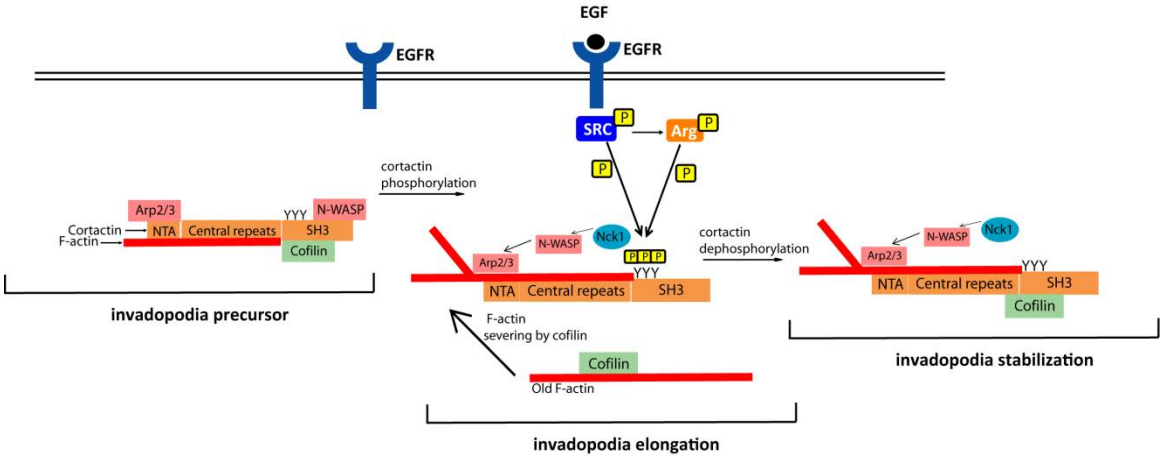

Figure 8: Scheme depicting the contribution of cortactin phosphorylation for invadopodia assembly and maturation. Cortactin binds to F-actin through its central repeats domain, to N-WASP through its SH3 domain, to Arp2/3 through its N-terminal acidic (NTA) region and to cofilin. All these proteins form a complex that constitutes the invadopodium precursor. Cortactin phosphorylation by SRC and Arg, that are activated by EGFR activation upon ligand binding, has two consequences: first phosphorylated cortactin binds to Nck1 that in turn activates cortactin-bound N-WASP that activates the branching activity of the Arp2/3 complex; second phosphorylated cortactin causes cofilin dissociation from cortactin and cofilin is then free to severe actin to generate free barbed ends that the Arp2/3 complex can use for efficient actin polymerization. Cortactin is then dephosphorylated, which stabilizes the invadopodium precursor for maturation.

1.4.3. Invadopodia degradation of ECM through the action of MMPs

Invadopodia precursors further mature into functional degradative structures upon accumulation of MT1-MMP, a membrane-anchored MMP that allows focal degradation of the matrix at the level of invadopodia (Artym et al., 2006; Clark et al., 2007; Monteiro et al., 2013; Sakurai-Yageta et al., 2008; Sato et al., 1994). Secretion of MMP2 and MMP9 also occurs at invadopodia (Artym et al., 2006; Clark et al., 2007) but the prominent role is exerted by MT1-MMP (Hotary et al., 2006; Hotary et al., 2003; Poincloux et al., 2009; Sabeh et al., 2004). Understanding how MT1-MMP is targeted to invadopodia is a subject of interest of my host lab and one of the aims of my

study. I will discuss later (section 1.5.), the main findings on MT1-MMP function and intracellular regulation.

1.4.4. Invadopodia in 3D matrix environment

Recent studies employing 3D matrices have shown that invadopodial structures enriched for F-actin together with cortactin, FAK, MT1-MMP, N-WASP, β1-integrin and other adhesive proteins such as paxillin and talin also form in 3D culture of mouse sarcoma, human melanoma, fibrosarcoma and breast cancer cells (Li et al., 2010; Tolde et al., 2010). Juin and colleagues in several cell types such as endothelial cells, macrophages, fibroblasts and breast cancer cells described structures that they named linear invadopodia (Juin et al., 2012). Similarly to classical dotty-like invadopodia on gelatin, N-WASP, TKS5 and cortactin colocalized with F-actin in linear invadopodia (Juin et al., 2012; Monteiro et al., 2013) and were also observed when cells are fully embedded in a 3D type I collagen matrix (Juin et al., 2012). Surprisingly β1 and β3 integrins are not present in linear invadopodia and not required for their formation (Juin et al., 2012). A recent study from my lab has shown that breast cancer cells plated on a layer of fibrillar type I collagen (that more faithfully mimics the fibrous interstitial stroma) and stained for F-actin and cleaved collagen I fibers (through a specific antibody that recognizes the collagen filament cleaved by proteases) revealed the formation of linear accumulations of F-actin on the inner face of the plasma membrane associated with collagen fibers, coincident with regions of collagenolytic activity (Monteiro et al., 2013) (Fig.9). In conclusion although these studies support the idea that invadopodia form also in 3D matrices that more faithfully mimic the *in vivo* environment, it will be important in the future to establish the characteristics of formation of these structures.

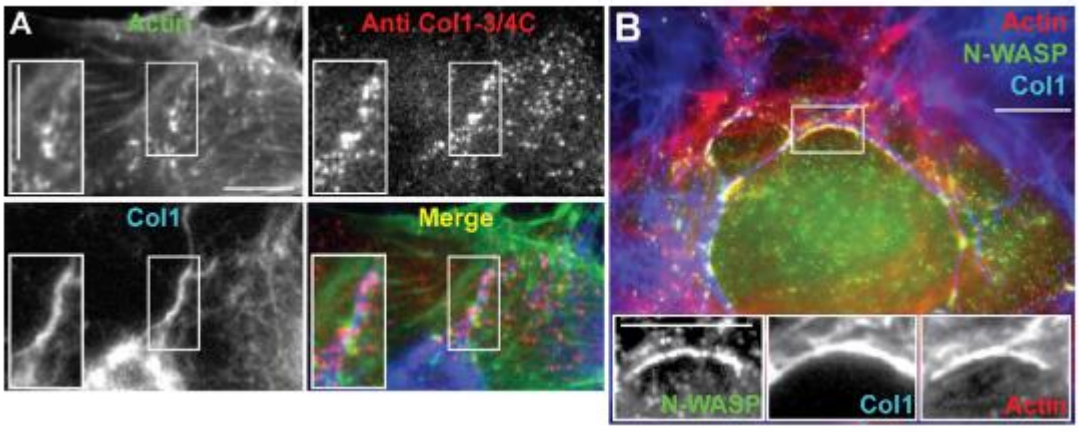

Figure 9: Picture showing linear invadopodia formed in MDA-MB-231 breast cancer cells plated on a layer of collagen I fibers (blue). In A cells were stained with anti-Col1-3/4C antibodies recognizing MMP-cleaved collagen I (red) and for F-actin (green) revealing collagenolytic linear invadopodia. Inset is a higher magnification of the boxed region. Scale bar: 5 μm. In B, cells were stained for N-WASP (green) and F-actin (red). Insets are higher magnification of boxed regions. Scale bar: 5 μm. Picture from Monteiro et al., 2013.

1.5. ECM degradation through the action of MT1-MMP

1.5.1. MMPs family

MMPs belong to the family of zinc-dependent endopeptidases and they are so called "metallo-proteases" because they rely on a zinc atom to carry out the hydrolysis of their substrates. MMPs are enzymes implicated in the degradation of pericellular proteins of the BM and the ECM and therefore they are involved in many physiological processes, like embryonal development, morphogenesis and remodelling of the tissues (Kessenbrock et al., 2010) and regulation of inflammatory processes (Khokha et al., 2013).

Interest in MMPs increased in the late 1960s and early 1970s following observations that several MMPs are upregulated in cancer. Importantly, high levels of MMPs often correlated with poor prognosis in human patients (Egeblad and Werb, 2002). Furthermore animal studies with transplantation assays showed that relatively benign cancer cells acquire malignant properties when MMP expression is upregulated. Conversely, highly malignant cells become less aggressive when MMP expression or activity is reduced. For instance, after intravenous injection, cancer cells are less capable of colonizing the lungs of *Mmp2*- or-*9*-deficient mice than the lungs of wild-type mice (Itoh et al., 1999; Itoh et al., 1998), while overexpression of MT1-MMP in the mammary gland of transgenic mice induce adenocarcinoma and mammary gland abnormalities (Ha et al., 2001).

All MMPs share a conserved domain structure that consists of a catalytic domain and an autoinhibitory pro-domain. The catalytic domain consists of five β-sheets and three α-helices and a catalytic zinc ion (Zn^{2+}). The pro-domain contains a conserved Cys residue that coordinates Zn^{2+} in the active-site, thereby inhibiting catalysis (Fig.10). When the pro-domain is destabilized or removed, the active site becomes available to cleave substrates. In addition, most MMP-family members also contain a hemopexin (HPX) domain attached at their carboxyl-termini by a flexible hinge (Fig.10). The HPX domain encodes a four-bladed β-propeller structure that mediates protein–protein interactions; this domain contributes to proper substrate recognition, activation of the enzyme, protease localization, internalization and degradation (Page-McCaw et al., 2007). Most MMPs are secreted proteins; however some MMP family members incorporate a transmembrane domain and are membrane-anchored (membrane-type MMPs, MT-MMPs), these include MT1-MMP, MT2-MMP, MT3-MMP and MT5-MMP (also called MMP14, MMP15, MMP16 and MMP24) (Sato et al., 1994) (Fig.10). Other membrane-bound MMPs are represented by MT4-MMP and MT6-MMP (also called MMP17 and MMP25) who feature a glycosphingolipid (GPI) anchor at the place of the transmembrare domain, and by a membrane-type II MMP, MMP23, characterized by a N-terminal signal anchor that targets it at the membrane (Egeblad and Werb, 2002).

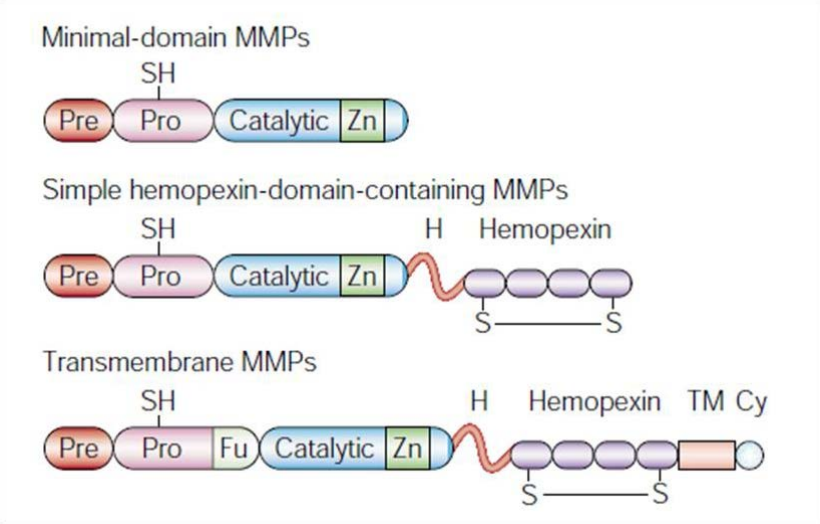

Figure 10: **Schematic structure of MMPs**. All MMPs share conserved domain structure of signal-peptide (pre), pro-domain (pro) and catalytic domain. All MMPs are synthesized with a signal peptide, which is cleaved during transport through the secretory pathway. The pro-domain contains a thiol-group (-SH) that interacts with the zinc ion (Zn^{2+}) of the catalytic domain and keeps the enzyme as an inactive zymogen. Pro is removed by proteolytic cleavage between the pro-domain and the catalytic domain. Most MMPs possess also a hemopexin-like region, a domain composed of four repeats and containing a disulfide bond (S-S) between the first and the last subdomain, which is linked to the catalytic domain through a flexible hinge region. Membrane typeI-MMPs also comprise a transmembrane domain and a short cytoplasmic tail. Figure adapted from Egeblad and Werb, 2002.

1.5.2. Role of MT1-MMP in cancer cell invasion

Although secreted MMPs have been implicated in cancer since decades, several converging studies, including some of my lab, implicate MT1-MMP as the major MMP implicated in the tissue invasive program of cancer cells (Hotary et al., 2006; Hotary et al., 2003; Li et al., 2008; Sabeh et al., 2004). In agreement with this, MT1-MMP strongly accumulates at invadopodia where it is required for focal pericellular degradation of the ECM (Artym et al., 2006; Sakurai-Yageta et al., 2008; Steffen et al., 2008; Poincloux et al., 2009; Monteiro et al., 2013).

MT1-MMP was shown to degrade several ECM components, including collagen type I, II, and III and IV, gelatin, fibronectin, laminin types1 and 5, fibronectin, vitronectin, aggrecan, and fibrin (d'Ortho et al., 1997; Ohuchi et al., 1997). It also participates in the activation of secreted MMPs such as pro-MMP-2 (Butler et al., 1998; Itoh et al., 2001; Kinoshita et al., 1998; Strongin et al., 1995) and pro-MMP-13 (Knauper et al., 1996), which, in turn, can cleave multiple matrix substrates. The cell surface activation of proMMP-2 by MT1-MMP has been considered to be a particularly important step in tumor invasion because MMP-2 degrades collagen type IV and laminin, which are the major components of the BM (Kalluri, 2003). The activation steps include the tri-molecular complex formation of MT1-MMP, TIMP-2 (an inhibitor of MMPs) and proMMP-2 (Butler et al., 1998; Kinoshita et al., 1998; Strongin et al., 1995). The interaction of MT1-MMP and TIMP-2 is through the active site of MT1-MMP and the inhibitory site of TIMP-

2; thus, the activity of MT1-MMP is inhibited in the complex. This MT1-MMP–TIMP-2 complex acts as a receptor to bind proMMP-2 to the cell surface through the interaction of the exposed TIMP-2 carboxyl-terminal domain and the hemopexin of proMMP-2 (Butler et al., 1998; Kinoshita et al., 1998). Since the ability of MT1-MMP in the complex to process the propeptide of MMP-2 proteolytically is inhibited by TIMP-2, a second molecule of MT1-MMP that is adjacent to the complex but not interacting with TIMP-2 is required for the processing of proMMP-2. Indeed homophilic oligomerisation of MT1-MMP via its hemopexin domain is needed for pro-MMP2 activation (Itoh et al., 2001). MT1-MMP is also the only MMP that is essential for survival, as mice deficient in this protease suffer severe complications in remodelling of skeletal and extra-skeletal connective tissues resulting in early death (Holmbeck et al., 1999).

Several studies, however, have shown that in metastatic dissemination MT1-MMP is the only MMP strictly required for the proteolysis of the interstitial collagen networks (Hotary et al., 2003; Li et al., 2008; Sabeh et al., 2004; Sodek et al., 2007). As shown by Weiss and coworkers, silencing of MT1-MMP impairs the invasive ability of tumor cells and tumor-associated fibroblasts to invade through fibrillar type I collagen matrices polymerized *in vitro* or through native chicken chorioallantoic membrane (strongly enriched in type I collagen) (Sabeh et al., 2004). On the contrary other secreted MMPs are dispensable for collagenolysis in these systems, confirming the primary role for MT1-MMP in invasion (Sabeh et al., 2004).

MT1-MMP seems to be indispensable for breaching of the BM and remodeling collagen fibres of interstitial tissues (Hotary et al., 2006). It was shown that over-expression of MT1-MMP in non-invasive COS or MCF-7 cells is sufficient to degrade native mesothelial BM in a way that is independent from MMP-2 and MMP-9, while silencing of MT1-MMP in highly aggressive breast adenocarcinoma-derived MDA-MB-231 cells inhibited BM perforation and invasion (Hotary et al., 2006). The same results were obtained for MT2-MMP and MT3-MMP suggesting that each of the three MT-MMPs is necessary and sufficient for mediating BM remodeling (Hotary et al., 2006). Surprisingly no such effect was observed upon depletion of MMP2 or MMP9, which can cleave BM-specific type IV collagen, suggesting that MT1-MMP action in invasion does not rely on the activation of secreted MMPs (Hotary et al., 2006).

MT1-MMP has been shown to be up-regulated in human cancer clinical samples and studies have reported elevated MT1-MMP expression in breast cancer. For instance it was observed a significant up-regulation of MT1-MMP mRNA levels in breast cancers samples associated with poorer prognosis (Jiang et al., 2006). More recent studies, including some from our lab also documented by immunohistochemical analyses an up-regulation of MT1-MMP in ER/PR-negative breast tumors, which are associated with higher risk of metastasis (Perentes et al., 2011; Rosse et al., 2014)(C. Lodillinsky, unpublished data).

MT1-MMP is produced as an inactive 64-kDa zymogen that is activated in the trans-Golgi network (TGN) by furin-like convertases, which cleave at the Arg108-Arg-Lys-Arg motif

located between the pro-peptide and the catalytic domain. Active MT1-MMP (55 kDa), starting at Tyr112, is then inserted into the plasma membrane with the catalytic domain facing the extracellular space, where it can cleave pericellular substrates (Mazzone et al., 2004). MT1-MMP proteolitic activity at the plasma membrane is subjected to various regulatory mechanisms, like gene transcription, proteolytic inactivation, inhibition by TIMPs and intracellular traffic and in cancer pathogenesis most of these processes are deregulated (Kessenbrock et al., 2010). I will focus below on the main aspects of MT1-MMP intracellular trafficking in cancer cell invasion and in its importance for the delivery of the protease to invadopodia.

1.6. MT1-MMP intracellular trafficking

One regulatory mechanism of MT1-MMP activity at the cell surface is through internalization and traffic through the endocytic compartments. Indeed it is known that at each time only a small fraction of MT1-MMP that is delivered to the plasma membrane remains at the surface as MT1-MMP is efficiently internalized (Poincloux et al., 2009; Remacle et al., 2003).

1.6.1. Endocytic pathway

Endocytosis is a major mechanism by which cells regulate the level of cell-surface proteins. Receptors, ligands and other endocytosed molecules are internalized using different routes of entry. The best-characterized one is the clathrin-dependent endocytosis through which several surface receptors are internalized including receptor tyrosine kinases (RTKs), G-coupled receptors (GPCRs), transferrin receptor low-density lipoprotein (LDL) receptors (McMahon and Boucrot, 2011). Cargoes are first recruited into specialized domains of the plasma membrane through interactions with adaptor protein complexes, such as adaptor protein-2 (AP-2). AP-2 recruits the coat protein clathrin, whose polymerization drives the progressive invagination of the membrane to form a clathrin-coated pits (CCPs) (Fig.11). Recruitment of the GTPase dynamin, which assembles in a helix around the neck of CCPs leads to the scission and formation of clathrin-coated vesicles (CCVs). These vesicles then uncoat and fuse with early endosomes (McMahon and Boucrot, 2011). Besides clathrin-dependent endocytosis, different forms of non-clathrin-mediated endocytic pathway have been identified that are less well-characterized (Doherty and McMahon, 2009; McMahon and Boucrot, 2011). Caveolae are one example of a clathrin-independent and cholesterol-sensitive uptake pathway (Fig.11) present in many but not all cell types (Parton and Simons, 2007). In addition, other less-known mechanisms of internalization which does not use clathrin, caveolin or dynamin exist (Doherty and McMahon, 2009; McMahon and Boucrot, 2011); one of these alternative pathways is mediated by the small GTP-binding protein ARF6 (see Fig.11 and chapter 2).

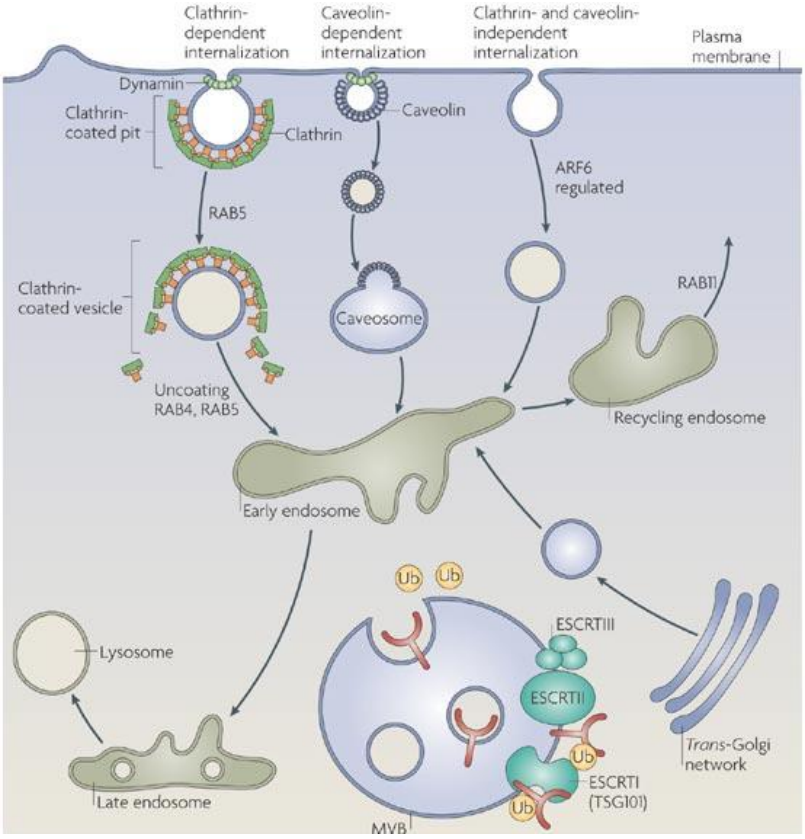

Figure 11: **Schematic representation of the endocytic-recycling-degradative pathway**. Figure from (Gould and Lippincott-Schwartz, 2009).

Independently from their route of entry, internalized cargoes are routed to early endosomes, which represent a sorting station in which receptors are sorted to late endosomes and lysosomes for degradation, or are recycled back to the cell surface (Fig.11) (Jovic et al., 2010; Sigismund et al., 2012). Sorting at different endosomal compartments is regulated mainly by small GTP-binding proteins of the Rab family, which determine the functional organization of different endosomal compartments by generating biochemically distinct RAB-containing membrane domains both in early and late endosomes (Stenmark, 2009). For example two critical RAB proteins, RAB5 and RAB7, are associated with early and late endosomes, respectively. Cargoes routed to recycling compartments are recycled back to the plasma either through a fast or a slow recycling route depending on RAB4 and RAB8/RAB11, respectively (Stenmark, 2009). Cargoes destined to degradation in lysosomes traffic through late endosomes and multivesicular bodies (MVBs) (Fig.11) depending on RAB7 (Stenmark, 2009). Receptor ubiquitination provides the crucial signal for entering the degradative pathway. Indeed, several protein complexes harbouring ubiquitin (UB)-binding domains recognize ubiquitinated cargoes and escort them along the degradative route to lysosomes (Gould and Lippincott-Schwartz, 2009) (Fig.11). ESCRT (endosomal sorting complex required for transport) multiprotein complexes I, II and III, recognize ubiquitylated cargo in the endosomal system and direct this cargo into MVBs (fig7). MVBs are late endocytic compartments, which are characterized by the presence of intraluminal vesicles (ILVs) that are generated by inward invagination of the limiting membrane of the endosomes

(Gould and Lippincott-Schwartz, 2009). MVBs fuse with lysosomes for cargo degradation or can also fuse with the plasma membrane in an exocytic fashion and release their vesicular content, the exosomes (Gould and Lippincott-Schwartz, 2009).

1.6.2. MT1-MMP regulation through clathrin-mediated and caveolar endocytosis

The first studies suggesting that MT1-MMP undergoes endocytosis were done in epithelial MDCK and CHO-K1 cells. Jiang and colleagues revealed that MT1-MMP colocalizes with clathrin at the plasma membrane and is internalized in CCPs in a dynamin-dependent pathway and routed to early endosomes (Jiang et al., 2001). At the same time Uekita *et al*. showed that the clathrin-mediated uptake of MT1-MMP requires the integrity of the cytoplasmic domain of MT1-MMP, in particular of a Leu-Ley-Tyr573 motif that binds with high affinity to the mu2 subunit of AP-2 (Uekita et al., 2001).

Two studies implicated a role for caveolae in MT1-MMP endocytosis. In different tumor cell lines MT1-MMP has been found in caveolar detergent-insoluble, glycolipid-rich membrane microdomains and was shown to co-precipitate with caveolin-1 (Annabi et al., 2001). In addition, MT1-MMP has been found to colocalise with caveolin-1 at the cell surface of endothelial cells (Puyraimond et al., 2001) and the cytoplasmic tail of MT1-MMP has been shown to interact with tyrosine (Tyr14)-phosphorylated caveolin-1, suggesting a possible mechanism for the caveolar association with MT1-MMP (Labrecque et al., 2004).

These studies suggested that MT1-MMP is efficiently internalized from the cell surface possibly as a way to control its proteolytic activity; later studies suggested that cancer cells may increase their invasive potential by blocking MT1-MMP endocytosis and retaining it to the surface. It was shown that SRC controls MT1-MMP endocytosis by phosphorylating Tyr573 in the cytoplasmic tail of the protease (Nyalendo et al., 2007), likely by impeding binding of AP-2 and therefore retaining the protease at the surface. This phosphorylation promotes endothelial and fibrosarcoma cell migration (Nyalendo et al., 2007), tumor cells proliferation and invasion in 3D type I collagen matrices and tumor progression in nude mice (Nyalendo et al., 2008; Nyalendo et al., 2010).

Furthermore, SRC suppresses MT1-MMP internalization by phosphorylating endophilin A2, a protein that generates membrane curvature through its F-BAR domain (Wu et al., 2005). Phosphorylated endophilin A reduces its affinity for dynamin resulting in reduced endocytosis of MT1-MMP and increased matrix degradation (Wu et al., 2005).

Consistently, in MDA-MB-231 breast cancer cells SRC was shown to block MT1-MMP endocyosis by phosphorylating and limiting the activity of the Cdc42 interacting protein 4 (CIP4). Indeed recruitment of CIP4 to invadopodia leads to MT1-MMP internalization probably by inducing invagination of membranes through its F-BAR domain; invaginations are stabilized by SH3-domain-mediated recruitment of N-WASP–Arp2/3 and branching of F-actin. SRC-induced

tyrosine phosphorylation of CIP4 might limit its ability to recruit N-WASP, and thereby reduce MT1-MMP internalization (Hu et al., 2011). Another study showed that type-I collagen can interfere with clathrin-mediated uptake of MT1-MMP by interacting with the HPX domain at the cell surface (Lafleur et al., 2006).

1.6.3. MT1-MMP exocytosis

Another mechanism that cancer cells use to promote MT1-MMP activity is by increasing its exocytosis rate to the plasma membrane in particular to invadopodia. Several studies, including some from my lab, have shown that a significant fraction of internalized MT1-MMP is recycled to the surface (Itoh and Seiki, 2006; Monteiro et al., 2013; Remacle et al., 2003; Sakurai-Yageta et al., 2008; Steffen et al., 2008).

Remacle and co-workers have shown that in fibrosarcoma cells internalized MT1-MMP reaches a Rab4-positive compartments where it is recycled back to the cell surface (Remacle et al., 2003). This study proposed a model in which internalization of MT1-MMP in addition to down-regulate the enzymatic activity, represents also a rapid response mechanism used by the cell for relocalizing active MT1-MMP at sites where it is needed (Remacle et al., 2003). As invadopodia are structures strongly enriched in MT1-MMP, it has been proposed that recycled MT1-MMP is re-targeted from the endosomes to invadopodia allowing localized proteolysis (Poincloux et al., 2009).

Another study found that MT1-MMP localizes to Rab8-positive secretory vesicles involved in polarized membrane transport of newly synthesized proteins to PM protrusions. Plasma membrane delivery of MT1-MMP from these compartments is Rab8-dependent manner (Bravo-Cordero et al., 2007). Internalized MT1-MMP and MT3-MMP trafficked from early endosomes to the TGN from where they recycle back to cell surface in 60 min. This route was dependent on a conserved motif in the cytoplasmic tail of MT1/MT3-MMP (DKV(582) of MT1-MMP) defining a novel recycling motif (Wang et al., 2004). All these studies suggest that MT1-MMP could be recycled from recycling endosomes or from secretory compartments back to invadopodia, but the underlying mechanisms were not investigated.

Several studies from our lab have shown that the majority of intracellular MT1-MMP in MDA-MB-231 breast adenocarcinoma-derived cells is stored in late endocytic compartments. Former colleagues in my lab in the attempt of exploring MT1-MMP subcellular localization in MDA-MB-231 cells, generated a stable cell lines expressing mCherry-tagged MT1-MMP [where mCherry was added N-terminal to the trans-membrane region, (Sakurai-Yageta et al., 2008)]; MT1-MMP-mCherry showed the same localization as endogenous MT1-MMP. The majority of MT1-MMP-mCherry colocalized with the late endosome/lysosomal compartment marker VAMP7 (Steffen et al., 2008) and the late endosome/MVBs marker Rab7 (Rosse et al., 2014; Steffen et al., 2008), whereas only a small fraction of MT1-MMP-mCherry was found in early

endosomes positive for EEA1 (Steffen et al., 2008). Based on these studies, it was proposed that MT1-MMP in these compartments represents a storage pool from where a significant fraction the protease could be actively transported and exocytosed to the plasma membrane at invadopodia (Monteiro et al., 2013; Rosse et al., 2014; Steffen et al., 2008).

In addition, several components of an exocytic machinery that is required for delivery of MT1-MMP to invadopodia have been identified, including actin cytoskeletal proteins including cortactin, the exocyst complex (required for docking of transport vesicles) and vesicle fusion SNARE proteins (Artym et al., 2006; Monteiro et al., 2013; Rosse et al., 2014; Sakurai-Yageta et al., 2008; Steffen et al., 2008).

1.6.3.1. Role of SNAREs in exocytosis of MT1-MMP

Anika Steffen, a former member of the lab first showed that MT1-MMP exocytosis requires the SNARE membrane fusion machinery (Steffen et al., 2008). SNARE (soluble NSF [N-ethylmaleimide-sensitive factor] attachment protein receptor) proteins constitute the basic machinery for membrane fusion that regulates trafficking of cellular material between the plasma membrane and intracellular compartment (Proux-Gillardeaux et al., 2005). The SNARE TI-VAMP/VAMP7 was identified as a vesicular (v-) SNARE mainly present on the TGN and late endosome/lysosomal structures and it was shown to be responsible for late endosome/lysosomal exocytosis (Proux-Gillardeaux et al., 2005). VAMP7 colocalizes with MT1-MMP in late endosomes and in lysosomal structures (corroborating MT1-MMP localization at late endocytic compartments) and at the plasma membrane at sites of matrix degradation. Upon siRNA knockdown of VAMP7 in MDA-MB-231 cells, significantly less MT1-MMP accumulated at the PM, the number of invadopodia decreased and invasion was impaired, suggesting a specific role of Ti-VAMP in targeting MT1-MMP to invadopodia and regulating the fusion of MT1-MMP-containing endosomes with the plasma membrane (Steffen et al., 2008). Later on, another group showed that dominant negative mutants of VAMP7 and Rab7 impair MT1-MMP exocytosis, cell migration and invasion of fibrosarcoma cells (Williams and Coppolino, 2011). Additional SNAREs have been implicated in the delivery of MT1-MMP to the surface including the plasma membrane target (t-) SNARE syntaxin 4 in human gastric cancer cells(Miyata et al., 2004). More recently, Coppolino and colleagues reported that inhibition of the plasma membrane t-SNARE SNAP23 and of the endosomal v-SNAREs VAMP3 and syntaxin-13 impairs the trafficking of MT1-MMP to the surface of fibrosarcoma cells and the secretion of MMP2 and MMP9 (Kean et al., 2009). Furthermore, blocking the functions of the three SNAREs impaired the proteolytic degradation of a gelatin matrix and cell invasion *in vitro* (Kean et al., 2009). Finally, a recent study showed by co-immunoprecipitation experiments that during invadopodia formation in MDA-MB-231 cells an increased association of SNAP23, Syntaxin4 and VAMP7 occurs and blocking the function of these SNAREs perturbed invadopodium-based ECM degradation and cell

invasion (Williams et al., 2014). These studies therefore reveal an important role for SNARE-regulated trafficking of MT1-MMP to invadopodia during cellular invasion of ECM.

1.6.3.2. Role of the actin cytoskeleton and exocyst-complex docking system in MT1-MMP exocytosis

A study from Mika Sakurai-Yageta in the lab proposed that cytoskeletal assembly and MT1-MMP exocytosis are coordinated at invadopodia based on the observation that IQGAP1 (IQ motif containing GTPase activating protein) and the exocyst vesicle-docking complex are required for invadopodium formation and activity (Sakurai-Yageta et al., 2008). IQGAP1 is an effector for the Rho GTPases Rac and Cdc42 and acts by stabilizing them in their active form (Noritake et al., 2005). IQGAP1 plays crucial roles in cell-cell adhesion, cell polarization and directional cell migration by linking Rho-family GTPases with the actin cytoskeleton and microtubules (Noritake et al., 2005). Several studies have also implicated IQGAP1 in the dissemination of invasive carcinoma cells in human tumors, supported by the over-expression and distinct membrane localisation of IQGAP1 observed in a range of tumours (White et al., 2009). The exocyst complex, which consists of eight subunits (Sec3, Sec5, Sec6, Sec8, Sec10, Sec15, Exo70 and Exo84), mediates the tethering of post-Golgi and endocytic recycling vesicles at the plasma membrane for exocytosis (Hertzog and Chavrier, 2011). In MDA-MB-231 cells, IQGAP1 and the exocyst component Sec8 colocalize at invadopodia (Sakurai-Yageta et al., 2008). IQGAP1 was identified as an interacting partner of the exocyst complex subunits Sec3 and Sec8 by yeast 2-hybrid and co-immunoprecipitation experiments. Interaction of IQGAP1 and the exocyst complex required activation of the Rho GTPases Cdc42 and RhoA, both of which are essential for invadopodium formation (Sakurai-Yageta et al., 2008). Knockdown of different exocyst-complex subunits or IQGAP1 prevented the focal delivery of MT1-MMP to invadopodia suggesting that the exocyst complex in association with IQGAP1 control the docking of MT1-MMP transport vesicles to the invadopodial plasma membrane (Sakurai-Yageta et al., 2008).

Another cytoskeletal protein, which is implicated in MT1-MMP exocytosis is cortactin (Artym et al., 2006; Clark et al., 2007). In addition to its role in accumulating F-actin and N-WASP at invadopodia precursors and in the regulation of several signaling pathway leading to invadopodia maturation (section 1.4.1.-1.4.2.), cortactin was also shown to regulate delivery of MT1-MMP to invadopodia (Clark et al., 2007). In fact cells depleted for cortactin exhibited a decrease, whereas cortactin-overexpressing cells show an increase in MT1-MMP cell surface expression and MMP2 and MMP-9 secretion pointing to a role for cortactin in coupling dynamic actin assembly at invadopodia to the secretory machinery (Artym et al., 2006; Clark et al., 2007). Although the mechanism trough which cortactin exerts this function is still not completely clear, recent studies from my lab and others have provided important insights into how cortactin, actin and other cytoskeletal proteins regulate the delivery of MT1-MMP to invadopodial plasma membrane. For

instance Yu and colleagues have shown that N-WASP localizes to and concentrates at the front of invading pseudopodia, which are long protrusions that MDA-MB-231 cells form when they migrate through a 3D matrigel matrix where F-actin, cortactin and the Arp2/3 complex are enriched (Yu et al., 2012). Silencing of N-WASP blocks pseudopodia formation and MT1-MMP-dependent matrix degradation. Indeed, MT1-MMP, which is transported to the plasma membrane via late endosome/lysosomal trafficking, is captured and anchored to N-WASP/F-actin patches due to an interaction occuring between MT1-MMP cytoplasmic tail and F-actin (Yu et al., 2012). In this way MT1-MMP gets enriched at degradation sites at the tip of pseudopodia (Yu et al., 2012).

In parallel recent studies from my lab have demonstrated that in MDA-MB-231 cells a second pool of F-actin, cortactin and other regulatory proteins is present on the MT1-MMP-positive late endosomes themselves (Monteiro et al., 2013; Rosse et al., 2014). In particular, Monteiro *et al.* showed that the Wiskott-Aldrich syndrome protein and Scar homolog (WASH), a recently discovered NPF for the Arp2/3 complex, interacts with the exocyst subunit Exo84 and Sec3 and localizes together with cortactin, F-actin and the exocyst complex on the cytosolic side of the MT1-MMP late endosomes as punctuate domains. Moreover loss of WASH or exocyst induces loss of F-actin domains on the endosomes and defects in MT1-MMP recycling and delivery to the invadopodial plasma membrane (Monteiro et al., 2013). Furthermore by measuring the exocytic events of MT1-MMP tagged with PHluorin (a fluorophore that turns green fluorescent when passes from an acidic to a neutral PH environment), it was shown that MT1-MMP endosomes engage with the plasma membrane and exocytose their content at the level of contacts with the matrix and that WASH and exocyst contribute to MT1-MMP exocytosis to these sites. This occurs both at the level of dotty invadopodia when cells are plated on a flat gelatin substrate and at the level of linear invadopodia when cells are plated on a coat of fibrillar type I collagen, suggesting that cells use a similar mechanism when they breach the BM or migrate through a 3D collagen environment (Monteiro et al., 2013). Monteiro and collaborators therefore proposed a model, summarized in figure 12, in which WASH localized at the endosomes drives actin assembly and gives rises to the formation of tubular endosomes intermediates which are targeted to the plasma membrane thanks to the tethering action of the exocyst complex (Monteiro et al., 2013).

Finally another recent study has shown that cortactin at the level of MT1-MMP endosomes gets phosphorylated by atypical protein kinase C ι (aPKCι), a kinase implicated in the development of apico-basal polarity in mammalian epithelial cells (Rosse et al., 2014). This phosphorylation favors the binding of cortactin with dynamin-2, which is involved in membrane scission and was previously shown to be required for the formation and function of invadopodia (Baldassarre et al., 2003). The recruitment of dynamin-2 to MT1-MMP containing endosomes would then favour the scission of endosomes intermediates and their target to the surface. Indeed depletion of aPKCι

give rise to a phenotype of tubulation of endosomal membranes due to impaired fission, and reduce trafficking and exocytosis of MT1-MMP to the cell surface as well as matrix degradation (Rosse et al., 2014).

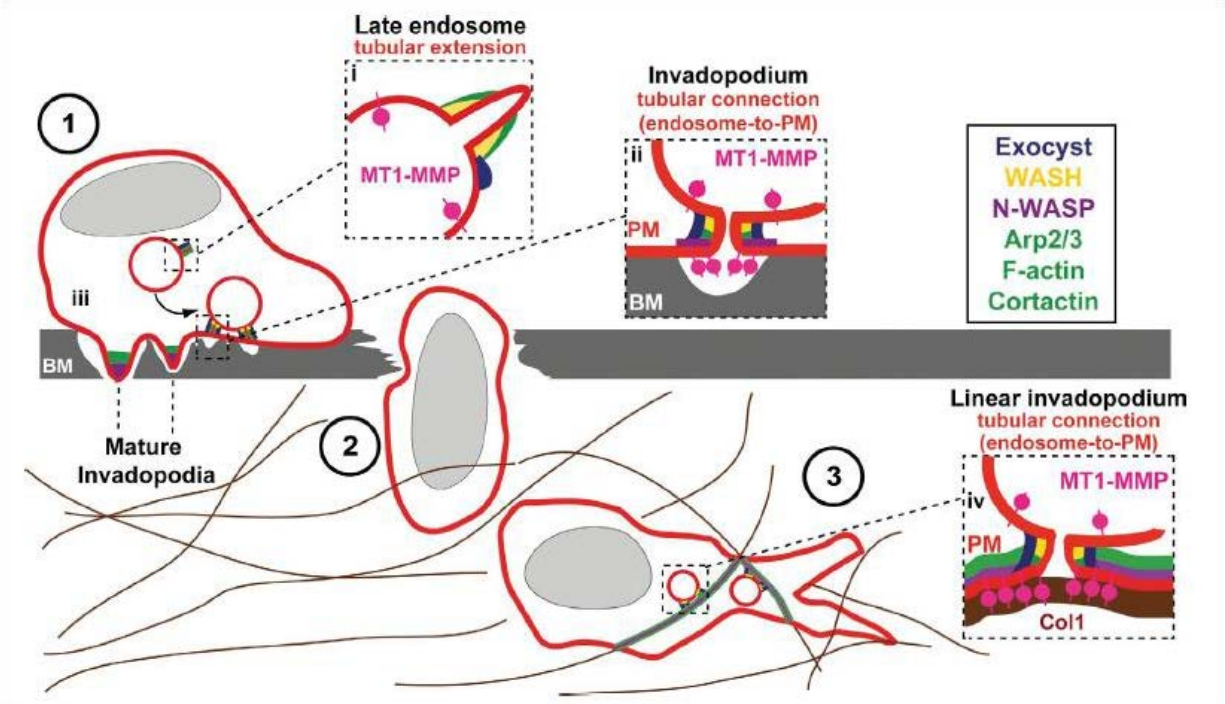

Figure 12: **Scheme summarizing the current view for exocytosis of MT1-MMP late endosomes at invadopodia in breast cancer cells**. (1-2) WASH activates the Arp2/3 complex and actin/cortactin assembly controls the dynamics of tubular endosomal membrane extensions (inset i) and which are then targeted to the plasma membrane where they allow the transfer and delivery of MT1-MMP from the endosome to the invadopodial plasma membrane (inset ii). The exocyst complex mediates tethering of MT1-MMP–positive late endosomes with the target membrane (ii). At invadopodia actin and cortactin assembly requires N-WASP that allows membrane protrusion formation and retention of MT1-MMP (insets ii and iii). (3) The same WASH- and exocyst- dependent mechanism is required for exocytosis of MT1-MMP in a fibrous, collagen 1-rich extracellular environment (inset iv). Picture from Monteiro et al., 2013.

1.6.3.3. Role of the microtubules transport in MT1-MMP exocytosis

Microtubules have been implicated in the latest stages of maturation of invadopodia (Schoumacher et al., 2010). Some lines of evidence indicate that the microtubules cytoskeleton could be implicated in the long-range intracellular transport of MT1-MMP and consequent delivery to invadopodial plasma membrane but the mechanism remains poorly understood.

In malignant human glioma U251 and breast carcinoma MCF7 cells and in non-malignant canine epithelial MDCK cells, MT1-MMP, once internalized, was shown to follow the microtubular cytoskeleton to reach recycling endosomes (Remacle et al., 2005), thus suggesting that MT1-MMP-positive transport vesicles could use microtubules for trafficking. Wiesner and colleagues showed that in primary human macrophages, MT1-MMP-positive vesicles move bidirectionally depending on (+)-end-directed kinesin family proteins and (-)-end-directed dynein (Wiesner et al., 2010). Moreover, kinesin-1 and kinesin-2 are required for delivery of MT1-MMP to the macrophage surface and for surface-localized activities of MT1-MMP such as shedding of the

matrix receptors CD44 and syndecan-1 and for ECM degradation at podosomes (Wiesner et al., 2010). These data showed that kinesin-mediated intracellular transport of MT1-MMP is a basal process that allows macrophages to dynamically modify their pericellular matrix environment (Wiesner et al., 2010). An ongoing study in our lab shows that kinesin1 and kinesin2 are also required for the transport of MT1-MMP-positive late endosomes to the surface of MDA-MB-231 breast cancer cells (Castro-Castro A. et al, unpublished data).

Another connection between MT1-MMP exocytosis and microtubules could be represented by IQGAP1 because of its known ability to capture microtubule plus-ends, via its association with plus-end-associated proteins such as CLIP-170 and APC (Fukata et al., 2002; Watanabe et al., 2004). The microtubules plus tips-associated proteins EB1, p150*Glued* and APC were also implicated in the establishment of endothelial cell apical-basal polarity vascular tube morphogenesis in 3D extracellular matrices that is a process that requires MT1-MMP (Kim et al., 2013), but no direct interaction was demonstrated. Therefore it will be important in the future to identify proteins involved in directional transport of MT1-MMP late endosomes along microtubules, as well as proteins that regulate the dynamics and anchoring of microtubules at the unvasive front of tumor cells.

1.6.3.4. Conclusions

The picture emerging from these last studies is that invadopodia are sites of coordination of local cytoskeleton assembly and MT1-MMP exocytosis. Several proteins from the actin cytoskeleton and the docking-fusion machinery have been identified as important for the exocytosis of MT1-MMP late endosomes to invadopodia. Microtubules-based endocytic transport could also be involved. With the attempt of identifying new cellular components and molecular pathways involved in MT1-MMP exocytosis that could provide future potential therapeutic targets, this study focused on the small GTP-binding protein ARF6. ARF6 is a implicated in the endocytic-recycling pathway and in actin cytoskeleton remodeling (D'Souza-Schorey and Chavrier, 2006) and is required for cancer cell invasion, in particular in breast cancer MDA-MB-231 cells where it localizes at invadopodia (Hashimoto et al., 2004; Morishige et al., 2008). Recent studies from my lab also implicated ARF6 in the microtubule-based transport of recycling endosomes (Montagnac et al., 2011; Montagnac et al., 2009). For all these reasons we hypothesized that ARF6 may regulate MT1-MMP trafficking at invadopodia.

Chapter 2: The ARF6 protein

2.2. Classification and discovery

ARF6 belongs to the family of the ADP-ribosylation factors (ARF) proteins, a subgroup of the Ras superfamily of small guanine triphosphate (GTP)-binding proteins. This superfamily comprises over 160 human members, with evolutionary conserved orthologues in *Drosophila*, *C.Elegans*, *S. Cerevisiae*, *S.pombe*, *Dictyostelium* and plants and that can be subdivided into five major families: Ras, Rho, Rab, Arf and Ran subfamilies according to difference in structures and functions. All Ras GTP-binding proteins share a common enzymatic mechanism, which consists in a binary molecular switch between an inactive GDP-bound state and active GTP-bound state. They exhibit high-affinity binding for GDP and GTP but possess low intrinsic GTP hydrolysis and GDP/GTP exchange activities. Therefore, to switch from one state to the other these proteins need assistance by two classes of proteins: guanine-nucleotide-exchange factors (GEFs), which catalyze GDP dissociation, and GTPase-activating proteins (GAPs) that catalyze GTP hydrolysis. The interplay between the GTP-binding proteins, their GEFs, GAPs and effectors regulate the functioning of a broad range of cell processes (Wennerberg et al., 2005).

The ARF subfamily comprises the most divergent members among the Ras proteins and are involved in vesicle trafficking and membrane remodeling. ARFs are already present in the protist *Giardia Lamblia* which lacks Ras and G protein α subunits (Murtagh et al., 1992), suggesting that they appear earlier in evolution than the other RAS.

Arfs were first purified from rabbit liver and bovine brain by Kahn and colleagues and identified as cofactors required for the cholera toxin-dependent ADP-ribosylation of the stimulatory regulatory component (G) of adenylate cyclase (Kahn and Gilman, 1984) hence their name, ADP-ribosylation factors (Arfs). Shortly after, they were shown to be GTP-binding proteins (Kahn and Gilman, 1986). The mammalian Arf family consists of six related gene products, Arf1-6, which are further divided into three subroups based on sequence homology. Class I includes Arf1, Arf2 and Arf3, class II Arf4 and Arf5, and class III Arf6. In human, ARF2 is a pseudogene. ARF6 in particular was identified by Tsuchiya and collaborators in 1991 by screening of a cDNA library using as a probe the cDNA of the bovine Arf2 (Tsuchiya et al., 1991).

Class I and II Arfs localize at the Golgi apparatus and endoplasmic reticulum, and primarily regulate vesicular trafficking between these two intracellular organelles (Volpicelli-Daley et al., 2005). ARF6, instead, predominantly localizes to the plasma membrane and endosomal compartments and plays important roles in endocytosis at the plasma membrane,

exocytosis, endosomal recycling, cytokinesis in coordination with actin cytoskeleton reorganization (D'Souza-Schorey and Chavrier, 2006).

2.2. ARF6 structure

ARF6 is a ~20 kDa monomeric protein. Like all the small G proteins, it contains a G domain responsible for nucleotide binding and hydrolysis that consists in six-stranded β sheets flanked by five α helices located on both sides (Menetrey et al., 2000). It contains also a N-terminal extension that folds in an amphipathic helix and which is instead unique to ARFs (Pasqualato et al., 2002). This N-terminal amphipathic helix together with the presence of a Glycine at position 2 in the N-terminus which is post-translationally modified by addition of a myrisystate fatty acid are critical for ARF6 binding and tethering to membranes (Franco et al., 1993) (Fig.13). The N-terminal helix is linked to the G-domain by a short flexible linker, which imposes ARF6 to be close to the membrane (Menetrey et al., 2000).

In the G domain, the segments of the polypeptide that are sensitive to the GDP/GTP cycle are called switch regions and correspond to the so-called switch-1 loop and switch-2, an helix. The γ phosphate of GTP interacts with switch-1 and -2 and stabilizes their conformation, allowing them to be the main binding sites for effectors. Differently from other GTP-binding proteins, ARF6 and the other ARFs contain two additional domains that are structurally sensitive to the GTP/GDP cycle: the β hairpin connecting the switch-1 and switch-2 regions or so-called interswitch region and the N-terminal helix (Menetrey et al., 2000; Pasqualato et al., 2001; Pasqualato et al., 2002).

In GDP-bound ARF6, the interswitch is retracted and forms a pocket to which the N-terminal helix binds serving as a molecular hasp to maintain the inactive conformation (Menetrey et al., 2000). The retracted interswitch positions a conserved aspartate (D) upstream of switch-2 to mimic the charges of γ- phosphate of GTP, thus preventing the binding of GTP. In the GTP-bound form, the interswitch undergoes a two-residue register shift that pulls switch-1 and switch-2 up, restoring the active conformation that can bind effectors, typical of the other GTP-binding proteins. In this conformation the interswitch projects out of the protein and obstructs the pocket where the myristoilated N-terminal helix binds, which is then free to associate with membranes through hydrophobic and lipidic interactions (Pasqualato et al., 2001) (Fig.13). This coupling of molecular switch with membrane binding was first described for ARF1. ARF1, indeed, is cytosolic in its GDP-bound state and, upon nucleotide exchange, it exposes its N-terminal myristoyl anchor and amphipathic helix and insert it into the membrane. Eventually ARF1 is released from membranes upon GTP hydrolysis (Goldberg, 1998). ARF6, despite showing the same structural framework of the dual membrane/nucleotide switch as ARF1 (Menetrey et al., 2000), remains essentially bound to membranes even in its inactive GDP-bound form, as

demonstrated by the fact that the localization to membranes is not affected in an ARF6 mutant locked in the GDP-form (D'Souza-Schorey et al., 1998).

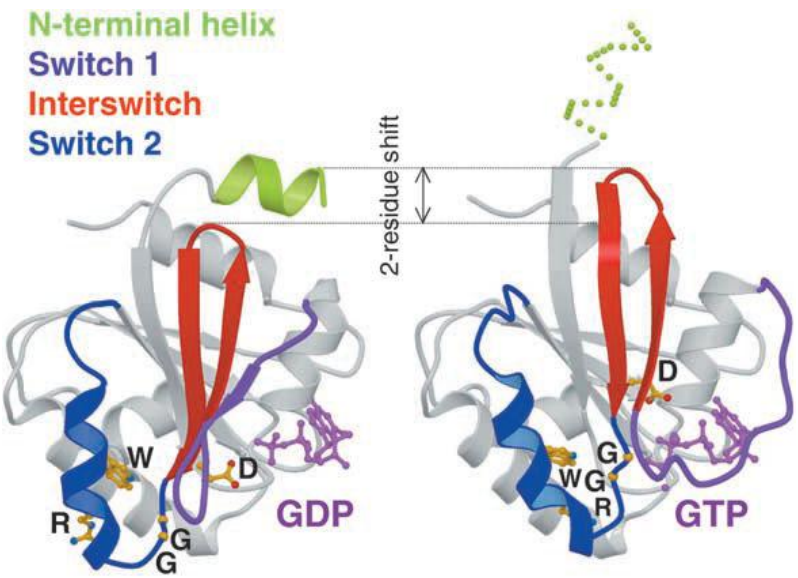

Figure 13: **The ARF6 GDP/GTP structural cycle.** The crystal structure of ARF6-GDP is shown on the left and of ARF6-GTPγS on the right. ARF6 in the GDP-bound form is retracted in an unusual retracted conformation with the interswitch region fastened by the N-terminal helix. In the GTP-bound form, the interswitch undergoes a two-residue register shift that pulls switch 1 and switch 2 up, projects out of the protein and obstructs the pocket where the myristoilated N-terminal helix binds, which is then free to associate with membranes. Residues with disordered electron density are indicated by a dashed line and are expected to interact with membranes in activated ARFs. The conserved residues W/GG/R/D of sequence signature typical of ARF family proteins are shown. In GDP-bound structure, tryptophan (W) fastens switch 2 and the interswitch in a conformation where the aspartate (D) and the glycine (G) are incompatible with GTP binding. In the GTP-bound form, the glycine pair, the tryptophan and the arginine (R) reorganize providing an interconnected network of hydrogen bonds necessary for GTP-binding and the stabilization of the active conformation. Picture from Pasqualato et al., 2002.

ARF6 mutants that affect its GDP/GTP cycle have been generated and used over the years to understand the functions of ARF6 in cells. The most commonly used have been the so called constitutively active and dominant negative mutants. The first, ARF6 Q67L (where a Glycine in position 67 is replaced by Leucine), is a mutant defective in GTP-hydrolysis and therefore is blocked in its active state, while the second, ARF6 T27N (where a Threonine in position 27 is replaced by an Asparagin), is defective in GTP binding and therefore is locked in its inactive state (D'Souza-Schorey et al., 1995; Peters et al., 1995). More recently another mutant called fast-cycling was generated. This mutant, ARF6 T157A or T157N (where the Threonine in position 157 is replaced by an Alanine or an Asparagine), is characterized by an increase rate of GTP association and GDP dissociation while still able to undergo normal GAP-mediated hydrolysis and therefore is more active than the wild-type ARF6 (Klein et al., 2006; Santy, 2002). This mutant is preferred to the dominant active and inactive ones since it was shown that the

completion of the GDP/GTP cycle is critical for many cellular functions of ARF6 (Klein et al., 2006).

2.3. ARF6 functions

ARF6 is ubiquitously expressed (Yang et al., 1998) and even though the subcellular distribution may vary from one cell type to the other, it generally localizes at the plasma membrane and endosomal compartments. In the last twenty years, indeed, ARF6 has been object of much interest since it was shown to be involved in several pathways from membrane trafficking to actin cytoskeleton remodeling and therefore implicated in many cell events, such us cell adhesion, cytokinesis, phagocytosis, cell migration and also tumor cell invasion (D'Souza-Schorey and Chavrier, 2006).
I will review some of the most important findings on ARF6 functions and implications in normal physiology and disease.

2.3.1. Role of ARF6 in lipid modifications

ARF6 has been implicated in the regulation of lipid modifying enzymes. First, it was shown that ARF6-GTP stimulates the activity of phospholipase D (PLD) *in vitro* to the same extent as ARF1 and ARF5 (Massenburg et al., 1994). PLD is responsible for the hydrolysis of phosphatidylcholine (PC) to produce phosphatidic acid (PA). Later on, Honda and colleagues identified ARF6 as an activator of phosphatidylinositol 4-Phospate 5-Kinase α [PI(4)P5Kα] (Honda et al., 1999). PIP5-kinases are responsible for generating phosphatidylinositol 4,5-bisphosphate [$PI(4,5)P_2$], by phosphorylating 4-phosphate [PI(4)P] [PI(4)P5Ks] at the D-5 position of the inositol ring. Although both ARF1 and ARF6 could stimulate the activity of PIP5-kinase *in vitro*, in cells it was ARF6 that co-localized with PIP 5-kinase to generate $PI(4,5)P_2$ and cause plasma membrane ruffling. They also showed that *in vitro,* PI(4)P5Kα needs a synergistic activation by ARF-GTP and PA, generated by PLD (Honda et al., 1999). These results therefore suggested that ARF6 by activating both PLD and PIP5-kinase contributes to increase $PI(4,5)P_2$ production.
These findings shed light on the cellular functions of ARF6 since $PI(4,5)P_2$ is a major plasma membrane phosphoinositide involved in membrane traffic and actin rearrangements. For instance $PI(4,5)P_2$ was shown to regulate local actin polymerization by binding to N-WASP and recruiting it at the plasma membrane (Miki et al., 1996). Moreover $PI(4,5)P_2$, contributes to N-WASP activation together with Cdc42 (Rohatgi et al., 2000) and to WAVE activation together with Rac1

(Chen et al., 2010). PI(4,5)P_2 has also been shown to regulate actin capping and the activities of several actin binding proteins (Hilpela et al., 2004).

Furthermore PI(4,5)P_2 has been also implicated in clathrin-mediated endocytosis by favouring the invaginations of CCPs (Rohde et al., 2002). The μ2 subunit of the AP-2 complex indeed binds to PI(4,5)P_2 which is thought to play a role in stabilizing the conformation of the complex, thus enabling cargo recognition by and facilitating the stable association of AP-2 with the membrane (Rohde et al., 2002). Therefore controlling PI(4,5)P_2 levels at the plasma membrane could represent one of the way through which ARF6 regulates membrane trafficking and actin remodeling.

2.3.2. Role of ARF6 in membrane trafficking

2.3.2.1. Regulation of endocytosis by ARF6

ARF6 has been shown to play a role in the post-endocytic internalization of several plasma membrane receptors and cargoes in both the clathrin dependent and –independent routes (see figure 11, chapter 1.6.1). However, whether ARF6 has a direct role on endocytosis remains still elusive.

2.3.2.1.1. Regulation of clathrin-dependent endocytosis by ARF6

One of the first hypotheses was that ARF6 may regulate the formation of clathrin-coated vesicles at the plasma membrane by recruiting adaptor and coat proteins, reminiscent of ARF1's function in recruiting different coat proteins on the Golgi apparatus (D'Souza-Schorey and Chavrier, 2006). This assumption was supported by the observation that PI(4,5)P_2 production is required for clathrin-coated vesicles formation in synaptic membranes in neurons and that ARF6 is able to stimulate PI(4,5)P_2 production by strongly activating PIP5K type Iγ (PIP5KI γ), the PIP5K isoform specific brain (Krauss et al., 2003). Paleotti and colleagues later showed that ARF6-GTP recruits the clathrin-adaptor protein complex AP2 (not AP1, the Golgi counterpart) both in a liposome-binding assay *in vitro* and by co-immunoprecipitation from cellular extracts (Paleotti et al., 2005). They could also show that expression of the GTP-locked mutant ARF6Q67L leads redistribution of AP-2 in ARF6-GTP-enriched areas of the plasma membrane and to the inhibition of transferrin receptor (TfnR) internalization, suggesting a direct role for ARF6 in controlling assembly of the AP-2/clathrin coat (Paleotti et al., 2005). This model, however, did not find confirmation in a study from our group where ARF6-GFP, although it was found in CCPs by total internal reflection (TIRF) microscopy and by electron microscopy, was neither required for CCPs assembly nor for TfR endocytosis (Montagnac et al., 2011). In addition, knocking-down the expression of ARF6 did not cause significant reduction of plasma membrane

association of clathrin or AP-2 into CCPs in HeLa cells, while, in contrast, AP-2 knockdown lead to a drastic reduction of plasma membrane accumulation of ARF6-GFP, including in few CCPs that persisted in AP-2-depleted cells. All together, these data rather suggested that AP-2 is necessary for ARF6 recruitment in CCPs (Montagnac et al., 2011). In addition, Montagnac *et al.* showed that ARF6 knockdown or expression of ARF6 T27N did not interfere with the initial rate of transferrin endocytosis or EGF uptake in HeLa cells, suggesting no role for ARF6 in clathrin-mediated endocytosis. The model that was proposed based on these data implied a function of ARF6 in post-endocytic trafficking of TfnR since they showed that ARF6-GTP, dormant in CCPs, becomes accessible after the recruitment of the clathrin uncoating component auxilin (Fig.14). Only then ARF6 is free to recruit its effectors, the JNK interactor proteins 3 and 4 (JIP3 and JIP4) that function as adaptor proteins for the microtubule motors (see chapter 3). ARF6 and JIPs interaction is then required for the post-endocytic recycling of the TfR endosomes back to the plasma membrane through the fast recycling pathway (Fig.14) (Montagnac et al., 2011).

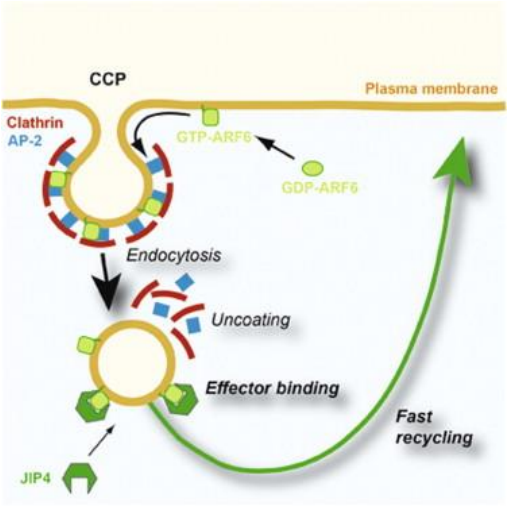

Figure 14: **The implication of ARF6 in post-endocytic trafficking.** The scheme shows how ARF6 resides in CCPs and becomes accessible for effectors only after the burst of auxillin in uncoated vesicles where it can bind to JIP3/JIP4 and regulate the recycling of TfnR cargoes back to the plasma membrane. Picture from Montagnac et al., 2011.

ARF6 is also implicated in clathrin-dependent internalization and desensitization of several G protein-coupled receptors (GPCRs) (Houndolo et al., 2005). GPCRs are seven transmembrane receptors that once activated by ligand binding lead to activation/phosphorylation of the heterotrimeric G protein that leads to a cascade of signaling event inside the cell. G proteins are composed of monomers of α, β, and γ subunits. The GTP bound form of the G protein α subunit and in some cases the free β-γ-subunits initiate cellular response by altering the activity of specific effector molecules. Most GPCRs are internalized from the cell surface following their activation to dampen the biological response, to recycle and resensitize the receptors, or to propagate signals through novel transduction pathways (Moore et al., 2007). Agonist-induced GPCR internalization is predominantly mediated by CCPs and is regulated by GPCR kinases (GRKs) and β-arrestins. The ligand-bound GPCR gets phosphorylated by GRK and β-arrestins binds to the phosphorylated receptors inducing receptor desensitization by preventing G protein

activation. Then, bound β-arrestin mediates GPCR internalization by directly binding to AP-2 complexes and clathrin recruitment. Indeed, it is well established that direct interaction of β-arrestins to ligand-activated, phosphorylated GPCRs leads to exposure of the carboxy-terminal domain of β-arrestin containing the AP-2 and clathrin-binding sites (Moore et al., 2007). ARF6 has been shown to play a role in the internalization of the luteinizing hormone/choriogonadotropin receptor (LH/CGR) in ovarian follicle cells since ARF6 activation by ARNO GEF promotes release of β-arrestin from the membrane, making it available for interaction with LH/CGR (Mukherjee et al., 2000). A similar mechanism was proposed for the internalization of the β2-adrenergic receptor (β2AR) where ARNO was shown to directly bind β-arrestin and to stimulate β2AR internalization when overexpressed (Claing et al., 2001). Upon agonist stimulation of the receptor, β-arrestin also interacts with ARF6-GDP, thereby facilitating ARNO-promoted activation of ARF6 (Claing et al., 2001). Defects in β2AR internalization have been observed following expression of the ARF6-GAP GIT1 presumably by stimulating GTP-hydrolysis on ARF6 (Premont et al., 1998). More recently, a new ARF6-dependent pathway was identified that couples the activation of β2AR with the inhibition of its recycling, contributing to receptor desensitization and down-modulation; β-arrestin was shown to bind directly to both ARF6 and its GEF EFA6 and ligand-induced stimulation of β2AR leads to colocalization with β-arrestin and EFA6 at the plasma membrane and subsequent activation of ARF6 by EFA6 in a β-arrestin-dependent manner (Macia et al., 2012). Overexpression of EFA6 or ARF6T157N does not affect the internalization rate of the receptor but leads to desensitization of β2AR by inhibiting its recycling through a Rab4-dependent pathway and by promoting its trafficking to late endosomes/lysosomes, suggesting that active ARF6 would favor ligand-bound β2AR degradation and desensitization. The agonist removal instead would stop the activation of ARF6 leading to the release from inhibition of Rab4-dependent fast recycling (Macia et al., 2012). It is however unclear how ARF6 regulates Rab4-dependent fast recycling for β2AR. One possibility could be by recruiting JIP3/4, another could be by regulating a Rab4 GAP.

The scheme in figure 15 summarizes the contribution of ARF6 in clathrin-dependent or independent (see next paragraph) endocytosis and trafficking of some of the most known receptors.

Figure 15: **The implication of ARF6 in clathrin-dependent and –independent endocytosis of membrane receptors.** (A) ARF6-GTP may participate in clathrin coat assembly, by directly interacting with AP-2 (Paleotti et al., 2005) and by increasing the $PI(4,5)P_2$ level at the plasma membrane (Krauss et al., 2003). Ligand-activated β2AR leads to β-arrestin–dependent internalization of the receptor and activation of ARF6 and active ARF6 inhibits the recycling of the ligand-bound β2AR and favors its degradation in the late endosomes/lysosomes The agonist removal instead stops activation of ARF6 leading to Rab4-dependent fast recycling of ligand-free β2AR (Macia et al., 2012). (B) ARF6 has also been implicated in the clathrin-independent endocytosis of receptors such as β1-integrin, MHC1 and CD59. Although the mechanism through which ARF6 induces membrane invagination is largely unclear, these receptors have been found in ARF6-positive endosomes that can subsequently either reach the early endosomes containing clathrin-dependent cargos or some Rab11-positive tubular endosomal compartments

for slow recycling. This step requires ARF6 inactivation since expression of ARF6Q67L or overexpression of ARF6 effector PIP5K leads to accumulation of these cargoes in PI(4,5)P_2-enriched vacuoles that do not proceed further (Brown et al., 2001; Nasvlasky N et al., 2004; 2003).

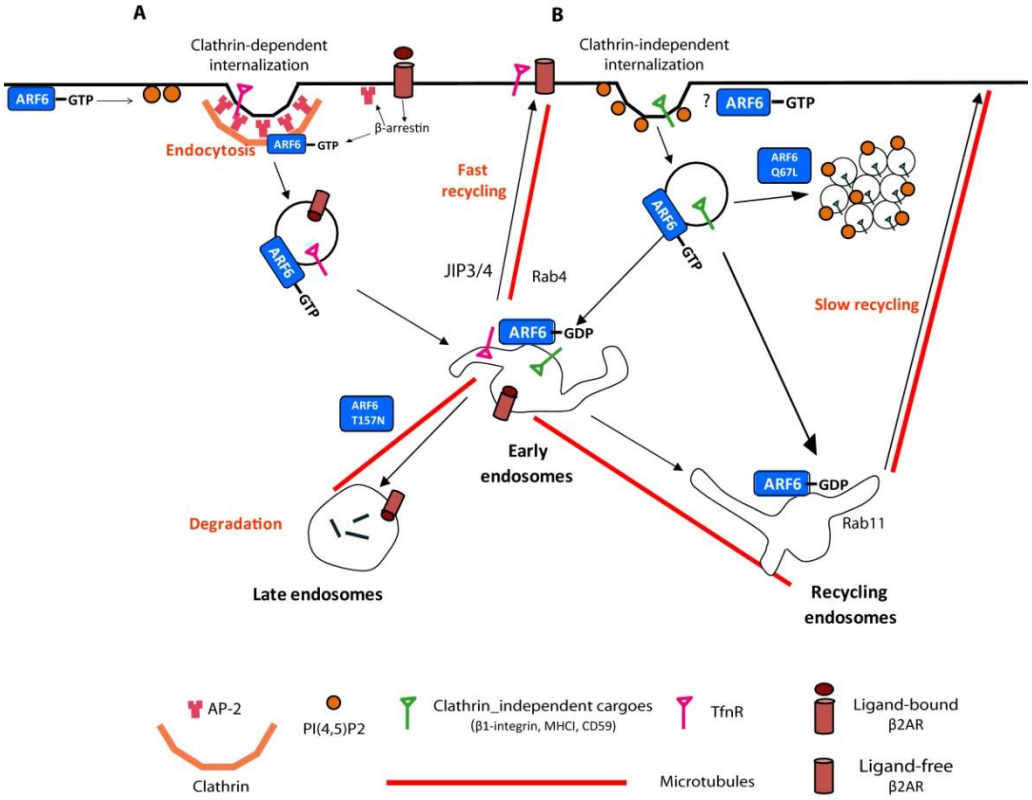

2.3.2.1.2. Regulation of clathrin-independent endocytosis by ARF6

A role for ARF6 in the internalization of cargoes through a unique clathrin-independent pathway has also been documented by several studies (Brown et al., 2001; Naslavsky et al., 2003; Naslavsky et al., 2004). As it has emerged during the last years, many cell surface transmembrane proteins lack cytoplasmic sequences for the recruitment and internalization into clathrin-coated vesicles and are therefore internalized by different clathrin-independent routes (Doherty and McMahon, 2009). ARF6 has been proposed as the main regulator of one of these pathways that is used by some specific membrane receptors that lack adaptor protein recognition sequences. Examples are the major histocompatibility complex class I protein (MHCI) (Naslavsky et al., 2003), β1-integrin (Brown et al., 2001; Powelka et al., 2004) and CD59, a protein anchored to the plasma membrane by a glycosylphosphatidyl inositol (GPI) moiety (Naslavsky et al., 2004).

This hypothesis came from the observation that expression of ARF6Q67L causes MHCI and CD59 to accumulate in enlarged PI(4,5)P_2-enriched vacuoles, which are segregated away from clathrin-dependent cargoes and from the degradative pathway (Naslavsky et al., 2003; Naslavsky et al., 2004), suggesting that this pathway requires ARF6 inactivation (GTP hydrolysis) shortly after internalization for cargoes to recycle back to the plasma membrane (Fig.15). Along the same

line, over-expression of the ARF6 effector PIP5K leads to accumulation of newly-internalized membranes that fuse in large vacuoles and further transport is blocked (Brown et al., 2001; Radhakrishna and Donaldson, 1997). It remains however completely unclear how ARF6 regulates this clathrin-independent internalization of membranes and cargoes. Neither adaptor proteins nor recognition sequences for ARF6 have been identified. One possibility could be that ARF6 functions as a membrane curvator regulator. ARF6-GTP is capable to generate positive membrane curvature through the insertion of the N-terminal amphipathic helix into the proximal lipid monolayer (Lundmark et al., 2008). Furthermore, ARF6 loads GTP in a curvature-sensitive manner (loading is stimulated by high positive curvature). These characteristics are positively reinforcing: exchange of GTP results in helix insertion, which, in addition to decreasing the off rates of these proteins from the membrane, results in greater membrane curvature and more GTP loading. Active ARF6 thus become clustered on membrane buds where they activate their effectors (Lundmark et al., 2008).

Independently on how ARF6 controls the internalization of these receptors, once internalized a fraction of these cargoes reaches some tubular recycling compartments positive for ARF6 and Rab11, while another fraction reaches the early endosomes containing clathrin-dependent cargos (Naslavsky et al., 2003) (Fig.15). Indeed in HeLa cells, CD59 and MHC1 have been shown to localize into clathrin-negative ARF6-positive endosomes at early-time of internalization and at later-time of internalization a fraction of these receptors co-localize with TfnR-containing early endosomes positive for Rab5 and EEA1, from where they can be either routed to the late endosomes or recycled back to the surface (Naslavsky et al., 2004).

2.3.2.2. Role of ARF6 in endocytic recycling to the plasma membrane

If the contribution of ARF6 in endocytosis remains elusive, it is generally well accepted that ARF6 plays important contributions in the endocytic recycling pathway of several cargoes to the plasma membrane, independently from their route of entry. A wide variety of cellular activities depends upon endocytic recycling like cell motility, cell division, cell polarity and tumor invasion. As a matter of fact, ARF6 has been implicated in all these processes (D'Souza-Schorey and Chavrier, 2006). I will now summarize the most important findings on ARF6-mediated endocytic recycling.

A requirement for ARF6 in endosomes recycling was first documented with over-expression studies that led to the discovery that the constitutively active mutant ARF6 Q67L was localized to the plasma membrane where it induced extensive membrane invaginations, decreased the rate of Tfn internalization and triggered a redistribution of Tfn receptors to the cell surface (D'Souza-Schorey et al., 1995; D'Souza-Schorey et al., 1998; Peters et al., 1995). In contrast, the dominant-inactive mutant ARF6 T27N is associated with a pericentriolar tubulovesicular compartment that contains TfnR and is morphologically reminiscent of the recycling endosomal compartments

(D'Souza-Schorey et al., 1995; D'Souza-Schorey et al., 1998; Peters et al., 1995). The conclusions of these early studies were that ARF6 activation could occur on these recycling endosomes and is required for the delivery of membranes and cargoes at the plasma membrane. The ability of ARF6 to cause actin remodeling at the plasma membrane and trigger protrusion formation and membrane ruffling was interpreted as the capacity of ARF6 to coordinate actin reorganization and polarized recycling of membranes at the cell surface [(D'Souza-Schorey et al., 1998; Radhakrishna and Donaldson, 1997) see also paragraph 2.3.5]. Along this line, M. Franco a former member of the lab, showed that overexpressed EFA6 that he identified as an ARF6-specific GEF, accumulated on the cytoplasmic side of the plasma membrane where it induced several invaginations. Consistently with earlier findings on cells expressing ARF6Q67L, EFA6 expression caused also reorganization of the actin cytoskeleton with the formation of membrane ruffles and affected the Tfn cycle by redistributing TfnR to the cell surface (Franco et al., 1999). These data suggested that recycling endosomes would be then incompetent for fusion with the plasma membrane until EFA6 activates ARF6 (Franco et al., 1999).

A possible mechanism through which ARF6 could regulate membrane recycling towards specialized regions of the plasma membrane could involve Sec10, a subunit of the exocyst complex found to interact with ARF6-GTP by yeast two-hybrid and pull-down assays (Prigent et al., 2003). Sec10 localizes to TfnR-containing recycling endosomes as observed by immunofluorescence and EM and expression of ARF6Q67L triggers its localization and of the exocyst complex to plasma membrane protrusions and invaginations that formed upon ARF6 activation. Moreover interfering with the exocyst complex activity partially inhibits Tf recycling and cell spreading, consistent with a role of the exocyst in the docking of recycling transport intermediates with the plasma membrane. Prigent and colleagues therefore suggested a model in which ARF6 activation at the plasma membrane is required for polarized membrane recycling and insertion through interaction of GTP-ARF6 with the vesicle-tethering exocyst complex (Prigent et al., 2003).

Evidences suggest that ARF6-regulated delivery and insertion of recycling endosomes at the cell surface requires PLD activity (Jovanovic et al., 2006; Padron et al., 2006). Silencing of PLD2 for instance inhibits the recycling of TfnR (Padron et al., 2006). Moreover inhibition of PLD with 1-butanol (that inhibits production of PA) or expression of an ARF6 mutant that cannot activate PLD (ARF6 N48I) inhibits recycling of membranes and MHCI cargo to the plasma membrane, resulting in an accumulation of tubular endosomal membranes (Jovanovic et al., 2006). ARF6 stimulation of PLD has also been implicated in dense core secretory granules exocytosis in neuroendocrine cells (Vitale et al., 2002) and for translocation of vesicles containing glucose transporter 4 (Glut4) to the plasma membrane (Huang et al., 2005). It is unclear how PLD regulates endosomal recycling and regulated exocytosis. It is not through the stimulation of PIP5K as it is shown by the abundant $PI(4,5)P_2$ on the tubular endosomes in cells treated with 1-

butanol (Jovanovic et al., 2006). Generation of PA in the membrane instead could lead to changes in membrane curvature that might facilitate vesicle fission or fusion (Huttner and Zimmerberg, 2001).

Interestingly ACAP1, a GAP for ARF6, was shown to play a role in cargo sorting by recognizing sorting signals in the cytoplasmic domain of TfnR for its endocytic recycling (Dai et al., 2004). ACAP1 also functions in the cargo sorting of recycling integrin (Li et al., 2005). Later it will be shown that ACAP1 is part of a novel clathrin coat complex that resides on the endosomes and is required for cargos sorting and recycling. This ACAP1-containing clathrin coat complex is regulated by ARF6 in two key physiological settings, stimulation-dependent recycling of integrin that is critical for cell migration and insulin-stimulated recycling of glucose transporter type 4 (Glut4), which is required for glucose homeostasis (Li et al., 2007).

Scheme in figure 16 summarizes ARF6 implication in endocytic recycling.

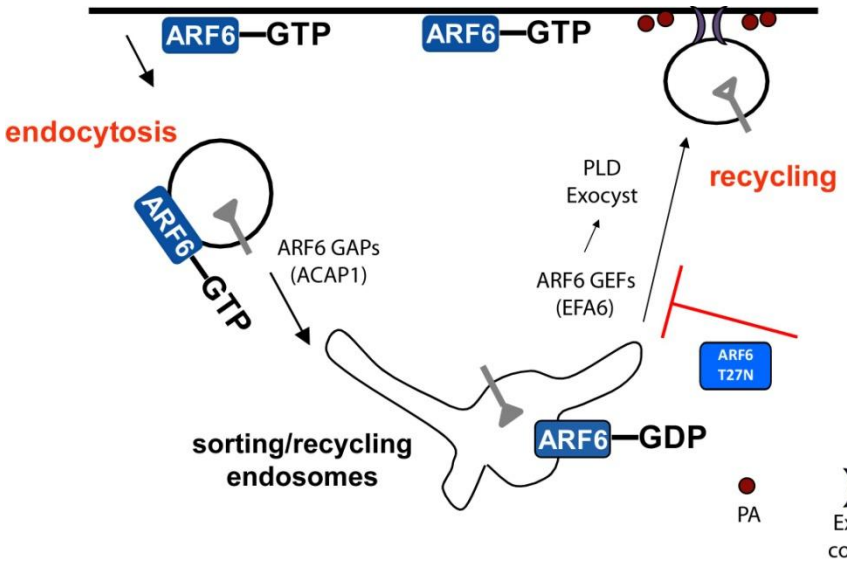

Figure 16: **Model for ARF6 recycling pathway**. Upon internalization from the plasma membrane from clathrin-dependent or –independent routes, ARF6-GTP undergoes GTP-hydrolysis probably through the action of GAPs such as ACAP1. The membranes fuse with the tubular-recycling endosomes which then return to the plasma membrane upon ARF6 activation through specific GEFs such as EFA6. The dominant inactive ARF6 T27N indeed blocks the return of ARF6 recycling endosomes to the plasma membrane. ARF6-dependent membrane recycling requires the activity of PLD and consequent PA generation and the action of the vesicle-tethering exocyst complex.

2.3.3. Cellular functions of ARF6

2.3.3.1. Regulation of cytokinesis by Arf6

In agreement with its role in providing focal and polarized membrane delivery at specific sites of the plasma membrane, ARF6 has been implicated in cytokinesis, the last step of cell mitosis (Dyer et al., 2007; Fielding et al., 2005; Montagnac et al., 2009; Schweitzer and D'Souza-

Schorey, 2002). During anaphase and telophase (early cytokinesis) in animal cells, the formation of an actomyosin-based contractile ring begins to divide the diving cell into two daughters and the plasma membrane ingresses in a region called the cleavage furrow between the two reforming nuclei. The cleavage furrow ingression results in the formation of a narrow cytoplasmic bridge connecting the two daughter cells throughout cytokinesis. This bridge is filled with anti-parallel microtubule bundles interdigitating in a central electron-dense matrix called the midbody, and is severed in a process termed abscission representing the terminal step of cell division (Montagnac et al., 2008). The microtubules bundles in the central spindle are thought to provide tracks for polarized transport of membranes towards the intercellular bridge (Montagnac et al., 2008) (Fig.17).

ARF6 appears to be important for targeting recycling endosomes to the cleavage furrow and to the midbody. Initially, the group of C. D'Souza-Schorey discovered that ARF6 was transiently activated during cytokinesis and localized first to the cleavage furrow and then to the midbody before separation of the two daughter cells (Fielding et al., 2005; Schweitzer and D'Souza-Schorey, 2002). The first strong evidence came from a study in *Drosophila* fly, where Arf6 is required during cytokinesis of spermatocytes (Dyer et al., 2007). Although Arf6 null (*Arf6-/-*) flies are viable with no morphological phentoype, males are due to defect in spermatogenesis (Dyer et al., 2007). In Arf6 null spermatocytes Arf6 ablation causes a regression of the cleavage furrow because of a failure in rapid membrane addition at the plasma membrane (Dyer et al., 2007). Arf6 is enriched in the recycling endosomes localized around the central mitotic spindle. Although Arf6 is not required for central spindle assembly or targeting of recycling endosomes to the central spindle, Arf6 is recruited there by interacting with the central spindle component Pavarotti, suggesting a mechanism in which Arf6 coordinates membrane recycling with the mitotic spindle and cleavage furrow ingression (Dyer et al., 2007).

The effect of ARF6 at the cleavage furrow may be explained by the interaction of ARF6 with the proteins FIP3 and FIP4 (also called Arfophilin-1 and 2) (Fielding et al., 2005)(Fig.16). FIP3 and FIP4 were initially known as Rab11 interacting proteins, which are also able to interact with ARF6-GTP and to form a ternary complex with ARF6 and Rab11 (the respective binding sites are different). Rab11 was previously shown to be implicated in mammalian cell cytokinesis and to be responsible for the recruitment of FIP3 to endosomes but not for its localization at the midbody (Wilson et al., 2005). ARF6 is responsible of the recruitment of FIP3 and FIP4 at the cleavage furrow since expression of ARF6T27N blocks the association of FIP3 and FIP4 at the cleavage furrow or the midbody (Fielding et al., 2005). FIP3 and FIP4 then are both capable to bind the Exo70 subunit of the exocyst complex, which also localizes at the furrow. These data suggested that recycling endosomes associated with Rab11/FIP3 and Rab11/FIP4 protein complexes traffic to the furrow and midbody in an ARF6-dependent way and in the midbody the interaction of FIP3/4-ARF6 may facilitate membrane tethering via the exocyst complex (Fig.17) (Fielding et al.,

2005). Furthermore, ARF6 appears to function as a switch to regulate the directionality of microtubule-based movement of endosomes in and out of the midbody area by controlling the dynein/dynactin and kinesin motors (Montagnac et al., 2009). ARF6 indeed binds to the JNK-interacting proteins 3 and 4 (JIP3 and JIP4), which in turn can bind both the subunit of the dynactin complex p150*Glued* and the light chain of kinesin1 (KLC). Both motors are responsible for the movements of Tfn-associated endosomes at the midbody since depetion of p150*Glued* and KLC affects endosome dynamics within the bridge and interferes with abscission. The observations that loss of ARF6 and JIP4 or perturbation of JIP4's interaction with ARF6 or KLC1 altered the dynamics and distribution of endosomes within the bridge and, similar to motors, reduced the efficacy of abscission, identified ARF6/JIP proteins as key regulators of kinesin-1/dynein-dependent movements of endosomes during cytokinesis (Montagnac et al., 2009). These data led to a model in which trafficking of endosomes towards the plus tip of microtubules involve a kinesin-1/JIP4-dependent mechanism that would assure ARF6 targeting to the bridge (Fig.17). Then upon ARF6 activation, movement out of the bridge would be allowed through a dynein-dynactin/JIP4 switch mechanism required for abscission (Fig.17). Scheme in figure 16 summarizes the implication of ARF6 in cytokinesis.

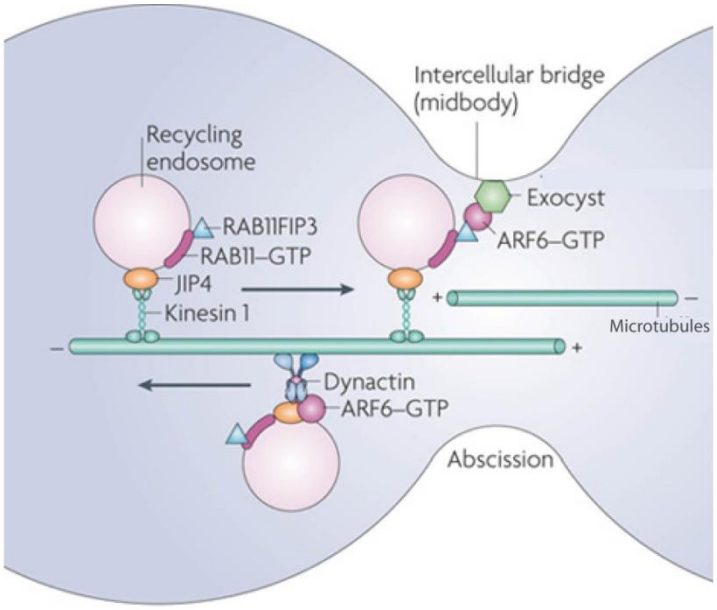

Figure 17: Model for ARF6 role in cytokinesis. During telophase, membrane is added to the cleavage furrow by recycling endosomes. RAB11/FIP3-positive recycling endosomes are recruited to the intercellular bridge. Transport to the bridge is mediated, at least in part, through the association of kinesin-1 with the recycling endosome adaptor JIP4. At the bridge, ARF6 is activated by specific GEFs and ARF6-GTP interacts with RAB11FIP3 and the exocyst promoting endosomes docking and fusion with the midbody. ARF6–GTP also interacts with JIP4, favoring dynactin binding to JIP4 and promoting exit of endosomes out of the intercellular bridge (Fielding et al., 2005; Montagnac et al., 2009). Picture adapted from the review (Grant and Donaldson, 2009).

2.3.3.2. ARF6-mediated control of cell-cell adhesion and cell polarity

ARF6 is an important regulator of cell-cell adhesions as it was shown to regulate the internalization and trafficking of E-cadherin (Palacios et al., 2001; Palacios et al., 2002; Palacios et al., 2005). E-cadherin is a major component of adherens junctions (AJs), the principal mediators of cell–cell adhesion in epithelial cells. AJs are markedly compromised during epithelial cell migration and their loss is therefore a hallmark of the epithelial-to-mesenchymal

transition (EMT) during cancer progression and tumor invasion. In polarized epithelial cells, E-cadherin is constitutively recycled between the basolateral plasma membrane and the early endosome system and ARF6 regulates E-cadherin turnover (Le et al., 1999). The lab of C. D'Souza-Schorey has demonstrated that ARF6 in epithelial Madin-Darby Canine Kidney (MDCK) cells is activated upon stimulation of hepatocyte growth factor (HGF) (Palacios et al., 2001). HGF and its receptor Met are potent regulators of EMT, cell scattering and invasion (Peschard and Park, 2007). Moreover, the expression of ARF6Q67L mutant causes a loss of AJs and the accumulation of E-cadherin in TfR-positive early endosomes (Palacios et al., 2001). In contrast, ARF6T27N stabilizes cell-cell adhesion and abolishes HGF-induced internalization of E-cadherin, thus avoiding EMT and stabilizing the epithelial phenotype (Palacios et al., 2001). The GTPase dynamin was shown to be downstream ARF6 in the endocytic mechanism of E-cadherin. In particular ARF6-GTP was shown to interact with Nm23-H1, a nucleoside diphosphate (NDP) kinase that was thought to provide GTP to dynamin (Palacios et al., 2002). Co-expression of an inhibitory mutant of Nm23-H1 together with the ARF6Q67L, inhibited ARF6-GTP-induced internalization of E-cadherin and the disassembly of AJs. Therefore, based on these data ARF6-dependent recruitment of Nm23-H1 may serve to facilitate clathrin-dependent uptake of E-cadherin at the basolateral membrane of polarized cells and thus may facilitate the disassembly of AJs (Palacios et al., 2002). Furthermore, activation of SRC by HGF promotes the targeting of internalized E-cadherin to lysosomes in an ARF6-dependent manner (Palacios et al., 2005). These studies therefore suggest that during EMT ARF6 is activated by HGF and together with SRC promotes E-cadherin internalization and degradation and consequent AJs dissolution.

Another way through which ARF6 could regulate EMT is by regulating the recycling of the HGF receptor c-Met (Parachoniak et al., 2011). Indeed, once ligand (HGF)-bound c-Met is internalized, the cargo adaptor protein Golgi-localized gamma ear-containing Arf-binding protein 3 (GGA3) interacts selectively with the activated c-Met in early-recycling endosomes and promotes access of c-Met into a recycling pathway while decreasing entry of c-Met into the degradative pathway (Parachoniak et al., 2011). It does so likely by mediating assembly of gyrating clathrin, a highly dynamic clathrin structure involved in rapid receptor recycling (Zhao and Keen, 2008). GGA3-dependent entry of c-Met into the recycling pathway promotes sustained ERK1/2 activation and relocalization of c-Met toward the leading edge to initiate localized signaling required for cell migration (Parachoniak et al., 2011). GGA3 is recruited to active-Met-positive endosomal membranes by the combined action of ARF6 and the adaptor protein of the RTKs Crk, both of which are necessary for GGA3-dependent c-Met recycling (Fig.18) (Parachoniak et al., 2011).

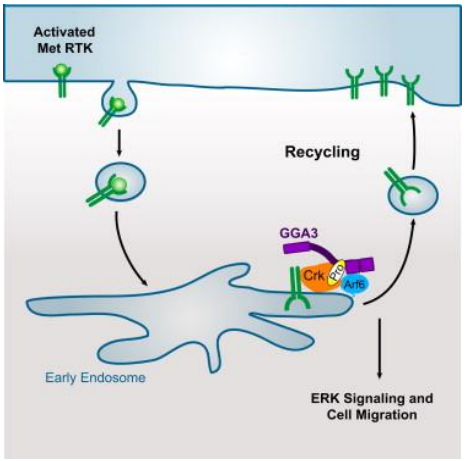

Figure 18: Scheme for ARF6 role in c-Met/HGF receptor recycling. Picture from Parachoniak et al., 2011.

In agreement with this role of Arf6 in HGF/c-Met signaling and trafficking, an *in vivo* study on a mouse model showed that Arf6 knock-out mice die at mid-gestation or shortly after birth and exhibit impaired liver development characterized by reduced size and aberrant structure, due to defective hepatic cord formation (Suzuki et al., 2006). *Arf6*-/- fetal hepatocytes cultured *in vitro* in collagen gel matrix exhibit defective hepatic cord-like structure formation in response to HGF stimulation (Suzuki et al., 2006).

ARF6 activity was also shown to be tightly regulated during AJ formation and epithelial polarization by the Par-3/Par-6/aPKC/Cdc42 complex, a multi-protein complex that has a key role in epithelial cell polarity and regulates the conversion of primordial AJs into mature belt-like AJs. Par-3 recruits a scaffolding protein, named FRMD4A (FERM domain containing 4A) that connects Par-3 and the ARF6-GEF ARNO (Ikenouchi and Umeda, 2010). Moreover ARF6 was shown to be required for the recruitment of the polarity complex Par-6/aPKC and Cdc42 and its GEF βPIX at the leading edge of migrating astrocytes (Osmani et al., 2010).

In conclusion all these data suggest that ARF6 by mediating the internalization of E-cadherin and recycling of HGFR and polarity proteins, strongly impacts cell-cell adhesion and cell polarity and possibly contribute to EMT. In agreement with this the effects of ARF6 on the internalization-recycling of E-cadherin and surface receptors have been shown to impact epithelial glandular organization (Tushir et al., 2010). Certain epithelial cells indeed form cysts and tubules and adopt tissue-like conformations when grown in 3D extracellular matrix (Matrigel) and represent a useful tool to study epithelial morphogenesis. In particular MDCK cells self-organize to form cysts when grown in collagen or matrigel, and these cysts develop tubules when exposed to mesenchymal growth factors such as HGF. In 3D cell cultures of MDCK cells, ARF6 is activated at early stages of tubule development and its nucleotide cycling is required for tubule initiation upon HGF stimulation (Tushir et al., 2010). On the other hand, sustained ARF6 activation, induces the formation of cell-filled glandular structures with multiple lumens and disassembled cadherin AJs (Tushir et al., 2010). Moreover HGFR internalization into signaling endosomes follows these aberrant alterations (Tushir et al., 2010). Similarly, in mammary epithelial cells acini, stimulation

with colony-stimulating factor-1 (CSF-1) induces endogenous ARF6 activation and formation of hyperproliferative and disorganized mammary acini coupled, phenotype that is reversed by ARF6 inhibition (Tushir et al., 2010).

2.3.3.3. Regulation of cell-matrix adhesion by ARF6

ARF6 has also been implicated in the regulation of cell-matrix adhesion by controlling the endocytic recycling of the ECM receptors β1-integrin and syndecans (Allaire et al., 2013; Dunphy et al., 2006; Powelka et al., 2004; Zimmermann et al., 2005).

Integrins are the major cell surface adhesion receptors for ligands in the ECM. They are heterodimeric proteins consisting of an α- and a β-chain and are involved in the transmission and interpretation of signals from the extracellular environment into various signaling cascades (Hynes, 2002). The endocytic recycling of integrins is supposed to play a crucial role during cell migration as well as the invasive migration of tumor cells since exocytosis of integrins at the leading edge may assist cell locomotion by providing fresh (unliganded) adhesion receptors, while integrins are internalized by endocytosis at the retracting trail of the cell (Caswell et al., 2009). As mentioned above, β1-integrin has been reported to accumulate in $PI(4,5)P_2$-positive vacuoles induced by constitutive ARF6 activation (Brown et al., 2001). In addition, it was later shown that internalized β1-integrin accumulates in recycling endosomes positive for ARF6 and Rab11 and that upon growth factor stimulation, β1-integrin exits these compartments and recycle back to the plasma membrane to promote cell migration (Powelka et al., 2004). ARF6, Rab11 and actin mediate this recycling since dominant inactive mutants of ARF6 and Rab11 or treatment with Cytochalasin D abrogate the ability of the cell to recycle β1-integrin to the plasma membrane and inhibit cell migration (Powelka et al., 2004).

Internalization of β1 integrins is mediated, at least in part, by the ARF6-GEF BRAG2/GEP100, through ARF6 activation at the plasma membrane (Dunphy et al., 2006). Silencing of endogenous BRAG2 leads to accumulation of β1 integrin at the cell surface, and increased binding fibronectin and cell spreading (Dunphy et al., 2006). Recycling of β1 integrin, instead, seems to be mediated by the ARF6-GAP, ACAP1 (Li et al., 2005). Li and co-workers showed that serum stimulation-induced phosphorylation of ACAP1 at Serine S554 by Akt, regulates ACAP1-β1-integrin interactions in endosomes (Li et al., 2005). SiRNA-mediated silencing of either ACAP1 or Akt impaired this interaction and inhibited integrin recycling (Li et al., 2005). These data are thus relevant to earlier findings showing that serum-induced recycling of β1 integrin involves ARF6 and Rab11 (Powelka et al., 2004).

More recently, it was also shown that β1 integrin internalization and traffic differ according to its active (ligand-bound) or inactive (ligand-free) conformations. In cancer-derived cell lines, inactive and active β1-integrins are internalized through the same endocytic route but while active β1-integrin traffics with slower kinetics to Rab7 endosomes, ligand-free adhesion receptors may

be diverted from this degradative pathway to a Rab4-dependent fast recycling pathway for recycling to the surface. ARF6 seems to control the recycling of inactive β1 integrins since they associate with a population of ARF6-positive endosomes and are then recycled back to ARF6-positive protrusions of the plasma membrane (Arjonen et al., 2012).

Even though ARF6 has been implicated in integrins recycling, the mechanism through which this is accomplished is still largely elusive. In MDA-MB-231 breast cancer cell line, β1 integrin recycling at invadopodia could be accomplished by a mechanism involving an ARF6 GAP AMAP1. ARF6 is activated in breast cancer cell upon EGF stimulation and recruits AMAP1 (see paragraph 2.4.1.) which binds to protein kinase D2 (PRKD2) and makes a complex with the cytoplasmic tail of β1 subunit, thus suggesting a mechanism where ARF6, activated upon EGFR signaling, recruits β1 integrins associated with AMAP1 via PRKD2 to the plasma membrane (Onodera et al., 2012).

Finally a recent study has unveiled how ARF6-dependent recycling of integrins and cadherins is also tightly regulated by Rab35 (Allaire et al., 2013). ARF6 was previously shown to inactivate Rab35 by binding several Rab35-GAPs: TBC1D10A, TBC1D10B and TBC1D24/Skywalker (Chesneau et al., 2012). Reciprocally, Rab35 may inactivate ARF6 by binding to the ARF6-GAP ACAP2 and by recruiting ACAP2 to ARF6-positive endosomes (Kobayashi and Fukuda, 2012). Allaire and colleagues have shown that Rab35 activity is essential to maintain E-cadherins at the cell surface to promote cell–cell adhesion, suggesting that the antagonistic effect of active ARF6 on E-cadherin recycling is mediated through inhibition of Rab35 (Allaire et al., 2013). Furthermore Rab35 negatively regulates integrin recycling and cell migration through its inhibition of ARF6, which requires endosomal ACAP2 recruitment by active Rab35 (Allaire et al., 2013). Consistently, Rab35 knockdown leads to enhanced ARF6 activity, recycling of integrins and EGFR, which are known to co-traffic with integrins (Muller et al., 2009) and increased cell migration (Allaire et al., 2013). Importantly, Rab35 mRNA expression is suppressed in high-grade gliomas, and in breast and squamous cancers, suggesting that ARF6 is active in those tumors (Allaire et al., 2013). Therefore the functional interplay between Rab35 and ARF6 in the recycling of integrins and cadherins is aimed at tuning cell adhesive behaviour towards cell migration or intercellular contact and at efficiently coordinating the two processes.

Interestingly ARF6 has also been implicated in the recycling of other adhesion receptors like syndecans. Syndecans are transmembrane heparan-sulfate proteoglycans that function as co-receptors attracting and concentrating various growth factors and adhesion molecules at the surface and facilitating their interaction with their specific receptors (Morgan et al., 2007). Through their cytoplasmic tails, syndecans recruit a variety of signaling and cytoskeleton proteins, including the PDZ-protein syntenin, which binds $PI(4,5)P_2$ through its PDZ domain (Zimmermann et al., 2002). Zimmermann and colleagues reported that in MCF-7 breast tumour cells, internalized syndecans interact with syntenin in ARF6-positive recycling endosomes and

recycling of syndecans/syntenin depends on the ability of syntenin to interact with PI(4,5)P_2 (Zimmermann et al., 2005). The production of PI(4,5)P_2 on these endosomes requires ARF6 activation through the recruitment of PIP5K. Expression of Arf6T27N, dominant-negative PIP5K or a syntenin mutant form defective for PI(4,5)P_2-binding all caused syndecan/syntenin co-accumulation in recycling endosomes, which ultimately results in the engorgement of the perinuclear recycling compartment. The consequent reduction in syndecans cell surface availability and activity results in an inhibition of cell spreading and other syndecans-dependent processes like FGF-receptor signaling (Zimmermann et al., 2005). Moreover, a recent study has shown that syndecan-4 regulates ARF6 activity in order to control recycling and engagement of different integrin heterodimers ($\alpha_5\beta_1$ or $\alpha_V\beta_3$) in a spatially and temporally restricted manner and to allow precise coordination of focal adhesion dynamics and cell migration (Fig.19) (Morgan et al., 2013). Indeed in migrating fibroblasts, SRC phosphorylates syndecan-4 and promotes syntenin binding, and this interaction suppresses ARF6 activity in a mechanism that is not clarified yet. In turn, ARF6 inactivation promotes the recycling of $\alpha_V\beta_3$ integrins at the surface, an integrin type that promotes reinforcement and stabilization of focal adhesions (Fig.19). On the other hand, abrogation of syndecan phosphorylation promotes recycling of $\alpha_5\beta_1$ integrins, which in turn increase focal adhesions turnover (Fig.19) (Morgan et al., 2013).This study then suggests that ARF6 activation or inactivation by syndecan-4/SRC acts as a molecular switch to determine whether $\alpha_5\beta_1$ or $\alpha_V\beta_3$ integrins are delivered to the membrane in order to dictate focal adhesions stability and to efficiently coordinate cell migration.

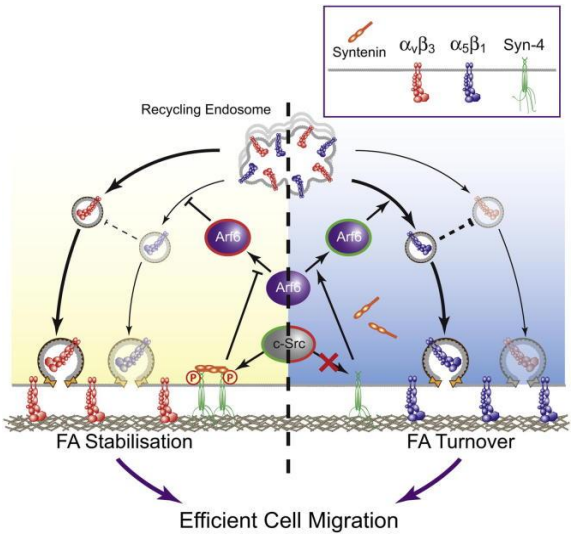

Figure 19: Model for Syndecan-4/SRC-dependent ARF6 regulation of integrin recycling. Picture from Morgan et al., 2013.

Another study had previously shown an ARF6 activation following ECM engagement (Balasubramanian et al., 2007). Fibronectin adhesion indeed triggers ARF6-dependent recycling of lipid rafts at the surface. Lipid rafts are plasma membrane microdomains enriched mainly in cholesterol, sphingolipids and GPI-linked proteins. They are small, dynamic structures that can

modulate many signalling pathways in diverse biological processes such as cell division, apoptosis, adhesion and chemotaxis and are anchoring points for Rho GTP-binding proteins such as Rac1. Balasubramanian and colleagues showed that upon detachment of cells from the substratum lipid rafts are removed from the plasma membrane through caveolar endocytosis. Endocytosed rafts traffic to recycling endosomes positive for Rab11 and ARF6 in a microtubule-dependent manner. Re-adhesion to fibronectin triggers rapid recycling of these membranes out of the recycling endosome by an ARF6-dependent pathway, also along microtubules. Moreover blocking the return of rafts to the plasma membrane by inhibiting ARF6 function or microtubule assembly inhibited the membrane targeting and activation of Rac1, and concomitantly impaired cell spreading (Balasubramanian et al., 2007).

In agreement with this last study, in HeLa cells ARF6 has been implicated in the recycling of Rac1 itself towards confined regions of the plasma membrane where circular dorsal ruffles (CDRs) form (Palamidessi et al., 2008). CDRs are highly dynamic actin-based structures that form in response of RTKs stimulation and are thought to have a role in fastly disassembling and remodeling actin prior lamellipodium formation and therefore in directed cell motility (Buccione et al., 2004). Palamidessi *et al.* showed that in response to growth factors stimulation of RTKs, such as HGF stimulation of the MET receptor, clathrin-mediated endocytosis and RAB5 activation promote the internalization of Rac1 and its GEF, TIAM1, into early endosomes. Here, activated GTP-bound Rac1 is subsequently recycled through the ARF6 endosomal pathway to regions of the plasma membrane where subsequently CDRs form, a step that occurs prior lamellipodium formation. Indeed ARF6 silencing or dominant negative mutant lead to abolishment of HGF-dependent CDRs formation and Rac1 translocation from endosomes to the plasma membrane (Palamidessi et al., 2008). In this way ARF6 assures localized Rac1 signaling and formation of migratory protrusions that promote a mesenchymal mode of cell motility.

All these studies together suggest that, ARF6, by controlling recycling of integrins, lipid rafts and Rac1 back to the surface, seems to play a critical role for coordinating directed cell migration and cell adhesion.

2.3.4. Role of ARF6 in late endosomal compartments

As said above, a role for ARF6 was shown in certain conditions for sorting surface proteins such as E-cadherin (Palacios et al., 2005) or β2AR (Macia et al., 2012) (Fig.15) to the late endosomal compartments for degradation, but no clear mechanism has been so far identified. Moreover there was no evidence in literature that reported a role for ARF6 in late endocytic events, before a very recent study that implicates ARF6 in exosomes biogenesis and budding into MVBs (Ghossoub et al., 2014). MVBs are late endocytic compartments which are characterized

by the presence of intraluminal vesicles (ILVs) that are generated by inward invagination of the limiting membrane of the endosomes. The vesiculation increases upon growth factor receptors signaling as a way to inactivate the receptors by depriving them from contact with the cytosol. MVBs can either fuse with lysosomes, where endocytosed cargoes are degraded, or they can fuse with the plasma membrane and induce the secretion of ILVs in the extracellular environment that are then called exosomes (Piper and Katzmann, 2007). The syndecan cytoplasmic adaptor syntenin was previously shown to be enriched in exosomes, to stimulate exosomes production and to be required for inward budding of ILVs associated with the tetraspanin CD63, an ILV and exosome marker (Baietti et al., 2012). A recent study (Ghossoub et al., 2014) identified ARF6 as a regulator of the production of syntenin-positive exosomes. Indeed, ARF6 inhibition leads to a significant decrease in exosomal proteins markers and exosome secretion, while expression of fast-cycling ARF6-T157N mutant increases syntenin-positive exosomal secretion, indicating that the full ARF6 GDP/GTP cycle is required for stimulating exosome production through the syntenin-dependent mechanism. Electron microscopy experiments show that ARF6 is necessary for CD63 intraluminal budding into MVBs since loss of ARF6 affects MVBs morphology whose lumen resulted largely empty, suggesting that ARF6 is not implicated in the delivery of cargo to late endosomes but rather in ILV biogenesis. ARF6 effector PLD2 was also implicated in ILV budding and syntenin-positive exosome biogenesis. ARF6 and PLD might favor endosomal intraluminal budding through the production of PA, that is generated in the inner leaflet of membranes and is likely to induce negative membrane curvature that could facilitate inward budding (Ghossoub et al., 2014). Interestingly, ARF6 controls sorting of EGFR in the late endocytic pathway as ARF6 depletion results in increased levels of EGFR and a lack of EGFR degradation upon EGF stimulation (Ghossoub et al., 2014). Thus, ARF6 may also have an impact on the formation of degradative late endosomes (MVBs destined for fusion with lysosomes).
Despite the large literature on ARF6, this study is the first to report a role for ARF6 in late endocytic events and exocytosis from MVBs/late endosomes.

2.3.5. Role of ARF6 in actin cytoskeleton remodeling

In concomitance with its role in membrane trafficking, ARF6 has been implicated in actin remodeling at the cell periphery and is involved in the formation of F-actin-driven structures and cell motility. How ARF6 achieves this function was so far difficult to recapitulate because probably it involves several distinct ARF6 activities. One of the mechanism by which ARF6 drives actin assembly is through the regulation of lipid metabolism, in particular through the production of $PI(4,5)P_2$. As a matter of fact, $PI(4,5)P_2$, contributes to N-WASP activation together with Cdc42 (Rohatgi et al., 2000) and to WAVE activation together with Rac1 (Chen et al., 2010).

Another way through which ARF6 modulates actin remodeling is by regulating upstream the Rho GTPase Rac1 and some of Rac1 effectors. Rac1 is a small G-protein of the Rho subgroup widely implicated in normal physiology and disease. It plays an important role in cytoskeleton rearrangements and it is a key regulator of cell proliferation, adhesion, migration and malignant transformation (Ridley, 2006; Wertheimer et al., 2012). Rac1 is activated by RTKs, GPCRs, integrins and stress and one of its main function is to promote actin polymerization during lamellipodia extension by activating the Arp2/3 activator WAVE and by increasing the availability of actin monomers for incorporation into actin filaments by regulating cofilin, an actin- depolymerization factor (Heasman and Ridley, 2008).

2.3.5.1. Regulation of Rac1 activity

The first observations that ARF6 had a role in actin cytoskeleton remodeling derive from the finding that at the plasma membrane of HeLa cells, accumulation of ARF6-GTP resulted in the formation of actin protrusions and membrane ruffles (Radhakrishna et al., 1996). These surface protrusions could be induced in transiently transfected HeLa cells expressing wild-type ARF6 by treatment with the G-protein activator aluminum fluoride (AlF). Similar protrusions were observed in cells expressing ARF6Q67L (Radhakrishna et al., 1996). Later on it was shown that Rac1 colocalized with ARF6 in a perinuclear recycling compartment in HeLa cells and that AlF treatment shifted the distribution of vesicle-associated ARF6 and Rac1 to the plasma membrane (Radhakrishna et al., 1999), suggesting a relationship between the two GTPases. Moreover ARF6-mediated surface actin protrusions are regulated by POR1, a Rac1-interacting protein that plays a role in Rac1-induced membrane ruffling. ARF6 in its GTP-bound state interacts with POR1 and deletion mutants of POR1 block ARF6-mediated cytoskeletal rearrangements (D'Souza-Schorey et al., 1997).

ARF6 was also associated with the formation of lamellipodia. Indeed, in MDCK epithelial cells, expression of the ARFGEF ARNO lead to cell morphological changes and a switch from an epithelial phenotype to a more scattered one together with increased lamellipodia formation and migratory activity. ARNO expression also resulted in activation of endogenous Rac1 that was activity required for acquisition of the migratory phenotype. This phenotypic transition, resembling EMT also required activation of the ARF6 effector PLD (Santy and Casanova, 2001). Later on it was shown that ARNO-mediated activation of Rac1 was dependent on the bipartite Rac1-GEF Dock180/Elmo complex. Both Dock180 and Elmo colocalize with ARNO at the lamellipodia induced by ARNO expression and expression of inactive mutants of both Dock180 and Elmo inhibited ARNO-induced Rac1 activation and MDCK cells motility (Santy et al., 2005), suggesting that ARNO and Dock180/Elmo can coordinate a localized activation of ARF6 and Rac1 at the leading edge of migrating MDCK cells. These data together with the observation that expression of ARF6Q67L or a constitutively active mutant of Rac1 induced formation of

membrane rufflings and protrusions but did not enhance motility, suggested that generalized activation of the two GTPases was inefficient for migration and ARF6 and Rac1 needed to be locally activated at the leading edge of the cells for efficient migration. Another study showed that ARF6 and consequently Rac1 activity was down-modulated at the rear and trailing edge of migrating cells (Nishiya et al., 2005). In particular paxillin binds selectively to the non-phosphorylated α4 chain of α4β1 integrin, which, differently from the phosphorylated form, locates only distally to the leading edge. In turn, paxillin binds the ARF-GAPs GIT1 and GIT2/Pkl whose presence leads to locally reduced levels of active ARF6, (and consequently Rac1) along the sides and trailing edge of these cells (Nishiya et al., 2005).

Another possible way through which ARF6 could regulate Rac1 activation is by binding and recruiting at the plasma membrane the Rac1 GEF Kalirin5. It was shown by co-immunoprecipitation that ARF6-GDP can bind to the spectrin repeat region of Kalirin5, as well as of other Kalirin family GEFs, such as Trio. The subsequent activation of ARF6 then allows Kalirin5 to activate Rac1 (Koo et al., 2007). Consistent with this, co-expression of wild type ARF6 increases the plasma membrane localization of Kalirin5, the steady state level of Rac1-GTP and the ability of Kalirin5 to induce membrane ruffling. ARF6T27N, however, being trapped in the GDP-bound state, recruits Kalirin5 to endosomal membranes but fails to allow activation of Rac1 through Kalirin (Koo et al., 2007), suggesting a new mechanism for the ARF6 GDP/GTP cycle to regulate Rac1 activity.

ARF6-dependent activation of Rac1 was also shown to play an important role in epithelial tubule development (Tushir and D'Souza-Schorey, 2007). As said above (paragraph 2.3.3.2), in 3D cell cultures of epithelial MDCK cells, ARF6 is activated at early stages of tubule development and its nucleotide cycling is required for tubule initiation upon HGF stimulation (Tushir et al., 2010; Tushir and D'Souza-Schorey, 2007). Indeed, expression of ARF6Q67L increases the number of immature HGF-induced tubule extensions, while expression of ARF6T27N completely blocks tubule extension in response to HGF. Moreover, ARF6 is responsible for the recruitment of Rac1 at the basolateral membrane of the cyst forming cells, since ARF6T27N-expressing cells showed a mislocation of Rac1 at the cytoplasm or apical membrane of epithelial cysts. In contrast, the increased levels of Rac1 at the cell surface observed upon expression of ARF6Q67L explain the hypertubulation phenotype (Tushir and D'Souza-Schorey, 2007). In addition, Rac1 activation during tubule initiation is dependent on ARF6-induced ERK activation. If it is not clear how ARF6 increases ERK phosphorylation levels, it is clear that ERK signalling controls Rac1 activation through the expression of urokinse-type plasminogen activator receptor (uPAR). The expression of this surface receptor indeed is regulated by the Ras/ERK pathway via the AP1 transcription factor and uPAR activates the DOCK180/Elmo/P130Cas complex, which mediates Rac1-GTP activation (Tushir and D'Souza-Schorey, 2007).

In conclusion, although Rac1 has been described as a downstream target of ARF6, the ARF6-dependent Rac1 regulation seems to be complex and varies depending on cell types.

2.3.5.2. Regulation of the SCAR/WAVE complex

More recently it has been shown that ARF6 regulates actin polymerization by activating the WAVE regulatory complex (WRC) (Humphreys et al., 2012; Humphreys et al., 2013). WRC is a heteropentameric complex (composed of WAVE, Abi, Cyfip, Nap1, and HSPC300 or their homologs), which associates to PI(4,5)P_2-enriched membranes and induces actin assembly by activating the ubiquitous Arp2/3 complex. Previous studies had shown that Rac1 is the main activator of the WAVE complex since purified Rac1 can bind and activate recombinant WRC in vitro and the crystal structure of the WRC identified a potential binding site for Rac1 in Cyfip (Chen et al., 2010). However, the Rac1 interaction with WRC *in vitro* is of very low affinity (Lebensohn and Kirschner, 2009), suggesting the involvement of an additional factor at the cell membrane. This factor was identified *in vitro* as ARF1 (Koronakis et al., 2011). Indeed, by reconstituting *in vitro* WRC-dependent actin assembly on lipid-coated beads in HeLa cells extracts, Rac1 was not sufficient for WRC recruitment to the membrane and for its activation, which instead requires direct binding with both Rac1 and ARF1 (Koronakis et al., 2011). Differently from ARF1, ARF6 does not directly bind to WRC, but it is required for WRC-mediated actin assembly in a mechanism involving the ARFGEF ARNO. ARF6, indeed, recruits and activates ARNO at the plasma membrane, both *in vitro* and *in vivo* and in turn activates ARF1 (Fig.20) (Humphreys et al., 2013). The ARF6-ARNO-ARF1 cascade was already described by Cohen and colleagues (Cohen et al., 2007), who showed how ARF6-GTP binds to the PH domain of ARNO and convert it from its cytosolic inactive form to its active membrane-bound form, which in turn further activates ARF1 at the membrane (Fig.20). This cascade is used by ARF6 to promote WRC activation and actin assembly and is usurped by the pathogen *Salmonella* to invade host cells (Humphreys et al., 2012; Humphreys et al., 2013). *Salmonella* indeed induces WRC-mediated membrane ruffling to facilitate cell macropinocytosis of *Salmonella* by recruiting ARF6 GEFs BRAG2 and EFA6 (Humphreys et al., 2013).

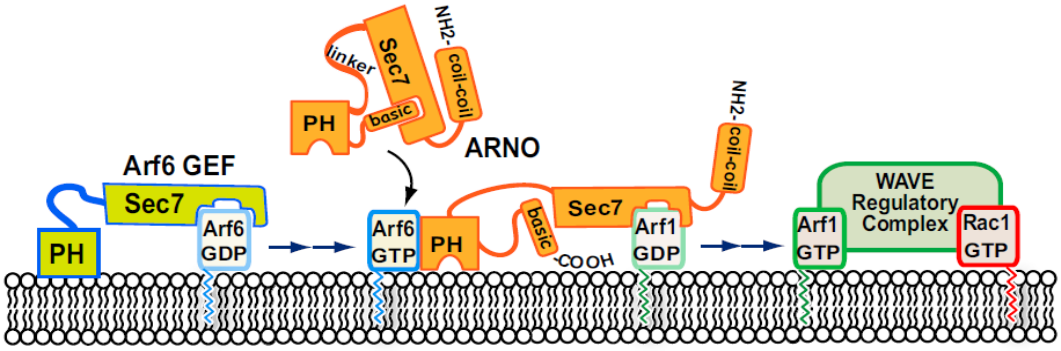

Figure 20: Model for ARF6 regulation of the WAVE regulatory complex. ARF6 GEFs such as EFA6 or BRAG activate ARF6. ARNO resides in a soluble autoinhibited conformation, and is recruited to the plasma membrane and activated by ARF6 binding of the ARNO PH domain. ARNO activates ARF1 that collaborates with Rac1 to drive WRC-dependent actin polymerization. Picture from Humphreys et al., 2013.

2.4. ARF6 and cancer cell invasion

Since ARF6 has been heavily implicated in the recycling and polarized delivery of membranes and factors important for cell adhesion, migration and polarity and in the actin cytoskeleton remodelling, it is not a surprise that it could also be implicated in cancer cell invasion where most of these processes are de-regulated.

2.4.1. ARF6 in breast cancer

The first evidence of a role for ARF6 in breast cancer invasion derives from a study of 2004 where Hashimoto and co-workers showed that ARF6 is required for the invasive capacities of breast tumor-derived cell lines (Hashimoto et al., 2004). In MDA-MB-231 cells, GFP-tagged ARF6 localized at invadopodia, in correspondence of sites of matrix degradation (Fig.21) and ARF6 knockdown led to a strong reduction in matrix degradation and transmigration through a matrigel barrier, without affecting cell adhesion.

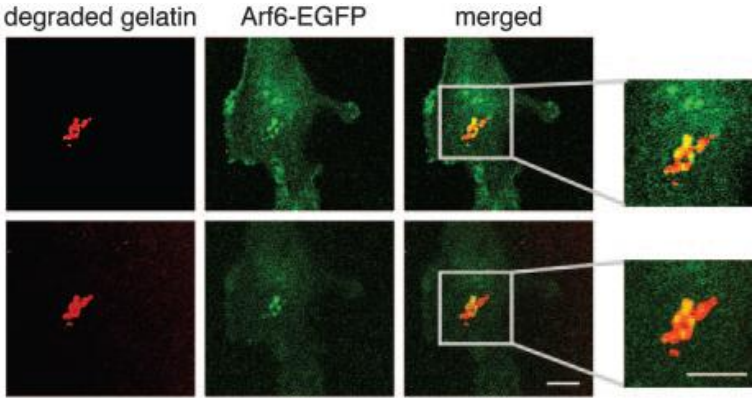

Figure 21: **ARF6 localizes at invadopodia of MDA-MB-231 cells**. Cells expressing Arf6-EGFP were cultured on a fluorescently labeled, cross-linked gelatin matrix for 16 h. Degraded gelatin zones are observed as spots (red), and EGFP-ARF6 was detected by autofluorescence (green). In upper panels focus was adjusted at the cell bottom, or at 0.7 µm below the cell bottom in lower panels. Scale bar represents 10 µm. Picture from Hashimoto et al., 2004.

The authors also analysed ARF6 protein expression levels in breast tumor-derived cell lines and found significantly higher levels in highly invasive cell lines such as BT549 or Hs578T, as compared to weak or non invasive cells and ARF6 silencing in these highly invasive cancer cell lines effectively blocked invasion. Moreover, both the expression of ARF6Q67L and ARF6T27N blocked invasion of MDA-MB-231 cells, suggesting the necessity of cycling of ARF6 cycle in

invasion. This was the first time in which ARF6 cycle, with its GEFs and GAPs, was proposed as a possible target for cancer therapy (Hashimoto et al., 2004).

Shortly after, it was shown that the ARF-GAP AMAP1 (also called DDEF1 in human, DEF1 in bovine and ASAP1/centaurin β4 in mouse) is an effector for ARF6-GTP in invasion and metastasis (Hashimoto et al., 2005; Onodera et al., 2005). AMAP1 has an ARF GAP domain and was originally reported to exhibit efficient GAP activity against ARF1 and ARF5, but very weak activity against ARF6. AMAP1, together with AMAP2, was shown to bind ARF6-GTP without GAP activity and therefore functioning as an ARF6 effector rather than a *bona fide* GAP. In particular ARF6 upon stimulation by EGF recruits AMAP1 from intracellular endosomal compartments to the plasma membrane (Hashimoto et al., 2005).

AMAP1 co-localizes with ARF6 at invadopodia of MDA-MB-231 cells and its knockdown blocks invadopodia formation and invasive activities (Onodera et al., 2005). Like ARF6, AMAP1 is also overexpressed (> 10 fold) in highly invasive breast cancer cell lines as compared with weakly- and noninvasive breast cancer cell lines and human mammary epithelial cells (HMECs) and silencing of AMAP1 blocks the *in vitro* invasive ability of these cells (Onodera et al., 2005). Immunohistochemical analysis of human tumor samples also revealed that AMAP1 protein expression was very high in infiltrating ductal carcinomas (IDCs), while its expression was at basal levels in most ductal carcinoma *in situ* (DCIS) and in peritumoral tissues. In addition, AMAP1 levels were high in all DCIS tumors harboring an invasive component (Onodera et al., 2005). Although the number of clinical samples was relatively low, these data indicated that AMAP1 levels increased with tumor progression. AMAP1 localizes at the invadopodia with cortactin and paxillin and it was shown by pull-down that a proline-rich sequence of AMAP1 binds to the SRC homology 3 (SH3) domain of cortactin, while the SH3 domain of AMAP1 binds to paxillin. A trimeric complex consisting of AMAP1, cortactin and paxillin was detected only in highly invasive breast cancer cells in which AMAP1 is abnormally overexpressed but not in noninvasive breast cancer cells or normal mammary epithelial cells. Moreover blocking of this trimeric protein complex inhibited invadopodia formation and *in vitro* invasive activities of breast cancer cells (Onodera et al., 2005). As described above (see paragraph 2.3.3.2), AMAP1 in MDA-MB-231 cells also makes a complex with the cytoplasmic tail of β1 integrin and is responsible for the ARF6-dependent recruitment of β1 integrins to the plasma membrane upon EGF stimulation (Onodera et al., 2012).

Later on it was shown that the ARF6-GEF GEP100/BRAG2 is implicated in breast cancer cell invasive activities since silencing of GEP100/BRAG2 lead to a strong decrease in matrigel invasion, in contrast to silencing other ARF6-GEFs (Morishige et al., 2008). GEP100/BRAG2 activates ARF6 downstream EGFR signalling and silencing of ARF6 or GEP100/BRAG2 leads to a strong decrease of EGF-dependent invasion. Moreover, it was shown by pull-down assays that GEP100/BRAG2 directly binds to ligand-activated EGFR via an interaction of the pleckstrin

homology (PH) domain of GEP100/BRAG2 either with phosphorylated Tyr1068- or Tyr1086 of EGF-R (Morishige et al., 2008). Overexpression of GEP100/BRAG2 together with ARF6 made otherwise noninvasive MCF7 cells to get a mesenchymal phenotype and to become highly invasive under EGF stimulation, whereas co-overexpression of ARNO and ARF6 did not. Finally injection of breast tumor cells stably depleted for GEP100/BRAG2 in the fat pad of mouse mammary glands blocked lung metastasis as compared to control mice. Immunohistochemical analysis also showed that GEP100/BRAG2 was expressed in the 70% of cases of a cohort of primary breast ductal carcinomas and was preferentially co-expressed with EGF-R in the most malignant cases (*i.e.* cases associated to pathological grade II and III) (Morishige et al., 2008). These studies indicate that GEP100/BRAG2 links EGF-R signalling to ARF6 activation, which, by recruiting AMAP1 and its effectors paxillin and cortactin, induces invasion of breast cancer cells. GEP100/BRAG2 is also activated in human umbilical vein (HUVEC) cells by the vascular endothelial growth factor receptor (VEGF-R) that triggers the same GEP100/BRAG2-ARF6-AMAP1-cortactin axis that is essential for angiogenesis activities (Hashimoto et al., 2011).

In conclusion all these studies from Sabe's group showed that in breast cancer cell models ARF6 is activated downstream RTKs such as EGFR, which was also shown to be associated with invasiveness and poor patient survival in breast cancer (Magkou et al., 2008) or VEGFR, strongly implicated in cancer-associated angiogenesis. Once activated, ARF6 could act by recruiting the effector AMAP1 to invadopodia where in turn it recruits paxillin and cortactin, and this trimeric complex is required for invadopodia formation and matrix degradation. ARF6 recruitment of AMAP1 seems also to be important for recycling of β1 integrin at the surface and for efficient breast cancer cell migration (Fig.22).

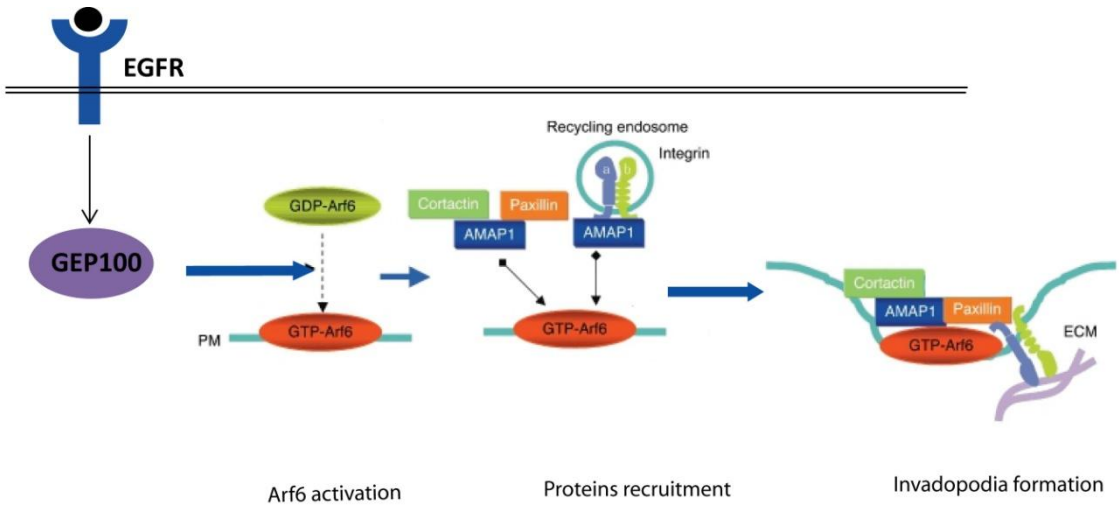

Figure 22: Model for ARF6 function in invadopodia. Picture adapted from Sabe et al., 2009.

2.4.2. ARF6 in other types of cancer

ARF6 has also been implicated in invasion in other types of aggressive and malignant tumors, such as melanoma and glioma (Li et al., 2006; Li et al., 2009; Muralidharan-Chari et al., 2009a; Muralidharan-Chari et al., 2009b; Tague et al., 2004).

Tague and colleagues showed that ARF6 localizes at invadopodia in a human melanoma invasive cell line (LOX cells) and overexpression of ARF6Q67L strongly increases degradation of gelatin, whereas expression of ARF6T27N abolishes invadopodia formation and decreases the percentage of degradative cells (Tague et al., 2004). The authors also showed that ARF6 is activated upon HGF stimulation and ARF6 activation leads to extracellular signal-regulated kinase (ERK) activation. In addition overexpressed ARF6Q67L partially colocalizes with phosphorylated ERK at invadopodia of LOX cells and inhibition of ERK by inhibitors blocks ARF6Q67L gelatin degradation, suggesting for the first time a mechanism in which ARF6 regulates melanoma cell invasion through activation of the ERK signaling pathway (Tague et al., 2004). ARF6's role in melanoma invasion was later studied in a mouse model (Muralidharan-Chari et al., 2009b). LOX cells expressing GFP as a control, ARF6Q67L or ARF6T27N were injected subcutaneously in the dorsal flank of mice. At 3 weeks post-injection in the mice injected with ARF6Q67L-expressing cells, the mass of the primary tumor was reduced but the invasive potential of LOX cells was increased, as measured by the extent of collagen border compromised and infiltration into surrounding tissues. Expression of ARF6T27N, instead, slowed down the growth rate of the primary tumor mass, decreased invasion and lung metastasis (Muralidharan-Chari et al., 2009b). The authors also showed that active ARF6 promotes melanoma cell invasion by inducing ERK phosphorylation in a mechanism dependent on PLD activity. Indeed, phospho-ERK levels in LOX-GFP and LOX-ARF6Q67L cells isolated from the primary tumors were decreased upon treatment with primary alcohols such as 1-butanol that inhibit PA production and inhibition of PLD and ERK blocked invadopodia formation. Moreover, ERK activation led to increased Rac1-GTP levels. Expression of a dominant-negative Rac1 mutant blocked basal as well as ARF6-GTP induced cell invasion (Muralidharan-Chari et al., 2009b). The role of Rac1 in invadopodia is not clear, even though the authors suggested it could promote actin remodeling required for invadopodia extension or facilitate the recruitment of actin-binding proteins. Taken together, these studies suggest the implication of an ARF6-PLD-ERK-Rac1 cascade to regulate melanoma cell invasion (Muralidharan-Chari et al., 2009b).

The same authors also described an ARF6-PLD-ERK pathway involved in shedding of microvesicles from LOX melanoma cells (Muralidharan-Chari et al., 2009a). Microvesicles shedding from the cell surface is a relatively poorly studied process that occurs in a spectrum of normal and, more frequently, tumor cells, both *in vivo* and *in vitro* (Cocucci et al., 2004). Invadopodia and microvesicles appear to be distinct structures and while invadopodia promote pericellular proteolysis at the leading/invading edge, microvesicles likely promote more distant

proteolysis and creation of an invasion path. It is possible that some tumor lines may exhibit both invasion mechanisms, whereas one of these mechanisms may dominate in other cell lines (Muralidharan-Chari et al., 2009a). The authors showed that LOX cells' microvesicles are capable to degrading a gelatin matrix and are loaded with proteases such us MMP2, MMP9 and MT1-MMP as well as with β1 integrin, which likely facilitates interaction of microvesicles with the ECM (Muralidharan-Chari et al., 2009a). ARF6-GTP is required for the shedding of microvesicles and their release is dependent on PLD activity, which in turn leads to ERK activation and activation of myosin light chain kinase (MLCK), a known substrate for ERK. MLCK, phosphorylates and activates MLC to allow actomyosin-based contraction at the necks of microvesicles, facilitating their release into the extracellular space (Muralidharan-Chari et al., 2009a). This study therefore suggests that ARF6, besides invadopodia formation, is coupled also to a distinct cellular process linked to matrix invasion, that is the release of surface vesicles into the surrounding environment and is the first study implicating ARF6 in the exocytosis of MT1-MMP and other proteases in tumor cells.

In addition, the ARF6-GEF EFA6A was shown to be upregulated at the mRNA level in both low-grade and high-grade human glioma as compared to normal brain tissues and overexpression of EFA6A in U373 cells (a glioblastoma cell line) lead to an increase of the migratory capacity of these cells both in a wound-healing assay and in transwell migration through matrigel (Li et al., 2006). Moreover, ERK signaling is required for EFA6A-mediated cell invasion because expression of both a GEF-defective mutant of EFA6A (E242K) or ARF6T27N, as well as treatment with ERK inhibitor markedly reduced levels of phosphorylated ERK and EFA6A-mediated invasive capacity, suggesting the implication of an EFA6-ARF6-ERK axis for glioma cells migration and invasion (Li et al., 2006). In addition, it was shown that EGF stimulation was able to up-regulate transcription of ARF6 in human glioblastoma U87 cells through two parallel and independent pathways: the MEK/ERK and the PI3K signaling pathways (Li et al., 2009). Finally, EGF-induced glioblastoma cell proliferation was shown to depend on ARF6 (Li et al., 2009). Another study (Hu et al., 2009), confirmed that ARF6 is abundantly expressed in invasive glioma cell lines and is required for invasion. Furthermore, the authors identified a mechanism whereby ARF6 activates Rac1 upon HGF stimulation by recruiting IQ-domain GTPase-activating protein 1 (IQGAP1) at the leading edge of HGF-stimulated cells. IQGAP1 was previously reported to function either as a target or regulator of Rac1 and to regulate cell adhesion and migration by binding and stabilizing Rac1-GTP (Noritake et al., 2005). Silencing of Rac1 and IQGAP1 abrogates HGF-stimulated cell migration, whereas knockdown of IQGAP1 by siRNA suppressed serum-stimulated cell migration and Rac1 activation. This study therefore suggests that ARF6 regulates HGF-stimulated and serum-stimulated glioma cell migration through formation of a Rac1-GTP/IQGAP1 complex and is critical for invasive behaviors of malignant glioma cells (Hu et al., 2009).

In conclusion, these different studies implicate ARF6 in the invasive behaviour of breast cancer, melanoma and glioma cells and suggest some interesting mechanisms through which ARF6 could regulate invasion. However, to our knowledge there are no data in the literature that clearly implicated ARF6 in the polarized delivery of MT1-MMP at the site of invasion of cancer cells. One of the aim of our study was to address this hypothesis in particular by focusing on the interaction between ARF6 and its two effectors JIP3 and JIP4, which we thought could regulate the microtubule-based transport of MT1-MMP at the surface.

Chapter 3: ARF6 effectors JIP3 and JIP4

3.1. The JIP family of scaffold proteins

3.1.1. The MAPK modules

JIP3 and JIP4 belong to the family of the c-Jun NH_2-terminal kinase (JNK) interacting proteins (JIPs), which have been identified in the late 1990s as putative scaffolding protein for regulating JNK- and p38-mediated mitogen activated-protein-kinase (MAPK) signaling (Ito et al., 1999; Kelkar et al., 2000; Kelkar et al., 2005; Lee et al., 2002).

MAPK signal transduction pathways are evolutionary conserved from yeast to mammals and consist of a cascade of kinase phosphorylation events which is triggered by extracellular stimuli such as growth factors or cytokines or stress and eventually ends in the activation of transcription factors which regulate cell proliferation, differentiation and survival (Gallo and Johnson, 2002). In mammals, four groups of MAPK modules have been described: the extracellular signal-regulated protein kinases 1 and 2 (ERK1/2), the extracellular signal-regulated protein kinase 5 (ERK5), the JNK, and the p38 MAPKs. Generally, the ERK pathways respond to growth factor signals, whereas the JNK and p38 modules typically respond to a variety of extracellular stress signals. Each of these groups of MAPKs is activated by dual phosphorylation on a Thr and a Tyr by a MAPK kinase (MAPKK or MKK), which, in turn is activated by a MAPKK kinase (MAPKKK or MKKK) (Fig.23).

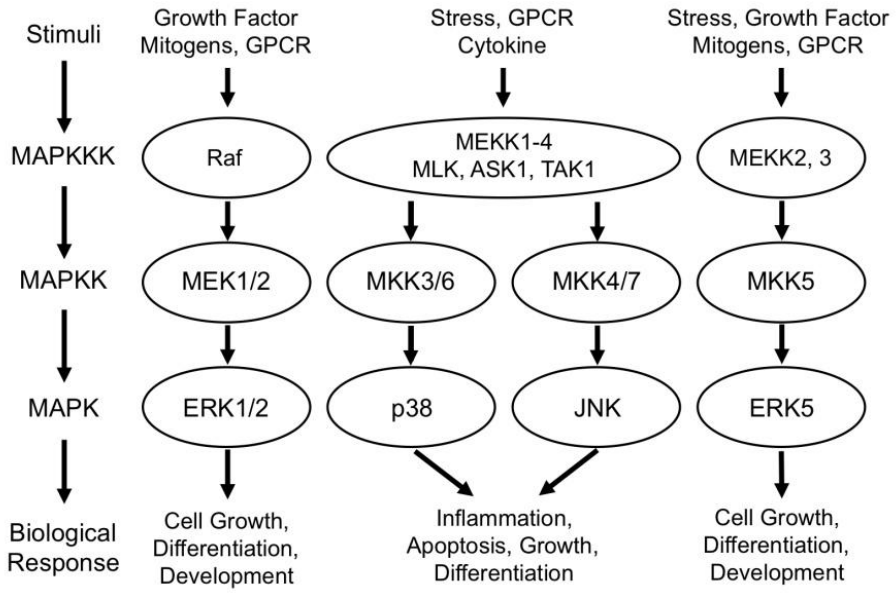

Figure 23: **Schematic representation of the four MAPKs modules**, ERK1/2, p38, JNK and ERK5, with their upstream MAPKKs and MAPKKKs and the different cellular responses.

In the JNK module, a variety of environmental stimuli activate the small GTPases of the Rho family (Rac, Rho and Cdc42) in the cell membrane that in turn lead to the activation of membrane proximal protein components such as MEKKs, ASK1, TAK1 or mixed-lineage kinase (MLKs). These protein kinases then phosphorylate and activate MKK4 and/or MKK7, which mediates the activation of JNK family members. There are three JNK isoforms: JNK1 and JNK2 that are ubiquitously expressed, and the brain-specific JNK3. Activated JNK can translocate to the nucleus where it can regulate the activity of multiple transcription factors, including c-Jun, to regulate gene expression. Many of the MAPKKK described for JNK have been shown to activate also the p38 module (Wagner and Nebreda, 2009) (Fig.23).

3.1.2. JIP1 and JIP2

The family of JIP scaffolding proteins is encoded by four genes. All JIPs share a number of common biochemical properties including functioning as binding partners and cargo molecules for microtubule motor proteins (see next paragraph 3.2) and as scaffold proteins for JNK and p38 signalling modules thanks to their ability to aggregate the different kinase components of the MAPK cascades, thereby facilitating MAPK module activation in discrete cellular compartments and in different contexts. Another common property of JIP proteins is that they function as dimers (Kelkar et al., 2000; Kelkar et al., 2005; Yasuda et al., 1999).

JIP1 was first identified in a screen for JNK-interacting proteins using a yeast two-hybrid assay (Dickens et al., 1997). Two isoforms of JIP1, namely JIP1a and JIP1b have been identified. Although both isoforms contain an N-terminal JNK binding domain (JBD), a SRC homology (SH3) domain and phosphotyrosine-binding (PTB) domain, JIP1b contains an additional c-terminal PTB domain (Fig.24) (Dickens et al., 1997). JIP1 interacts with both JNK1 and JNK2 (Whitmarsh et al., 1998; Yasuda et al., 1999). Moreover it interacts with the MAPKKKs MEKK3, MLK2 and MLK3 and neuronal MLK dual leucine zipper-bearing kinase (DLK). MKK7 is the only JNK-specific MAPKK that interacts with JIP1 (Fig.24) (Whitmarsh et al., 1998; Yasuda et al., 1999). In accordance with the scaffolding role of JIP1 in the JNK-signaling pathway, the coexpression of JIP1 has been shown to enhance the activation of JNK via MLK3 and MKK7 (Whitmarsh et al., 1998). JIP1 was also shown to bind the phosphatases MKP7 and M3/6 which downregulate JNK activation, suggesting a more complex and dynamic role for JIP1 in the regulation of JNK activity by balancing upstream stimulatory kinases and attenuating phospatases (Fig.24) (Willoughby et al., 2003).

JIP2 was then identified (Yasuda et al., 1999). Similar to JIP1, it contains a JNK binding domain, a PTB domain as well as an SH3 domain (Fig.24) (Yasuda et al., 1999). Northern blot analysis indicates that JIP2 is expressed in the brain but not in other tissues, differently from JIP1 which is also expressed in other tissues (Yasuda et al., 1999). MAPKKKs that interact with JIP2 include DLK, MLK2 and MLK3. Also similar to JIP1, JIP2 specifically interacts with MKK7

(Fig.24). JIP2, therefore, appears to assemble a JNK-signaling complex involving MKK7 as the MAPKK (Yasuda et al., 1999). However, although JIP2 has been shown to interact with all JNK isoforms (Whitmarsh et al., 1998; Yasuda et al., 1999), the binding affinity is lower as compared to JIP1 for JNK (Yasuda et al., 1999). Moreover JIP2 has also been shown to interact with p38 MAPK and with the p38-specific MAPKK MKK3 (Fig.24) (Buchsbaum et al., 2002), suggesting a role for JIP2 in bringing the JNK and the p38 modules together.

The observation that JIP2 PTB domain can also bind the Rac1 GEFs Tiam1 and Ras-GFR1 and that Rac1 is an activator of MLK3, suggest a role for JIP2 in coupling Rac1 signaling and p38 activation (Fig.24) (Buchsbaum et al., 2002). Similarly JIP1 PTB domain was shown to physically interact with the RhoGEF p190, suggesting the possibility that JIP1 couples Rho signaling with JNK activation (Fig.24) (Meyer et al., 1999).

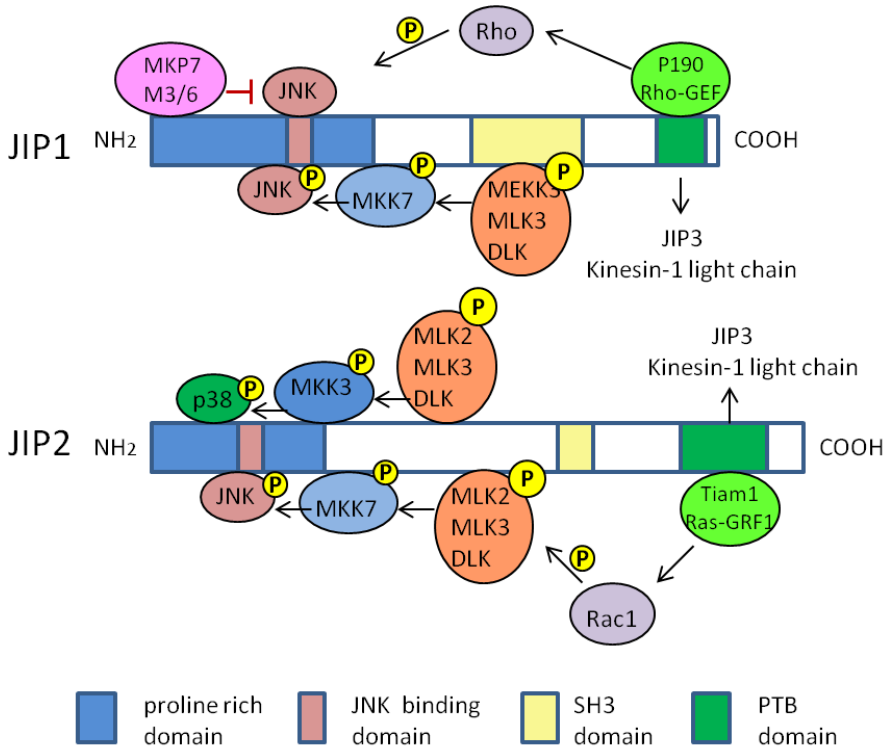

Figure 24: **Schematic representation of JIP1 and JIP2 primary sequences with their putative structural domains and their known interacting partners of the JNK and p38 MAPK signaling modules and of the Rho GEFs family.** The PTB domain of JIP1 and JIP2 binds to JIP3 to form heterodimers (Hammond et al., 2008). The C-terminus domain of JIP1 and JIP2 was shown to interact with the light chain of kinesin1 (Verhey et al., 2001*;* see paragraph 3.2.2.)

3.1.3. JSAP1/JIP3

3.1.3.1 JSAP1/JIP3 as scaffold protein for the JNK signaling module

JIP3, also called JNK/stress activated protein kinase-associated protein 1 (JSAP1), has been independently discovered by two groups (Ito et al., 1999; Kelkar et al., 2000) that were

screening mouse embryo cDNA libraries by yeast-2 hybrid for identifying novel JNK3 (Ito et al., 1999) and JNK1 (Kelkar et al., 2000) partners. Sequence analysis demonstrated the lack of the SH3 domain typical of JIP1/2 and the presence of an extended coiled-coil domain in the NH_2-terminal region, which also contained a leucine zipper (LZ) domain (Fig.25) (Kelkar et al., 2000). LZ domains are characterized by the presence of heptad repeats containing a conserved hydrophobic residue, usually a leucine, at every seventh residue in a coiled-coil α-helical structure (Lupas, 1996). JIP3 is predominantly expressed in the brain both at the mRNA and protein levels as demonstrated by Northern and Western blot analysis, with lower levels in the heart and other tissues (Kelkar et al., 2000). By Western blot analysis we could detect significant levels of JIP3 in HeLa and MDA-MB-231 cell lines (Montagnac et al., 2009) (my unpublished data).

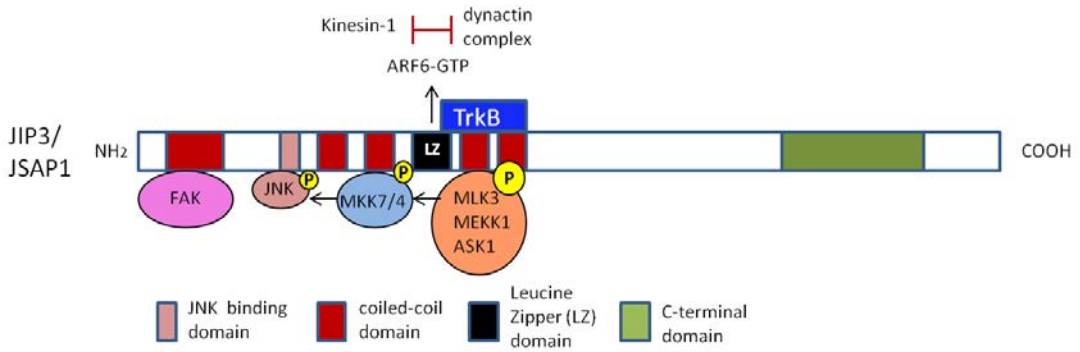

Figure 25: **Schematic representation of JIP3 primary sequence with its putative structural domains and its known interacting partners. JIP3 mainly functions as a scaffold protein for the JNK signalling module** (Ito et al., 1999; Kelkar et al; 2000). JIP3 also binds to FAK and forms a scaffold complex that couples JNK activation with cell migration upon fibronectin adhesion (Takino et al., 2002; 2005). ARF6 binds to JIP3 through the LZ domain of JIP3 (Montagnac et al., 2009) (see paragraph 3.2.2.6.). The LZ domain of JIP3 is also critical for JIP3 binding to the plus-tip-directed microtubules motor kinesin-1 (Bowman et al., 2000) and the (-)-end directed microtubules motor dynein/dynactin complex (Montagnac et al., 2009). The two motors bind to JIP3 in a mutually-exclusive way (Montagnac et al., 2009) (see paragraph 3.2.2.). The neuronal receptor TrkB also binds to JIP3 in a region comprised between the LZ and the two following coiled-coil domains (Huang et al., 2011) (see paragraph 3.2.2.1).

By co-immunoprecipitation analysis, JIP3 was shown to selectively interact with all JNK isoforms but not with ERK or p38 MAPKs (Ito et al., 1999; Kelkar et al., 2000). JIP3 is phosphorylated by JNK and enhances JNK activation, which in turn increases complex formation with JIP3 (Ito et al., 1999; Kelkar et al., 2000). By using deletion mutants, the JNK binding site was localized in the NH_2-terminal region and is very similar to the JNK binding site of JIP1 (Fig.25) (Kelkar et al., 2000). In addition, Kelkar and colleagues showed that JIP3 binds to the MKK7 (MAPKK) and to MLK3 (MAPKKK), suggesting therefore a role for JIP3 as scaffold protein of the module MLK3-MKK7-JNK1-3 (Fig.25) (Kelkar et al., 2000). Later on, it was shown that JIP3 can also bind to the MLK ASK1 (Kelkar et al., 2005). However, Ito and colleagues showed that JIP3/JSAP1 binds to MEKK1 (MAPKKK) and to the MKK4 (MAPKK)

(Ito et al., 1999). These conflicting findings might be due to the fact that four alternatively spliced isoforms of JIP3/JSAP1 exist (called JSAP1a-d) (Ito et al., 2000), that could have different affinity for distinct MAPKs. For instance, JSAP1c and JSAP1d have weaker affinity for JNK3 and it is likely that different isoforms could assemble distinct JNK modules in a tissue-specific manner. Indeed, while all four isoforms are abundantly expressed in the brain, they do exhibit isoform-specific expression in other tissues (Ito et al., 2000).

3.1.3.2. JSAP1/JIP3 localization and biological functions

Immunofluorescence analysis in PC12 neuronal cells demonstrated that JIP3 is mainly cytosolic (Kelkar et al., 2000). Other studies reported that JIP3 associates to post-Golgi vesicles (Bowman et al., 2000) and to some membrane compartments in the axon of sciatic nerves (Abe et al., 2009; Cavalli et al., 2005), suggesting that JIP3 may be membrane-associated. Bowman *et al*. proposed that the *Drosophila* JIP3 orthologue Sunday Driver may be a transmembrane protein because of the presence of a predicted transmembrane domain located near the C-terminal domain (Bowman et al., 2000). However, Cavalli *et al.* using sucrose flotation gradient, could finally show that JIP3 exists in two pools: a soluble cytosolic pool and a peripherally membrane-associated one (Cavalli et al., 2005), although to date it remains unclear how JIP3 associates to membrane.

JIP3 expression is induced during neuronal differentiation in response to nerve growth factor (NGF), while it is down-regulated during NGF withdrawal-induced apoptosis (Kelkar et al., 2000), suggesting a role for JIP3 in neuronal differentiation. Moreover experiments on knock-out mice showed that JIP3, even though it is not required for embryonic viability, is essential for mammalian life after birth since *Jip3*-/- mice are unable to breathe and exhibit severe defects in the development of the telencephalon (Kelkar et al., 2003). This observation is consistent with a previous study reporting that the brain-specific MLK isoform DLK can activate JNK in the developing mouse telencephalon and that altered DLK-JNK signaling disrupts telencephalon morphogenesis (Hirai et al., 2002). Moreover, the observation that the telencephalic commissure (a major interhemispheric connection in the brain) is absent in *Jip3* KO mice suggested some severe axonal pathfinding defects, a phenotype that could be explained by a role for JIP3 in axonal transport during development (see paragraph 3.2) (Kelkar et al., 2003).

3.1.3.3. JSAP1/JIP3 role in cell migration

JIP3 interacts with focal adhesion kinase (FAK) (Takino et al., 2002) (Fig.25) and is involved in fibronectin-mediated cell migration (Takino et al., 2005). Several lines of evidence indicate that activated JNK and some molecules of its signaling pathway are localized not only in the nucleus but also in focal adhesions (FAs) (Almeida et al., 2000), suggesting that FAs function as MAPK signaling platforms. Along this line, Takino *et al.* showed that JIP3 binds to the N-

terminal domain of FAK and mediates association between FAK and JNK (Takino et al., 2002). Complex formation is further stimulated by SRC, resulting in tyrosine phosphorylation of JIP3/JSAP1 and recruitment of additional FAK/SRC signaling molecules. Expression of JSAP1 in Hela cells facilitated formation of well-organized focal contacts and actin stress fibers and promoted cell spreading onto fibronectin (Takino et al., 2002). This study then suggested that JIP3 is involved in an integrin-mediated signaling pathway through FAK/SRC resulting in promotion of cell spreading onto fibronectin. Later the same group showed that JIP3 also co-localizes with JNK and phosphorylates FAK at the leading edge of migrating cells, suggesting that a JSAP1/FAK scaffold may cooperatively enhance FAK and JNK activation at the leading edge. Migration *per se* is stimulated by JIP3 over-expression, which depends on its JNK-binding domain and is suppressed by inhibition of JNK (Takino et al., 2005). The findings that JIP3-deficient mice show several abnormalities in brain development including axon guidance defects (Kelkar et al., 2003) and JIP3-null embryonic stem cells are deficient in the formation of lamellipodial protrusions (Takino et al., 2005), attest of the critical role played by JIP3 in cell motility. The authors also showed that JIP3 mRNA levels were significantly higher in samples derived from highly aggressive glioblastoma tumors rather than in samples derived from normal brain tissues or low-grade brain tumors (Takino et al., 2005). This is the first and only evidence linking JIP3 to cancer cell invasion.

3.1.4. JIP4/JLP/SPAG9

JIP4 was the last JIP family member to be discovered. Three JIP4 isoforms generated by alternative splicing have been identified and named: JNK-associated leucine zipper protein (JLP) (Lee et al., 2002), JNK-interacting protein 4 (JIP4) (Kelkar et al., 2005) and sperm associated antigen 9 (SPAG9) (Jagadish et al., 2005), respectively (Fig.26). The corresponding locus is located on mouse chromosome 11 (human chromosome 17) and consists of 31 exons.

3.1.4.1. JIP4/JLP/SPAG9 as scaffold protein for JNK and p38 MAPK modules

JLP shows 69% homology with JIP3, but differently from neuronal-specific JIP3, northern blot analysis showed that JLP is ubiquitously expressed. Immunofluorescence staining revealed that JLP is mainly cytosolic similarly to JIP3 (Lee et al., 2002). The NH_2 domain of JLP has been shown to interact with the two transcription factors c-Myc and Max (Fig.26), suggesting a role for JLP as a scaffold to bring together the MAPK signaling and their target transcription factors. Pull down assays showed that JLP can directly bind both to JNK1 and to p38 MAPKs, through two distinct domains spanning amino acids 1–110 and 210–398 of JLP (Fig.26). Thus JLP can tether JNK and p38 together and could be designed to link JNK and p38 MAPK signaling modules. Moreover, JLP binds to the MKK4 (MAPKK) and MEKK3 (MAPKKK), suggesting it is a scaffold for the MEKK3-MKK4-JNK/p38 module (Fig.26) (Lee et al., 2002). JIP4 splice

variant and JIP3 were identified simultaneously by Kelkar and colleagues (Kelkar et al., 2000; Kelkar et al., 2005). JIP4 features an extended coiled-coil and a LZ domain in the NH_2-terminal region together with a JNK binding domain and a predicted transmembrane domain (Fig.26). Differently from JIP3, JIP4 lacks an NH_2-terminal extension (170 amino acids) and it also differs from JLP as it lacks a unique NH_2-terminal domain of JLP allowing binding to c-Myc and Max transcription factors (Fig.26). Moreover JIP4 shows a strong expression in testis, brain, kidney and liver and weaker expression in heart (Kelkar et al., 2005). Although JIP4 is able to bind to JNK, it does not appear to function as a scaffold for the JNK pathway, since it does not bind to MKK7 and MLK3 (as does JIP3) and does not contribute to MLK3-dependent activation of JNK. In contrast JIP4 binds to p38 and potentiates its activation by binding to the ASK1 (MAPKKK) (Fig.26) (Kelkar et al., 2005).

Finally, SPAG9 is an 84-kDa protein apparently uniquely expressed in haploid spermatid cells during spermatogenesis in macaque, baboon and human species (Shankar et al., 2004). Sequence analysis of SPAG9 showed two coiled-coil regions with an embedded LZ domain and a predicted transmembrane region at the C-terminus (Jagadish et al., 2005). Like JIP4, SPAG9 lacks the N-terminal and C-terminal domains present in JLP (Fig.26), but differently from all other JIPs that are mainly cytosolic, SPAG9 appears to be membrane associated in transfected COS-7 cells and its localization depends on the presence of the transmembrane domain. SPAG9 can bind all the three JNK isoforms but with higher affinity for JNK2 and JNK3 and it does not bind to other MAPKs including p38 (Jagadish et al., 2005) (Fig.26). MAPKKs and MAPKKKs possibly interacting with SPAG9 have not been identified and SPAG9's role in spermatid function remains to be established.

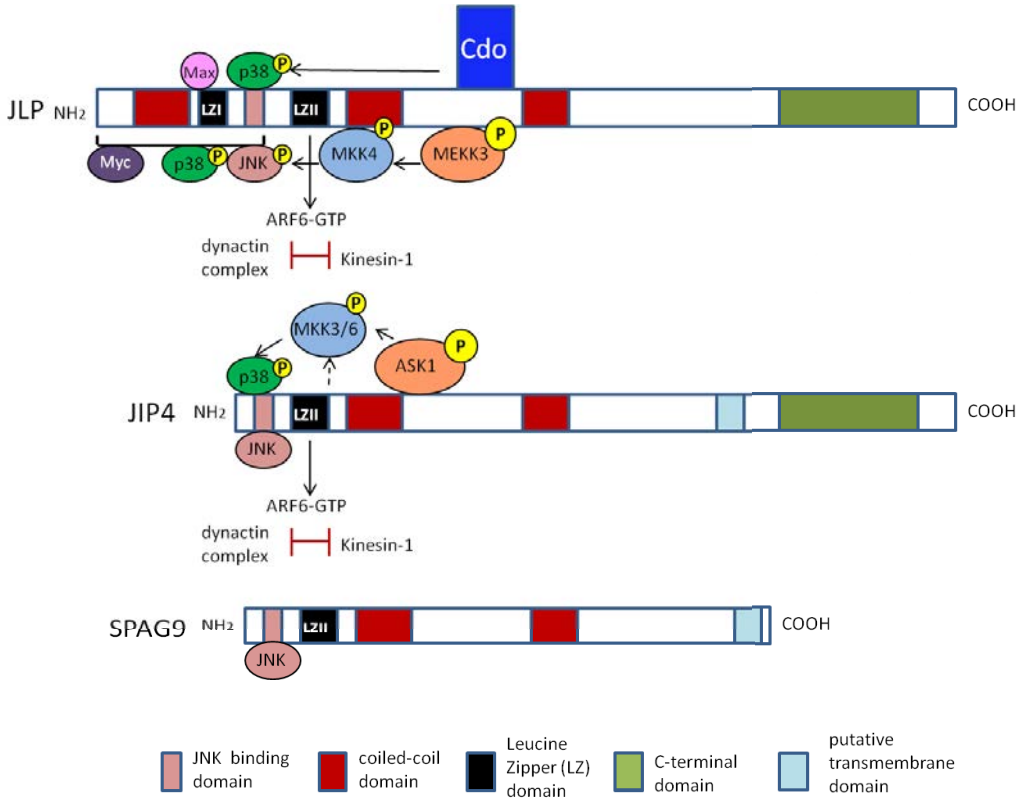

Figure 26: **Schematic representation of the primary sequences of the three JIP4 splice variants, JLP, JIP4, SPAG9, with their putative structural domains and their known interacting partners.** JLP mainly functions as a scaffold protein for the JNK and p38 MAPK signalling modules (Lee et al; 2002). It also binds to the two transcription factors c-Myc and Max (Lee et al; 2002). JLP also binds to the surface receptor Cdo member of the Ig superfamily and their interaction facilitates p38 activation (Takaesu et al., 2006). ARF6 binds to JIP4/JLP through the LZII domain (Montagnac et al., 2009) (see paragraph 3.2.2.6.). The LZII domain of JIP4 is also critical for JIP4 binding to the (+)-tip-directed microtubules motor kinesin-1 (Bowman et al., 2000) and the (-)-end directed microtubules motor dynein/dynactin complex (Montagnac et al., 2009). The two motors bind to JIP4 in a mutually-exclusive way (Montagnac et al., 2009) (see paragraph 3.2.2.). JIP4 lacks the NH_2-terminal domain that binds to Max and c-Myc and is manly a scaffold for p38 even though it can binds also to JNK (Kelkar et al., 2005). Spag9 is the shortest splice variant since it misses the NH_2-terminal domain and the C-terminal domain. It binds to JNK (Jagadish et al., 2005).

3.1.4.2. Role of JLP in myogenesis

Interestingly JLP has been associated also to a role in myogenesis by binding to the surface trans-membrane receptor Cdo and by mediating Cdo-dependent p38 activation (Takaesu et al., 2006). It is well known that the p38 MAPK pathway plays an important role in myogenesis since p38 phosphorylates several proteins involved in muscle-specific gene expression. Indeed, p38 activity increases and persists in differentiating myoblasts, and differentiation is blocked by the p38 inhibitor SB203580. Cdo is a cell surface Ig superfamily member with a long intracellular region, which is known to promote myogenesis *in vivo* and *in vitro* (Krauss et al., 2005). JLP was identified as a binding partner for Cdo in a two-hybrid screen (Takaesu et al., 2006). *Takaesu* et al. showed that the cytoplasmic domain of Cdo binds JLP (amino acids 465-647; Fig.26) and this interaction is necessary for p38 activation in co-transfected cells. Endogenous Cdo, JLP and p38 also form complexes during myogenesis in myoblasts and binding of Cdo with JLP potentiates

p38 activation. Moreover Cdo-deficient satellite cells derived from *Cdo−/−* mice cells are impaired in their ability to activate p38 (Takaesu et al., 2006). Thus, JLP has a function in linking Cdo receptor signaling to p38 activation and this interaction is important for Cdo's effect during myogenesis. A later study also showed that Cdo binds to Bnip-2, a scaffold protein for Cdc42, and the Bnip-2/Cdc42 and JLP/p38 complexes associate in a Cdo-dependent manner, resulting in Bnip-2/Cdc42-dependent p38 activation and stimulation of myoblast differentiation (Kang et al., 2008).

3.1.4.3. *In vivo* implication of JIP4/JLP/SPAG9

An *in vivo* study on *Jip4* knock-out mice experiments showed that differently from JIP3 that is essential for life (Kelkar et al., 2003), JIP4 seems to be indispensable only in later stages of sperm development. Indeed, in comparison to wild-type mice, male fertility, sperm number and sperm function are reduced in homozygous knockout animals (Iwanaga et al., 2008). Interestingly, no activated JNK could be detected in testis of homozygous mice knockout, whereas activated JNK levels in the brain did not differ from heterozygotes or wild-type mice suggesting that JNK activation is dependent upon JIP4 specifically in sperm development (Iwanaga et al., 2008). An explanation of why the knockout experiment did not lead to more severe effects despite the ubiquitous expression of JIP4/JLP and its possible roles in various fundamental processes such as cellular transport (Bowman et al., 2000), cytokinesis (Montagnac et al., 2009) or myogenesis (Takaesu et al., 2006; Kang JS et al., 2008) could be that the exon targeted in this knockout model was the first ATG exon. In this way only the longer Jip4 isoforms are affected in knockout mice, leaving shorter isoforms such as JIP4 and SPAG9 intact. This suggests that the functions of these proteins in cellular transport, cytokinesis and myogenesis may not be affected by the specific loss of JLP or that JLP function can be compensated by the presence of other isoforms.

3.1.4.4. SPAG9 and cancer

The expression of the isoform SPAG9 was shown by RT-PCR and immunohistochemestry to be elevated in a variety of human cancers including renal, breast, cervical, thyroid, colon and lung carcinoma and it has been proposed to be used as a marker for early cancer detection (Garg et al., 2009a; Garg et al., 2009b; Garg et al., 2009c; Kanojia et al., 2009; Kanojia et al., 2011; Wang et al., 2013). Moreover SPAG9 silencing leads to a decrease in lung carcinoma-derived cells invasion and proliferation and to a down-regulation of mRNA and protein levels of MMP9 (Wang et al., 2013). However, no mechanism for SPAG9 role in invasion has been identified.

3.2. JIP3 and JIP4 in microtubule-based transport

Besides their role as scaffold proteins of the MAPK signaling pathways, JIP3 and JIP4 have been implicated in microtubule and molecular motor-based transport. Indeed a conserved function of all JIP proteins is their ability to interact with kinesin-1 the plus-tip directed microtubule motor (Bowman et al., 2000; Kelkar et al., 2005; Lee et al., 2002; Nguyen et al., 2005; Verhey et al., 2001). JIP3 and JIP4 have also been shown to interact with the (-)-end-directed dynein/dynactin motor (Cavalli et al., 2005; Montagnac et al., 2009).

In order to better understand JIP3 and JIP4 functions in microtubule-based transport I will shortly introduce the main aspects and functions of the two most known microtubule motors, kinesin-1 and cytoplasmic dynein associated to the dynactin complex, as they specifically interact with JIP3 and JIP4.

3.2.1. Microtubules motors

Two large families of molecular motors, kinesins and dyneins, drive intracellular transport along microtubule filaments. Kinesins control mainly the transport of cargoes towards the plus tips of microtubules, while (-)-end-directed transport is powered mainly by the cytoplasmic dynein. As molecular motors, these enzymes convert the chemical energy of ATP hydrolysis into mechanical energy and force production (Verhey and Hammond, 2009).

3.2.1.1. Kinesin-1

Kinesins are a wide family that comprises more than 45 mammalian genes and twice as many proteins due to alternative splicing (Hirokawa et al., 2009). All these proteins have a common kinesin motor domain that contains nucleotide- and microtubule-binding sites. Evolution has adapted this core motor domain by adding divergent non-motor regions that are important for isoform-specific functions such as cargo binding, regulation and localization. Most of the kinesin family members bear the motor domain at the NH_2-domain (they are named N-Kinesins) and drive microtubules (+)-end-directed motility (Hirokawa et al., 2009; Verhey and Hammond, 2009). Very important for understanding the cellular roles of kinesins is deciphering how these motors attach to specific cargoes but, even though many binding partners for individual motors have been identified, it is still largely unknown how motors distinguish and bind to specific cargoes in a time and spatially-controlled manner (Verhey and Hammond, 2009).

Kinesin-1, known as conventional kinesin, drives the transport of a variety of molecules including protein complexes, vesicles, RNA granules, and cytoskeletal components (Hirokawa et al., 2009). Kinesin-1 is a tetramer of two heavy chains (KHC or KIF5), each of them harboring the motor domain, and two accessory light chains (KLC), which do not posses any motor activity (Fig.27). There are three subtypes of KIF5 in mammals, KIF5B which is mainly ubiquitous and KIF5A and

KIF5C that are specific to neurons. There are four types of KLC (KLC1-4) that associate with approximately one-half of KIF5 dimers to produce tetramers. Kinesin-1, indeed, can also exist as a dimer composed only by the two heavy chains (Hirokawa et al., 2009). The association of cargoes to kinesin-1 is mediated by adaptor proteins that directly bind either KHC or KLC. The growing number of identified KLC and KHC binding partners is thought to reflect the complexity of the molecular machinery controlling kinesin-1's cargo selectivity (Hirokawa et al., 2009).

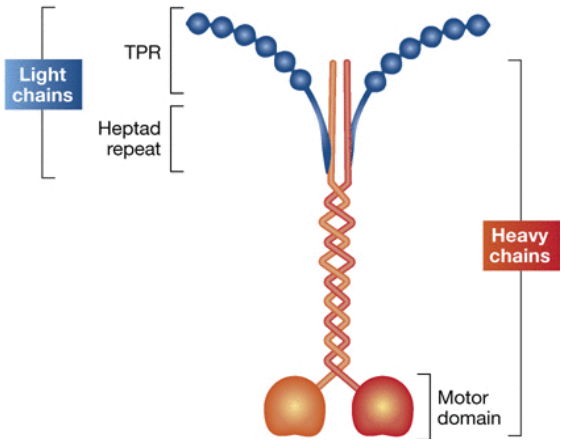

Figure 27: **Molecular composition of the motor kinesin1.** Kinesin-1 is a heterotetramer composed of two motor-containing heavy chains (orange) and two light chains (blue). The light chains associate with the heavy chains via heptad repeat regions in their N-terminus. The C-terminal half of the light chains is composed of six tetratricopeptide repeats (TPR), which represent cargo binding domains. Picture from the review (Dodding and Way, 2011).

In addition the binding of adaptor proteins to kinesin-1 is not only important for cargo transport but it is also believed to promote activation of the motor for microtubule binding and motility. When not transporting cargo, kinesin-1 is thought to be inactive due to a folded conformation positioning the KHC tail domain near the enzymatically active motor domain, thereby preventing ATP hydrolysis (Verhey and Hammond, 2009) (Fig.28, left part). In this folded state, kinesin exhibits decreased ATPase activity and diminished binding to microtubules. The KHC tail has also been shown to contain an ATP-independent microtubule-binding domain, which was suggested to 'park' kinesin on microtubules when not transporting cargo (Dietrich et al., 2008). Additionally, in the folded state, KLC is thought to contribute to the autoinhibition of kinesin-1 by pushing the KHC motor domains apart (Verhey et al., 1998). Binding to both KHC and KLC appears to be required to release the inhibition and to activate microtubule-dependent transport of kinesin-1 (Blasius et al., 2007; Verhey and Hammond, 2009). For instance Blasius and colleagues provided the first evidence that activation of Kinesin-1 needs the binding of two proteins, fasciculation and elongation protein-zeta1 (FEZ1) and JIP1 that bind to the two inhibitory regions of the kinesin1 (the KHC tail and the KlC subunit, respectively) for activation of microtubule binding and motility (Fig.28) (Blasius et al., 2007).

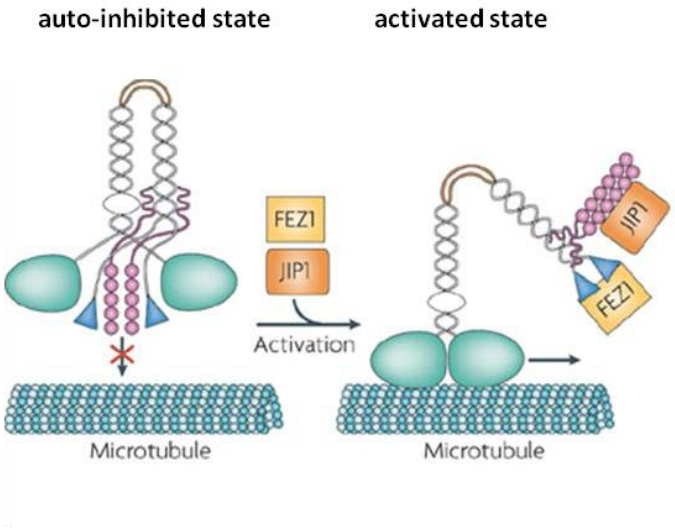

Figure 28: **Scheme representing kinesin-1 activation upon cargo-binding.** In the left, kinesin-1 is depicted in its auto-inhibited state with the tail of KHC folded near the motor domains and KLC pushing the motor domains apart. Autoinhibition of Kinesin-1 motor can be relieved (right part) by the interaction with two binding partners FEZ1 and JIP1, which release the restraints of microtubule binding and processive motility (Blasius et al., 2007). Pictures derived from the review Verhey and Hammond, 2009.

3.2.1.2. The dynein/dynactin complex

Cytoplasmic dynein is a giant 1.6 MDa complex that drives the transport of membrane-bound vesicles and tubules, together with their resident molecules, towards microtubule (-)-ends, which typically lie in the microtubule-organizing centre (MTOC) near the nucleus in non-dividing cells. Examples of organelles trafficked by cytoplasmic dynein include endosomes, lysosomes, phagosomes, melanosomes, peroxisomes, lipid droplets, mitochondria, vesicles from the endoplasmic reticulum (ER) destined for the Golgi, transcription factors, cytoskeletal filaments and mRNA-containing ribosomes (Roberts et al., 2013). Cytoplasmic dynein is also involved in clearing material from the periphery of the cell for degradation and recycling: at the distal tip of neurons, organelles and proteins are engulfed into autophagosomes and transported in a dynein-dependent manner towards the cell body for breakdown (Roberts et al., 2013).

Dynein (Fig.29A) consists of two copies of dynein heavy chain (DHC), each of them comprising six ATPase subunits called AAAs (ATPase associated with various cellular activities). ATP hydrolysis in AAA1 and AAA3 is the most important for motility. DHC binds to microtubules via a small globular domain at the end of an anti-parallel coiled-coil stalk domain that extends between AAA4 and AAA5. Two intermediate chains (ICs) bind directly to DHC, and three different light chains (LCs), Tctex1, LC8 and LC7/roadblock bind to the IC at separate sites. Two light intermediate chains (LICs) bind independently to DHC (Fig.29A). The ICs, LICs and LCs are each encoded by two genes in vertebrates and ICs and LICs may be alternatively spliced and present in different phospho-isoforms. This variation suggests that different versions of dynein may perform distinct tasks by binding preferentially to specific cargoes (Allan, 2011).

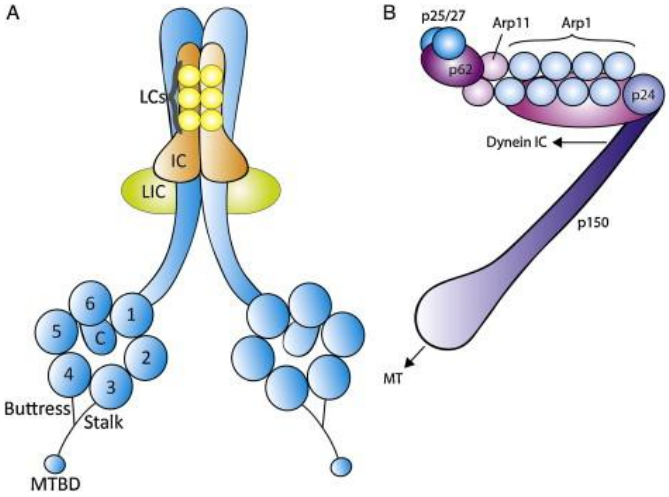

Figure 29: Molecular composition of the dynein (A) and dynactin complex (B). Picture from the review (Granger et al., 2014).

The dynactin complex (Fig.29B) is needed for virtually all dynein functions. Dynactin is a 1 MDa, multi-subunit protein complex involved in most aspects of cytoplasmic dynein function (Vallee et al., 2012). It consists of a filament of actin-related protein 1 (Arp1), decorated by capping proteins at the barbed (+)-end and a subcomplex of Arp11 and accessory subunits at the pointed (-)-end. The long projecting arm of dynactin (Fig.29B) is a 150 kDa protein called p150*Glued*. P150*Glued* contains a small microtubule-binding CAP-Gly (cytoskeleton-associated protein-glycine-rich) domain near its N-terminus, followed by two predicted α-helical coiled-coil regions (the first of which binds dynein through its intermediate chains) and a C-terminal Arp1-binding site (Vallee et al., 2012) (Fig.29B).

Dynactin regulation of dynein is complex and still not completely understood (Vallee et al., 2012). It was shown in vitro that dynactin enhances dynein's processivity (the number of steps a motor takes along the microtubule before falling off) of about two-fold (Kardon et al., 2009), without affecting its rate of movement or its ability to step backwards. The contribution of dynactin to dynein processivity was abolished by N-terminal truncation of p150*Glued* through coiled-coil domain 1. This domain has also been implicated in dynein binding and whether it contributes directly or indirectly to processivity remains to be explored (Vallee et al., 2012).

Many studies indicate that dynactin helps linking dynein to its cargoes (Kardon and Vale, 2009). For example it was shown an interaction between the ARP1 filament of dynactin and βIII spectrin, a filamentous protein that is found on the cytosolic surface of the Golgi and other cellular membranes (Muresan et al., 2001). P150*Glued* also links dynein to cargoes by binding to GTPases. For example an interaction occurs between the C terminus of p150*Glued* and SEC23, a GAP for SAR1, which assembles as part of the COPII coat on transport vesicles budding from the endoplasmic reticulum (ER) (Watson and Stephens, 2005). This interaction seems to be important for trafficking, as overexpression of the C terminus of p150*Glued* strongly inhibits the delivery of secretory proteins from the ER to the Golgi (Watson and Stephens, 2005). A similar set of

interactions facilitates dynein-dependent transport of late endosomes. The C terminus of p150*Glued* interacts with Rab-interacting lysosomal protein (RILP), a RAB7 effector that is found on late endosomes. This interaction is required for the localization of p150*Glued* to late endosomes and their subsequent transport by dynein (Johansson et al., 2007).

Dynactin was also shown to target dynein to the plus tips of microtubules. Although dynein is a (-)-end-directed motor, it often accumulates at the (+)-ends of microtubules, and dynactin has been shown to modulate this localization. The association of dynactin with the microtubule (+)-end, which has been best characterized in budding yeast, has been implicated in delivering dynein to sites where it is needed for transport. Indeed deletion or mutation of many dynactin subunits causes dynein to accumulate at astral microtubule (+)-ends and abolishes its localization to the bud cortex (Kardon et al., 2009). In metazoan the situation is more complex since localization of dynactin to the microtubule (+)-end requires the interaction with CAP-Gly domain-containing linker protein 170 (CLIP170) and end-binding 1 (EB1) in a mechanism not clearly understood. Following recruitment to microtubule (+)-ends dynein is loaded with cargo and dynactin promote its release from the microtubule (+)-end and the initiation of motility through an as yet unknown mechanism (Kardon and Vale, 2009).

In conclusion dynactin is essential for nearly every cellular function of cytoplasmic dynein. Dynactin helps to target dynein to specific cellular locations, links dynein to cargos and increases dynein processivity, although a comprehensive model of how these activities are integrated has yet to emerge (Kardon and Vale, 2009).

3.2.2. JIP3 and JIP4 functions in microtubule and molecular motor-based transport

3.2.2.1. Binding of JIP3 to microtubule (+)-end motor kinesin-1

JIP3 was initially identified as a kinesin-1-binding protein in a screen for adaptor proteins required for the interaction of kinesin-1 with axonal organelles and vesicles in *Drosophila* (Bowman et al., 2000). The screen led to the identification of a mutation in the gene Sunday Driver (SYD) resulting in a strong tail flipping phenotype characteristic of mutation in axonal transport and defect in microtubule motor function. SYD is the *Drosophila* orthologue of mammalian JIP3. SYD mutants displayed accumulation of several membranous axonal cargoes within the axons of the larval segmental nerve, phenotype nearly indistinguishable from that of mutants lacking kinesin1 (Bowman et al., 2000). This phenotype, together with the notion that JIP3 is a neuron-enriched protein (Ito et al., 1999; Kelkar et al., 2000), led the authors to hypothesize that SYD is a kinesin-1 binding protein required for microtubule-dependent axonal transport. The localization of JIP3 to the Golgi and to post-Golgi vesicles of the secretory pathway in mammalian epithelial cells transfected with JIP3-GFP suggested that JIP3 is a membrane-associated protein that could also functions in kinesin-1-based transport of post-Golgi

vesicles. Finally, the authors could demonstrate a physical interaction of JIP3/SYD with kinesin-1 using different techniques including two-hybrid, pull-down and co-immunoprecipitation of JIP3 from mouse brain extracts with kinesin-1 antibodies (Bowman et al., 2000). They also showed that this interaction occured between the NH_2-terminal half of JIP3/SYD and the TPR domain of kinesin light chains KLC1 and KLC2 (Bowman et al., 2000).

Similarly, Verhey *et al.* identified JIP1, JIP2 and JIP3 as partners for kinesin-1 and showed that they all bind to the TPR domain of KLC and that their cellular localization required kinesin-1 activity, indicating that JIPs are functional cargoes for kinesin1 (Verhey et al., 2001). They also proposed that JIP1 and JIP2 may interact with vesicles by binding directly to the cytoplasmic domain of transmembrane low density lipoprotein (LDL) receptors such as ApoER2. In fact, with co-immunoprecipitation and microtubule-binding assays, kinesin-1, JIP1, ApoER2 and the JNK MAPKKK kinase DLK were all found in the same complex. In addition, the localization of JIP1, JIP2 and DLK to the tip of neurites could be perturbed by over-expression of the TPR domain of KLC. Thus, kinesin-1 may be linked to transport vesicles through JIP1/2 scaffold proteins, which bind to transmembrane receptors of the LDL family (Verhey et al., 2001). However, evidence for such a mechanism for JIP3 are missing and it is still unclear how JIP3 associates to cargo membrane.

Interestingly, Hammond *et al* demonstrated that JIP1 and JIP3 are co-transported by kinesin-1 since besides binding to each other (JIP3 binds to the PTB domain of JIP1 (Fig.24) and form heterodimers) they also bind to separate sites on the KLC TPR bundle and may facilitate each other's binding and transport (Hammond et al., 2008). Indeed, although JIP1 and JIP3 can interact independently with KLC in yeast two-hybrid and co-immunoprecipitation experiments, they bind with higher affinity when they are part of a tripartite JIP1/JIP3/KLC complex. Thus, it was speculated that this complex could facilitate the inclusion of many proteins into the transport complex and cross talk between JNK and its different substrates.

Therefore an intriguing issue arising from these studies is whether JIP3 could function as a link between JNK signaling and microtubule-based transport. Byrd and colleagues indeed showed that in the motor neuron of *C. elegans larvae,* loss-of-function mutations of *unc-16* (JIP3/SYD orthologue) result in mislocalization of synaptic vesicles and glutamate receptor markers (Byrd et al., 2001). UNC-16, similarly to mammalian JIP3, physically interacts with *C. elegans* JNK-signaling proteins JNK-1, JKK-1 and SEK-1 and mutations in *jnk-1* and *jkk-1* result in synaptic vesicle mislocalization similar to *unc-16* mutants, supporting a role for JNK signaling in the transport process of synaptic vesicles. Consistent with an interaction of conventional kinesin-1, mutations in *unc-116* (*C. elegans* orthologue of kinesin heavy chain/KIF5) display phenotypes similar to *unc-16* and mislocalize GFP-tagged UNC-16. All together these data suggest that UNC-16 regulates vesicle transport through its association with both JNK-signaling

components and kinesin1 motor (Byrd et al., 2001). A recent study also showed that mammalian JIP3 binds the neuronal receptor tyrosine kinase receptor B (TrkB) which is required for brain-derived neutrophic factors (BDNFs) signaling and mediates TrkB anterograde transport by making a complex with KLC (Huang et al., 2011).

In conclusion, these studies suggest a role for JIP3 (and its orhologues unc-16 in *C. elegans* and SYD in *Drosophila*) not only as a cargo for kinesin-1 but also as an adaptor protein mediating the binding of axonal vesicles to kinesin-1 and regulating their transport towards axonal compartments.

Interestingly, a recent study described a novel function of JIP3/SYD as a positive regulator of kinesin-1 by interacting directly with the tail domain of KHC in addition to and independently of its interaction with KLC (Sun et al., 2011). Using an *in vitro* motility assay, the authors showed that JIP3/SYD promotes efficient motility of KHC along microtubules, increasing both its run length and velocity. Importantly, JIP3/SYD binding to KHC is functional in rat hippocampal neurons as JIP3/SYD mutants that bind KHC but not KLC are transported to axons and dendrites similarly to wild-type JIP3/SYD (Sun et al., 2011). These data suggest that JIP3/SYD binding to the KHC tail domain relieves an inhibition by the KHC tail domain, activating or opening KHC to bind microtubules for long-range motility.

3.2.2.2. Binding of JIP4/JLP to KLC

JIP4 and JLP have also been shown to interact with KLC. Kelkar and colleagues showed that KLC co-immunoprecipitates with both JIP3 and JIP4 and they identified the TPR domain of KLC and the LZII domain of JIP3/4 as being responsible for this interaction (Fig.25-26) (Kelkar et al., 2005). Similarly, a 2-hybrid interaction was observed between the LZII domain of JLP and the TPR domain of KLC1 (Nguyen et al., 2005). In addition, over-expression of a dominant negative form of KLC1 resulted in the mislocalization of endogenous JLP arguing that this interaction is functional (Nguyen et al., 2005).

3.2.2.3. Binding of JIP3/4 to microtubule (-)-end motor dynactin/dynein

Importantly, JIP3 and JIP4 have also been shown to bind to the dynein/dynactin complex and to regulate (-)-end directed vesicle motility and retrograde transport in neurons (Abe et al., 2009; Cavalli et al., 2005; Drerup and Nechiporuk, 2013; Montagnac et al., 2009).

Cavalli *et al*. for the first time showed that JIP3 is transported together with JNK3 in both anterograde and retrograde routes and binds to dynactin (Cavalli et al., 2005). The authors performed nerve ligation experiments, in which mouse sciatic nerves were subjected to ligature at the midpoint, and nerve portions proximal or distal to the ligation were analyzed by immunofluorescence microscopy (Fig.30). While amyloid precursor protein (APP), a typical marker for anterograde transport, accumulated primarily on the proximal side of the ligation,

phospho-TrkA, a typical marker for retrograde transport, accumulated on the distal side and JIP3 and JNK3 accumulated on both proximal and distal sides (Fig.30) (Cavalli et al., 2005).

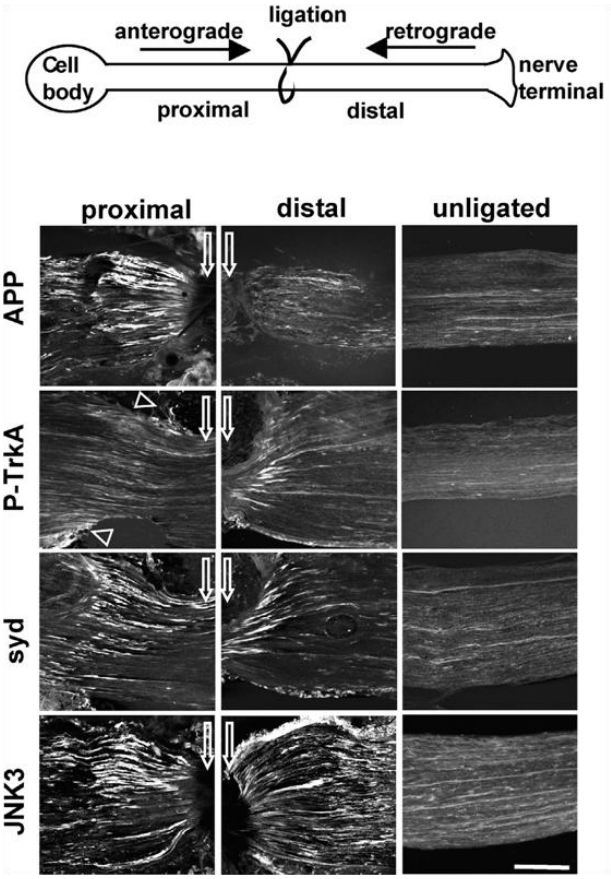

Figure 30: **Picture showing that JIP3/SYD and JNK3 are transported in both the anterograde and the retrograde pathways.** The drawing on the top shows the procedure of nerve ligation, in which sciatic nerves are ligated unilaterally at the midpoint and processed for immunofluorescence. APP accumulates primarily on the proximal side of the ligation, whereas phospho-TrkA primarily accumulates on the distal side (arrowheads point to nonspecific staining of the perineurium). JIP3/SYD and JNK3 accumulate on both proximal and distal sides. White arrows point to ligation site. Scale bar:100 µm. Picture from Cavalli et al., 2005.

Moreover JIP3 and JNK3 are associated to synaptic vesicles, suggesting that they are transported on axonal vesicles, which are transported in both directions. Co-immunoprecipitation experiments from mice sciatic nerve extracts showed that JIP3 interacts with the two subunits of the dynactin complex p50-dynamitin and p150*Glued* and immunofluorescence analysis in axons showed that JIP3 colocalizes with p150*Glued* and to some extent to DHC (Cavalli et al., 2005). Moreover, the authors showed that sciatic nerve injury provoked by ligation induced JNK activation and increased association of JIP3 with dynactin and consequently increased retrograde transport of JIP3 and JNK3 to the cell body (Cavalli et al., 2005). Based on these findings, a model was proposed in which JIP3 is part of a damage surveillance system in axons; JNK is activated at injury sites and this favors binding of JIP3 to dynactin and retrograde transport of JNK and JIP3 on axonal vesicles towards the cell body, where JNK can initiate gene transcription for axon repair.

Therefore, JIP3 may function as a scaffold that favors transport of JNK and its associated MAPKKs and MAPKKKs bidirectionally along microtubules, a notion that could be experimentally verified in a later study (Abe et al., 2009). Indeed using a biochemical approach, Abe *et al.* identified two pools of vesicles associated with JIP3 with distinct protein composition

and morphology; a population of small anterogradely trafficking vesicles that contain mainly adhesion and cytoskeletal proteins with a possible function in neurite outgrowth and guidance (Abe et al., 2009), and a second pool of large vesicles positive for endosomal markers such as Rab5, Rab7, Rab11, dynamin, AP2, clathrin and therefore belonging to the endocytic pathway. In vivo labeling of endocytic endosomes with fluorescently-tagged endocytic tracer dextran confirmed JIP3 colocalization with these endosomes (Abe et al., 2009). These endosomes trafficked both retrogradely and anterogradely and JIP3 by binding to both kinesin-1 and dynactin was proposed to function as a regulatory switch for motors of opposing directions. Moreover because JIP3-associated endosomes contain the synaptic vesicle proteins synaptophysin and syntaxin 1, JIP3 may also function to transport synaptic vesicle components to the synapse, similarly to its *C. elegans* homolog UNC-16 whose loss of function also results in mislocalization of synaptic vesicle marker synaptobrevin (Byrd et al., 2001; Sakamoto et al., 2005). In addition, the observation that JIP3 associates with Rab5-containing endosomes is in agreement with another study that showed that loss of function of UNC-16, lead to an accumulation of enlarged Rab5-containing compartments and decreased number of synaptic vesicles in GABAergic synapses (Brown et al., 2009). JIP3 therefore may play a key role in synaptic transmission by regulating synaptic vesicle formation and recycling (Abe et al., 2009).

C. elegans UNC-16 (JIP3) was also shown to bind dynein intermediate light chain (LIC, DLI-1 in *C. elegans*) and to form a complex with kinesin-1 (Arimoto et al., 2011), suggesting that UNC-16 could signal changes in cargo direction through physical interaction with both a (+)-end–directed and a (-)-end–directed microtubule motor. By 2-hybrid, UNC-16 bound DLI-1 through its N-terminal region. However, interaction did not occur between full-length UNC-16 and DLI-1, suggesting that full-length UNC-16 was in a closed conformation. UNC-16 co-immunoprecipitated with DLI-1 when KLC-2 was co-expressed, suggesting that KLC-2, which binds to UNC-16 via a distinct domain could convert UNC-16 to a conformation accessible by DLI-1. In addition, localization of DLI-1 at (+)-ends of nerve microtubules depended both on kinesin-1 and UNC-16 suggesting that kinesin-1 and UNC-16 are required for the localization of cytoplasmic dynein to microtubule (+)-ends (Arimoto et al., 2011). The authors finally proposed a model in which the interaction between UNC-16 and KLC-2 may trigger loading of the dynein complex to the kinesin-1 motor at microtubule (-)-ends in cell bodies. Thus, the UNC-16–kinesin-1 complex would act as a motor for anterograde transport of the dynein complex in neurons, with UNC-16 functioning as an adaptor between kinesin-1 and dynein (Arimoto et al., 2011).

3.2.2.4. JIP3 controls lysosome retrograde transport

In zebrafish, JIP3 was also shown to mediate retrograde transport of two distinct cargoes: active JNK and lysosomes (Drerup and Nechiporuk, 2013). In this animal model, JIP3 loss of function mutants caused abnormal accumulation of phosphorylated-JNK and lysosomes at axon

terminal resulting in swelling of the terminus. Loss of JIP3 decreased frequency of retrograde transport of active JNK and lysosomes but not of other components of the endosomal system, such as late endosomes and autophagosomes, and did not affect anterograde transport (Drerup and Nechiporuk, 2013). This study thus contrasts with Abe *et al*., who showed that JIP3 binds to different types of endocytic cargoes that traffic in both directions (Abe et al., 2009). Drerup *et al*. showed that direct interaction of JIP3 and JNK was necessary to prevent accumulation of active JNK and axon terminal swelling suggesting that JIP3 functions as a carrier for JNK. JIP3 also mediated retrograde lysosome transport by facilitating lysosome interaction with the dynein motor through binding to the DLIC (Drerup and Nechiporuk, 2013).

3.2.2.5. JIP3 and JIP4 control endosome movement required for cytokinesis

Another contribution to the understanding of the role of JIP3/JIP4 in microtubule-based traffic came from a study from our laboratory using a non-neuronal system, during cytokinesis in HeLa cells (also see paragraph 2.3.3.1). By yeast 2-hybrid and *in vitro* pull-down assays Montagnac *et al*. showed that JIP3 and JIP4 binds to GTP-bound ARF6 through their LZII domain, previously known to mediate binding of mammalian JIP3 and JIP4 and drosophila SYD to the TPR domain of KLC (Bowman et al., 2000; Nguyen et al., 2005; Verhey et al., 2001). In addition, the authors identified the LZII domain as the binding site for p150*Glued* and p50 dynactin complex subunits (Fig.25-26). Moreover, in solution, GTP-ARF6 competed with kinesin-1 for binding to JIP3 or JIP4 and favored a complex of JIP3 or JIP4 with dynactin (Montagnac et al., 2009). The authors proposed a model in which when ARF6 is inactive (GDP bound) JIP3 and JIP4 would be free to interact with kinesin-1 and to move along towards microtubules (+)-ends. Upon activation of ARF6 and interaction of GTP-ARF6 with JIP3 or JIP4, occurring likely at the plasma membrane, kinesin-1 would be replaced by dynactin on JIP3 or JIP4, thus switching movement of JIPs' cargos towards microtubule-(-)-end (Montagnac et al., 2009). As a biological consequence, interfering with ARF6, JIP4, KLC and p150*Glued* affected early endosome (TfR-positive) trafficking in and out of the intracellular bridge of dividing cells during late cytokinesis and delayed abscission (Montagnac et al., 2009).

This study identified ARF6 as a molecular switch that controls JIP3/JIP4-dependent directionality of vesicles along the microtubules. JIP3 and JIP4 were also shown to interact with active ARF6 in neurons (Suzuki et al., 2010). Pull-down assays with mouse brain extract showed that JIP3 and JIP4 interacts with ARF6Q67L, but not with ARF6T27N and overexpression of a mutant of ARF6 unable to interact with JIP3, called ARF6TriM (T53E/K58C/N60T), or JIP3 knockdown in mouse cortical neurons stimulated neurites elongation and branching (Suzuki et al., 2010). In this study the authors speculated that ARF6 through interaction with JIP3 could be responsible for the retrograde transport of endosomal cargoes, which could contain membrane-

constituting materials essential for neurites elongation, thereby negatively regulating elongation and branching of axons and dendrites (Suzuki et al., 2010).

3.2.2.6. GTP-ARF6 interaction with JIP3 and JIP4

The use of an ARF6 mutant (ARF6iSW) in which the interswitch region was replaced with the corresponding ARF1 region completely disrupted interaction between ARF6 and JIP4 suggesting that JIP4 specifically recognizes the interswitch region of ARF6 and not that of ARF1 (Montagnac et al., 2009). Expression of ARF6iSW lead to cytokinesis defects similar to those observed when ARF6 or JIP4 function was inhibited, showing that these proteins work together during abscission (Montagnac et al, 2009).

The crystal structure of a complex between *E. coli*-expressed ARF6Q67L (ARF6-GTP) and the LZII domain of JIP4 was later solved (Isabet et al., 2009). It showed an ARF6-$(JIP4)_2$-ARF6 heterotetramer with the JIP4-LZII homodimer recruiting two ARF6 molecules at its centre in a dyad-symmetric manner (Fig.31) (Isabet et al., 2009). ARF6 molecules in complex with JIP4 contain the G-domain typical of the Ras superfamily with a central six-stranded β sheet flanked by five α helices (Fig.31) and were overall very similar to uncomplexed ARF6-GTPγS solved previously by *Pasqualato* and colleagues (Pasqualato et al., 2001) (Fig.13, section 2.2.). The LZII domain of JIP4 consisted of nine-heptad repeats with the characteristic leucine residue in position -d- except in the seventh heptad repeat, showing a valine residue (alanine residue in JIP3) in place of the characteristic leucine. The JIP4-LZII domain complexed to ARF6 consisted of two α-helices that wind around each other in a long and straight parallel coiled-coil structure (Fig.31). This structure was similar to that of JIP4-LZII in solution in the absence of ARF6 (Isabet et al., 2009). Each JIP4 helix bridges two opposing ARF6 molecules, and conversely, each ARF6 molecule interacts with both helices that comprise the LZ. No interaction is observed between the two ARF6 molecules bound to JIP4-LZII in the crystal suggesting that ARF6 molecules do not cooperate for binding to JIP4 (Isabet et al., 2009).

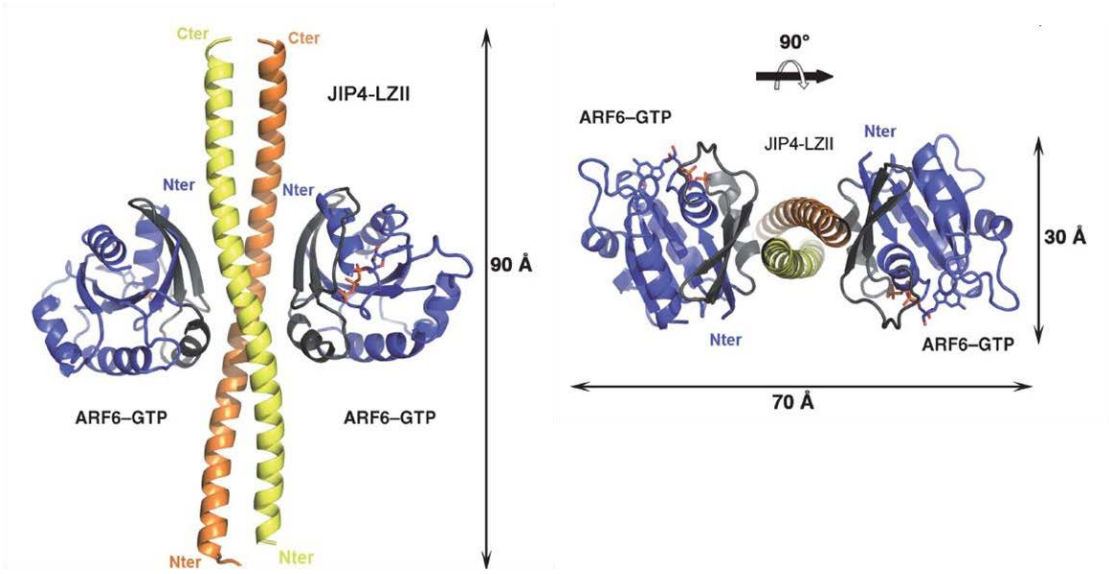

Figure 31: **The overall structure of the ARF6–JIP4-LZII heterotetrameric complex.** ARF6–GTP is drawn in blue with the switch regions in grey and the two monomers of JIP4-LZII are drawn in yellow and orange. Two orthogonal views of the complex are shown. Picture from Isabet et al., 2009.

Importantly, this heterotetrameric complex occurs between GTP-ARF6 and JIP4/LZII domain when the two molecules are in solution. In the *in vivo* situation where GTP-ARF6 is presumably bound to membrane through its myristoylated N-terminal helix, it is likely that the complex would be unable to attain a 2:2 stoichiometry. Indeed, modeling of the ARF6–$(JIP4)_2$–ARF6 heterotetramer at the membrane interface according to the orientation of membrane- bound ARF6, revealed that JIP4-LZII would stand perpendicular to the membrane, generating a severe clash between the membrane and the C-terminal part of the straight coiled-coil of JIP4-LZII (Fig.32A). Therefore, the elongated LZII of JIP4 more likely aligns tangentially to the membrane (Isabet et al., 2009), and in that case only one ARF6-GTP molecule can be membrane-anchored at a time. Indeed, the second ARF6–GTP molecule is oriented with its myristoylated N-terminal helix opposite to the membrane (Fig.32B). Thus, this model supports the idea that when GTP-ARF6 is associated to the membrane, a dimer of JIP4 interacts with only one GTP-ARF6 molecule forming a heterotrimer (Fig.32C) (Isabet et al., 2009).

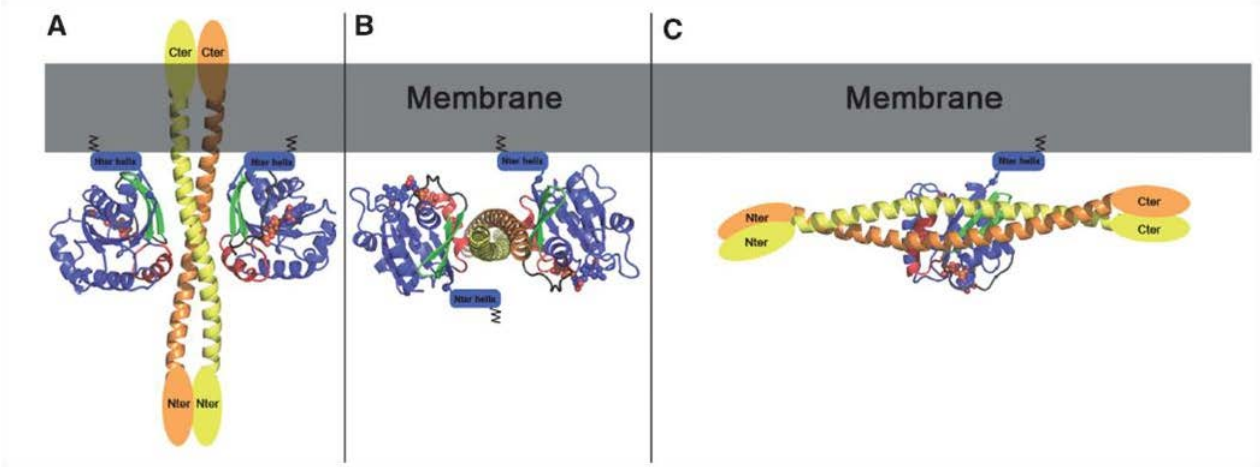

Figure 32: **ARF6–JIP4 interactions at the membrane.** (A) Model of the ARF6–$(JIP4)_2$–ARF6 heterotetramer at the membrane obtained when both ARF6 molecules are anchored to the membrane. ARF6 molecules are shown in blue with switch II in red and the interswitch in green. The myristoylated amphipatic N-terminal helix of ARF6 that is critical for interaction with membrane is indicated as a blue cylinder lying against the membrane (B) Model of the ARF6–$(JIP4)_2$–ARF6 heterotetramer at the membrane considering that JIP4 is positioned tangentially with respect to the membrane. In this model, one ARF6 molecule is oriented with its N-terminal part close to the membrane, whereas that of the second ARF6 molecule is turned toward the cytosol, suggesting that only one ARF6 molecule interacts with JIP4 at the membrane. (C) Model of an ARF6–$(JIP4)_2$ heterotrimer at the membrane. Picture from Isabet et al., 2009.

Therefore the model previously proposed based on interaction of the different proteins in solution (Montagnac et al., 2009) in which ARF6 by binding to JIP4 favors interaction of JIP4 with dynactin, needs to be partially revisited. Indeed, *in vivo*, if the monomer of JIP4 bound to ARF6 and oriented towards the membrane is favored in binding the dynactin subunits, the cytosolic face of the coiled-coil of JIP4 is still available for binding either to kinesin-1 or dynactin. Thus the role of ARF6 in the regulation of JIPs' interaction with motors and endosomes trafficking as was described by Montagnac *et al.* needs to be better understood.

3.2.2.7. A general scheme of JIP3/JIP4 function in vesicle transport

Figure 33 summarizes most of the functions described so far for JIP3 and JIP4 in microtubules-based intracellular transport. JIP3 and JIP4, in addition to their role as scaffold proteins in MAPK signaling pathways, physically interact with kinesin-1 and dynein/dynactin and functions as adaptor proteins linking motors to cargoes. The mammalian JIP3, its *C. elegans* orthologue UNC-16 and the *Drosophila* orthologue SYD all bind to KLC (Bowman et al., 2000; Byrd et al., 2001; Montagnac et al., 2009) and SYD and UNC-16 loss-of-function mutants have neuronal defects similar to those of *Drosophila* and *C. elegans* kinesin-1 mutants, with accumulation of axonal and synaptic vesicles along the axon (Bowman et al., 2000; Byrd et al., 2001). The findings that JIP3 associates with vesicles containing the synaptic markers synaptobrevin, synaptophysin and syntaxin 1 (Abe et al., 2009; Byrd et al., 2001) suggest a role

for JIP3 in transport of synaptic vesicles to the synapse but this hypothesis needs further investigation. These data also suggest a role for JIP3 as an adaptor protein for kinesin-1 carrying axonal and synaptic vesicles and the components of the JNK kinase cascades in the neuronal anterograde transport.

Moreover JIP3 positively regulates kinesin-1 activity by binding to KHC and enhancing motor activity (Sun et al., 2011). Indeed, JIP3 binding to KHC tail domain efficiently relieves the autoinhibition by the KHC tail domain, activating or opening KHC to bind microtubules for long-range motility. It is currently not known whether JIP3/SYD may fulfill activation of tetrameric kinesin-1 via its ability to interact with both KHC and KLC or, similar to the JIP1–Fez1 complex (Blasius et al., 2007), JIP3/SYD may require additional interacting partners for the activation of tetrameric kinesin-1.

JIP4 was also shown to interact with KLC and to be transported by kinesin-1 in the cytosol (Kelkar et al., 2005; Nguyen et al., 2005) but its function in microtubule-based anterograde transport was not investigated yet. However considering JIP4 structural similarities with JIP3 and its more ubiquitous distribution in mammalian tissues, it is possible to speculate that also JIP4 could have an important role in intracellular transport.

Importantly JIP3 and JIP4 have been implicated also in the retrograde transport of several cargoes thanks to their ability to bind to two subunits of the dynactin complex (Cavalli et al., 2005; Montagnac et al., 2009). JIP3 has been found associated with vesicles of the endocytic pathway that are transported mainly retrogradely (Abe et al., 2009) and JIP3 loss of function in zebrafish causes an abnormal accumulation of lysosomes at the axon termini (Drerup and Nechiporuk, 2013), suggesting a role for JIP3 in the clearance of endosomes at the axon terminal and in transporting them retrogradely to the cell body. JIP3 is also clearly involved in the retrograde transport of JNK (Cavalli et al., 2005; Drerup and Nechiporuk, 2013). Activation of JNK might also block kinesin-1-driven transport and favor the retrograde transport. A work in *Drosophila melanogaster* has shown that activation of JNK by its upstream kinases results in dissociation of the kinesin-1 motor from the JIP1 cargo protein (Horiuchi et al., 2007). It is not known whether a similar mechanism occurs also for JIP3, but it was demonstrated that under some stress conditions such as neuronal injury, local activation of JNK is induced and results in a shift from anterograde transport to retrograde transport of JIP3 and JNK by favoring the binding of JIP3 with dynactin (Cavalli et al., 2005). GTP-bound ARF6 has also been identified as a possible molecular switch that could drive JIP3 and JIP4 binding to dynactin complex and influence the trafficking of endocytic vesicles along the microtubules (Montagnac et al., 2009; Suzuki et al., 2010). Active ARF6 indeed binds to JIP3 and JIP4 and this interaction inhibits the binding of kinesin-1, while it favors the binding with dynactin (Montagnac et al., 2009).

ARF6 binding to JIP3 and JIP4 could also represent one of the possible ways through which JIP3 and JIP4 are linked to their specific cargo vesicles. Indeed, even though JIP3 was

shown to be a protein peripherically associated to membranes (Cavalli et al., 2005) and JIP3 and JIP4 have been shown to interact with some membrane receptors such us TrkB and Cdo respectively (Huang et al., 2011; Takaesu et al., 2006), to date how JIP3 and JIP4 associate to membranes and recognize their specific cargo vesicles still remains elusive.

In conclusion, even though JIP3 and JIP4 seem to be strongly implicated in intracellular transport, there are still many open questions regarding their precise functions in neuronal and non-neuronal cells and very little is known about their implications in normal physiology and diseases.

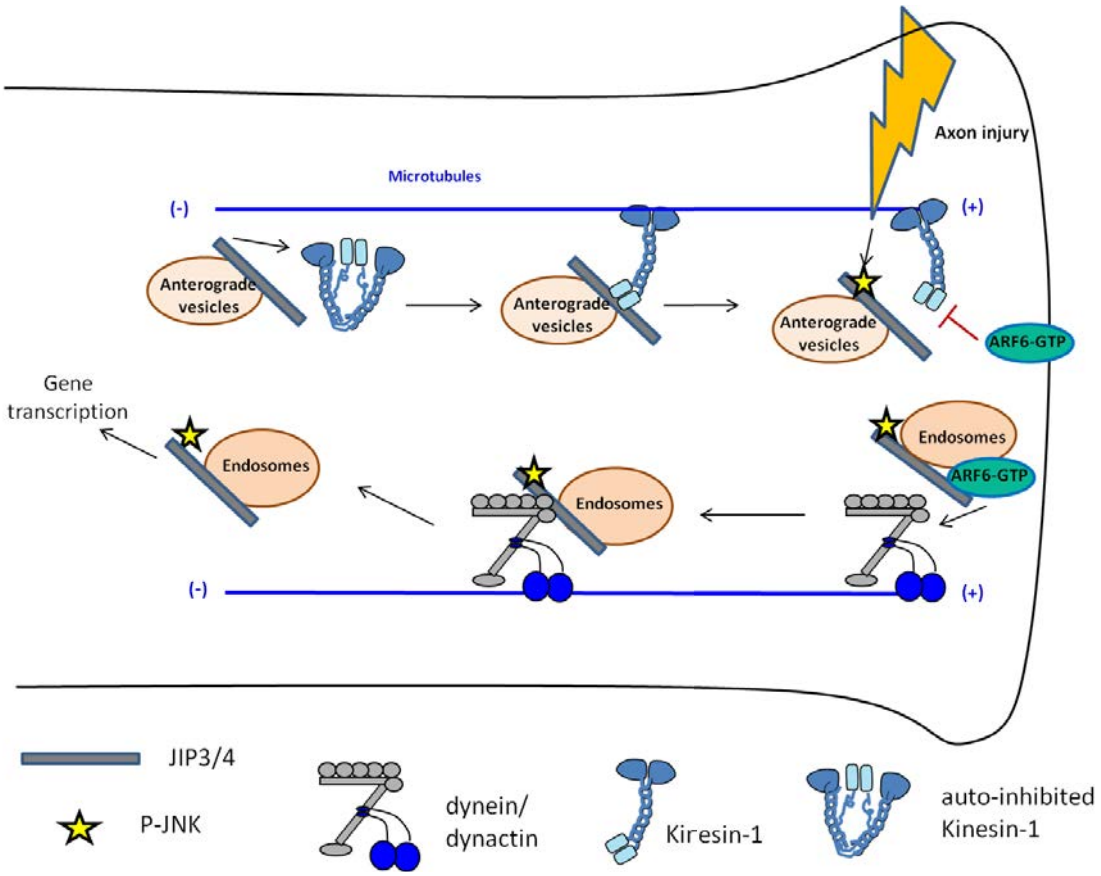

Figure 33: **Schematic representation of the role of JIP3/JIP4 in microtubules-based transport.** JIP3 activates the motor activity of kinesin-1 and by binding to KLC functions as an adaptor for axonal and synaptical vesicles. JIP3 also binds to dynactin and it mediates the retrograde transport of several endocytic vesicles and lysosomes. Activation of JNK by axon injury causes the release of JIP3 cargos from kinesin-1 and the dynactin/dynein-mediated transort of phospho-JNK towards the nucleus to trigger gene expressions. Binding with ARF6-GTP also causes a switch from JIP3/4-kinesin-1-mediated transport to JIP3/4-dynactin-mediated one.

Chapter 4: ARF6-JIP3/4-MT1-MMP axis controls a matrix invasion program during breast cancer progression

4.1. Introduction to Article 1

The main purpose of my experimental work was to investigate the role of ARF6 in breast cancer cell invasion. As previously said, ARF6 represents a good candidate for the regulation of the invasive programs of cancer cells thanks to its ability to regulate the actin cytoskeleton remodelling and the recycling and polarized delivery of membranes and surface receptors important for cell adhesion, migration and polarity (D'Souza-Schorey and Chavrier, 2006; Donaldson and Jackson, 2011). Although ARF6 has been already implicated in cancer cell invasion and several lines of evidence underlined a role for ARF6 downstream EGFR activation in breast cancer cells (Hashimoto et al., 2004; Morishige et al., 2008; Onodera et al., 2005), to our knowledge there are no data in the literature that implicated ARF6 in the trafficking and polarized delivery of MT1-MMP at the site of invasion of cancer cells.

MT1-MMP trafficking and regulation is a major subject of interest of my host lab. Indeed, in order to provide future potential therapeutic targets it is of crucial importance to understand the cellular components and molecular pathways involved in MT1-MMP exocytosis and MT1-MMP-dependent ECM pericellular proteolysis.

The work of G. Montagnac, a former member of the lab, delineated a mechanism through which ARF6, by interacting with two previously unknown effectors JIP3/JIP4, controlled a motor switch mechanism that moved recycling endosomes in opposite directions, necessary for completion of cytokinesis in HeLa cells (Isabet et al., 2009; Montagnac et al., 2009). An intriguing hypothesis was that breast cancer cells could use a similar ARF6/JIP3/4 axis to regulate the microtubule-based transport of MT1-MMP at the surface.

The article manuscript that will follow in this session was aimed to test the validity of this hypothesis. In particular I assessed the implication of ARF6 and JIP3/4 loss of function with different cell invasion assays and in MT1-MMP trafficking and exocytosis by live-cell imaging techniques. Moreover in collaboration with the pathological department of the Curie hospital of Paris and the project PIC-BIM (“Projet incitatif et coopératif-Breast cancer invasion and motility”, coordinated by Drs. A. Vincent-Salomon and P.Chavrier), we could analyze for the first time by immunohistochemestry ARF6 expression in a wide cohort of human breast cancer samples.

4.2. Article 1: ARF6-JIP3/4-MT1-MMP axis controls a matrix invasion program during breast cancer progression

Article to be submitted

Authors: Valentina Marchesin, Catalina Lodillinsky, Joanna Cyrta, Laetitia Fuhrmann, Marie Irondelle, Asma Soltani, Alan Guichard, Anne Vincent-Salomon, Guillaume Montagnac and Philippe Chavrier

ARF6-JIP3/JIP4-MT1-MMP axis controls a matrix invasion program during breast cancer progression

Valentina Marchesin[1,2], Catalina Lodillinsky[1,2], Joanna Cyrta[1,2], Laetitia Fuhrmann[1], Marie Irondelle[1,2], Asma Soltani[1,2], Alan Guichard[1,2], Anne Vincent-Salomon[1,3], Guillaume Montagnac[1,2,†] and Philippe Chavrier[1,2,*]

[1] Institut Curie, Research Center, 75005 Paris, France

[2] Membrane and Cytoskeleton Dynamics, Centre National de la Recherche Scientifique UMR144, 75005 Paris, France

[3] Institut Curie, Pathology Department, 75005, Paris, France

* Corresponding author (e-mail: philippe.chavrier@curie.fr)

[†] Present address: Institut Gustave Roussy, Inserm U1009, Villejuif, France

ABSTRACT

Initial steps in breast cancer dissemination require tumor epithelial cells to cross tissue barriers through a matrix invasion program involving the trans-membrane type 1 matrix metalloproteinase (MT1-MMP). Here we address the contribution of ARF6 and its downstream effectors JIP3 and JIP4 to the regulation of MT1-MMP endosomal trafficking and consequences for the invasive potential of breast tumor cells. Depletion of ARF6 or JIP3/JIP4 attenuates matrix remodeling and invasive potential of breast tumor cell lines in a 3D type collagen environment *in vitro,* reduces exocytosis of MT1-MMP from late endosomes and correlates with MT1-MMP-positive endosome mispositioning through a mechanism involving microtubule minus-end directed dynactin/dynein motor activity. ARF6 is overexpressed in clinical samples of invasive ductal breast cancers, translocates to the plasma membrane of breast tumor cells and correlates with elevated levels of plasma membrane MT1-MMP in a subset of high-grade triple-negative breast cancers. Our results identify ARF6 as a regulator of dynamic microtubule-based trafficking of MT1-MMP-containing endosomes to support exocytosis and surface expression of MT1-MMP essential for pericellular matrix remodeling during breast cancer invasion.

INTRODUCTION

Metastasis - the process by which cells from a primary tumor invade local tissues and disseminate to distant sites - marks the transition from a benign tumor to a lethal, malignant cancer. One intrinsic property of metastatic tumor cells that allows them to breach tissue barriers is their ability to degrade proteins of the extracellular matrix (ECM). ECM remodeling by cancer cells depends on matrix-degrading proteases (Kessenbrock et al., 2010). Membrane-anchored matrix metalloproteinases (MMPs) including membrane type (MT)1-MMP (Sato et al., 1994) have been recognized as important proteases involved in invasive tumor growth and metastasis (Bartolome et al., 2009; Devy et al., 2009; Hotary et al., 2003; Perentes et al., 2011; Szabova et al., 2008). The current view based on *in vitro* work using native or reconstituted matrix is that expression of MT1-MMP at the surface of neoplastic cells is essential for remodeling and transmigration through the basement membrane and for invasive migration through fibrillar collagen gels (Hotary et al., 2006; Monteiro et al., 2013; Sabeh et al., 2004; Sabeh et al., 2009; Sodek et al., 2007; Wolf et al., 2013; Wolf et al., 2007).

The current view is that interaction of matrix receptors on the tumor cell surface with components of the ECM leads to assembly of plasma membrane protrusions containing F-actin and cortactin called invadopodia, which mature into matrix-degrading structures upon accumulation of MT1-MMP (Artym et al., 2006; Murphy and Courtneidge, 2011). In MDA-MB-231 human breast adenocarcinoma cells, newly synthesized MT1-MMP reaches the plasma membrane where it is rapidly endocytosed (Poincloux et al., 2009). The majority of internalized MT1-MMP is located in late endosomes (LEs)/multivesicular bodies from where it can recycle to plasma membrane invadopodia (Hoshino et al., 2013; Monteiro et al.,

2013; Rosse et al., 2014; Steffen et al., 2008; Sung et al., 2011; Williams and Coppolino, 2011; Yu et al., 2012). Various studies, including our own, identified components of the machinery required for exocytosis of MT1-MMP-positive LEs to the invadopodial plasma membrane; these include the WASH complex (Arp2/3 complex activator present on MT1-MMP-containing LEs) and cortactin (regulator of Arp2/3-dependent F-actin networks), the exocyst complex (octameric complex required for docking MT1-MMP-positive LEs to the invadopodial plasma membrane), the exocytic Rab27a small GTPase and VAMP7 (v-SNARE protein involved in LE-plasma membrane fusion events) (Artym et al., 2006; Clark et al., 2007; Hoshino et al., 2013; Monteiro et al., 2013; Sakurai-Yageta et al., 2008; Steffen et al., 2008; Sung et al., 2011; Williams and Coppolino, 2011). We recently proposed that through the coordinated functions of WASH and exocyst complexes, formation of LE-to-plasma membrane connections ensure MT1-MMP targeting to invadopodia (Monteiro et al., 2013). One implication of this model is that MT1-MMP-positive LEs should be positioned close to the PM to allow membrane connections to form. Along this line, MT1-MMP-positive vesicles were found to travel along microtubules and microtubule plus-end-directed kinesin-family motor proteins control exocytosis of MT1-MMP in human macrophages (Wiesner et al., 2010).

ARF6, a member of the ADP-ribosylation factor subfamily of Ras-related monomeric GTP-binding proteins, is present at the plasma membrane where it regulates the internalization and recycling of plasma membrane components and receptors through its GTPase cycle (D'Souza-Schorey and Chavrier, 2006). A large body of work implicates ARF6 in the motile phenotype of epithelial cells and the invasive and metastatic potential of breast carcinoma cells (Donaldson and

Jackson, 2011). Overexpression of ARF6 correlates with increased matrix invasion activity of melanoma and breast tumor-derived cell lines (Hashimoto et al., 2004; Tague et al., 2004). A pathway consisting of ARF6, the ARF6 guanine exchange factor (GEF) GEP100/BRAG2 and AMAP1 (DDEF1 or ASAP1), an ARF6 downstream effector, promotes tumor invasion and metastasis in breast cancer in response to epidermal growth factor receptor (EGF-R) activation (Morishige et al., 2008; Sabe et al., 2009). Enhanced invasiveness through the ARF6 pathway is associated with disruption of E-cadherin-based cell-cell contacts and increased beta1-integrin recycling in tumor epithelial cells (Palacios et al., 2001; Onodera et al., 2012).

Sometime ago we identified the microtubule motor adaptor proteins JNK interactor proteins 3 and 4 (JIP3 and JIP4) as ARF6 downstream effectors (Isabet et al., 2009; Montagnac et al., 2009). We found that GTP-bound ARF6 interacts with JIP3/JIP4 to control a motor switch mechanism involving kinesin-1 and dynactin/dynein microtubule-based motors that move cargoes in opposite directions (Montagnac et al., 2011; Montagnac et al., 2009). Here, we analyzed ARF6 and JIP3/JIP4's contribution to the regulation of MT1-MMP-positive LE movement and found that silencing of these proteins in breast tumor cell lines resulted in endosome mispositioning. As a consequence, exocytosis and surface delivery of MT1-MMP were impaired and breast tumor cells were defective in ECM remodeling and invasion through three-dimensional (3D) matrix environment. Immunohistochemistry analysis of ARF6 expression in a tissue microarray of invasive breast tumors revealed that ARF6 is up-regulated in carcinoma cells as compared to peritumoral tissues and accumulated at the plasma membrane in a subset of high-grade triple-negative breast carcinomas.

Co-up-regulation of ARF6 and MT1-MMP was observed in this tumor subset identifying ARF6-JIP3/JIP4-MT1-MMP axis in breast cancer invasion.

MATERIAL AND METHODS

Cell culture. Human breast adenocarcinoma MDA-MB-231 cells (American Type Culture Collection HTB-26) were maintained in L-15 culture medium (Sigma–Aldrich, St. Louis, MO, USA) with 2 mM glutamine (GIBCO) and 15% FBS (GIBCO) at 37 °C in 1% CO_2. MDA-MB-231 cells stably expressing MT1-MMPmCherry were cultured in the presence of 0.5 mg/mL G418 (Sakurai-Yageta et al., 2008). MCF10DCIS.com (hereafter DCIS.com) cell line was purchased from Asterand (Detroit, MI) and maintained according to the supplier's guidelines.

Immunoblotting analysis. Cells were lysed and proteins were eluted in SDS sample buffer, separated by SDS-PAGE, and detected by immunoblotting analysis with the following primary antibodies: anti-ARF6 (clone 6ARF01, Millipore), anti-JIP3 (clone H-140, Tebu-Bio), anti-JLP (ab12331, Abcam), anti-MT1-MMP (clone MAB3328, Millipore), anti-p150*Glued* (612708, BD transduction Lab), anti-β-actin (A1978, Sigma), anti-α-tubulin (T-9026, Sigma), anti-ERK (06-182, Millipore), anti anti-β1-integrin (a kind gift from C. Albiges-Rizo, Institut Albert Bonniot, Grenoble, France). Secondary antibodies used were goat HRP-conjugated anti-rabbit IgG (Sigma A0545) and anti-mouse IgG antibodies (Jackson ImmunoResearch 61871). Bound antibodies were detected with ECL Western Blotting Detection Reagents (GE Healthcare Life Sciences) and reveled by auto-radiographic film (Amersham Hyperfilm MP, GE Healthcare) or by camera detection (BioRad ChemiDoc MP).

siRNA treatment and lentiviral vectors for shRNA expression. siRNA transfection was performed using 50 nM siRNA with Lullaby reagent (OZ Biosciences) according to manufacturer’s instructions and analyzed 72 h after treatment. All siRNAs (see Table S2) were purchased from Dharmacon/Thermo Fischer Scientific with the exception of the siRNA ARF6#f that was designed as described (Hashimoto et al., 2004) and purchased from Ambion. Lentiviral shRNA sequence against human ARF6 and MT1-MMP inserted in pLKO.1-puro vector were purchased from Sigma (see Table S2). For lentivirus production, HEK293T cells were transfected using GeneJuice (Novagen) with a mix of expression vector and psPAX2 (AddGene) and pVSV-G (Clonetech) packaging

vectors in OPTIMEM (Invitrogen). After 72 hrs, virus-containing supernatant was collected, filtered and used for transduction of a subconfluent monolayer of MDA-MB-231 or DCIS.com cells. Puromycin (1 µg/ml, GIBCO) was added after 48 hrs for selection.

Fluorescent gelatin degradation assay. MDA-MB-231 cells were incubated for 5 h on FITC-conjugated cross-linked gelatin (Invitrogen) as described (Sakurai-Yageta et al., 2008), and then fixed and stained for F-actin using Alexa546-phalloidin (A22283, Invitrogen, 1/200) and cortactin using monoclonal anti-cortactin (Clone 4F11, Millipore, 1/200). Cells were imaged with the x63 objective of a wide-field microscope DM6000 B/M (Leica Microsystems) equipped with a CCD CoolSnap HQ camera (Roper Scientific) and steered by Metamorph (Molecular Devices Corp., Sunnyvale, CA). For quantification of degradation, the total area of degraded matrix in one field (black pixels) measured with the Threshold command of MetaMorph was divided by the number of phalloidin-labeled cells in the field to define a degradation index, which was normalized to the degradation index of control siNT-treated cells set to 100 as described (Sakurai-Yageta et al., 2008).

Multicellular spheroid invasion assay. Stably or transiently knocked down cells were used. For transient silencing, we used a double-round siRNA treatment for prolonged (up to 6 days) silencing; cells were first electroporated with 100 nM siRNA using Amaxa kit V and Nucleofector; after overnight incubation, cells were transfected with lullaby reagent (OZ Bioscience) with 50 nM siRNA. Six hours after treatment, multicellular spheroids were prepared using $3x10^3$ cells in 20 µl of complete medium for 3 days using the hanging droplet method as previously described (Rey et al., 2011). Spheroids were then embedded in 2.2 mg/ml acid extracted rat tail type I collagen (BD Biosciences), fixed immediately (T0) or after 2 days at 37°C (T2) and then stained with Alexa546-phalloidin and DAPI. Images were taken with a LSM 510 Meta confocal microscope (Zeiss) with a 5X dry objective, collecting stack of optical sections along the Z axis with 10µm interval. Quantification of invasion was done with ImageJ software (http://rsb.info.nih.gov/ij/) by estimating the diameter of spheroids at T0 and T2 as

described (Rey et al., 2011). Values were averaged and used to calculate the mean invasion area (πr^2). Mean invasion area at T2 was normalized to mean invasion area at T0.

Quantification of pericellular collagenolysis. Quantification of pericellular collagenolysis using anti-Col1$^{3/4}$C antibody was performed as previously described (Monteiro et al., 2013). Cells treated with siRNAs against ARF6, MT1-MMP, JIP3 and JIP4, or Non-Targeting siRNA for 48 hours, trypsinized and resuspended into in 0.2 ml of 2.2 mg/ml collagen I solution (2.5 x 10^5 cells/ml) loaded on a glass coverslip. After gelling for 30 min at 37°C, complete medium was added and collagen-embedded cells were incubated for 24 hrs at 37°C in 1% CO_2. After fixation in 4% PFA in PBS at 37°C for 30 min, samples were incubated with anti Col1$^{3/4}$C antibody (collagenase-cleaved ¾ fragment of collagen I, ImmunoGlobe GmbH, 2.5 µg/ml) for 2h at 4°C, washed extensively with PBS and counterstained with Cy3-conjugated anti-rabbit IgGs (Jackson ImmunoResearch Laboratories, 1/800), DAPI and AlexaFluor 488-phalloidin (Molecular Probes, 1/400) to see the cell shape. Image acquisition was performed with A1R Nikon confocal microscope with a 40x oil objective. Quantification of degradation spots was performed with a homemade Image J macro. Images were preprocessed by a laplacian of Gaussian filter (Sage et al., 2005), with variance reflecting the expected spot size. The spot detection then consists in finding the local minima, sorting them in ascending order of intensity, applying a flood-fill algorithm to each of them using a fixed noise tolerance value set up for all experiments at 10,000 and discarding higher minima whose fill-regions touch those of lower minima. Detected spots are then counted and saved for visual verification. No manual correction was done. Degradation index is the number of degradation spots divided by the number of cells present in the field, normalized to the degradation index of control cells set to 100.

Live-cell spinning disk confocal microscopy. MDA-MB-231 cells stably expressing MT1-MMPmCherry were plated on glass-bottom dishes (MatTek) coated with cross-linked gelatin and kept in a humidified atmosphere at 37°C and 1% CO2. The movement of MT1-MMP-mCherry vesicles was monitored by acquiring 3D time-series images by confocal spinning-disk microscopy (1 z-

stack/2 s) for a duration of 3 minutes using a spinning disk microscope (Roper Scientific) based on a CSU22 Yokogawa head mounted on the lateral port of an inverted TE-2000U Nikon microscope equipped with a 60X 1.45NA oil-immersion objective, a PIFOC Objective stepper and a dual output laser launch which included 491 and 561 nm 50 mW DPSS lasers (Roper Scientific). Images were acquired with a CoolSNAP HQ^2 CCD camera (Roper Scientific) steered by Metamorph software.

Analysis of endosome distribution. Software has been developed with MATLAB to determine the relative position of MT1-MMP endosomes to the cell centroid as previously described (Castro-Castro et al., 2012). First, cells are automatically segmented from the phase-contrast image. A polar coordinate system is created, where the main (longest) axis of the cell becomes the 0-180 degree axis with the cell centroid as the center. Vesicles are then automatically segmented from the matching fluorescence image using a Laplacian of Gaussian filter and mathematical morphology. Each vesicle is then expressed in the cell polar coordinate system, where its radius is expressed relatively to the length of the line going from the cell centroid through the vesicle centroid to the cell periphery. Segmentation was manually corrected if needed. Results are represented by classes according to the distance between each MT1-MMP segmented vesicle and the cell centroid (expressed as % of the total distance between the cell centroid and the cell periphery, where 0 represent the cell centroid and 100 the periphery).

Indirect immunofluorescence and confocal microscopy. For endosome staining, MDA-MB-231 cells stably expressing MT1-MMPmCherry treated with siRNAs against ARF6, JIP3 and JIP4, or Non-Targeting siRNA were cultured on gelatin-coated cover-slips, fixed in 4% PFA in PBS at room temperature for 20 min and permeabilized with Triton-X100 0.1% in PFA for 4 min. Then cells were stained for Rab7 with a rabbit anti-Rab7 (Cell Signaling Technology, 1/50) and counterstained with a goat Alexa488-conjugated anti-rabbit IgG (Jackson ImmunoResearch Laboratories, 1/200), or for EEA1 with a goat anti –EEA1 (sc-6415, Santa Cruz Biotechnology, 1/100) and counterstained with a donkey Alexa488-conjugated anti-goat IgG (Molecular¨Probes, 1/500). Image acquisition

was performed with A1R Nikon confocal microscope with a 60x oil objective and a z-dimension series of images was taken every 0.5 µm. For visualizing the positioning of MT1-MMP-mCherry vesicles in cells in a 3D-collagen environment, glass cover-slips were layered with a solution of type I collagen mixed with AlexaFluor 647-conjugated type I collagen (10% final) at a final concentration of 5 mg/ml. After gelling for 3 min at 37°C, the collagen layer was washed gently in PBS and a cell suspension in L15 medium with 15% FCS (1.5-2.5 x 10^5 cells/ml) was added. Cells were incubated for 30 min at 37°C in 1% CO_2, then medium was removed and a 40 µl drop of a solution of type I collagen mixed with AlexaFluor 647-conjugated type I collagen (10% final) at a final concentration of 2.5 mg/ml was added and allowed to polymerize for 1 hour at 37°C in 1% CO_2, before medium was added. Five hours after cells were permeabilized with 0.5 % Triton-X100 and 4% PFA in PBS, fixed in 4% PFA in PBS and stained for DAPI and cortactin to visualize the shape of the cells. Image acquisition was performed with A1R Nikon confocal microscope with a 63x oil objective and a z-dimension series of images was taken every 1 µm.

MT1-MMP-pHLuorin exocytosis assay. MDA-MB-231 cells stably expressing MT1-MMP-pHluorin (Lizarraga et al., 2009) were treated with non-targeting, ARF6 or JIP3 and JIP4 siRNA for 72 hours, plated on MatTek dishes layered with a drop of polymerized type I collagen mixed with AlexaFluor 549-conjugated type I collagen (10% final) at a final concentration of 2.5 mg/ml. Cells were incubated for 30 min at 37°C in 1% CO2 and imaged by multi-color confocal spinning disk microscopy (2 images/min). Number of exocytic events of MT1-MMP-phLuorin (*i.e.* GFP flashes) was scored as described in (Monteiro et al., 2013).

Linear invadopodia assay. MDA-MB-231 cells were treated with non-targeting, ARF6, MT1-MMP or JIP3 and JIP4 siRNA for 72 hours, plated atop of cover-slips layered with a drop of polymerized type I collagen mixed with AlexaFluor 549-conjugated type I collagen (10% final) at a final concentration of 2.5 mg/ml and allowed them to spread for 1 hour and 30 minutes. Cells were then permeabilized with 0.5 % Triton-X100 in 4% PFA, fixed in 4% PFA in PBS and stained with rabbit anti-TKS5 antibodies (clone M-300, Santa Cruz Biotechnology) and Alexa488-conjugated anti-rabbit IgG. Images were acquired with a wide-field

Eclipse 90i Upright Microscope (Nikon) using a 100x Plan Apo VC 1.4 oil immersion objective and a highly sensitive cooled interlined charge-coupled device (CCD) camera (Roper CoolSnap HQ2). A z-dimension series of images was taken every 0.2 μm by mean of a piezoelectric motor (LVDT, Physik Instrument). Quantification of linear invadopodia area was done with ImageJ software on the z-projected images after manual background substraction. A region was drawn with the Region Tool of ImageJ to define the shape of the cell and a threshold was applied to cover the bright linear invadopodia. The total thresholded area (in $pixel^2$) was measured with the Analyze particles command and normalized for the total surface of the cell measured with the ImageJ Measure command.

Cell growth assay. Proliferation curve of the different stable cell lines was measured using a MTT Cell Growth kit (CT02, Millipore) according to the manufacturer's instruction.

Human sample analysis. Analyses of human samples were performed in accordance with the French Bioethics Law 2004-800, the French National Institute of Cancer (INCa) Ethics Charter and after approval by the Institut Curie review board and ethics committee (*Comité de Pilotage du Groupe Sein*) that waived the need for written informed consent from the participants. Women were informed of the research use of their tissues and did not declare any opposition for such research. Data were analyzed anonymously.

Immunohistochemistry analysis of breast cancer tissue microarray. Samples of primary breast tumors surgically removed prior to any radiation, hormonal or chemotherapy treatment at Institut Curie from 2005 to 2006 have been analyzed. Tumors were classified as intravasive ductal carcinoma (IDC) based on clinicopathological examination. Breast molecular subtypes were defined as follows: Luminal A+B according to (Prat et al., 2013): (Luminal A: estrogen-receptor (ER)≥10%, progesterone-receptor (PR)≥20%, Ki-67<14%; Luminal B: ER≥10%, PR<20%, Ki-67≥14%); ER- PR- HER2+: ER<10%, PR<10%, HER2 2+ amplified or 3+ according to (Allred et al., 2008); ER- PR-

HER2- (Triple negative breast cancers, TNBCs): ER<10%, PR<10%, HER2 0/1+ or 2+ non-amplified according to the ASCO guidelines (Wolff et al., 2007). Our series of invasive breast tumors for which acidified formal alcohol (AFA)-fixed paraffin-embedded samples were available comprised all TNBC and HER2 tumors available and equal number of consecutively treated Luminal A and Luminal B tumors from the same period following the same criteria. The tissue microarray (TMA) consisted of replicate 1mm-diameter tumor cores selected from whole tumor tissue section in the most representative tumor areas (high tumor cell density) of each tumor sample and a matched tissue core from adjacent non-tumoral breast epithelium (referred to as normal breast tissue). For IHC staining, EnVision™ FLEX, High pH kit (Dako) was used according to the manufacturer's instructions and following previously published protocols (Vincent-Salomon et al., 2007). For ARF6 IHC staining we used a mouse anti-ARF6 antibody (clone 6ARF01, 05-1149, Millipore, 1/100).

Statistics. Statistical analyses were performed using Mann-Whitney t-test, one-way or two-way ANOVA and X^2 test, using GraphPad Prism (GraphPad Software) as specified in each figure legend with $p < 0.05$ considered significant.

RESULTS

ARF6 is required for matrix degradation and invasive migration of breast tumor cells through 3D type I collagen environment

First, we investigated whether ARF6 is required for the invasive capacity of breast cancer cells. The effect of ARF6 loss of function on cell invasion was assessed in MDA-MB-231 cells, classified as highly invasive triple-negative breast cancer (Neve et al., 2006). Confirming earlier reports (Hashimoto et al., 2004; Tague et al., 2004), silencing of ARF6 using two independent siRNAs (siARF6#a and #f, see Fig. S1A) diminished by ~2-fold the proportion of MDA-MB-231 cells able to degrade gelatin and decreased by 60% the total area of degraded matrix as compared to cells treated with a non-targeting siRNA (siNT) (Fig. 1A). Silencing of MT1-MMP led to almost complete inhibition of gelatin degradation by MDA-MB-231 cells ((Artym et al., 2006; Sakurai-Yageta et al., 2008), Fig.1A). Inhibition of matrix degradation by ARF6 knockdown was not due to overall alteration of MT1-MMP levels (Fig. S1B).

We then investigated the effect of ARF6 silencing on the capacity of breast cancer cells to invade in a 3D type I collagen matrix. As compared to multicellular spheroids of MDA-MB-231 cells treated with siNT control siRNA, the average invasion area of ARF6-depleted spheroids after two days in collagen was decreased by about 40% similar to MT1-MMP knocked-down spheroids (Fig. 1B-C and Fig. S1C).

The generality of these findings was assessed by analyzing ARF6's contribution to the invasive potential of another triple-negative breast cancer cell line, MCF10DCIS.com cells (hereafter named DCIS.com). In contrast to MDA-MB-231

cells, DCIS.com cells retain E-cadherin expression and may represent an earlier step in breast cancer progression (data not shown). DCIS.com cells were depleted for ARF6 or MT1-MMP by stable lentiviral shRNA expression and knockdown efficiency was estimated by comparison to DCIS.com cells expressing non-targeting shRNA sequence (shNT, Fig. S2A). Similar to the situation in MDA-MB-231 cells, ARF6 or MT1-MMP depletion led to 50% decrease of invasion capacity of DCIS.com multicellular spheroids in collagen I (Fig. S2B-C). All together, these data show for the first time a requirement for ARF6 in the invasive migration of breast cancer cells in a 3D collagen environment.

We then sought to investigate whether inhibition of cell invasion upon ARF6 knockdown was due to a requirement for ARF6 in the ability of the cells to proteolytically cleave the surrounding collagen. In MDA-MB-231 cells embedded in type I collagen, depletion of MT1-MMP strongly reduced pericellular collagen degradation as indicated by a 70% reduction of the Col1$^{3/4}$C antibody signal (Fig1D-1E), an antibody that recognizes the cleaved fragment of collagen I by collagenases (Monteiro et al., 2013; Wolf et al., 2007). Thus, collagen degradation by MDA-MB-231 cells strongly relies on MT1-MMP activity. Silencing of ARF6 led to a similar decrease of collagen cleavage (Fig. 1D-E), suggesting that ARF6 is implicated in MT1-MMP-dependent pericellular collagen degradation.

JIP3 and JIP4 are required for invasive migration through 3D type I collagen environment

As we previously reported, MT1-MMP accumulated mostly in Rab7-positive late endosomes (LEs) in MDA-MB-231 cells (Fig. S3A and C) (Monteiro et al., 2013; Steffen et al., 2008)), with limited overlap with EEA1-positive early endosomal compartments (Fig. S3B-C). We recently identified JIP3 and JIP4 as ARF6 downstream effectors involved in the control of endosome movement through the regulation of microtubule-based motors kinesin-1 and dynactin/dynein complex (Isabet et al., 2009; Montagnac et al., 2009). Thus we hypothesized that ARF6 may control microtubule-dependent movement of MT1-MMP-positive LEs in a JIP3 and/or JIP4-dependent manner.

Both JIP3 and JIP4 were expressed in MDA-MB-231 cells and could be efficiently silenced upon siRNA treatment (Fig. S4A). Knockdown of JIP3 or JIP4 led to a significant decrease of both the percentage of cells able to degrade gelatin and of their degradative capacity (Fig. S4B). In addition, silencing of JIP3 or JIP4 led to a significant 30-40% decrease of the invasion potential of multicellular spheroids in 3D type I collagen (Fig. 2A and Fig. S4C-D). Simultaneous knockdown of JIP3 and JIP4 using two independent pairs of siRNAs resulted in a similar inhibition of the invasion capacity of MDA-MB-231 cells suggesting mutually dependent functions of these two proteins (Fig. 2B and Fig. S4D). Moreover, the role of JIP3 and JIP4 on invasive migration was paralleled by a 50-65% decreased capacity of JIP3 or JIP4-depleted cells to cleave type I collagen (Fig. 2C and Fig. S4E). Thus our data identify JIP3 and JIP4 as important components of the matrix remodeling and invasion program of MDA-MB-231 breast tumor cells.

The ARF6/JIP pathway controls MT1-MMP-positive endosome positioning

The intracellular late endosome-enriched pool of MT1-MMP represents a major reservoir of the protease for exocytosis and surface delivery to support pericellular matrix degradation by invasive breast tumor cells (Monteiro et al., 2013; Rosse et al., 2014; Steffen et al., 2008; Williams and Coppolino, 2011; Yu et al., 2012). We thus looked at ARF6 and JIPs' capacity to affect the distribution of MT1-MMP-positive LEs. Automated image analysis of endosome position between the cell center (position 0) and the periphery (position 100) showed that MT1-MMPmCh accumulated in large centrally located endosomes and in smaller and scattered endosomal compartments, which were all positive for Rab7 (Fig. 3A-B and Fig. S3A). Analysis of vesicle movement based on spinning disk confocal movies revealed that pheripheral MT1-MMP-positive endosomes were highly dynamics having bidirectional movement, while larger centrally-located ones were more static (Fig. 3B, lower panel). Silencing of ARF6 led to a dramatic redistribution of MT1-MMP-positive endosomes to the central cell region where these large vacuolar structures remained essentially static (Fig. 3A-B). Strikingly, cells double-knocked down for JIP3 and JIP4 had a scattered distribution of MT1-MMP endosomes and accumulated clusters of MT1-MMP-positive vesicles at the cell periphery, which were mostly non motile (Fig. 3A-B). Knockdown of ARF6 or JIP did not affect the overlap between MT1-MMP and Rab7 (Fig. S3A and C) indicating that loss of ARF6 or JIP functions resulted in mispositioning of Rab7/MT1-MMP-positive endosomes with minimal effect on endosomal cargo sorting and/or endosome maturation. Similarly, we looked at the distribution of MT1-MMP-positive endosomes in cells incubated in a 3D fibrous collagen matrix. Despite cells adopted a more elongated morphology in the 3D collagen environment as compared to spread shape on 2D gelatin substratum, changes in

MT1-MMP-positive endosome distribution in knocked down cells were clearly visible; *i.e.* accumulation of large perinuclear vacuolar structures in ARF6-depleted cells *vs.* scattered and more peripheral MT1-MMP endosomal clusters upon JIP depletion (Fig. 3C). All together, we conclude that defects in matrix remodeling and invasive migration correlate with dramatic and opposite changes in the distribution of MT1-MMP-positive LEs in MDA-MB-231 cells depleted for ARF6 or JIP3/JIP4, respectively.

Regulation of MT1-MMP endosome position by ARF6 requires JIP3/JIP4 and p150Glued dynactin complex subunit

JIP3 and JIP4 have been shown to interact with kinesin-1 and with the dynein/dynactin complex (Bowman et al., 2000; Cavalli et al., 2005; Montagnac et al., 2009) and ARF6 regulates JIPs' interaction with motors (Bowman et al., 2000; Cavalli et al., 2005; Montagnac et al., 2009). Correct positioning of LEs involves a balance of kinesin-1 and dynein opposite-direction motor activity (Bananis et al., 2004; Granger et al., 2014), thus perinuclear location of MT1-MMP-positive endosomes could indicate unbalanced dynein minus-end directed motor activity in ARF6-depleted MDA-MB-231 cells. This hypothesis was tested by knocking down the dynactin complex subunit p150*Glued* (Fig. S5A), which interacts with JIP3/JIP4 (Montagnac et al., 2009). In agreement with a positive role of dynactin complex on dynein minus-end directed motor activity, silencing of p150*Glued* led to a redistribution of MT1-MMP endosomes to a more scattered and peripheral distribution as compared to control siNT-treated cells (Fig. 4A). In addition, double ARF6 and p150*Glued* knockdown rescued a scattered and peripheral

(normal-like) distribution of MT1-MMP endosomes as compared to a central one in ARF6-depleted cells (compare siARF6 + sip150 *vs.* siARF6, Fig. 4A, upper graph and Fig. 4B), thus indicating that loss of ARF6 favors dynein/dynactin complex function. Similarly, depletion of ARF6 and JIP3/JIP4 together also reverted the phenotype of clustered perinuclear MT1-MMP endosomes seen in ARF6-depleted cells and led to the accumulation of endosomes at the cell periphery (compare siARF6 + siJIP3/JIP4 *vs.* siARF6, Fig.4A, lower graph and Fig. 4B), indicating a requirement for JIP3/JIP4 function in the regulation of endosome positioning by ARF6 through control of dynein/dynactin complex function. Double p150*Glued* and JIP3/JIP4 knockdown resulted in a scattered and peripheral distribution of MT1-MMP-positive endosomes as in the single knockdown of each protein (Fig.4A, middle graph), supporting the conclusion that JIP and dynactin complex work within the same pathway.

Regulation of MT1-MMP exocytosis by ARF6 and JIP3/JIP4

As surface MT1-MMP is directly responsible for pericellular matrix degradation by tumor cells, we investigated the role of ARF6 and JIP3/JIP4 in MT1-MMP exocytosis in relation with their identified function in endosome positioning. MDA-MB-231 cells expressing MT1-MMPpHLuorin were cultured on fibrillar type I collagen and we monitored the apparition of green fluorescence flashes by confocal spinning-disk microscopy corresponding to de-quenching of the florescence of the extracellular pHLuorin tag upon exocytosis (Monteiro et al., 2013; Rosse et al., 2014). As previously reported (Monteiro et al., 2013), exocytic events of MT1-MMP-containing LEs occurred mainly on the portion of the plasma

membrane in association with collagen I fibers and led to surface accumulation of MT1-MMP along the fibers (Fig. 5A-B). Quantification of MT1-MMPpHLuorin flashes revealed a decrease in the frequency of MT1-MMP exocytic events upon knocking down ARF6 (Fig. 5C), suggesting that ARF6 is required for MT1-MMP exocytosis. Knockdown of JIP3/JIP4 also decreased the frequency of exocytic events (Fig. 5C). Therefore, mispositioning of MT1-MMP-containing LEs as a consequence of ARF6 or JIP3/JIP4 loss-of-function function impairs exocytosis.

ARF6 and JIP3/JIP4 are required for linear invadopodia formation

(Juin et al., 2012; Monteiro et al., 2013)MDA-MB-231 cells were plated on a layer of fibrous type I collagen and stained for the specific invadopodia marker TKS5 (Seals et al., 2005). TKS5 accumulated in linear invadopodia forming in association with collagen fibers (Juin et al., 2012; Monteiro et al., 2013) (Fig. 5D). Strikingly, depletion of MT1-MMP in MDA-MB-231 cells drastically diminished TKS5 recruitment and thus the formation of linear invadopodia indicating that MT1-MMP, besides its role in collagen fiber remodeling is also essential for linear invadopodia formation (Fig. 5D and E). In agreement with their role in plasma membrane delivery of MT1-MMP, silencing of ARF6 and JIP3/JIP4 also led to a strong inhibition of linear invadopodia formation as revealed by scoring TKS5 accumulation (Fig. 5D and F). Thus we conclude that ARF6 and JIP3/JIP4 together control intracellular trafficking of MT1-MMP-positive endosomes and exocytosis for efficient targeting of the protease to invadopodia and to promote pericellular matrix remodeling.

Plasma membrane accumulation of ARF6 in hormone receptor-negative breast tumors and correlation with MT1-MMP surface expression

Changes in ARF6 levels in breast carcinoma cells and association with breast cancer markers were investigated by immunohistochemistry (IHC) analysis of a tissue microarray (TMA) including 496 cases of invasive ductal carcinoma (IDC) (patient characteristics are summarized in Table S1). To our knowledge there is no previous report of IHC analysis of ARF6 expression in human cancer. Several anti-ARF6 antibodies were tested; one monoclonal was selected based on specificity of ARF6 IHC staining on paraffin sections of multicellular spheroid of DCIS.com cells expressing non-targeting or ARF6 shRNA (Fig. S6A). In peritumoral breast epithelial tissues, we observed diffuse cytosolic ARF6 staining in luminal epithelial cells surrounding the duct lumen (Fig. 6A). ARF6 expression was also detected in myoepithelial cells and in stromal cells including fibroblasts and immune cells (not shown). Cytosolic ARF6 expression in carcinoma cells in IDCs was semi-quantitatively scored using an H-score method. Based on analysis of 426 IDCs available for scoring, levels of cytosolic ARF6 were significantly lower in epithelial cells in peritumoral tissues (mean H-score of 146.9) as compared to adjacent carcinoma cells (Fig. S6B), while levels were not significantly different comparing in situ (mean H-score of 171.0) *vs.* invasive (mean H-core of 161.5) components of IDCs (Fig. 6A and Fig. S6B). In addition to cytosolic ARF6 expression, a subset of breast tumors (107/426, 25.1%) showed striking ARF6 staining at cell-cell contacts, probably representing ARF6 association with the inner face of the plasma membrane (Fig. 6A). Plasma membrane-associated ARF6 was never detected in normal breast epithelial cells in peritumoral tissues (Fig. 6B) and was restricted to carcinoma cells in which it

was semi-quantitatively scored. Plasma membrane ARF6 level was significantly higher in invasive (mean H-score of 22.9) *vs.* in situ (mean H-core of 8.6) components of IDCs (Fig. 6B), and we also found a positive correlation of plasma membrane ARF6 with the tumor pathological grade (Fig. S6C). When segregating tumors into the different molecular subtypes according to hormone receptor and HER2 status and considering the invasive component of IDCs, plasma membrane ARF6 was lower in hormone receptor-positive (Luminal A+B) tumors (mean H-score of 5.4), intermediate in hormone receptor-negative/HER2-positive tumors (mean H-score of 25.3) and highest in TNBCs (mean H-score of 57.7) (Fig. 6C).

Our *in vitro* data based on TNBC cell lines pointed to a role for ARF6 in MT1-MMP-dependent breast tumor cell invasion. Thus, H-scores of plasma membrane ARF6 were compared to H-score values obtained by scoring expression of plasma membrane MT1-MMP in breast carcinoma cells by IHC analysis of the same TMA (Lodillinsky *et al.* submitted). Tumors for which both ARF6 and MT1-MMP H-scores were available (N=398) were stratified in two groups according to low (H-score<100) or high (H-score≥100) expression of plasma membrane ARF6 or MT1-MMP (Table 1). In the overall cohort, plasma membrane ARF6 was correlated with MT1-MMP expression (p=0.0001, Table 1). When IDCs were further segregated into hormone receptor-positive (Luminal A+B) and hormone receptor-negative (HER2 and TNBC) subgroups, a significant correlation between levels of plasma membrane ARF6 and MT1-MMP was observed in hormone receptor-negative breast tumors (p=0.0058, Table 1 and Fig. 6D). Thus, we conclude that ARF6 accumulates at the plasma membrane of high-grade

hormone receptor-negative invasive breast tumors and this redistribution correlates with increased surface expression of MT1-MMP in these tumors.

DISCUSSION

ARF6 was shown early on to localize to invadopodia, the specialized matrix-degradative structures of tumor cells and to be required for invadopodia activity (Hashimoto et al., 2004; Tague et al., 2004). In MDA-MB-231 cells, ARF6 controls the recruitment of invadopodial components cortactin and paxillin and invadopodia assembly through its downstream effector AMAP1 (Onodera et al., 2005), and ARF6 activation has been linked to EGF signaling via its GEF GEP100/BRAG2, which interacts with ligand-activated EGF-R (Morishige et al., 2008). Moreover, IHC analysis demonstrated that GEP100/BRAG2 is overexpressed in 80% of IDCs and is preferentially co-expressed with EGF-R in ductal carcinomas in situ (Morishige et al., 2008). Besides increased matrix invasion activity, the ARF6 pathway has been associated with epithelial-to-mesenchymal transition (EMT) through disruption of E-cadherin-based cell-cell contacts and increased beta1-integrin recycling in tumor epithelial cells (Morishige et al., 2008; Onodera et al., 2012; Palacios et al., 2001; Sabe et al., 2009).

In the present study, we found by IHC analysis of a TMA including a large collection of primary IDCs that ARF6 is overexpressed in carcinoma cells as compared to normal epithelial cells. In addition, a striking plasma membrane accumulation of ARF6 signal was observed in hormone receptor-negative invasive breast tumors. Plasma membrane recruitment of ARF6 was higher in

infiltrating components of IDCs as compared to in situ tumor regions and in higher-grade tumors and correlated with breast cancer progression. Consistent with several studies that reported accumulation of GTP-bound active ARF6 at the plasma membrane and colocalization with ARF6-GEFs including GEP100/BRAG2 (D'Souza-Schorey and Chavrier, 2006; Someya et al., 2001), it is likely that its plasma membrane enrichment represents hyperactivation of ARF6 in invasive carcinoma cells. Furthermore, in hormone receptor-negative IDCs, ARF6 translocation at the cell periphery correlated with increased surface expression of MT1-MMP, a major component of the matrix invasion program of breast carcinoma cells. Along this line, we found that ARF6 was not only required for degradation of gelatin but also for linear invadopodia-mediated collagen remodeling and for MT1-MMP-dependent invasive migration of TNBC cell lines in a 3D fibrous collagen environment. Thus, besides promoting EMT, these data suggest a novel pro-invasive role of ARF6 in regulating MT1-MMP transport to the cell surface for pericellular ECM degradation by breast tumor cells.

In MDA-MB-231 cells, the majority of MT1-MMP accumulated in endosomal compartments positive for LE/lysosomal marker VAMP7 (Steffen et al., 2008) and Rab7 ((Rosse et al., 2014) and this study). Our recent findings support a mechanism whereby MT1-MMP exocytosis involves formation of long-lasting (over several minutes) connections between MT1-MMP-containing LEs and the invadopodial plasma membrane (Monteiro et al., 2013). Based on the fact that loss of ARF6 function resulted in mispositioning of MT1-MMP-LEs in the perinuclear region, one function for ARF6 is probably to control negatively the clearance and inward movement of MT1-MMP endosomes from the cell periphery, thus promoting MT1-MMP exocytosis. Rescue of MT1-MMP

endosome positioning in ARF6-depleted cells by knockdown of p150*Glued* dynactin complex subunit strongly supports the implication of dynactin/dynein minus-end-directed motor activity in MT1-MMP endosome clearance in agreement with dynein's role in LE motility (Bananis et al., 2004; Granger et al., 2014). In addition, we showed that JIP3/JIP4 silencing led to mispositioning of MT1-MMP-positive LEs at the cell periphery, dominantly over ARF6 knockdown, indicates that JIP3/JIP4 are required for dynactin/dynein-mediated inward movement and for negative regulation by ARF6. This hypothesis is also supported by JIP3/JIP4's ability to bind to the dynactin complex in ARF6-controled manner and by recent observations in zebrafish neurons, in which retrograde transport of LE/lysosomes is mediated by JIP3 (Cavalli et al., 2005; Drerup and Nechiporuk, 2013; Montagnac et al., 2009). A recent study very elegantly reported that mammalian dynein exists in a resting inactive state in the cytoplasm requiring simultaneous binding of cargo adaptor proteins and dynactin, which has low affinity for dynein in the absence of adaptors (McKenney et al., 2014). Cargo adaptors are coiled-coil proteins such as Bicaudal D2 (BicD2) or FIP3 that link dynein to Rab6- and Rab11-positive vesicles, respectively (McKenney et al., 2014). By analogy, we postulate that JIP3/JIP4 coiled-coil proteins may act as cargo adaptors to link dynein/dynactin to MT1-MMP-positive LEs, while at the periphery of breast cancer cells, activated ARF6 may negatively regulate the JIP3/JIP4/dynactin/dynein complex and inward movement by interacting with the JIP3/JIP4 coiled-coil (LZII) domain (Isabet et al., 2009; Montagnac et al., 2009).

Bidirectional endosome movement depends on a "tug-of-war" equilibrium of dynactin/dynein and kinesin motors of opposite directions (Granger et al., 2014),

and we do not exclude the possibility that the ARF6-JIP3/JIP4 pathway may also influence plus-end-directed, kinesin-1-dependent transport of MT1-MMP endosomes (Bowman et al., 2000; Byrd et al., 2001; Kelkar et al., 2005; Montagnac et al., 2009; Nguyen et al., 2005). Noticeably, although JIP3/JIP4 knockdown resulted in peripheral accumulation of MT1-MMP LEs, it interfered with MT1-MMP exocytic events and ECM degradation, indicating that the invasive potential of breast cancers cells requires MT1-MMP endosomes to move and switch direction dynamically to adapt to changing ECM microenvironments. In conclusion we have delineated a possible mechanism through which ARF6 through JIP3/JIP4 could control intracellular trafficking of MT1-MMP-positive endosomes and exocytosis for efficient targeting of the protease to invadopodia and to promote pericellular matrix remodeling.

ACKNOWLEDGEMENTS

The authors wish to acknowledge the Breast Cancer Study Group and patients of Institut Curie for the breast tumor samples, the Nikon Imaging Centre @ Institut Curie-CNRS and Cell and Tissue Imaging Facility of Institut Curie for help with image acquisition and P.Paul-Gilloteaux and Dr. A. Casto-Castro for help with endosomes positioning quantification. V.M. was supported by fellowships from Domaine d'Intérêt Majeur de la Région Ile-de-France and Ligue Nationale contre le Cancer, C.L. was supported by grants from Agence Nationale pour la Recherche and Fondation Pierre-Gilles de Gennes pour la Recherche, L.F. and M.I. by the Incentive and Cooperative Research Programme 'Breast cancer: cell Invasion and Motility' of Institut Curie and A.G. by a grant from Appel à Projet "Biologie des Systèmes" 2012 du Plan cancer 2009-2013 (INVADE project). Funding for this work was provided by grants from ARC (SL220100601356 & SLR20130607099) and Institut National du Cancer (2012-1-PL BIO-02-IC-1) to P.C. and by core funding from Institut Curie and Centre National pour la Recherche Scientifique (CNRS).

REFERENCES

Allred, D.C., Y. Wu, S. Mao, I.D. Nagtegaal, S. Lee, C.M. Perou, S.K. Mohsin, P. O'Connell, A. Tsimelzon, and D. Medina. 2008. Ductal carcinoma in situ and the emergence of diversity during breast cancer evolution. *Clin Cancer Res*. 14:370-378.

Artym, V.V., Y. Zhang, F. Seillier-Moiseiwitsch, K.M. Yamada, and S.C. Mueller. 2006. Dynamic interactions of cortactin and membrane type 1 matrix metalloproteinase at invadopodia: defining the stages of invadopodia formation and function. *Cancer Res*. 66:3034-3043.

Bananis, E., S. Nath, K. Gordon, P. Satir, R.J. Stockert, J.W. Murray, and A.W. Wolkoff. 2004. Microtubule-dependent movement of late endocytic vesicles in vitro: requirements for Dynein and Kinesin. *Mol Biol Cell*. 15:3688-3697.

Bartolome, R.A., S. Ferreiro, M.E. Miquilena-Colina, L. Martinez-Prats, M.L. Soto-Montenegro, D. Garcia-Bernal, J.J. Vaquero, R. Agami, R. Delgado, M. Desco, P. Sanchez-Mateos, and J. Teixido. 2009. The chemokine receptor CXCR4 and the metalloproteinase MT1-MMP are mutually required during melanoma metastasis to lungs. *Am J Pathol*. 174:602-612.

Bowman, A.B., A. Kamal, B.W. Ritchings, A.V. Philp, M. McGrail, J.G. Gindhart, and L.S. Goldstein. 2000. Kinesin-dependent axonal transport is mediated by the sunday driver (SYD) protein. *Cell*. 103:583-594.

Byrd, D.T., M. Kawasaki, M. Walcoff, N. Hisamoto, K. Matsumoto, and Y. Jin. 2001. UNC-16, a JNK-signaling scaffold protein, regulates vesicle transport in C. elegans. *Neuron*. 32:787-800.

Castro-Castro, A., C. Janke, G. Montagnac, P. Paul-Gilloteaux, and P. Chavrier. 2012. ATAT1/MEC-17 acetyltransferase and HDAC6 deacetylase control a balance of acetylation of alpha-tubulin and cortactin and regulate MT1-MMP trafficking and breast tumor cell invasion. *Eur J Cell Biol*. 91:950-960.

Cavalli, V., P. Kujala, J. Klumperman, and L.S. Goldstein. 2005. Sunday Driver links axonal transport to damage signaling. *J Cell Biol*. 168:775-787.

Clark, E.S., A.S. Whigham, W.G. Yarbrough, and A.M. Weaver. 2007. Cortactin is an essential regulator of matrix metalloproteinase secretion and

extracellular matrix degradation in invadopodia. *Cancer Res*. 67:4227-4235.

D'Souza-Schorey, C., and P. Chavrier. 2006. ARF proteins: roles in membrane traffic and beyond. *Nat Rev Mol Cell Biol*. 7:347-358.

Devy, L., L. Huang, L. Naa, N. Yanamandra, H. Pieters, N. Frans, E. Chang, Q. Tao, M. Vanhove, A. Lejeune, R. van Gool, D.J. Sexton, G. Kuang, D. Rank, S. Hogan, C. Pazmany, Y.L. Ma, S. Schoonbroodt, A.E. Nixon, R.C. Ladner, R. Hoet, P. Henderikx, C. Tenhoor, S.A. Rabbani, M.L. Valentino, C.R. Wood, and D.T. Dransfield. 2009. Selective inhibition of matrix metalloproteinase-14 blocks tumor growth, invasion, and angiogenesis. *Cancer Res*. 69:1517-1526.

Donaldson, J.G., and C.L. Jackson. 2011. ARF family G proteins and their regulators: roles in membrane transport, development and disease. *Nat Rev Mol Cell Biol*. 12:362-375.

Drerup, C.M., and A.V. Nechiporuk. 2013. JNK-interacting protein 3 mediates the retrograde transport of activated c-Jun N-terminal kinase and lysosomes. *PLoS Genet*. 9:e1003303.

Granger, E., G. McNee, V. Allan, and P. Woodman. 2014. The role of the cytoskeleton and molecular motors in endosomal dynamics. *Semin Cell Dev Biol*. 31:20-29.

Hashimoto, S., Y. Onodera, A. Hashimoto, M. Tanaka, M. Hamaguchi, A. Yamada, and H. Sabe. 2004. Requirement for Arf6 in breast cancer invasive activities. *Proc Natl Acad Sci USA*. 101:6647-6652.

Hoshino, D., K.C. Kirkbride, K. Costello, E.S. Clark, S. Sinha, N. Grega-Larson, M.J. Tyska, and A.M. Weaver. 2013. Exosome secretion is enhanced by invadopodia and drives invasive behavior. *Cell Rep*. 5:1159-1168.

Hotary, K., X.Y. Li, E. Allen, S.L. Stevens, and S.J. Weiss. 2006. A cancer cell metalloprotease triad regulates the basement membrane transmigration program. *Genes Dev*. 20:2673-2686.

Hotary, K.B., E.D. Allen, P.C. Brooks, N.S. Datta, M.W. Long, and S.J. Weiss. 2003. Membrane type I matrix metalloproteinase usurps tumor growth control imposed by the three-dimensional extracellular matrix. *Cell*. 114:33-45.

Isabet, T., G. Montagnac, K. Regazzoni, B. Raynal, F. El Khadali, P. England, M. Franco, P. Chavrier, A. Houdusse, and J. Menetrey. 2009. The structural basis of Arf effector specificity: the crystal structure of ARF6 in a complex with JIP4. *EMBO J*. 28:2835-2845.

Juin, A., C. Billottet, V. Moreau, O. Destaing, C. Albiges-Rizo, J. Rosenbaum, E. Genot, and F. Saltel. 2012. Physiological type I collagen organization induces the formation of a novel class of linear invadosomes. *Molecular biology of the cell*. 23:297-309.

Kelkar, N., C.L. Standen, and R.J. Davis. 2005. Role of the JIP4 scaffold protein in the regulation of mitogen-activated protein kinase signaling pathways. *Mol Cell Biol*. 25:2733-2743.

Kessenbrock, K., V. Plaks, and Z. Werb. 2010. Matrix metalloproteinases: regulators of the tumor microenvironment. *Cell*. 141:52-67.

Lee, C.M., D. Onesime, C.D. Reddy, N. Dhanasekaran, and E.P. Reddy. 2002. JLP: A scaffolding protein that tethers JNK/p38MAPK signaling modules and transcription factors. *Proc Natl Acad Sci U S A*. 99:14189-14194.

Lizarraga, F., R. Poincloux, M. Romao, G. Montagnac, G. Le Dez, I. Bonne, G. Rigaill, G. Raposo, and P. Chavrier. 2009. Diaphanous-related formins are required for invadopodia formation and invasion of breast tumor cells. *Cancer Res*. 69:2792-2800.

McKenney, R.J., W. Huynh, M.E. Tanenbaum, G. Bhabha, and R.D. Vale. 2014. Activation of cytoplasmic dynein motility by dynactin-cargo adapter complexes. *Science*. 345:337-341.

Montagnac, G., H. de Forges, E. Smythe, C. Gueudry, M. Romao, J. Salamero, and P. Chavrier. 2011. Decoupling of activation and effector binding underlies ARF6 priming of fast endocytic recycling. *Curr Biol*. 21:574-579.

Montagnac, G., J.B. Sibarita, S. Loubery, L. Daviet, M. Romao, G. Raposo, and P. Chavrier. 2009. ARF6 Interacts with JIP4 to control a motor switch mechanism regulating endosome traffic in cytokinesis. *Curr Biol*. 19:184-195.

Monteiro, P., C. Rosse, A. Castro-Castro, M. Irondelle, E. Lagoutte, P. Paul-Gilloteaux, C. Desnos, E. Formstecher, F. Darchen, D. Perrais, A. Gautreau, M. Hertzog, and P. Chavrier. 2013. Endosomal WASH and

exocyst complexes control exocytosis of MT1-MMP at invadopodia. *J Cell Biol*. 203:1063-1079.

Morishige, M., S. Hashimoto, E. Ogawa, Y. Toda, H. Kotani, M. Hirose, S. Wei, A. Hashimoto, A. Yamada, H. Yano, Y. Mazaki, H. Kodama, Y. Nio, T. Manabe, H. Wada, H. Kobayashi, and H. Sabe. 2008. GEP100 links epidermal growth factor receptor signalling to Arf6 activation to induce breast cancer invasion. *Nat Cell Biol*. 10:85-92.

Murphy, D.A., and S.A. Courtneidge. 2011. The 'ins' and 'outs' of podosomes and invadopodia: characteristics, formation and function. *Nature reviews. Molecular cell biology*. 12:413-426.

Neve, R.M., K. Chin, J. Fridlyand, J. Yeh, F.L. Baehner, T. Fevr, L. Clark, N. Bayani, J.P. Coppe, F. Tong, T. Speed, P.T. Spellman, S. DeVries, A. Lapuk, N.J. Wang, W.L. Kuo, J.L. Stilwell, D. Pinkel, D.G. Albertson, F.M. Waldman, F. McCormick, R.B. Dickson, M.D. Johnson, M. Lippman, S. Ethier, A. Gazdar, and J.W. Gray. 2006. A collection of breast cancer cell lines for the study of functionally distinct cancer subtypes. *Cancer Cell*. 10:515-527.

Nguyen, Q., C.M. Lee, A. Le, and E.P. Reddy. 2005. JLP associates with kinesin light chain 1 through a novel leucine zipper-like domain. *J Biol Chem*. 280:30185-30191.

Onodera, Y., S. Hashimoto, A. Hashimoto, M. Morishige, Y. Mazaki, A. Yamada, E. Ogawa, M. Adachi, T. Sakurai, T. Manabe, H. Wada, N. Matsuura, and H. Sabe. 2005. Expression of AMAP1, an ArfGAP, provides novel targets to inhibit breast cancer invasive activities. *The EMBO journal*. 24:963-973.

Onodera, Y., J.M. Nam, A. Hashimoto, J.C. Norman, H. Shirato, S. Hashimoto, and H. Sabe. 2012. Rab5c promotes AMAP1-PRKD2 complex formation to enhance beta1 integrin recycling in EGF-induced cancer invasion. *J Cell Biol*. 197:983-996.

Palacios, F., L. Price, J. Schweitzer, J.G. Collard, and C. D'Souza-Schorey. 2001. An essential role for ARF6-regulated membrane traffic in adherens junction turnover and epithelial cell migration. *Embo J*. 20:4973-4986.

Perentes, J.Y., N.D. Kirkpatrick, S. Nagano, E.Y. Smith, C.M. Shaver, D. Sgroi, I. Garkavtsev, L.L. Munn, R.K. Jain, and Y. Boucher. 2011. Cancer cell-associated MT1-MMP promotes blood vessel invasion and distant

metastasis in triple-negative mammary tumors. *Cancer Res*. 71:4527-4538.

Poincloux, R., F. Lizarraga, and P. Chavrier. 2009. Matrix invasion by tumour cells: a focus on MT1-MMP trafficking to invadopodia. *J Cell Sci*. 122:3015-3024.

Prat, A., M.C. Cheang, M. Martin, J.S. Parker, E. Carrasco, R. Caballero, S. Tyldesley, K. Gelmon, P.S. Bernard, T.O. Nielsen, and C.M. Perou. 2013. Prognostic significance of progesterone receptor-positive tumor cells within immunohistochemically defined luminal A breast cancer. *J Clin Oncol*. 31:203-209.

Rey, M., M. Irondelle, F. Waharte, F. Lizarraga, and P. Chavrier. 2011. HDAC6 is required for invadopodia activity and invasion by breast tumor cells. *Eur J Cell Biol*. 90:128-135.

Rosse, C., C. Lodillinsky, L. Fuhrmann, M. Nourieh, P. Monteiro, M. Irondelle, E. Lagoutte, S. Vacher, F. Waharte, P. Paul-Gilloteaux, M. Romao, L. Sengmanivong, M. Linch, J. van Lint, G. Raposo, A. Vincent-Salomon, I. Bieche, P.J. Parker, and P. Chavrier. 2014. Control of MT1-MMP transport by atypical PKC during breast-cancer progression. *Proc Natl Acad Sci U S A*. 111:E1872-1879.

Sabe, H., S. Hashimoto, M. Morishige, E. Ogawa, A. Hashimoto, J.M. Nam, K. Miura, H. Yano, and Y. Onodera. 2009. The EGFR-GEP100-Arf6-AMAP1 signaling pathway specific to breast cancer invasion and metastasis. *Traffic*. 10:982-993.

Sabeh, F., I. Ota, K. Holmbeck, H. Birkedal-Hansen, P. Soloway, M. Balbin, C. Lopez-Otin, S. Shapiro, M. Inada, S. Krane, E. Allen, D. Chung, and S.J. Weiss. 2004. Tumor cell traffic through the extracellular matrix is controlled by the membrane-anchored collagenase MT1-MMP. *J Cell Biol*. 167:769-781.

Sabeh, F., R. Shimizu-Hirota, and S.J. Weiss. 2009. Protease-dependent versus -independent cancer cell invasion programs: three-dimensional amoeboid movement revisited. *J Cell Biol*. 185:11-19.

Sage, D., F.R. Neumann, F. Hediger, S.M. Gasser, and M. Unser. 2005. Automatic tracking of individual fluorescence particles: application to the

study of chromosome dynamics. *IEEE transactions on image processing*. 14:1372-1383.

Sakurai-Yageta, M., C. Recchi, G. Le Dez, J.B. Sibarita, L. Daviet, J. Camonis, C. D'Souza-Schorey, and P. Chavrier. 2008. The interaction of IQGAP1 with the exocyst complex is required for tumor cell invasion downstream of Cdc42 and RhoA. *J Cell Biol*. 181:985-998.

Sato, H., T. Takino, Y. Okada, J. Cao, A. Shinagawa, E. Yamamoto, and M. Seiki. 1994. A matrix metalloproteinase expressed on the surface of invasive tumour cells. *Nature*. 370:61-65.

Seals, D.F., E.F. Azucena, Jr., I. Pass, L. Tesfay, R. Gordon, M. Woodrow, J.H. Resau, and S.A. Courtneidge. 2005. The adaptor protein Tks5/Fish is required for podosome formation and function, and for the protease-driven invasion of cancer cells. *Cancer Cell*. 7:155-165.

Sodek, K.L., M.J. Ringuette, and T.J. Brown. 2007. MT1-MMP is the critical determinant of matrix degradation and invasion by ovarian cancer cells. *Br J Cancer*. 97:358-367.

Someya, A., M. Sata, K. Takeda, G. Pacheco-Rodriguez, V.J. Ferrans, J. Moss, and M. Vaughan. 2001. ARF-GEP(100), a guanine nucleotide-exchange protein for ADP-ribosylation factor 6. *Proc Natl Acad Sci U S A*. 98:2413-2418.

Steffen, A., G. Le Dez, R. Poincloux, C. Recchi, P. Nassoy, K. Rottner, T. Galli, and P. Chavrier. 2008. MT1-MMP-dependent invasion is regulated by TI-VAMP/VAMP7. *Curr Biol*. 18:926-931.

Sun, F., C. Zhu, R. Dixit, and V. Cavalli. 2011. Sunday Driver/JIP3 binds kinesin heavy chain directly and enhances its motility. *EMBO J*. 30:3416-3429.

Sung, B.H., X. Zhu, I. Kaverina, and A.M. Weaver. 2011. Cortactin controls cell motility and lamellipodial dynamics by regulating ECM secretion. *Current biology*. 21:1460-1469.

Szabova, L., K. Chrysovergis, S.S. Yamada, and K. Holmbeck. 2008. MT1-MMP is required for efficient tumor dissemination in experimental metastatic disease. *Oncogene*. 27:3274-3281.

Tague, S.E., V. Muralidharan, and C. D'Souza-Schorey. 2004. ADP-ribosylation factor 6 regulates tumor cell invasion through the activation of the MEK/ERK signaling pathway. *Proc Natl Acad Sci U S A*. 101:9671-9676.

Vincent-Salomon, A., J.Y. Pierga, J. Couturier, C.D. d'Enghien, C. Nos, B. Sigal-Zafrani, M. Lae, P. Freneaux, V. Dieras, J.P. Thiery, and X. Sastre-Garau. 2007. HER2 status of bone marrow micrometastasis and their corresponding primary tumours in a pilot study of 27 cases: a possible tool for anti-HER2 therapy management? *British journal of cancer*. 96:654-659.

Wiesner, C., J. Faix, M. Himmel, F. Bentzien, and S. Linder. 2010. KIF5B and KIF3A/KIF3B kinesins drive MT1-MMP surface exposure, CD44 shedding, and extracellular matrix degradation in primary macrophages. *Blood*. 116:1559-1569.

Williams, K.C., and M.G. Coppolino. 2011. Phosphorylation of membrane type 1-matrix metalloproteinase (MT1-MMP) and its vesicle-associated membrane protein 7 (VAMP7)-dependent trafficking facilitate cell invasion and migration. *The Journal of biological chemistry*. 286:43405-43416.

Wolf, K., M. Te Lindert, M. Krause, S. Alexander, J. Te Riet, A.L. Willis, R.M. Hoffman, C.G. Figdor, S.J. Weiss, and P. Friedl. 2013. Physical limits of cell migration: control by ECM space and nuclear deformation and tuning by proteolysis and traction force. *J Cell Biol*. 201:1069-1084.

Wolf, K., Y.I. Wu, Y. Liu, J. Geiger, E. Tam, C. Overall, M.S. Stack, and P. Friedl. 2007. Multi-step pericellular proteolysis controls the transition from individual to collective cancer cell invasion. *Nat Cell Biol*. 9:893-904.

Wolff, A.C., M.E. Hammond, J.N. Schwartz, K.L. Hagerty, D.C. Allred, R.J. Cote, M. Dowsett, P.L. Fitzgibbons, W.M. Hanna, A. Langer, L.M. McShane, S. Paik, M.D. Pegram, E.A. Perez, M.F. Press, A. Rhodes, C. Sturgeon, S.E. Taube, R. Tubbs, G.H. Vance, M. van de Vijver, T.M. Wheeler, and D.F. Hayes. 2007. American Society of Clinical Oncology/College of American Pathologists guideline recommendations for human epidermal growth factor receptor 2 testing in breast cancer. *Journal of clinical oncology : official journal of the American Society of Clinical Oncology*. 25:118-145.

Yu, X., T. Zech, L. McDonald, E.G. Gonzalez, A. Li, I. Macpherson, J.P. Schwarz, H. Spence, K. Futo, P. Timpson, C. Nixon, Y. Ma, I.M. Anton, B. Visegrady, R.H. Insall, K. Oien, K. Blyth, J.C. Norman, and L.M. Machesky. 2012. N-WASP coordinates the delivery and F-actin-mediated capture of MT1-MMP at invasive pseudopods. *The Journal of Cell Biology*. 199:527-544.

FIGURES

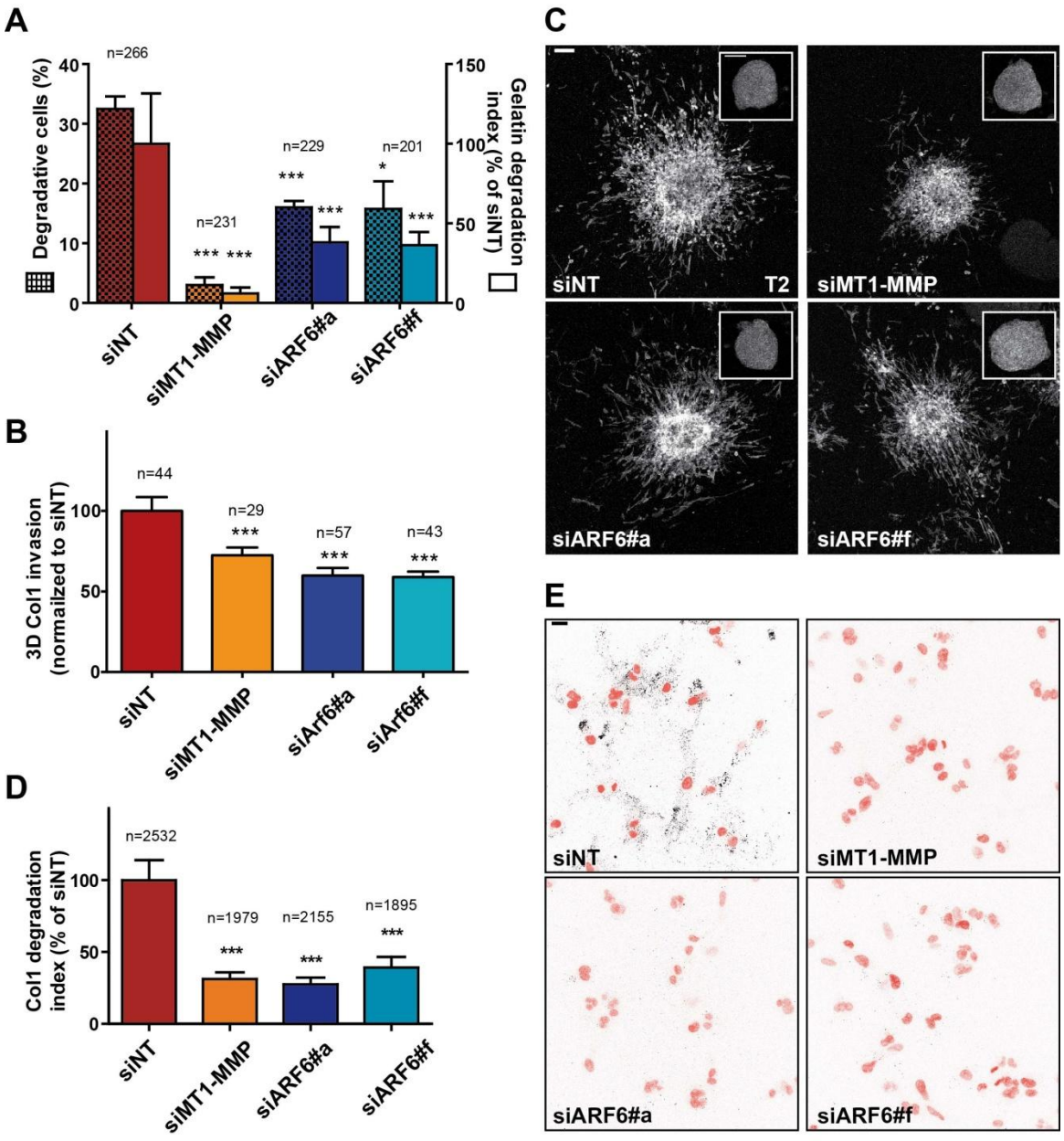

Fig.1

Figure 1: ARF6 is required for matrix degradation and invasive migration of breast tumor cells through 3D type I collagen environment. (A) MDA-MB-231 cells treated with indicated siRNAs were plated on cross-linked FITC-labeled gelatin and percentage of degradative cells (patterned bars) and degradation index (clear bars) were calculated. Values are mean ± SEM from two independent experiments. *n* represents the number of cells scored for each cell population. Comparisons were made with Mann-Whitney t-test (one-sided). *, P < 0.05; ***, P < 0.001 (compared with siNT-treated cells). **(B)** Multicellular spheroids of MDA-MB-231 cells treated with indicated siRNAs were embedded in 3D acid-extracted type I collagen, fixed immediately (T0) or incubated for 2 days (T2). Data represent average invasion area of spheroids at T2 normalized to the mean invasion area at T0 ± SEM and normalized to invasion of siNT spheroids, from four (siNT, siARF6#a) or three (siMT1-MMP, siARF6#f) independent experiments (*n,* number of spheroids analyzed for each cell population). Comparisons were made with ANOVA test. ****P* < 0.001. **(C)** Representative images showing phalloidin-labeled spheroids for each cell population collected at T2. Insets correspond to spheroids at T0. Scale bars: 200 µm. **(D)** Quantification of collagenolysis by MDA-MB-231 cells treated with indicated siRNAs and embedded in type I collagen. Values are mean normalized degradation index ± SEM from three independent experiments (*n*, number of cells analyzed for each cell population). Comparisons were made with Mann-Whitney t-test (one-sided) ***, P < 0.001 (as compared with siNT-treated cells). **(E)** Confocal images of MDA-MB-231 cells treated with the indicated siRNAs embedded in type I collagen and stained for the anti-Col1-$^{3/4}$C antibody (in black in the inverted image) and for DAPI (in red). Scale bar, 20 µm.

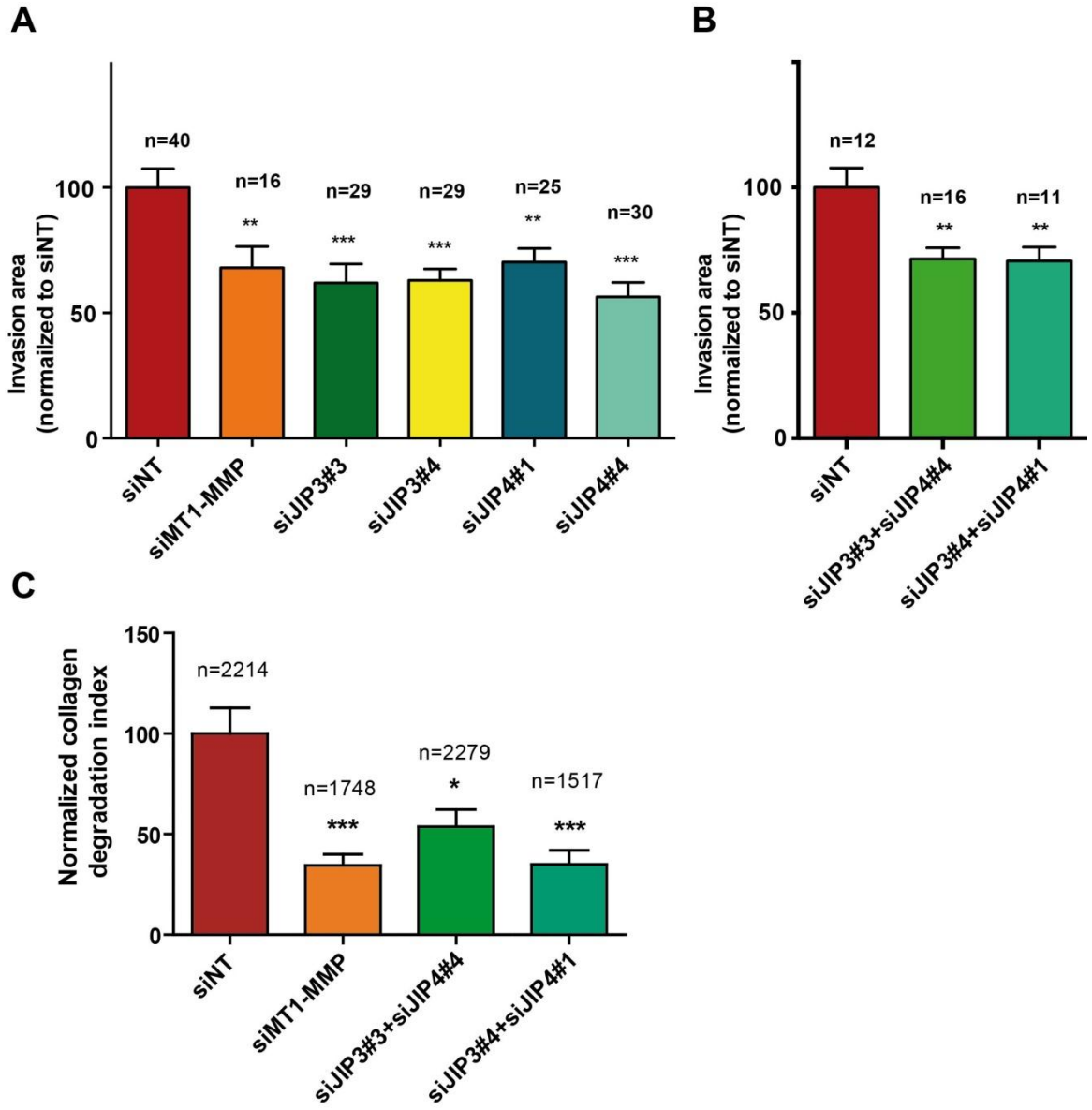
A
Invasion area (normalized to siNT)
100
50
0
n=40
n=16
n=29
n=29
n=25
n=30
**
***
***
**
***
siNT
siMT1-MMP
siJIP3#3
siJIP3#4
siJIP4#1
siJIP4#4
B
Invasion area (normalized to siNT)
100
50
0
n=12
n=16
n=11
**
**
siNT
siJIP3#3+siJIP4#4
siJIP3#4+siJIP4#1
C
Normalized collagen degradation index
150
100
50
0
n=2214
n=1748
n=2279
n=1517
***
*
***
siNT
siMT1-MMP
siJIP3#3+siJIP4#4
siJIP3#4+siJIP4#1

Fig. 2

Figure 2: JIP3 and JIP4 are required for invasive migration through 3D type I collagen matrix. (A-B) Quantification of spheroid invasion assay for cells treated with indicated siRNAs. Data represent average mean invasion area of spheroids at T2 normalized to the mean invasion area at T0 and further normalized to the invasion of siNT spheroids ± SEM from 2 to 3 independent experiments (*n,* number of spheroids analyzed for each cell population). Comparisons were made with ANOVA test. ***$P < 0.001$. **(C)** Quantification of collagenolysis by MDA-MB-231 cells treated with indicated siRNAs. Values are mean normalized degradation index ± SEM from two independent experiments (*n*, number of cells analyzed for each cell population). Comparisons were made with Mann-Whitney t-test (one-sided). *, $P < 0.05$; ***, $P < 0.001$ (as compared with siNT-treated cells).

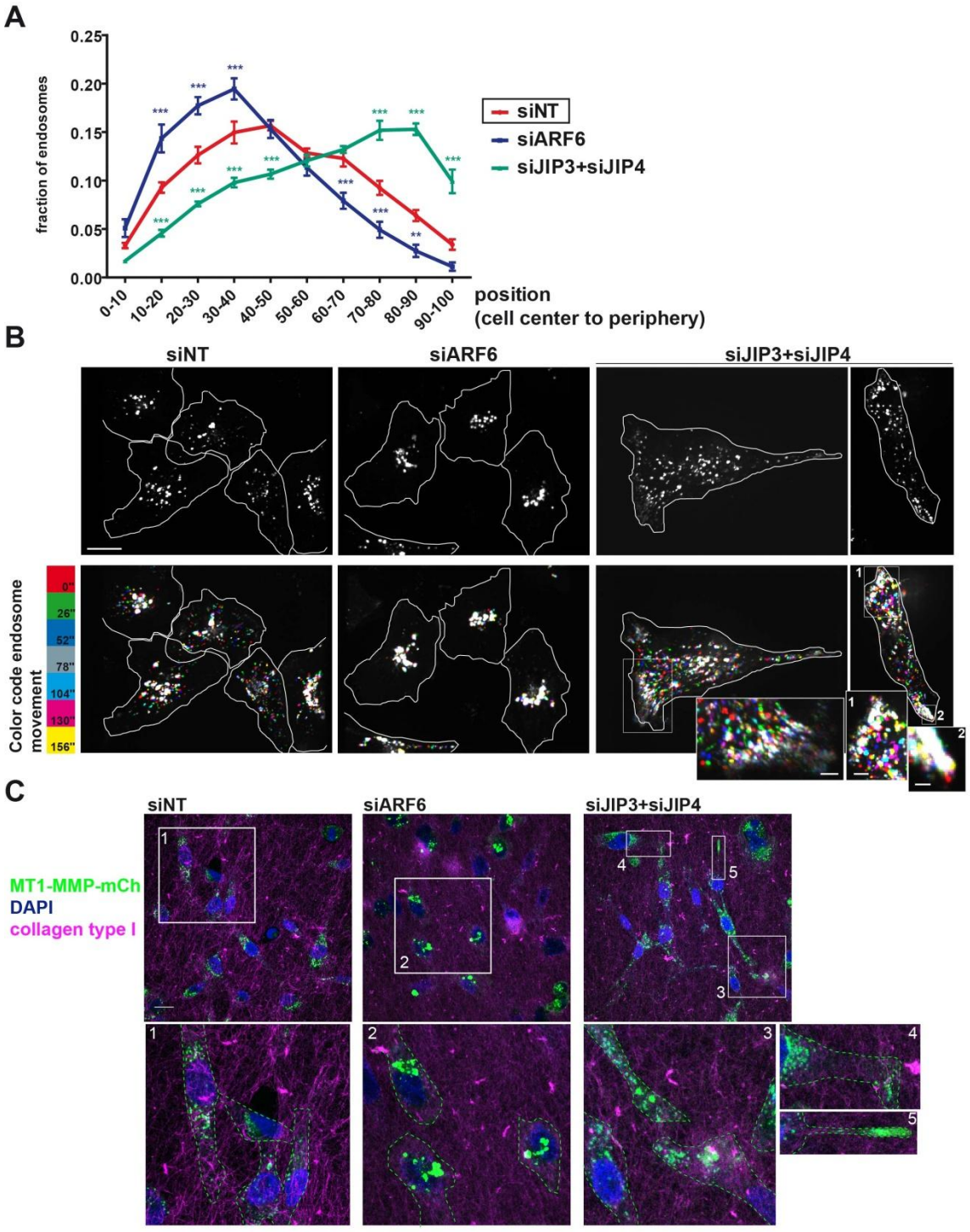
A
fraction of endosomes
0.25
0.20
0.15
0.10
0.05
0.00
0-10
10-20
20-30
30-40
40-50
50-60
60-70
70-80
80-90
90-100
position
(cell center to periphery)
siNT
siARF6
siJIP3+siJIP4
B
siNT
siARF6
siJIP3+siJIP4
Color code endosome movement
0"
26"
52"
78"
104"
130"
156"
C
siNT
siARF6
siJIP3+siJIP4
MT1-MMP-mCh
DAPI
collagen type I

Fig.3

Figure 3: The ARF6/JIP pathway is implicated in MT1-MMP-positive endosome positioning. (A) Automated quantification of intracellular distribution of MT1-MMP-mCherry-containing endosomes in cells treated with siNT (red curve), siARF6#a (blue curve) or a pair of siJIP3#3 and siJIP4#4 (green curve) siRNAs plated on 2D gelatin. Position “0” represents the cell center, position “100”, the cell periphery. Values are mean ± SEM from five to ten independent experimants scoring a total of 100 cells for each cell population. Comparisons were made with two-way ANOVA test. **, $P < 0.01$; ***, $P < 0.001$ (compared with siNT distribution). **(B)** The upper row are the first frame of confocal spinning-disk microscopy time-lapse sequences showing MT1-MMP-mCherry-expressing MDA-MB-231 cells treated with indicated siRNAs and plated on gelatin as in A. Lower row are the superimposition of seven time frames from the time-lapse sequences selected with an interval of 26 seconds and pseudocolored with color code shown on the left. Insets show magnification of the boxed regions. Scale bars, 20 µm, 5 µm (insets). **(C)** Confocal scanning images of MDA-MB-231 cells expressing MT1-MMP-mCherry treated with the indicated siRNAs and embedded in a 3D type I collagen matrix. Insets are magnification of the boxed regions. Scale bar, 20 µm.

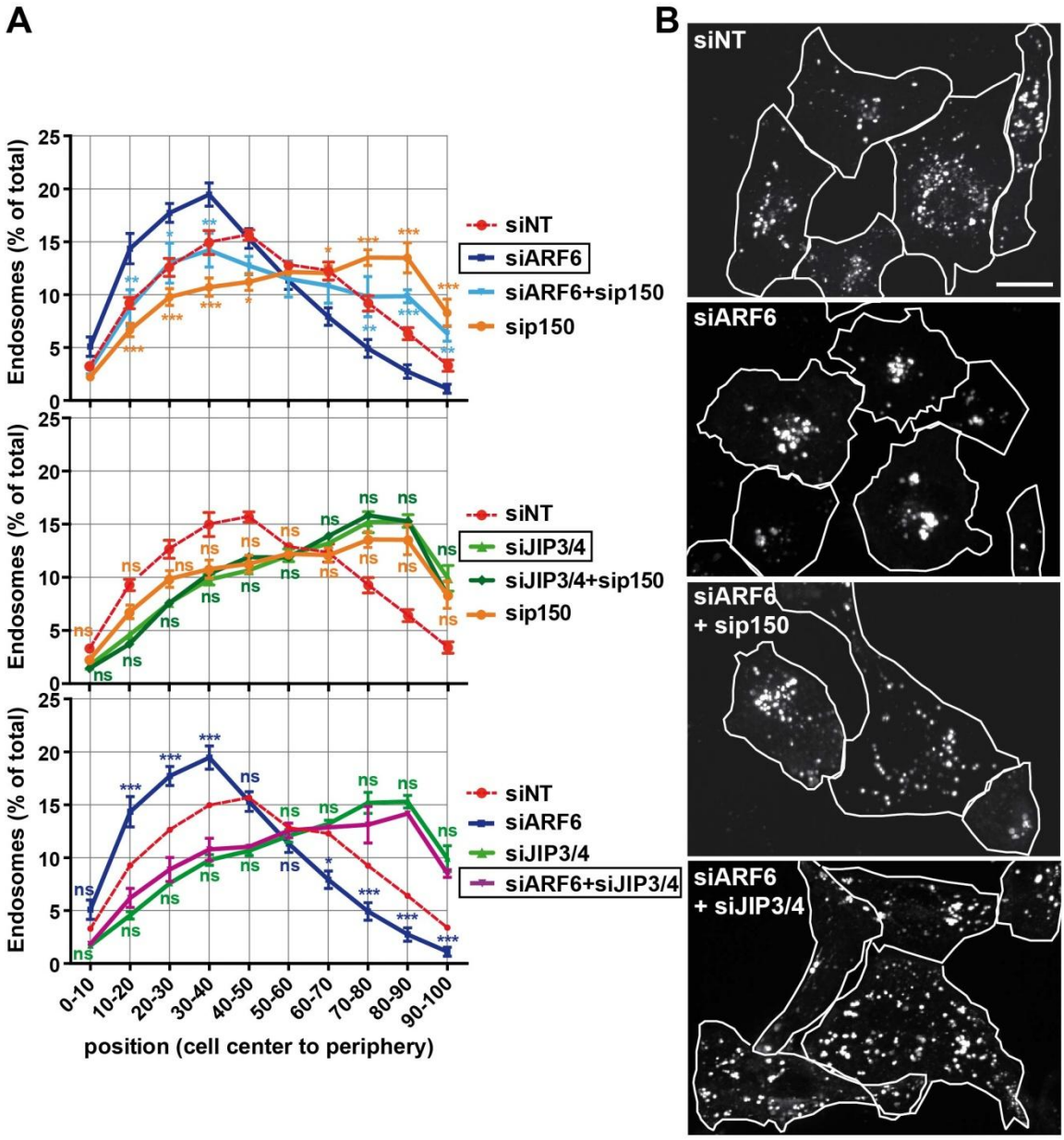
A
B
Endosomes (% of total)
position (cell center to periphery)
0-10
10-20
20-30
30-40
40-50
50-60
60-70
70-80
80-90
90-100
siNT
siARF6
siARF6+sip150
sip150
siJIP3/4
siJIP3/4+sip150
siARF6+siJIP3/4
siARF6
+ sip150
+ siJIP3/4

Fig.4

Figure 4: Regulation of MT1-MMP-positive endosome position by ARF6 requires JIP3/JIP4 and p150Glued dynactin complex subunit. (A) Automated quantification of the intracellular distribution of MT1-MMP-mCherry containing endosomes as in Fig. 3A. All values are mean ± SEM. Upper graph corresponds to three independent experiments analyzing a total of 50-60 cells for siARF6+p150*Glued* and sip150*Glued* siRNA conditions. Middle graph represents two independent experiments scoring a total of 40-50 cells for siJIP3/JIP4+sip150*Glued* condition. Lower graph represents two independent experiments scoring a total of 42 cells for siARF6+siJIP3/JIP4 condition. Comparisons were made with two-way ANOVA test. ns, non-significant, *, $P < 0.05$; **, $P < 0.01$; ***, $P < 0.001$ as compared to siARF6 treatment (upper graph), siJIP3/JIP4 (middle graph) or siARF6+siJIP3/JIP4 (lower graph). **(B)** MDA-MB-231 cells stably expressing MT1-MMP-mCherry plated on gelatin and treated with indicated siRNAs. Scale bar, 20 µm.

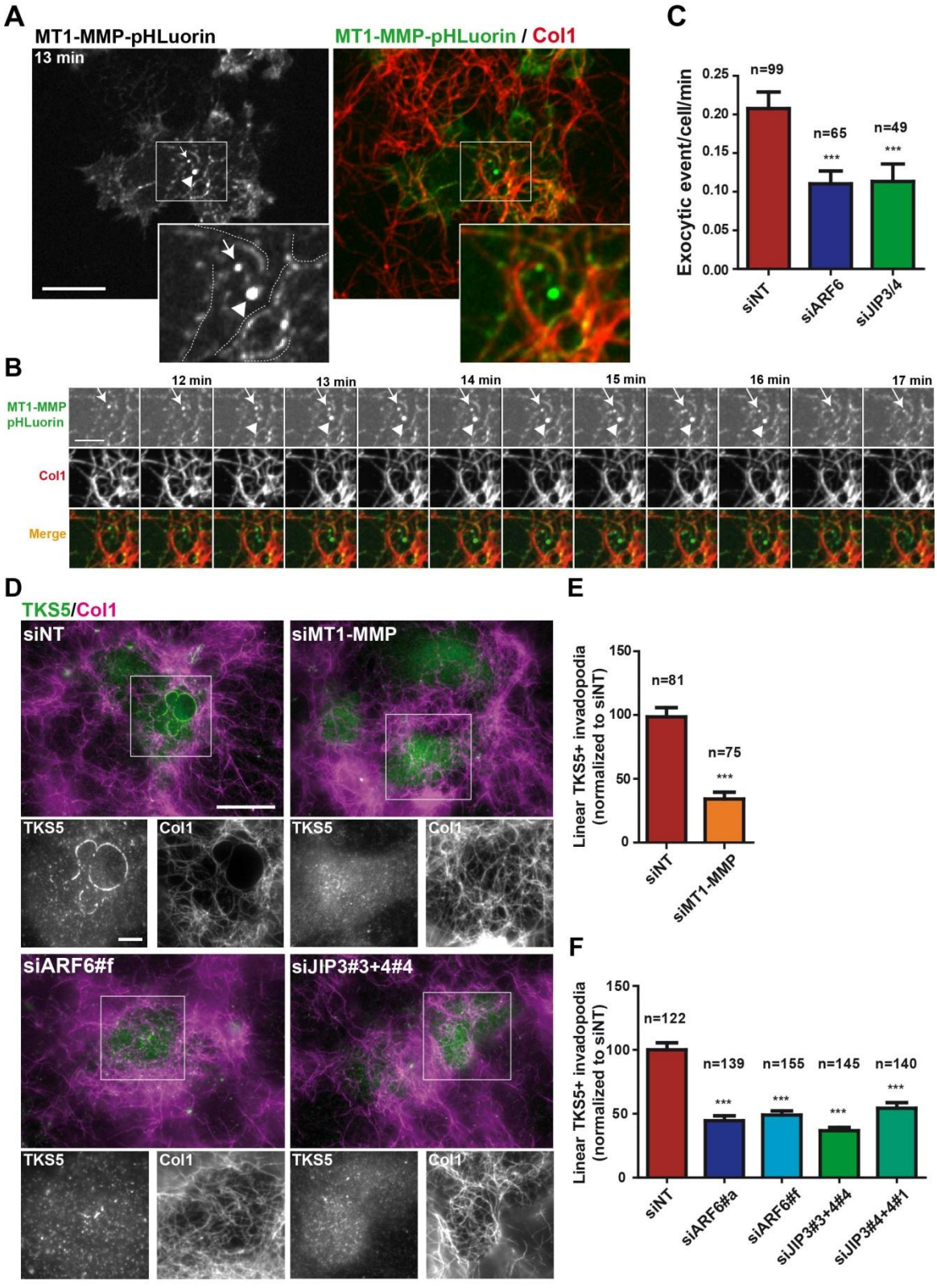
A
MT1-MMP-pHLuorin
13 min
MT1-MMP-pHLuorin / Col1
C
Exocytic event/cell/min
0.25
0.20
0.15
0.10
0.05
0.00
n=99
n=65
n=49
***
***
siNT
siARF6
siJIP3/4
B
12 min
13 min
14 min
15 min
16 min
17 min
MT1-MMP pHLuorin
Col1
Merge
D
TKS5/Col1
siNT
siMT1-MMP
TKS5
Col1
TKS5
Col1
siARF6#f
siJIP3#3+4#4
TKS5
Col1
TKS5
Col1
E
Linear TKS5+ invadopodia (normalized to siNT)
150
100
50
0
n=81
n=75
***
siNT
siMT1-MMP
F
Linear TKS5+ invadopodia (normalized to siNT)
150
100
50
0
n=122
n=139
n=155
n=145
n=140
***
***
***
***
siNT
siARF6#a
siARF6#f
siJIP3#3+4#4
siJIP3#4+4#1

Fig.5

Figure 5: ARF6 and JIP3/JIP4 are required for MT1-MMP exocytosis and for linear invadopodia formation. (A, B) Still image of a confocal spinning-disk microscopy time-lapse sequence of MDA-MB-231 cells expressing MT1-MMPpHLuorin (left panel, pseudocolored in green in the merge image in right panel) plated on a layer of type I collagen fibers (red). Two exocytic flashes of MT1-MMPpHLuorin are visible on the selected frame (pointed by arrow and arrowhead). Insets are high magnification of the boxed region. MT1-MMPpHLuorin accumulates along collagen I fibers (underlined with dashed lines). Scale bar, 20 µm. **(B)** Galleries correspond to the boxed region in panel A and show exocytosis of MT1-MMPpHluorin–positive endosomes (arrow and arrowhead) in the vicinity of collagen I fibers. Time is in min. Scale bar, 10 µm. **(C)** MDA-MB-231 cells expressing MT1-MMPpHLuorin silenced with siARF6#a or siJIP3#3+siJIP4#4 siRNAs seeded on a layer of type I collagen fibers and imaged over a 30-min time period. The frequency of MT1-MMPpHLuorin exocytic events was quantified (plotted as mean events/cell/min ± SEM with n, number of cells analyzed for each cell population Comparisons were made with Mann-Whitney t-test (one-sided). ***, $P < 0.001$ (compared with siNT-treated cells). **(D)** MDA-MB-231 cells treated with indicated siRNAs were seeded on a layer of type I collagen (magenta) for 90 min,, fixed and stained for TKS5 (green). Images are merged channels, insets showed magnifications of the boxed regions with separate channels. Scale bars, 20 µm, 5 µm (insets). **(E-F)** Quantification of linear invadopodia measured as total TKS5 fluorescence signal area in cells treated with indicated siRNAs, seeded and stained as in D. Values are mean ± SEM from three (E) and two (F) independent experiments (n, number of cells

analyzed for each cell population). Comparisons were made with Mann-Whitney t- test (one-sided). ***, $P < 0.001$ (compared with siNT-treated cells).

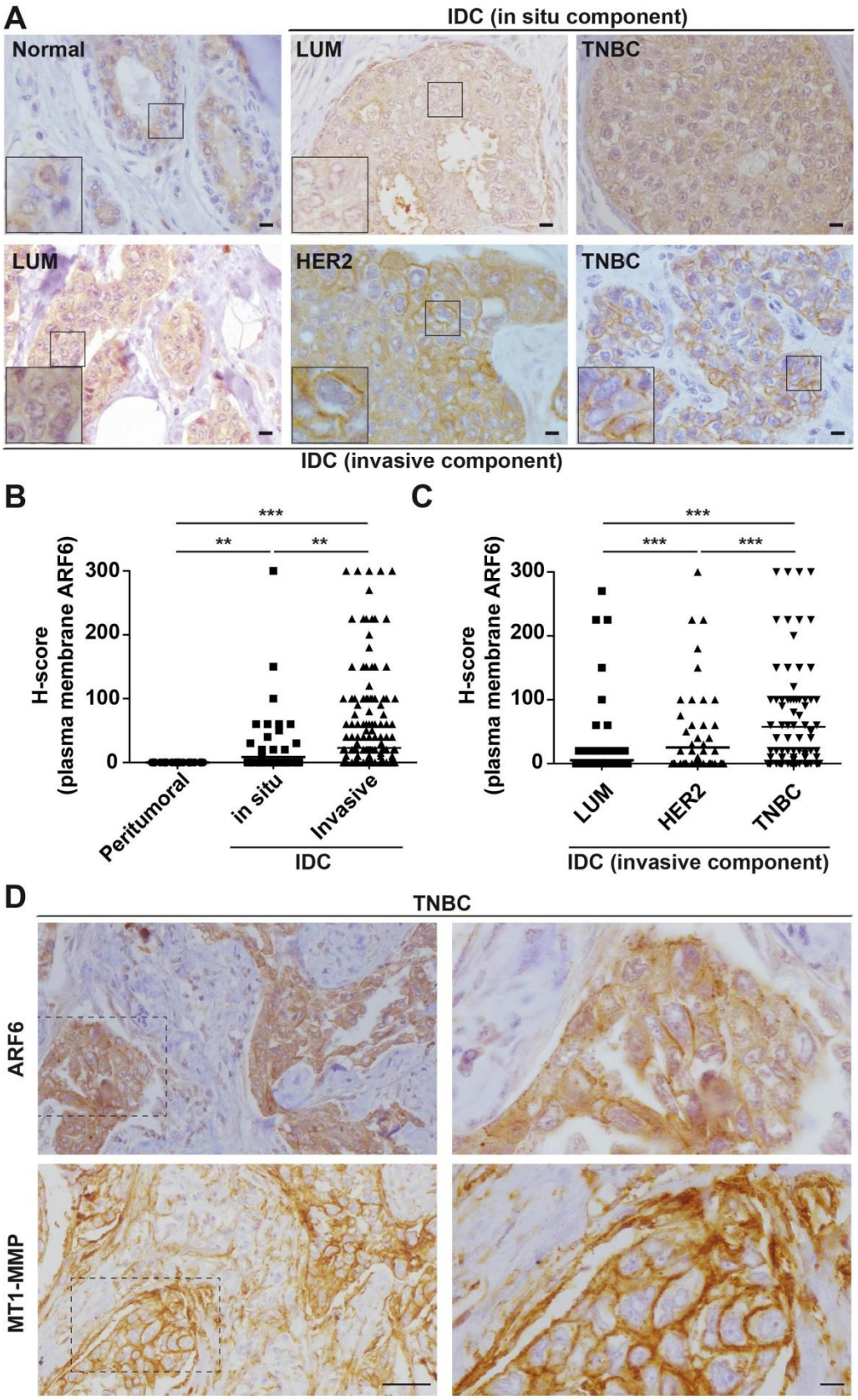
A
IDC (in situ component)
Normal
LUM
TNBC
LUM
HER2
TNBC
IDC (invasive component)
B
C
H-score (plasma membrane ARF6)
300
200
100
0
***
**
**
Peritumoral
in situ
Invasive
IDC
***
***
***
LUM
HER2
TNBC
IDC (invasive component)
D
TNBC
ARF6
MT1-MMP

Fig.6

Figure 6. Correlation of plasma membrane ARF6 and MT1-MMP expression in carcinoma cells in hormone receptor-negative breast tumors. (A) Representative regions of peritumoral breast epithelial tissue (Normal) and in situ and invasive components of invasive ductal carcinoma (IDC) of the indicated molecular subtypes stained for ARF6 by immunohistochemistry. LUM, hormone receptor-positive (Luminal A+B); TNBC, hormone receptor-negative, HER2-negative; HER2, hormone receptor-negative, HER2-positive. Insets show higher magnification of boxed regions. Scale bars, 10 μm. **(B, C)** Semiquantitative analysis of plasma membrane ARF6 expression by the H-score method comparing peritumoral breast epithelial tissue (n=324) and in situ (n=131) and invasive (n=426) components of IDCs (B) and the invasive component of IDCs segregated into the three molecular subtypes (LUM=234; HER2=80; TNBC=112) (C). Comparisons were made with Kruskal-Wallis test. **, $P < 0.01$; ***, $P < 0.001$. **(D)** Same region of non-consecutive sections of the invasive component of a TNBC immunostained for ARF6 and MT1-MMP. Images on the right row correspond to the boxed regions in the lower magnification pictures on the left row. Scale bars, 50 μm (left row), 10 μm (right row).

Table 1. Correlation between ARF6 and MT1-MMP plasma membrane H-score values in IDCs

	All cases N=398 Total population (%)		Hormone Receptor Positive N=222 Total population (%)		Hormone Receptor Negative N=176 Total population (%)	
	ARF6 <100	ARF6 ≥ 100	ARF6 < 100	ARF6 ≥ 100	ARF6 < 100	ARF6 ≥100
N	356 (89,4)	42 (10,6)	217 (97,7)	5 (2,3)	139 (79)	37 (21)
MT1-MMP <100	209 (58,7)	7 (16,7)	157 (72,4)	2 (40)	52 (37,4)	5 (13,5)
MT1-MMP ≥100	147 (41,3)	35 (83,3)	60 (27,6)	3 (60)	87 (62,6)	32 (86,5)
p value X^2	0,0001		NS		0,0058	

398 IDC cases were available for scoring plasma membrane ARF6 and MT1-MMP expression levels. Expression at the plasma membrane of both markers was analyzed in the overall cohort or after segregation based on hormone receptor status. Groups were divided in two categories based on the H-score values in <100 or ≥100. Analysis was done using X^2 test, one-sided.

SUPPLEMENTAL INFORMATION

ARF6-JIP3/JIP4-MT1-MMP axis controls tumor cell invasion during breast cancer progression

Valentina Marchesin, Catalina Lodillinsky, Joanna Cyrta, Laetitia Fuhrmann, Marie Irondelle, Asma Soltani, Alan Guichard, Anne Vincent-Salomon, Guillaume Montagnac and Philippe Chavrier

SUPPLEMENTAL FIGURES:

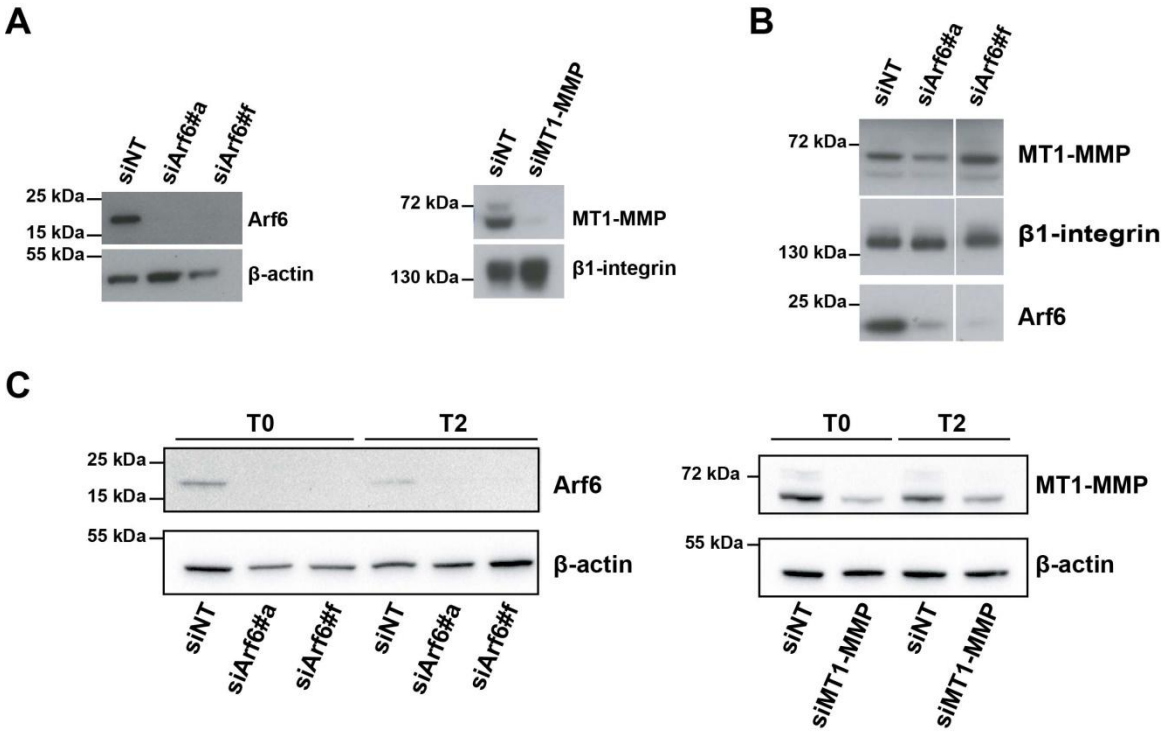

Suppl.1

Supplemental Figure S1 accompanying Figure 1: Immunoblotting analysis of siRNA-treated cells. (A–C) Immunoblotting analysis of lysates of MDA-MB-231 cells treated with indicated siRNAs for 72 hrs. In panel C corresponding to multicellular spheroid invasion assay shown in Fig. 1D, protein levels in the different cell populations were analyzed after 72 (T0) and 120 hrs (T2) after siRNA treatment. Antibodies are indicated on the right. Immunoblotting analysis with anti-β actin and anti β1-integrin was used as loading control.

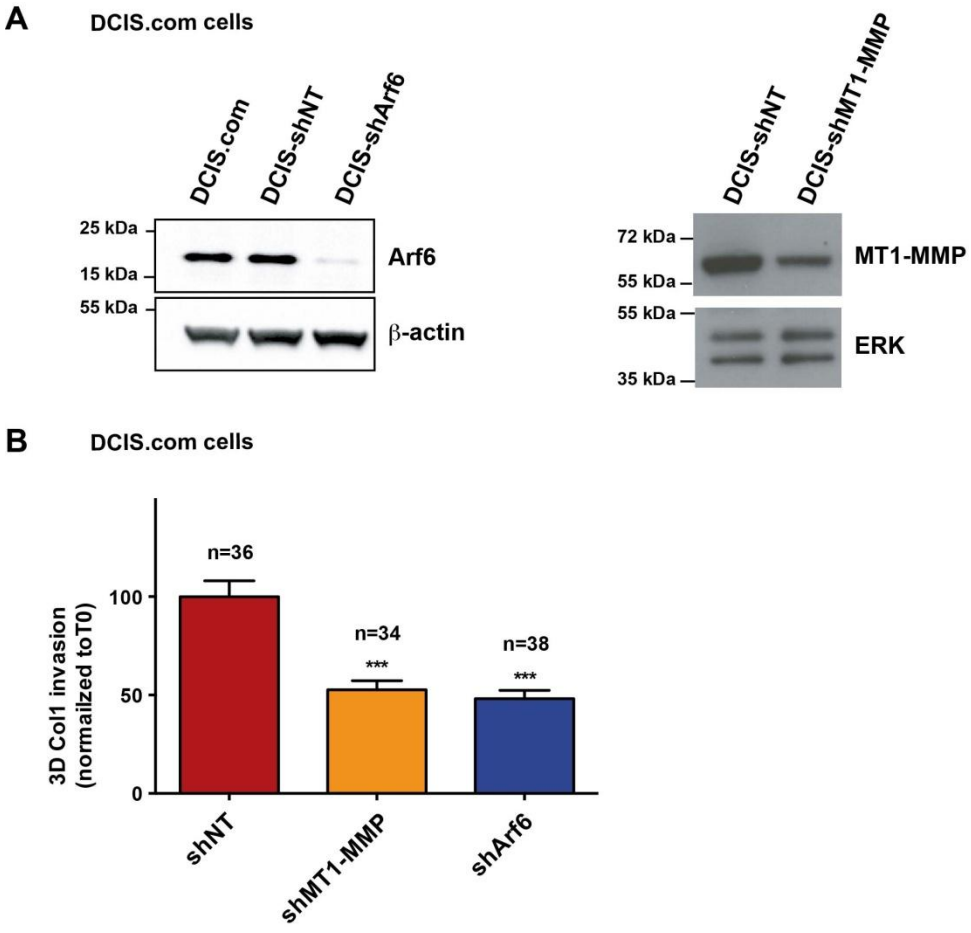
A
DCIS.com cells
DCIS.com
DCIS-shNT
DCIS-shArf6
25 kDa
15 kDa
55 kDa
Arf6
β-actin
DCIS-shNT
DCIS-shMT1-MMP
72 kDa
55 kDa
55 kDa
35 kDa
MT1-MMP
ERK
B
DCIS.com cells
3D Col1 invasion (normailzed toT0)
100
50
0
n=36
n=34
n=38
***
***
shNT
shMT1-MMP
shArf6
C
DCIS.com cells
T0
T0
T0
shNT
T2
shMT1-MMP
T2
shArf6
T2

Suppl. 2

Supplemental Figure S2 accompanying Figure 1: ARF6 is required for invasion of DCIS.com cells. (A) Immunobloting analysis of DCIS.com cells stably knocked-down for ARF6 or MT1-MMP expression by lentiviral shRNA expression. Antibodies for β actin and ERK1/2 were used as loading control. **(B)** Multicellular spheroids of DCIS.com cells stably expressing the indicated shRNA were embedded in 3D acid-extracted type I collagen and either fixed immediately (T0) or further incubated for 2 days (T2). Data represent average invasion area of spheroids at T2 normalized to the mean invasion area at T0 ± SEM from three independent experiments (*n*, number of spheroids analyzed for each cell population). Comparisons were made with ANOVA test. ***$P < 0.001$ (compared to shNT multicellular spheroids). **(C)** Phalloidin-labeled multicellular spheroids representative of each cell population collected after two days in 3D collagen I (T2). Insets correspond to spheroids at T0. Scale bars: 200 µm.

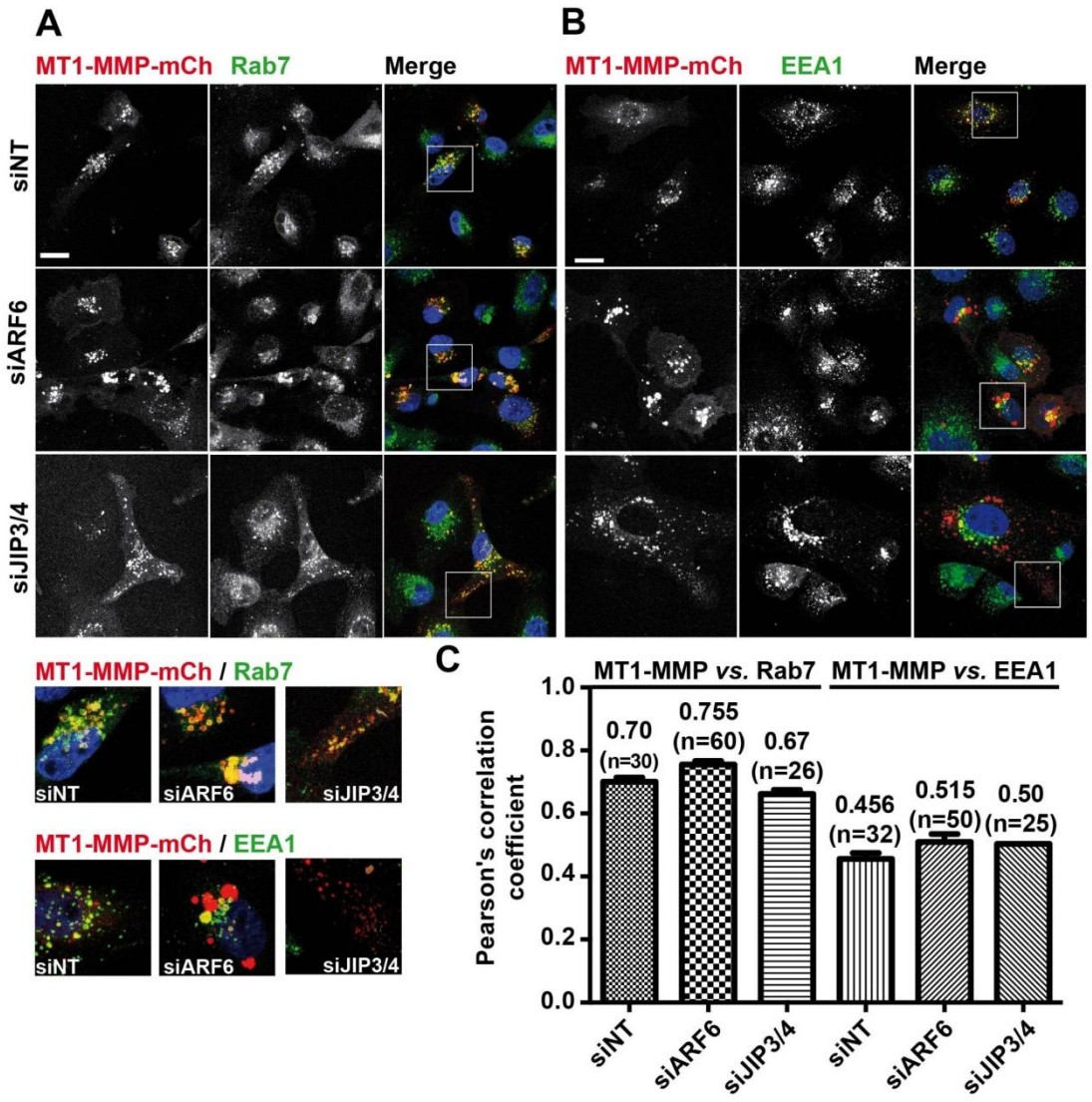
A
MT1-MMP-mCh
Rab7
Merge
siNT
siARF6
siJIP3/4
B
MT1-MMP-mCh
EEA1
Merge
MT1-MMP-mCh / Rab7
siNT
siARF6
siJIP3/4
MT1-MMP-mCh / EEA1
siNT
siARF6
siJIP3/4
C
MT1-MMP vs. Rab7
MT1-MMP vs. EEA1
Pearson's correlation coefficient
1.0
0.8
0.6
0.4
0.2
0.0
0.70 (n=30)
0.755 (n=60)
0.67 (n=26)
0.456 (n=32)
0.515 (n=50)
0.50 (n=25)
siNT
siARF6
siJIP3/4
siNT
siARF6
siJIP3/4

Suppl.3

Supplemental Figure S3 accompanying Figure 2 and 3: MT1-MMP accumulates in Rab7-positive late endosomes in MDA-MB-231 cells. (A-B) MDA-MB-231 cells stably expressing MT1-MMP-mCherry treated with the indicated siRNAs were plated on gelatin, fixed and stained for Rab7 (A) or EEA1 (B). Insets are higher magnification of the boxed regions. Scale bars: 20 µm. (C) Pearson's correlation coefficients of MT1-MMP *vs.* Rab7 or EEA1 markers in the different cell populations (n, number of cells analyzed).

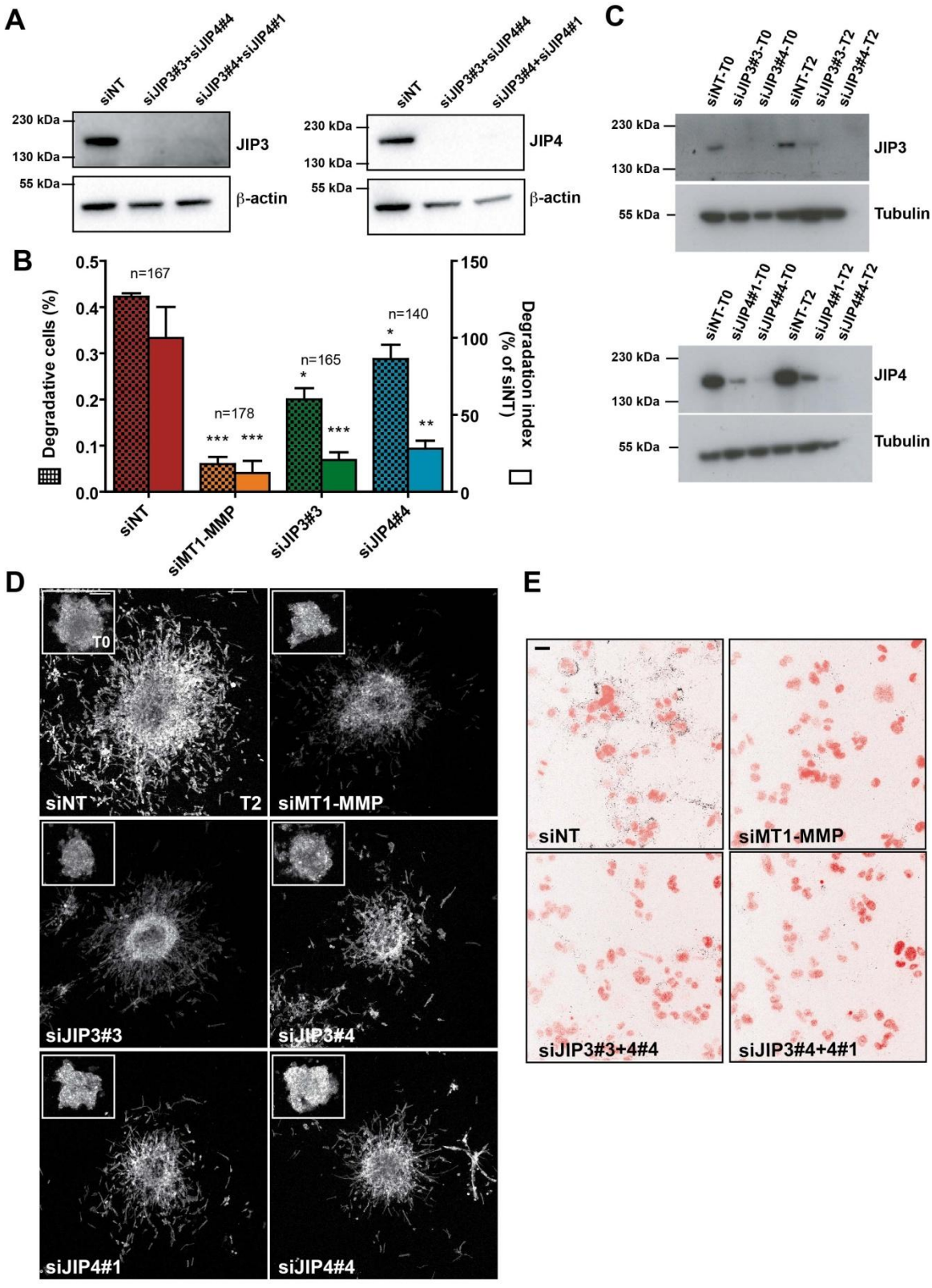
A
siNT
siJIP3#3+siJIP4#4
siJIP3#4+siJIP4#1
230 kDa
130 kDa
55 kDa
JIP3
β-actin
JIP4
B
Degradative cells (%)
Degradation index (% of siNT)
n=167
n=178
n=165
n=140
siNT
siMT1-MMP
siJIP3#3
siJIP4#4
C
siNT-T0
siJIP3#3-T0
siJIP3#4-T0
siNT-T2
siJIP3#3-T2
siJIP3#4-T2
Tubulin
siJIP4#1-T0
siJIP4#4-T0
siJIP4#1-T2
siJIP4#4-T2
D
T0
T2
siJIP4#1
E
siJIP3#3+4#4
siJIP3#4+4#1

Suppl.4

Supplemental Figure S4 accompanying Figure 2: JIP3 and JIP4 are required for gelatin degradation and invasive migration in 3D collagen. (A) Immunoblot analysis of JIP-knocked down MDA-MB-231 cells after 72 hrs siRNA treatment. Immunoblotting analysis with anti-βactin was used to check for equal loading. **(B)** Percentage of degradative cells (patterned bars) and degradation index (clear bars) of MDA-MB-231 cell populations depleted for JIP3 or JIP4. Values are mean ± SEM from two independent experiments (*n*, number of cells scored for each cell population). Comparisons were made with Mann-Whitney t-test (one-sided). *, $P < 0.05$; **, $P < 0.01$; ***, $P < 0.001$ (compared with siNT-treated cells). **(C)** Immunoblot analysis of MDA-MB-231 cells treated with JIP3 or JIP4 siRNAs for 72 (T0) or 120 hrs (T2) using anti-α tubulin antibodies as a loading control. **(D)** Phalloidin-labeled multicellular spheroids after 2 days in 3D collagen I gel. Insets correspond to spheroids at T0. Scale bars, 200 µm. **(E)** Confocal images of MDA-MB-231 cells treated with the indicated siRNAs embedded in type I collagen and stained for the anti-Col1$^{3/4}$C antibody (in black in the inverted image) and for DAPI (in red). Scale bar, 20 µm.

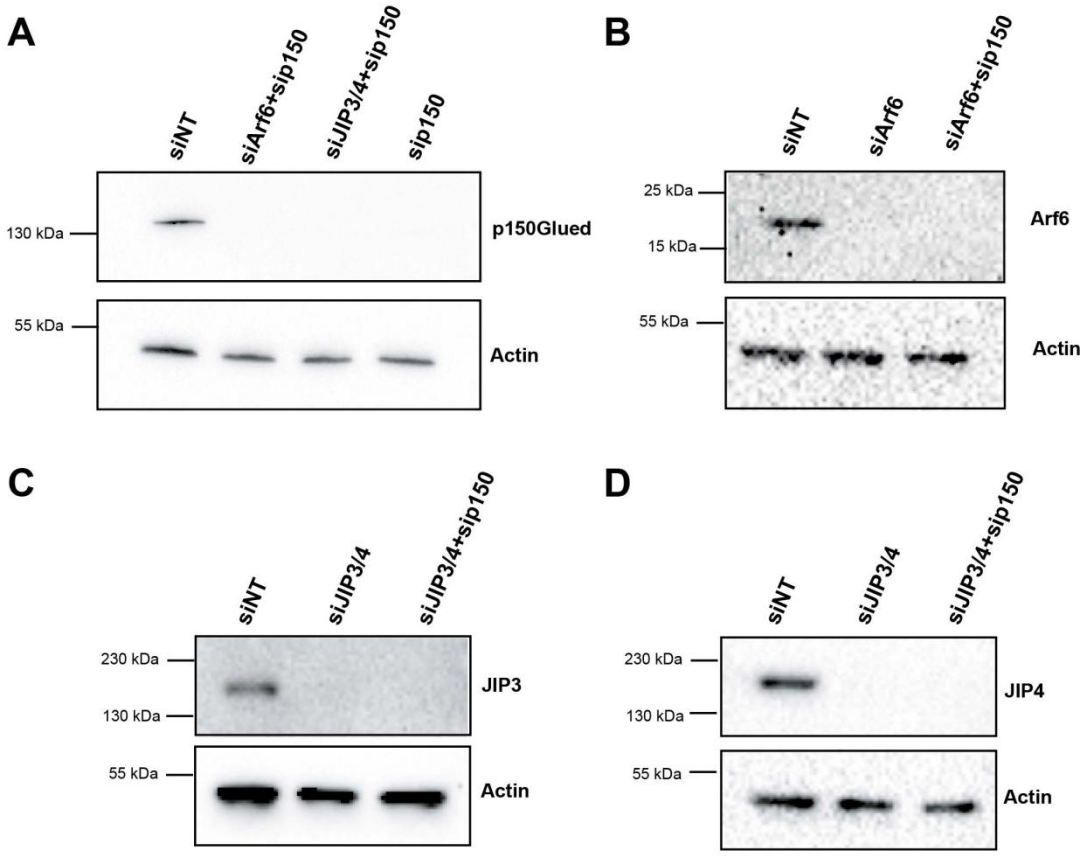

Suppl.5

Supplemental Figure S5 accompanying Figure 4: Immunoblotting analysis of siRNA-treated cells. (A–D) Immunoblotting analysis of MDA-MB-231 cells stably expressing MT1-MMP-mCherry treated with the indicated siRNAs. Antibody specificity is indicated on the right. Immunoblotting with anti-β actin was used as a loading control.

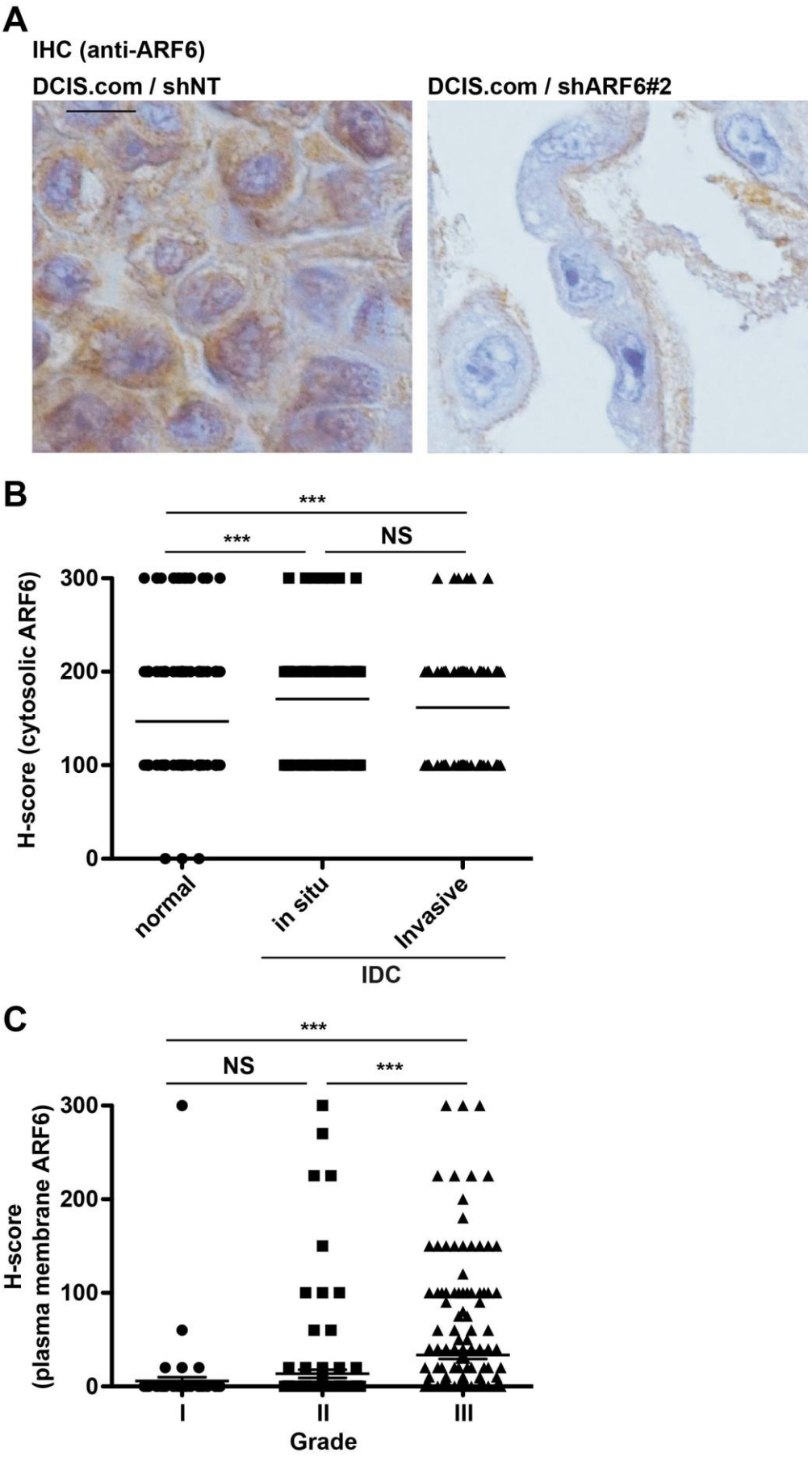
A
IHC (anti-ARF6)
DCIS.com / shNT
DCIS.com / shARF6#2
B
***
***
NS
H-score (cytosolic ARF6)
300
200
100
0
normal
in situ
Invasive
IDC
C
***
NS
***
H-score (plasma membrane ARF6)
300
200
100
0
I
II
III
Grade

Suppl.6

Figure S6 accompanying Figure 6. Analysis of ARF6 IHC staining of breast tumor TMA. (A) Specificity control of IHC anti-ARF6 antibody. Paraffin-embedded sections of multicellular spheroids of DCIS.com cells stably expressing non-relevant (shNT, left panel) or ARF6-specific shRNA (#2, right panel) stained by IHC by Millipore clone 6ARF01 anti-ARF6 monoclonal antibody. Scale bar, 10 µm. **(B)** Semiquantitative analysis of cytosolic ARF6 staining by the H-score method comparing peritumoral breast epithelial tissue (Normal, n=326) and in situ (n=131) and invasive (n=426) components of IDCs. **(C)** Semiquantitative analysis of membrane ARF6 staining by the H-score method comparing the three histological grades (grade I, n=73; grade II, n=127; grade III, n=226). Comparisons were made with Kruskal-wallis test. NS, non-significant; ***, $P < 0.001$.

Table S1, Related to Figure 6. Characteristics of primary tumors included in the TMA

Characteristics	IDC N=496 (%)
Histological grade [a]	
I	83 (16.7)
II	154 (30.0)
III	258 (52.0)
Unknown	1 (0.2)
Nuclear grade [b]	
High	NA
Non high	NA
Histological subtype	
Ductal carcinoma	487 (98.2)
Lobular carcinoma	6 (1.2)
Others	3 (0.6)
Tumour size (cm) [c]	
Tis	NA
T1mic	NA
T1 (<2)	330 (66.5)
T2 (2 NA 5)	148 (29.8)
T3 (>5)	14 (2.8)
T4	4 (0.8)
N stage [d]	
N0	272 (54.8)
N1	149 (30.0)
N2	55 (11.1)
N3	17 (3.4)
Unknown	3 (0.6)

ER status		
	Positive	286 (57.7)
	Negative	210 (42.3)
PR status		
	Positive	255 (51.4)
	Negative	241 (48.6)
	ND	0 (0.0)
HER2 status		
	Positive	93 (18.7)
	Negative	403 (81.3)
	ND	0 (0.0)
Ki67		
	Positive (≥20%)	363 (74.0)
	Negative (<20%)	133 (26.0)
	NA	0 (0.0)
Molecular subtype		
	TNBC	131 (26.4)
	HER2	79 (15.9)
	Luminal A	147 (29.6)
	Luminal B	139 (28.0)
	ND	0 (0)

Molecular subtypes were based on estrogen receptor (ER), progesterone receptor (PR) and HER2 status as described (Prat et al., 2013; Wolff et al., 2007) (see Experimental procedures). [a] Invasive breast cancers classified based on the Elston-Ellis classification system (grade I-III) (Elston and Ellis, 1993). [b] Grading of DCIS and microinvasive tumors based on Bloom-Richardson nuclear grading system (Bloom and Richardson, 1957) or EORTC. [c, d] Based on TNM staging (Singletary et al., 2003). NA, non applicable. After IHC staining with anti-ARF6 antibodies, 426 IDC cases were available for scoring.

Table S2: siRNAs and shRNAs used for this study.

siRNA Gene	Sequence (Sens)	Company
ARF6 #a	5'-CGGCAUUACUACACUGGGA-3'	Thermo Fisher Scientific
ARF6#f	5'-GCACCGCAUUAUCAAUGAC-3'	Ambion
MT1-MMP	5'-GGAUGGACACGGAGAAUUU-3', 5'-GGAAACAAGUACUACCGUU-3', 5'-GGUCUCAAAUGGCAACAUA-3', 5'-GAUCAAGGCCAAUGUUCGA-3'	Thermo Fisher Scientific
MAPK8IP3 (JIP3)#3	5'-GUUUGAAGAUGCUCUGGAA-3'	Thermo Fisher Scientific
MAPK8IP3 (JIP3)#4	5'-GAACAAAGCUUUCGGCAUC-3'	Thermo Fisher Scientific
SPAG9(JIP4)#1	5'-GAGCAUGUCUUUACAGAUC-3'	Thermo Fisher Scientific
SPAG9 (JIP4)#4	5'-GCAUCACAGUGGUUGGUUG-3'	Thermo Fisher Scientific
DCTN1(p150*Glued*)	5'-CUGGAGCGCUGUAUCGUAA-3', 5'-GAAGAUCGAGAGACAGUUA-3', 5'-GCUCAUGCCUCGUCUCAUU-3', 5'-CGAGCUCACUACUGACUUA-3'	Thermo Fisher Scientific
Non targeting		Thermo Fisher Scientific

shRNA Gene	Sequence (Sens)	Company
Non targeting	CCGGCAACAAGATGAAGAGCACCAACT CGAGTTGGTGCTCTTCATCTTGTTGTTTT T	Sigma
ARF6 #2	CCGGGTCAAGTTCAACGTATGGGATCTC GAGATCCCATACGTTGAACTTGACTTTTT G	Sigma *TRCN0000048003*
MT1-MMP	CCGGCGATGAAGTCTTCACTTACTTCTC GAGAAGTAAGTGAAGACTTCATCGTTTT TG	Sigma *TRCN0000050855*

Chapter 5: ARF6 implication in a mouse model of breast cancer

5.1. Introduction

As described in chapter 1.2, breast cancer progression is characterized first by *in situ* lesion, ductal carcinoma in situ (DCIS), which stays confined within the lumen of the ductal system. DCIS can progress to an invasive ductal carcinoma (IDC) when tumor cells cross the myoepithelium and perforate the BM to subsequently invade through the stroma. Close genetic resemblance between DCIS and their invasive counterparts supports the idea that DCIS is a precursor of the invasive form (Cowell et al., 2013). However the mechanism of transition from DCIS to invasive breast carcinoma is not yet well understood and the risk of progression cannot be predicted. Understanding this process is of key importance, as it might help to identify DCIS with a higher risk of recurrence and to develop therapeutic approaches for blocking the invasive activity in tumors.

Recently Dr Medina's lab developed a new xenograft model consisting in injecting intraductally a suspension of human breast carcinoma cells in 6-10 weeks old virgin female SCID mice via the cleaved nipple into the primary duct system (Behbod et al., 2009) (Fig. 34). Using cell lines representative of *in situ* breast carcinoma, including the DCIS.com cells, Behbod *et al.* observed the formation of *in situ* tumors filling the ducts at 4-8 weeks after injection (Fig.34), which were histopathologically reminiscent of human DCIS lesions. These lesions further progressed to invasive tumors in approximately 10 weeks (Behbod et al., 2009).

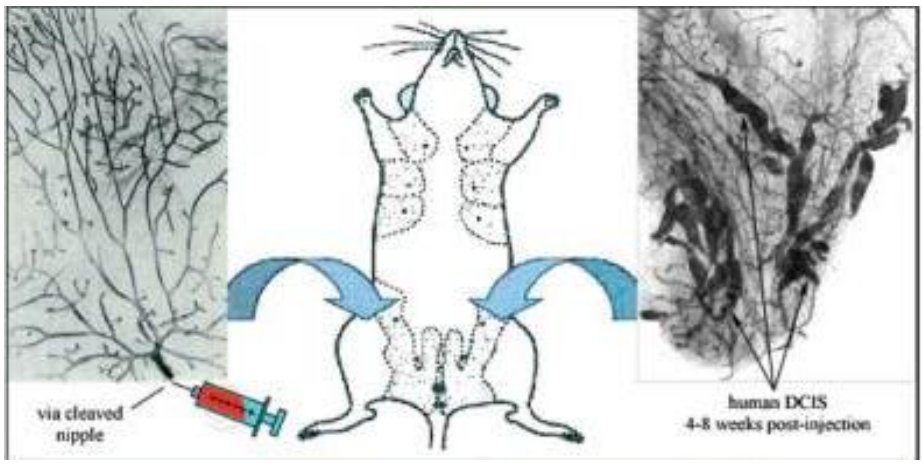

Figure 34: Human in mouse intraductal xenograft model. Picture from Behbod et al., 2009.

This intraductal xenograft therefore provides a useful model to analyze the molecular and cellular mechanisms of breast cancer progression and to study the earliest stage of invasion, such as the intraductal cancer cell growth or the capacity of cells to breach the BM and break out of the milk

duct. This model was established and developed in my host laboratory to assess the requirement for MT1-MMP in tumour invasion (Lodillinsky et al., submitted). In this study DCIS.com cells depleted for MT1-MMP and injected intraductally, gave rise to *in situ* tumors that did not progress further into invasive tumors, as compared to control mice in which the 100 % of *in situ* lesions were associated with adjacent invasive tumors (Lodillinsky et al., submitted). This study therefore provides strong evidences for a critical role of MT1-MMP in the in situ to invasive transition in breast cancer. Lodillinsky *et al.* also generalized these findings by injecting MDA-MB-231 cells in the intraductal system as a representative of highly invasive triple-negative breast cancer. Upon intraductal injection, MDA-MB-231 cells did not form *in situ* lesions; however, 2-3 weeks after injection it was possible to observe growth of infiltrating tumor foci through the mammary stroma. In contrast, MDA-MB-231 cells depleted for MT1-MMP failed to generate tumor foci, suggesting that MT1-MMP expression is required for MDA-MB-231 cells to cross the BM and reach the mammary stroma where these cells give rise to invasive growth and generate tumor foci (Lodillinsky et al., submitted).

Our *in vitro* data point to a role for ARF6 in MT1-MMP-dependent breast cancer cell invasion and our human samples analysis revealed an accumulation of ARF6 at the plasma membrane of cells in aggressive tumor types associated with poorer prognosis. Moreover this redistribution correlates with increased plasma membrane expression of MT1-MMP in these tumors (see chapter 4).

Therefore, our goal was to use the intraductal xenograft model in order to investigate whether ARF6 is also required for cells to breach the BM and for the *in situ* to invasive transition of breast cancer. To our knowledge, this would also be the first study to assess the role of ARF6 in invasion *in vivo* using cancer cell lines of an epithelial origin.

5.2. Materials and Methods

Lentiviral vectors for shRNA expression.

Lentiviral shRNAs inserted in pLKO.1-puro vector against human ARF6 (TRCN0000048003; TRCN0000294069) were purchased from Sigma (see Table1).

For lentivirus production, HEK293T cells were transfected using GeneJuice (Novagen) with a mix of expression vector and psPAX2 (AddGene) and pVSV-G (Clonetech) packaging vectors in OPTIMEM (Invitrogen). After 72 hrs, virus-containing supernatant was collected, filtered and used for transduction of a subconfluent monolayer of MDA-MB-231 cells. Puromycin (1 µg/ml, GIBCO) was added after 48 hrs for selection.

Table1: shRNAs used for generation of stable cell lines

shRNA		
Non targeting	CCGGCAACAAGATGAAGAGCACCAACTC GAGTTGGTGCTCTTCATCTTGTTGTTTTT	Sigma
ARF6 #2	CCGGGTCAAGTTCAACGTATGGGATCTCG A GATCCCATACGTTGAACTTGACTTTTTG	Sigma
ARF6 #3	CCGGCTTGCTGTAGATGGCTTATTTCTCGA GAAATAAGCCATCTACAGCAAGTTTTTG	Sigma

Intraductal transplantation method.

Intraductal injection was performed as previously described (Behbod et al., 2009). Briefly, 8-10 week-old virgin female SCID mice were anesthetized and a Y-incision was made on the abdomen to expose the inguinal glands after peeling back the skin covering the fat pads. Nipples of both inguinal glands #4 were snipped for insertion of a blunt-ended 1/2-inch needle from a 30-gauge 50-µl Hamilton syringe. Two microliters of cell suspension containing 10^5 cells/µl MDA-MB-231 cells in PBS were injected (with 0.1% trypan blue allowing visual detection of the injected cell suspension in the ductal tree). Mice were sacrificed between 5 to 7 weeks after injection by cervical dislocation. The care and use of animals were strictly applying European and National Regulation for the Protection of Vertebrate Animals used for Experimental and other Scientific Purposes in force (facility licence #C75-05-18). They comply also with internationally established principles of replacement, reduction and refinement in accordance with Guide for the Care and Use of Laboratory animals (NRC 2011) and Guidelines for the Welfare and Use of Animals in Cancer Research (Workman et al., 2010).

Histological analysis of mouse tissue sections. Whole-mount carmine and Hematoxylin and Eosin staining were performed as described (Teuliere et al., 2005).

Cell growth assay. The proliferation curve of the different stable cell lines was measured using a MTT Cell Growth kit (CT02, Millipore), a colorimetric assay based on the capability of living cells to cleave the substrate MTT 3-(4,5-dimethylthiazol-2-yl)-2,5-diphenyltetrazolium bromide that has a yellow pale color to its insoluble formazan, which has a purple color. The kit was used according to the manufacturer's instruction.

5.3. Results and discussion

We injected intraductally MDA-MB-231 stably knocked-down for ARF6 with two independent shRNAs (shARF6#2, shARF6#3). The depletion was checked by immunoblotting analysis (Fig. 35A). Cells depleted for ARF6 did not show significant defects in proliferation ability as compared to control MDA-MB-231 cells or cells treated with a Non-Targeting shRNA as measured with a cell growth assay (Fig.35B). Analysis of the mice mammary glands by whole-mount carmine staining showed that mice injected with cells depleted for ARF6 developed significantly fewer tumors than mice injected with control cells (Fig.35C-D), suggesting that ARF6 could be required for MDA-MB-231 cells to cross the BM and give rise to tumor growth in the fat pad. We could not rule out whether tumor growth observed in some shARF6#2-injected glands (Fig.35D) was due to a possible recovery of ARF6 protein expression that we observed by immunoblot in cells cultured for five weeks (data not shown). This was due to a technical issue, since IHC staining with ARF6 antibody requires an acidic fixation which is not compatible with a whole mount-carmine staining.

These results therefore suggest a possible requirement for ARF6 in the capacity of breast cancer cells to breach the BM and to give rise to invasive growth in the stroma, thereby further supporting our *in vitro* and human samples data.

However, this experimental work presents several limits that cannot allow us to strongly conclude that ARF6 is required for breast cancer formation *in vivo*. For instance, although silencing of ARF6 did not affect proliferation of MDA-MB-231 cells *in vitro* (Fig.35B), we cannot exclude that ARF6 KD may reduce cell growth in the particular environments of the mammary duct lumen or in the fat pad for the cells that reached this environment, and thus decrease in number of tumor foci/gland may be due to an effect of ARF6 KD on cell tumor growth. An experimental control that could be done to rule out a reduction of cell growth in the stromal environment would be to perform an injection of MDA-MB-231 cells depleted for ARF6 or control shRNAs directly in the fat pad of the mammary gland and to check for tumor growth.

Another important limitation derives from the use of MDA-MB-231 cells in this model. C. Lodillinsky, indeed, showed that most of the injected cells die inside the duct (as visualized by staining with the apoptotic marker caspase-3, C. Lodillinsky, unpublished data). This is in contrast to DCIS.com or SUM225 breast tumor-derived cells that generate highly proliferative intraductal xenograft tumors. One

A major difference between these two cell lines and MDA-MB-231 is the absence of E-cadherin expression in the latter and incapacity to make cell-cell contacts and thus generate a compact tumor mass. We therefore do not exclude the possibility that the decrease in the number of tumor foci we observed in glands injected with ARF6 shRNAs is due to a lower capacity of MDA-MB-231 cells to survive in the duct.

For these reasons DCIS.com cells would represent a better model to document the *in situ* to invasive transition. We attempted to inject intraductally DCIS.com cells depleted for ARF6 or expressing control shRNAs. Unfortunately, already after a few weeks in culture, we observed a strong recovery of ARF6 expression in DCIS.com cells in culture; in the intraductal xenograft model, we found formation of invasive tumors adjacent to *in situ* lesions with no significant difference between ARF6-depleted and non-depleted cells (data not shown). Thus, given these experimental limitations data on ARF6 implication *in vivo* should be taken with caution and further control experiments should be done in the future.

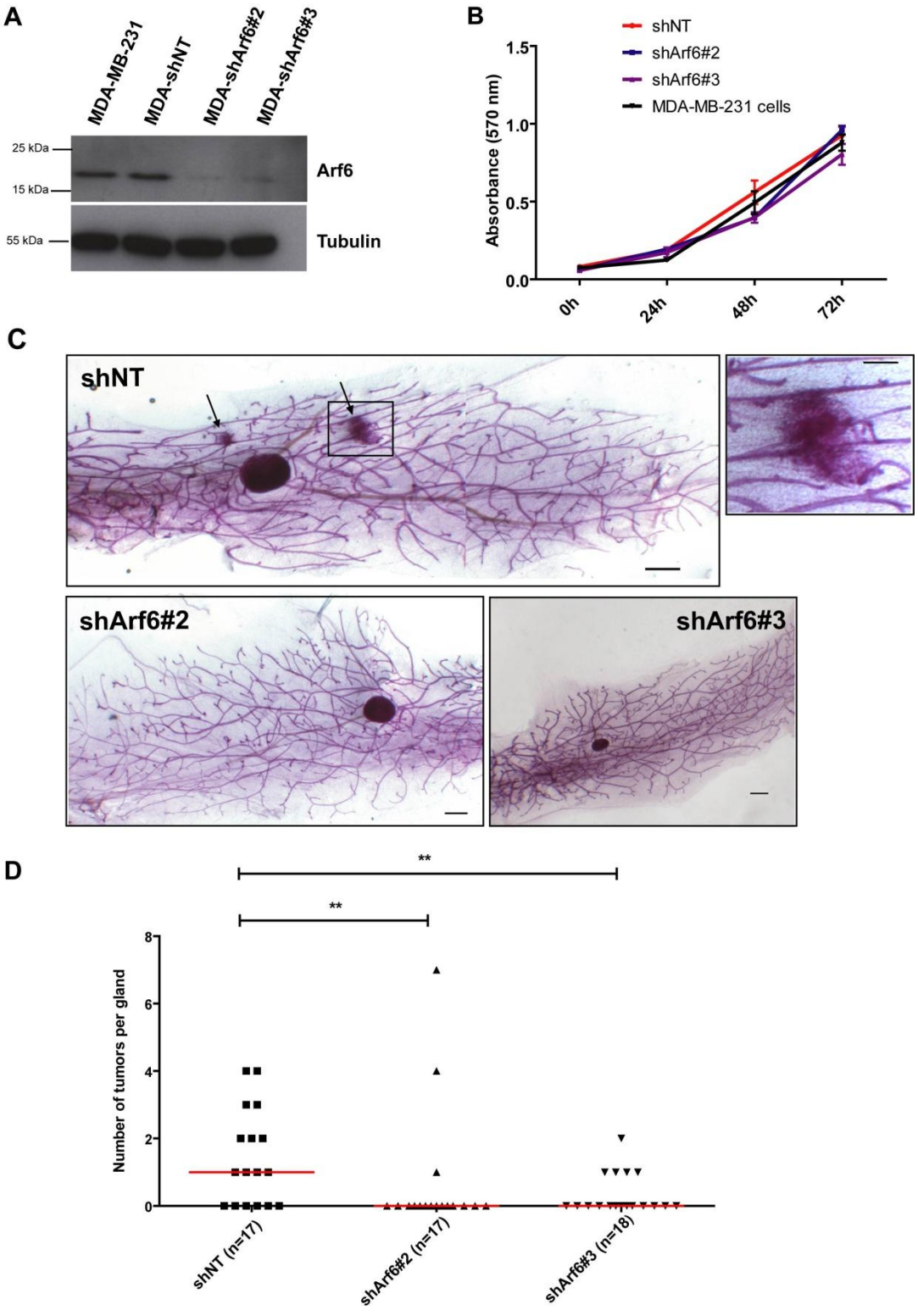

Figure 35: (A) Immunoblots for MDA-MB-231 stable cell lines depleted with the indicated shRNAs and revealed for ARF6 and α tubulin as loading control. (B) Proliferation curve of MDA-MB-231 stable cell lines depleted with the indicated shRNAs up to 72 hours of seeding. An MTT colorimetric cell growth assay was used and the capability of cells to cleave the substrate MTT to the insoluble formazan in the different time points was monitored with absorbance at 570

nm. Values are mean of repeated measurements from two independent experiments. The distribution curve compared with a one-way ANOVA test resulted non significantly different (C) Pictures showing whole-mount carmine stained sections of mice mammary glands injected with cells treated with the indicated shRNAs. Arrows point to two tumor foci. Scale bar: 2 mm. Inset is a magnification of one of them. Scale bar: 1 mm. (D) Scattered-plot graph showing the number of tumor foci scored in each mammary gland analyzed. Number of mammary glands analyzed is indicated between brackets. Values represent three independent experiments. Comparisons were made with Mann-Whitney t-test (one-sided); **, $P < 0.01$.

Chapter 6: ARF6 implication in ventral actin organization in breast cancer cells

6.1. Introduction to Article 2

In this second study I addressed the contribution of ARF6 on actin cytoskeleton remodeling in breast cancer cells with possible implication for cell motility. I used a gain of function approach to mimic upregulation of ARF6 activity reported in breast tumor cells. By expressing a hyper-activated mutant of ARF6 (ARF6T157N) in MDA-MB-231 cells, I observed the formation of highly dynamic actin structures at the ventral surface of the cells that we hypothesized as part of a process of lamellipodia extension. By immunofluorescence and live-imaging experiments I characterize these structures by identifying their main components and a possible mechanism through which ARF6 triggers their formation.

6.2. Article 2: ARF6 implication in ventral actin organization in breast cancer cells

Article to be submitted

Authors: Valentina Marchesin and Philippe Chavrier

ARF6 implication in ventral actin organization in breast cancer cells

Valentina Marchesin[1,2] and Philippe Chavrier[1,2,*]

[1] Institut Curie, Research Center, 75005 Paris, France

[2] Membrane and Cytoskeleton Dynamics, Centre National de la Recherche Scientifique UMR144, 75005 Paris, France

ABSTRACT

Coordination between actin cytoskeleton assembly and localized polarization through the endocytic and exocytic routes of surface receptors, signaling molecules and proteases in response to extracellular cues, is crucial for cancer cell migration. ARF6 has been implicated in the endocytic recycling of surface receptors and membrane components and in actin cytoskeleton remodeling. Here we show that expression of a hyper-activated mutant of ARF6 in MDA-MB-231 breast cancer-derived cell line, mimicking ARF6 hyperactivation in some invasive breast tumors induced a striking rearrangement of the actin cytoskeleton at the ventral surface of the cells. This phenotype consisted in the formation of dynamic rosettes or wave-like structures positive for markers of the actin cytoskeleton like cortactin, the Arp2/3 complex, the SCAR/WAVE complex and its most prominent regulator Rac1. These ventral actin structures were induced in control cells in response to epidermal growth factor (EGF) stimulation. We therefore hypothesize a role for ARF6 in EGF-dependent lamellipodia formation and breast cancer cell directed migration. We showed that interference with ARF6 expression

attenuated activation and plasma membrane targeting of Rac1 in response to EGF treatment, suggesting a role for ARF6 in linking EGF-R signaling to Rac1 recruitment and activation at the plasma membrane.

INTRODUCTION

Cancer cell invasion relies on two essential processes: the ability of tumor cells to interact with and remodel the extracellular matrix (ECM) to breach tissues barriers and the ability to reorganize their actin cytoskeleton in order to form protrusions for cell motility (Friedl and Wolf, 2009; Poincloux et al., 2009; Sanz-Moreno and Marshall, 2009). In almost all steps of metastatic spread, the reorganization and reassembly of the actin cytoskeleton is a critical process for invasive cell behavior, such as the dissolution of cell-cell contacts, protrusions formation, force generation to overcome physical resistance of three-dimensional tissue networks and motility (Nurnberg et al., 2011). Cancer cells migrating on 2D matrices *in vitro* form typical protrusive structures known as invadopodia, the ventral degradative protrusions enriched in matrix-metalloproteases (MMPs), the enzymes responsible for the proteolytic cleavage of ECM components, and lamellipodia, the sheet-like protruding leading edges of migrating cells (Ridley, 2011). Both structures are dependent on the assembly of filamentous (F-) actin, a process which is regulated by various proteins such as the Arp2/3 complex that mediates *de novo* branching of new F-actin filaments and its upstream activators N-WASP or the pentameric SCAR/WAVE complex (Campellone and Welch, 2010; Goley and Welch, 2006).

The protrusion activity of invasive tumor cells is enhanced by upregulation of several genes involved in cell motility like for example the actin nucleation promoting factor cortactin (MacGrath and Koleske, 2012). Another example is the epidermal growth factor receptor (EGF-R), a tyrosine kinase receptor with growth-promoting and migratory effects which is expressed in several carcinomas and stimulates actin-driven protrusions in response to EGF cues from the

surrounding microenvironment during chemotactic cell migration. EGFR signaling was associated with invasiveness and poor patient survival in breast cancer (Magkou et al., 2008).

The small GTP-binding protein ADP-ribosylation factor 6 (ARF6) is known to coordinate endocytosis, post-endocytic recycling, exocytosis and actin cytoskeletal organization at the plasma membrane (D'Souza-Schorey and Chavrier, 2006; Donaldson and Jackson, 2011). By controlling the recycling of lipids and surface proteins in the endocytic pathway, ARF6 is implicated in several events implying cell polarization including cell migration and cancer invasion. Recent studies suggest a link between up-regulation of ARF6 expression and activity and the invasive capacity of breast cancer cells (Hashimoto et al., 2004; Li et al., 2006; Morishige et al., 2008; Tague et al., 2004). For instance in MDA-MB-231 breast adenocarcinoma-derived cells, ARF6 controls the recruitment of invadopodial components cortactin and paxillin and invadopodia assembly through its downstream effector AMAP1 (Onodera et al., 2005), and ARF6 activation has been linked to EGF signaling via its guanine exchange factor (GEF) GEP100/BRAG2, which interacts with ligand-activated EGF-R (Morishige et al., 2008). Several studies also showed that ARF6 stimulates actin reorganization and membrane ruffling and promotes the acquisition of a migratory phenotype likely through activation of Rac1 (Nishiya et al., 2005; Palacios and D'Souza-Schorey, 2003; Radhakrishna et al., 1996; Santy and Casanova, 2001). The Rho GTPase protein Rac1 is another small G-protein widely implicated in normal physiology and disease. It plays an important role in cytoskeleton rearrangements and it is a key regulator of cell proliferation, adhesion, migration and malignant transformation (Ridley, 2006). Rac1 is

activated by tyrosine-kinase receptors, G-coupled receptors, integrins and stress and one of its main function is to promote actin polymerization during lamellipodia extension by activating the Arp2/3 activator WAVE and by increasing the availability of actin monomers for incorporation into actin filaments by regulating cofilin, an F-actin-depolymerization factor (Heasman and Ridley, 2008). Rac1 is overexpressed or hyperactive in breast cancer tissues (Schnelzer et al., 2000) and similarly, some Rac1-GEFs are overexpressed in high-grade poor-prognosis breast tumors (Wertheimer et al., 2012). ARF6 has been implicated in the recycling and upstream activation of Rac1 (Palacios and D'Souza-Schorey, 2003; Palacios et al., 2002; Palamidessi et al., 2008; Santy et al., 2005). However the ARF6-dependent Rac1 regulation seems to be complex and varies depending on cell types and needs to be better understood.

In this study we used a gain of function approach to mimic upregulation of ARF6 activity reported in breast tumor cells and to unravel the mechanism through which ARF6 controls cancer cell migration. Expression of a hyper-activated mutant of ARF6 (ARF6T157N) (Klein et al., 2006; Santy, 2002) in MDA-MB-231 cells induced a striking rearrangement of the actin cytoskeleton at the ventral surface of the cells, consisting in the formation of structures positive for markers like cortactin, the Arp2/3 complex, the SCAR/WAVE complex and its most prominent regulator Rac1; this brought us to hypothesize a role for ARF6 in lamellipodia formation and breast cancer cell directed migration. In addition, we showed that ARF6 depletion inhibits Rac1 activation and its targeting to the plasma membrane in response to EGF treatment, suggesting a role for ARF6 in linking EGFR signaling to Rac1 recruitment and activation at the plasma membrane.

MATERIAL AND METHOD

Cell culture. Human breast adenocarcinoma MDA-MB-231 cells (American Type Culture Collection HTB-26) were maintained in L-15 culture medium (Sigma–Aldrich, St. Louis, MO, USA) with 2 mM glutamine (GIBCO) and 15% FBS (GIBCO) at 37 °C in 1% CO_2.

Immunoblotting analysis. Cells were lysed and proteins were eluted in SDS sample buffer, separated by SDS-PAGE, and detected by immunoblotting analysis with indicated antibodies. Bound antibodies were detected with ECL Western Blotting Detection Reagents (GE Healthcare Life Sciences).

Antibodies. The antibodies used in this study are listed in Table S1.

Plasmid constructs and DNA transfection. Full length rat cortactin cDNA provided by Dr M.A. McNiven (Mayo Clinic, Rochester, MI, USA) was subcloned in pDsRed1-N1 and pEGFP-N1 (Clontech) in fusion with carboxy-terminal DsRed or GFP, respectively. Lentiviral ARF6-T157N expression vector was obtained by insertion of ARF6T157N cDNA into a pDEST vector (adapted for lentiviral transduction) through a Gateway Cloning technology (Invitrogen). The cDNA was amplified from a pcDNA3 plasmid containing human ARF6 T157N tagged with HA at the carboxy-terminal end (gift from Dr M. Franco, Univ Sophia-Antipolis, France). For transient expression, MDA-MB-231 cells were transfected with plasmid constructs (1µg) by using Lipofectamine LTX (Invitrogen) or Nucleofector (Lonza) according to the manufacturer's instructions. Cells were analyzed 48 h after transfection.

siRNA treatment and lentiviral transduction for protein expression. siRNA transfection was performed using 50 nM siRNA with Lullaby reagent (OZ Biosciences) according to manufacturer's instructions and analyzed 72 h after treatment. The siRNAs used in this study are listed in Table S2.

For lentivirus production, HEK293T cells were transfected using GeneJuice (Novagen) with a mix of ARF6-T157N expression vector and psPAX2 (AddGene) and pVSV-G (Clonetech) packaging vectors in OPTIMEM (Invitrogen). After 72 hrs, virus-containing supernatant was collected, filtered and used for transduction of a subconfluent monolayer of MDA-MB-231 cells.

Live-cell spinning disk confocal microscopy. MDA-MB-231 cells stably expressing ARF6T157N and transiently transfected with GFP-cortactin were plated on MatTek dishes layered with a drop of polymerized type I collagen mixed with AlexaFluor 549-conjugated type I collagen (10% final) at a final concentration of 2.5 mg/ml. Cells were incubated for 30 min at 37°C in 1% CO2 and formation of cortactin-positive structures was monitored by acquiring z-stack sequences by confocal spinning disk microscopy (2 z-stack/min) with a Nikon Eclipse TE2000-U microscope equipped with a 60x 1.45NA oil immersion objective, a PIFOC Objective stepper, a Yokogawa CSU22 confocal unit and a Roper HQ2 CCD camera steered by Metamorph and a temperature controller.

Total interference reflection fluorescence microscopy (TIRFM). MDA-MB-231 cells stably expressing ARF6T157N and transiently transfected with dsRed-cortactin were plated on glass-bottom dishes coated with cross-linked unlabeled gelatin and kept in a humidified atmosphere at 37°C and 1% CO2. Time-laps images were acquired on a Nikon TE2000 inverted microscope equipped with a ×100 TIRF objective (NA=1.47), a TIRF arm, an image splitter (DV, Roper Scientific) installed in front of the CCD camera and a temperature controller. dsRed was excited with a 560 nm laser (100 mW, Roper Scientific), controlled for power by an acousto-optic tunable filter. Fluorescent emissions were selected with bandpass and longpass filters (Chroma) and captured by a QuantEM EMCCD camera (Roper Scientific). The system was driven by Metamorph.

For EGF stimulation experiment, MDA-MB-231 cells were transiently transfected with dsRed-cortactin, starved for 16 hours and plated on glass-bottom dishes coated with cross-linked unlabeled gelatin and a z-stack of images (1/5 sec) was acquired for 1 min before adding EGF. EGF (Preprotech) was added directly to the medium at 100 ng/mL final concentration (from a 100 ng/µL stock solution). Immediately after acquisition was restarted for other 15 min.

Indirect immunofluorescence and epifluorescence microscopy. MDA-MB-231 cells stably expressing ARF6T15TN, cultured on gelatin-coated cover-slips, were permeabilized with 0.5 % Triton-X100 and 4% PFA in PBS for 90 seconds, fixed in 4% PFA in PBS and stained for cortactin and/or the indicated antibodies. For β1-integrin staining cells were fixed in 4% PFA in PBS and permeabilized with 0.05% saponin in PBS before proceeding with the staining. For Rac1 staining MDA-MB-231 cells, cultured on gelatin-coated cover-slips, were fixed in 4% PFA in PBS and permeabilized with Triton-X100 0.1% in PFA for 4 min, before proceeding with staining.

Cells were imaged with the 60X objective of a wide-field microscope DM6000 B/M (Leica Microsystems) equipped with a CCD CoolSnap HQ camera (Roper Scientific) and steered by Metamorph (Molecular Devices Corp., Sunnyvale, CA).

For quantification of Rac1 edge intensity profile, a line of 160 pixels was drown perpendicularly to the leading edges of cells and the fluorescence intensity for each pixel was measured with the Linescan tool of Metamorph software that than was averaged for all the cells analyzed.

EGF stimulation experiments and G-LISA activation assays. MDA-MB-231 cells, cultured on gelatin-coated cover-slips, were serum starved for 12-16 hours. Then medium was removed and replaced with EGF diluted in L-15 medium at 100 ng/mL final concentration for the indicated time points. Then stimulation was blocked on ice and cells were immediately permeabilized with 0.5 % Triton-X100 and 4% PFA in PBS for 90 seconds, fixed in 4% PFA in PBS and stained for cortactin.

For measuring ARF6 and Rac1 activation levels, we used G-LISA™-ARF6 Activation Assay kit (Cytoskeleton Inc, BK133) and G-LISA™-Rac1 Activation Assay kit (Cytoskeleton Inc, BK126). Briefly the G-LISA™ kits contain an ARF6- or Rac1-GTP-binding protein linked to the wells of a 96 well plate. Active, GTP-bound ARF6 or Rac1 in cell lysates bind to the wells while the inactive GDP-bound form is removed during washing steps. Bound active ARF6 or Rac1 is detected with an ARF6 or Rac1 specific antibody and the signal is developed with optical density or chemiluminescence reagents. MDA-MB-231 cells were treated with the indicated siRNAs for 72 hours, plated on gelatin-coated wells of a 6-well plate, serum starved and EGF-stimulated as described above. EGF stimulation was blocked on ice and cells were immediately lysed with lysis buffer and processed following the manufacturer's instructions.

Statistics. Statistical analyses were performed using, Student's t test or one-way (Kruskall-Wallis) using GraphPad Prism (GraphPad Software) as specified in each figure legend with $p < 0.05$ considered significant.

RESULTS AND DISCUSSION

ARF6 guanine exchange factors (GEFs) are associated with invasion and metastasis in breast cancer, suggesting that up-regulation of ARF6 activity may be pro-metastatic (Bill et al., 2010; Li et al., 2006; Morishige et al., 2008). The ARF6-GEF GEP100 is over-expressed in breast tumors and is required for the invasive activity of MDA-MB-231 cells (Morishige et al., 2008). Thus, we generated by lentiviral transduction a MDA-MB-231 cell line stably expressing a fast-cycling mutant of ARF6 (ARF6T157N). This mutant is characterized by increased spontaneous dissociation of GDP and GTP association (Klein et al., 2006), thus mimicking the effect of over-expression of an ARF6-GEF in breast carcinoma cells. By pull-down experiments, expression of ARF6T157N resulted in a 5-fold increase in the levels of GTP-ARF6 in MDA-MB-231 cells (data not shown). By immunofluorescence microscopy we observed that, compared to control MDA-MB-231 cells, cells stably expressing of ARF6T157N plated on gelatin showed a striking accumulation of pro-invasive F-actin and F-actin-binding protein cortactin in rosettes or wave-like structures forming at the ventral cell surface (Fig.1A, arrowhead and Fig. S1A). This phenotype occurred in the 50% of the cells imaged. These cells also displayed an enrichment of cortactin at the plasma membrane (Fig.1A, arrows). The presence in these structures of the invadopodial/podosomal markers SRC and phosphorylated-tyrosine residues (Fig.S1B) and their morphological similarities with podosomes brought us to hypothesize that they could correspond to some matrix degradative structures. However, we could exclude this possibility since cortactin-positive rosettes did not degrade gelatin and cells expressing ARF6T157N showed similar gelatin degradative ability as compared to control cells (data not shown). By TIRF

microscopy we confirmed that cortactin-positive structures occurred ventrally and we observed that they were highly dynamic usually forming as rosettes, expanding outwardly as waves and disassembling in a few minutes (Fig.1B, upper panel). When these structures formed in close proximity with a leading edge, they often merged with the peripheral plasma membrane (Fig.1B, lower panel). These data led us to hypothesize an implication for these structures in lamellipodium formation.

We also observed that the focal adhesion proteins paxillin and vinculin, together with β1-integrin, co-localized with these structures (Fig.S1C), suggesting an implication of ECM adhesion in their formation. This assumption was supported by the observation that, when MDA-MB-231-ARF6T157N cells were seeded on dishes coated with fibrillar type I collagen and imaged by confocal spinning-disk microscopy, cortactin waves almost exclusively formed at contact sites with the collagen fibers (Fig.1C). In addition to cortactin and F-actin, these structures were positive for the actin-nucleating Arp2/3 complex (Fig.2A), suggesting that their formation depends on the branched-dendritic actin machinery.

We then investigated the distribution of nucleation promoting factors (NPFs) known to activate the Arp2/3 complex; the WASP family proteins N-WASP, SCAR/WAVE and WASH. WAVE2, a subunit of the SCAR/WAVE complex, showed the strongest colocalization with these structures (Fig.2A). On the contrary WASH was absent, while N-WASP colocalized with these structures although weekly (Fig.2A). The effect of knocking down these different components was then assessed (Fig.S2A). Silencing of the Arp2/3 complex subunit p34 dramatically decreased the percentage of cells displaying cortactin-rosettes, while silencing of WASH did not cause any significant effect (Fig.2B-C).

Knock-down of WAVE2 with two independent siRNAs (#1 and #2) decreased the percentage of cells displaying cortactin-positive rosettes from 50% in control cells to 20-25% in WAVE2-depleted cells (Fig.2B-C). However, the pentameric SCAR/WAVE complex exists in different variants and three different isoforms of WAVE can assemble into different complexes (Soderling and Scott, 2006). Thus, we knocked-down Nap1, a conserved subunit of all SCAR/WAVE complexes. Silencing of Nap1 dramatically diminished the formation of cortactin-positive waves (Fig.2B-C). Given the role of SCAR/WAVE as major NPF involved in lamellipodia regulation (Ridley, 2011), these data suggest a role for ARF6 as an upstream regulator of the SCAR/WAVE complex and therefore of lamellipodia formation in breast cancer cells. Interestingly in cells depleted for N-WASP we observed a decrease in the percentage of cells displaying cortactin-rosettes from 50% in control cells to 20% (Fig.2B-C), also suggesting a possible implication of N-WASP in the formation of ventral cortactin-positive structures. These findings are compatible with a reported role of N-WASP in lamellipodia regulation, through its function in endocytosis (Campellone and Welch, 2010).

Since EGFR signaling has been implicated in the formation of migratory protrusions, such us lamellipodia and circular dorsal ruffles (CDRs) (Buccione et al., 2004; Palamidessi et al., 2008) and in ARF6 activation (Campellone and Welch, 2010), we checked whether EGF may induce the formation of these structures in serum-starved MDA-MB-231 cells. By wide-field fluorescence microscopy, we observed a rearrangement of cortactin distribution already 30 sec-2 min after EGF stimulation, and between 5-10 min formation of cortactin rosettes was visible in up to 40% of cells (Fig.3A). By TIRF microscopy we confirmed that these structures occurred at the ventral surface (Fig.3B) and that

their dynamics is similar to ARF6T157N-induced structures. These data suggest that EGFR signaling through activation of ARF6 may trigger the formation of cortactin ventral structures and increased ARF6 activation levels mimicked by expression of ARF6T157N may exacerbate this phenotype. Recent studies have also described similar F-actin ventral waves in different cell types, although their function is not fully understood. In neutrophilis actin propagating waves positive for Nap1 are thought to play a role in spatial organization and protrusion of the leading edge during cell motility of the immune cells (Weiner et al., 2007). Fibroblast and human osteosarcoma cells also exhibit ventral F-actin waves positive for Arp2/3, β1-integrin, paxillin, vinculin and other adhesive proteins such as talin and zyxin that propagate as spots and wavefronts along the ventral plasma membrane and are thought to play a role in coupling ventral actin polymerization and ECM adhesion (Case and Waterman, 2011). Thus, we hypothesize that ARF6, activated by EGFR signaling, could regulate upstream the SCAR/WAVE and Arp2/3 complex and consequently trigger the formation of ventral actin structures that may play a role in leading edge organization and ECM adhesion and control invasive migration of cancer cells. Given this hypothesis, we sought to understand how ARF6 activates upstream SCAR/WAVE. We hypothesized that ARF6 could activates SCAR/WAVE and triggers ventral cortactin structures formation through activation of Rac1, the most prominent activator of SCAR/WAVE. Consistent with this hypothesis, we observed that in cells stably expressing ARF6T157N, Rac1 colocalized with cortactin ventral structures (Fig.4A) and active GTP-bound Rac1 levels increased by 50% as compared to control cells (Fig.4B). These data suggest that hyper-activated ARF6 could enhance cortactin ventral structures formation through

hyper-activation of Rac1. This would also explain why ARF6T157N-expressing cells resulted twice less motile than control cells in a cell motility assay in 3D collagen type I (data not shown). Rac1 indeed needs to be spatially redirected and polarized towards extracellular cues for efficient cell migration (Disanza et al., 2009). On the contrary, non-polarized activation of Rac1, with cortactin propagating waves and several lamellipodia forming in an unpolarized manner in ARF6T157N-expressing cells may interfere with cell motility.

Based on these observations, we investigated the potential role of ARF6 in the spatial polarization of Rac1 in MDA-MB-231 cells. By immunofluorescence staining we observed that in serum-starved cells, EGF stimulation induced increased recruitment of Rac1 and F-actin at the lamellipodia, while ARF6 knock-down resulted in a 50% reduction of peripheral recruitment of Rac1 (Fig.4C-D). Based on these data, we propose that ARF6 regulates the localized targeting of Rac1 to the leading edge of breast cancer cells where Rac1 triggers actin polymerization for efficient cell migration. We used the ARF6 and Rac1 G-LISA activation assays to monitor ARF6 and Rac1 activation levels under EGF stimulation of serum-starved MDA-MB-231 cells. Both ARF6 (Fig.4E) and Rac1 (Fig.4F) activation levels increased 1 min and 15 min after EGF addition. Moreover, silencing of ARF6 decreased by six-fold the levels of GTP:Rac1 both in non-stimulated condition and in response to EGF stimulation (Fig.4F). All together, these findings strongly suggest that ARF6 is required for Rac1 activation. Although it is not clear how ARF6 can control Rac1 activation, we hypothesize that in breast cancer cells, ARF6 controls the recycling and targeting to the plasma membrane of Rac1 and a Rac1GEF and in absence of ARF6, EGF-induced Rac1 targeting to the plasma membrane and activation cannot take

place. These data are in agreement with a previous study in HeLa cells that showed how in response to HGF stimulation, Rac1 and its GEF, TIAM1, is internalized into early endosomes and then activated Rac1 is subsequently recycled in an ARF6-dependent manner to regions of the plasma membrane where subsequently CDRs form, a step that occurs prior lamellipodium formation (Palamidessi et al., 2008). CDRs are indeed highly dynamic actin-based structures that form dorsally in response of RTKs stimulation and are thought to play a role in fastly disassembling and remodeling actin prior lamellipodium formation (Buccione et al., 2004; Palamidessi et al., 2008). Therefore we propose that the cortactin ventral structures we described could play a similar role as CDRs in actin remodeling for lamellipodia formation and that ARF6, by controlling the formation of these structures through the EGF-mediated targeting and activation of Rac1 at the plasma membrane, could be required for directed cell motility. This last hypothesis, however, should be tested in future experiments by checking ARF6 implication in EGF-directed migration of breast cancer cells.

In conclusion in this study we propose that in breast cancer cells ARF6 links EGFR signaling to Rac1 activation and targeting to the leading edge where it activates the SCAR/WAVE complex and regulates ventral actin polymerization during lamellipodia extension and that this process could be important for efficient breast cancer cell motility.

REFERENCES

Bill, A., A. Schmitz, B. Albertoni, J.N. Song, L.C. Heukamp, D. Walrafen, F. Thorwirth, P.J. Verveer, S. Zimmer, L. Meffert, A. Schreiber, S. Chatterjee, R.K. Thomas, R.T. Ullrich, T. Lang, and M. Famulok. 2010. Cytohesins are cytoplasmic ErbB receptor activators. *Cell*. 143:201-211.

Buccione, R., J.D. Orth, and M.A. McNiven. 2004. Foot and mouth: podosomes, invadopodia and circular dorsal ruffles. *Nature reviews. Molecular cell biology*. 5:647-657.

Campellone, K.G., and M.D. Welch. 2010. A nucleator arms race: cellular control of actin assembly. *Nature reviews. Molecular cell biology*. 11:237-251.

Case, L.B., and C.M. Waterman. 2011. Adhesive F-actin waves: a novel integrin-mediated adhesion complex coupled to ventral actin polymerization. *PloS one*. 6:e26631.

D'Souza-Schorey, C., and P. Chavrier. 2006. ARF proteins: roles in membrane traffic and beyond. *Nature reviews. Molecular cell biology*. 7:347-358.

Disanza, A., E. Frittoli, A. Palamidessi, and G. Scita. 2009. Endocytosis and spatial restriction of cell signaling. *Molecular oncology*. 3:280-296.

Donaldson, J.G., and C.L. Jackson. 2011. ARF family G proteins and their regulators: roles in membrane transport, development and disease. *Nature reviews. Molecular cell biology*. 12:362-375.

Friedl, P., and K. Wolf. 2009. Proteolytic interstitial cell migration: a five-step process. *Cancer metastasis reviews*. 28:129-135.

Goley, E.D., and M.D. Welch. 2006. The ARP2/3 complex: an actin nucleator comes of age. *Nature reviews. Molecular cell biology*. 7:713-726.

Hashimoto, S., Y. Onodera, A. Hashimoto, M. Tanaka, M. Hamaguchi, A. Yamada, and H. Sabe. 2004. Requirement for Arf6 in breast cancer invasive activities. *Proceedings of the National Academy of Sciences of the United States of America*. 101:6647-6652.

Heasman, S.J., and A.J. Ridley. 2008. Mammalian Rho GTPases: new insights into their functions from in vivo studies. *Nature reviews. Molecular cell biology*. 9:690-701.

Klein, S., M. Franco, P. Chardin, and F. Luton. 2006. Role of the Arf6 GDP/GTP cycle and Arf6 GTPase-activating proteins in actin remodeling and intracellular transport. *The Journal of biological chemistry*. 281:12352-12361.

Li, M., S.S. Ng, J. Wang, L. Lai, S.Y. Leung, M. Franco, Y. Peng, M.L. He, H.F. Kung, and M.C. Lin. 2006. EFA6A enhances glioma cell invasion through ADP ribosylation factor 6/extracellular signal-regulated kinase signaling. *Cancer research*. 66:1583-1590.

MacGrath, S.M., and A.J. Koleske. 2012. Cortactin in cell migration and cancer at a glance. *Journal of cell science*. 125:1621-1626.

Magkou, C., L. Nakopoulou, C. Zoubouli, K. Karali, I. Theohari, P. Bakarakos, and I. Giannopoulou. 2008. Expression of the epidermal growth factor receptor (EGFR) and the phosphorylated EGFR in invasive breast carcinomas. *Breast cancer research : BCR*. 10:R49.

Morishige, M., S. Hashimoto, E. Ogawa, Y. Toda, H. Kotani, M. Hirose, S. Wei, A. Hashimoto, A. Yamada, H. Yano, Y. Mazaki, H. Kodama, Y. Nio, T. Manabe, H. Wada, H. Kobayashi, and H. Sabe. 2008. GEP100 links epidermal growth factor receptor signalling to Arf6 activation to induce breast cancer invasion. *Nature cell biology*. 10:85-92.

Nishiya, N., W.B. Kiosses, J. Han, and M.H. Ginsberg. 2005. An alpha4 integrin-paxillin-Arf-GAP complex restricts Rac activation to the leading edge of migrating cells. *Nature cell biology*. 7:343-352.

Nurnberg, A., T. Kitzing, and R. Grosse. 2011. Nucleating actin for invasion. *Nature reviews. Cancer*. 11:177-187.

Onodera, Y., S. Hashimoto, A. Hashimoto, M. Morishige, Y. Mazaki, A. Yamada, E. Ogawa, M. Adachi, T. Sakurai, T. Manabe, H. Wada, N. Matsuura, and H. Sabe. 2005. Expression of AMAP1, an ArfGAP, provides novel targets to inhibit breast cancer invasive activities. *The EMBO journal*. 24:963-973.

Palacios, F., and C. D'Souza-Schorey. 2003. Modulation of Rac1 and ARF6 activation during epithelial cell scattering. *The Journal of biological chemistry*. 278:17395-17400.

Palacios, F., J.K. Schweitzer, R.L. Boshans, and C. D'Souza-Schorey. 2002. ARF6-GTP recruits Nm23-H1 to facilitate dynamin-mediated endocytosis during adherens junctions disassembly. *Nature cell biology*. 4:929-936.

Palamidessi, A., E. Frittoli, M. Garre, M. Faretta, M. Mione, I. Testa, A. Diaspro, L. Lanzetti, G. Scita, and P.P. Di Fiore. 2008. Endocytic trafficking of Rac is required for the spatial restriction of signaling in cell migration. *Cell*. 134:135-147.

Poincloux, R., F. Lizarraga, and P. Chavrier. 2009. Matrix invasion by tumour cells: a focus on MT1-MMP trafficking to invadopodia. *Journal of cell science*. 122:3015-3024.

Radhakrishna, H., R.D. Klausner, and J.G. Donaldson. 1996. Aluminum fluoride stimulates surface protrusions in cells overexpressing the ARF6 GTPase. *The Journal of cell biology*. 134:935-947.

Ridley, A.J. 2006. Rho GTPases and actin dynamics in membrane protrusions and vesicle trafficking. *Trends in cell biology*. 16:522-529.

Ridley, A.J. 2011. Life at the leading edge. *Cell*. 145:1012-1022.

Santy, L.C. 2002. Characterization of a fast cycling ADP-ribosylation factor 6 mutant. *The Journal of biological chemistry*. 277:40185-40188.

Santy, L.C., and J.E. Casanova. 2001. Activation of ARF6 by ARNO stimulates epithelial cell migration through downstream activation of both Rac1 and phospholipase D. *The Journal of cell biology*. 154:599-610.

Santy, L.C., K.S. Ravichandran, and J.E. Casanova. 2005. The DOCK180/Elmo complex couples ARNO-mediated Arf6 activation to the downstream activation of Rac1. *Current biology : CB*. 15:1749-1754.

Sanz-Moreno, V., and C.J. Marshall. 2009. Rho-GTPase signaling drives melanoma cell plasticity. *Cell cycle*. 8:1484-1487.

Schnelzer, A., D. Prechtel, U. Knaus, K. Dehne, M. Gerhard, H. Graeff, N. Harbeck, M. Schmitt, and E. Lengyel. 2000. Rac1 in human breast cancer: overexpression, mutation analysis, and characterization of a new isoform, Rac1b. *Oncogene*. 19:3013-3020.

Soderling, S.H., and J.D. Scott. 2006. WAVE signalling: from biochemistry to biology. *Biochemical Society transactions*. 34:73-76.

Tague, S.E., V. Muralidharan, and C. D'Souza-Schorey. 2004. ADP-ribosylation factor 6 regulates tumor cell invasion through the activation of the MEK/ERK signaling pathway. *Proceedings of the National Academy of Sciences of the United States of America*. 101:9671-9676.

Weiner, O.D., W.A. Marganski, L.F. Wu, S.J. Altschuler, and M.W. Kirschner. 2007. An actin-based wave generator organizes cell motility. *PLoS biology*. 5:e221.

Wertheimer, E., A. Gutierrez-Uzquiza, C. Rosemblit, C. Lopez-Haber, M.S. Sosa, and M.G. Kazanietz. 2012. Rac signaling in breast cancer: a tale of GEFs and GAPs. *Cellular signalling*. 24:353-362.

FIGURES

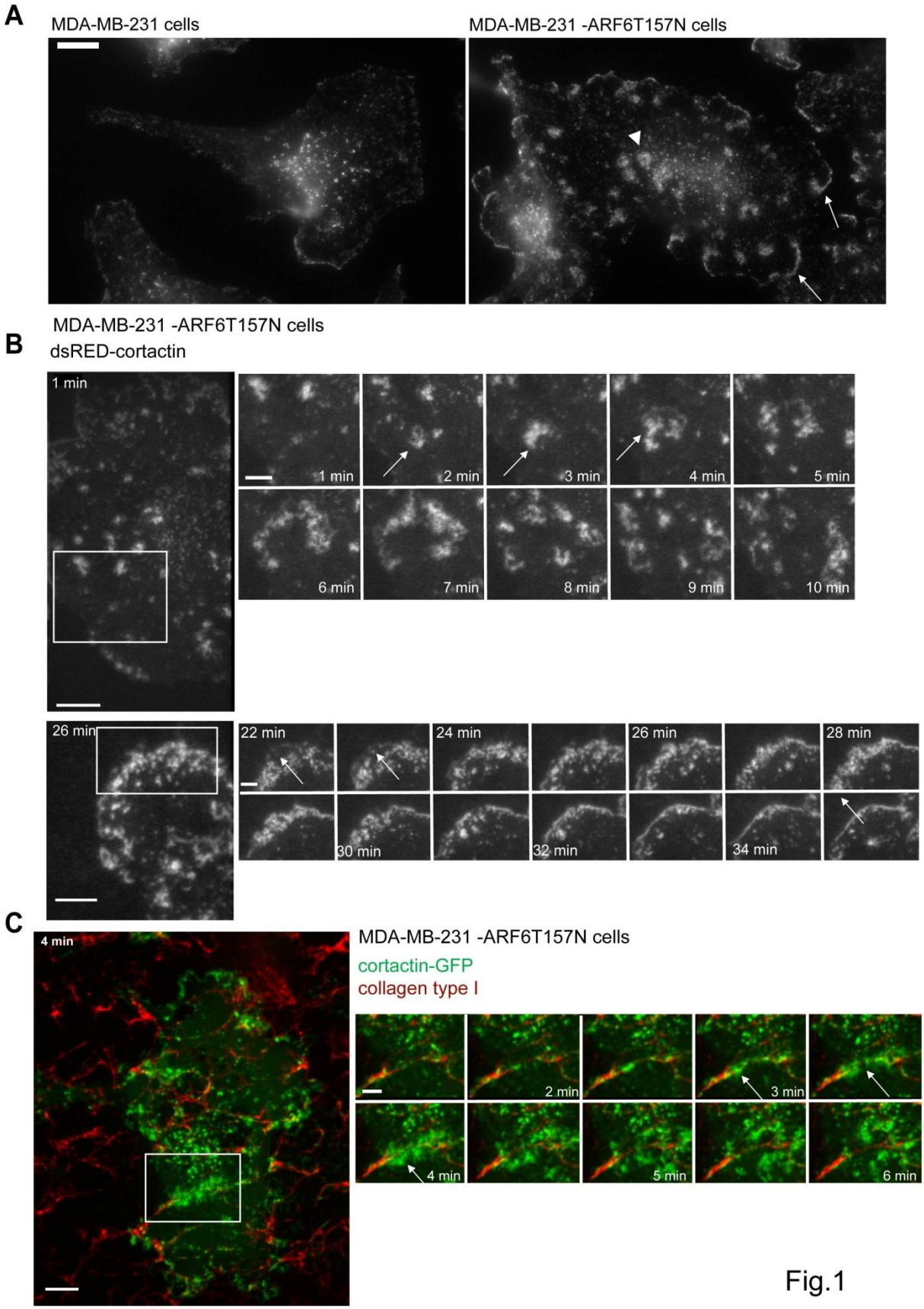

Fig.1

Figure 1: ARF6 hyper-activation induces the formation of ventral actin structures. (A) MDA-MB-231 cells and cells stably expressing ARF6T157N were plated on cross-linked unlabeled gelatin, fixed and stained for cortactin. Images were acquired with epifluorescence microscopy. Arrowhead points to a cortactin-positive structure and arrows show cortactin-enriched lamellipodia. Scale bar, 5 µm. **(B)** Still images of a TIRF microscopy time-lapse sequence of MDA-MB-231 cells stably expressing ARF6T157N and transiently transfected with dsRed-cortactin (left panels), plated on cross-linked unlabeled gelatin. Scale bars, 10 µm. Galleries correspond to the boxed regions of the still images and show a cortactin-positive rosette (arrows) forming and expanding outwardly before disassembling (upper example) or forming in proximity with a leading edge and merging with the plasma membrane (lower example). Time is in min. Scale bars, 5 µm. **(C)** Still image of a confocal spinning-disk microscopy time-lapse sequence of MDA-MB-231 cells expressing ARF6T157N and transiently transfected with GFP-cortactin (green) plated on a layer of type I collagen fibers (red) (left panel). Scale bar, 10 µm. The gallery corresponds to the boxed region and show a cortactin–positive structure (arrows) forming on contact sites with a collagen I fiber before propagating away. Time is in min. Scale bar, 5 µm.

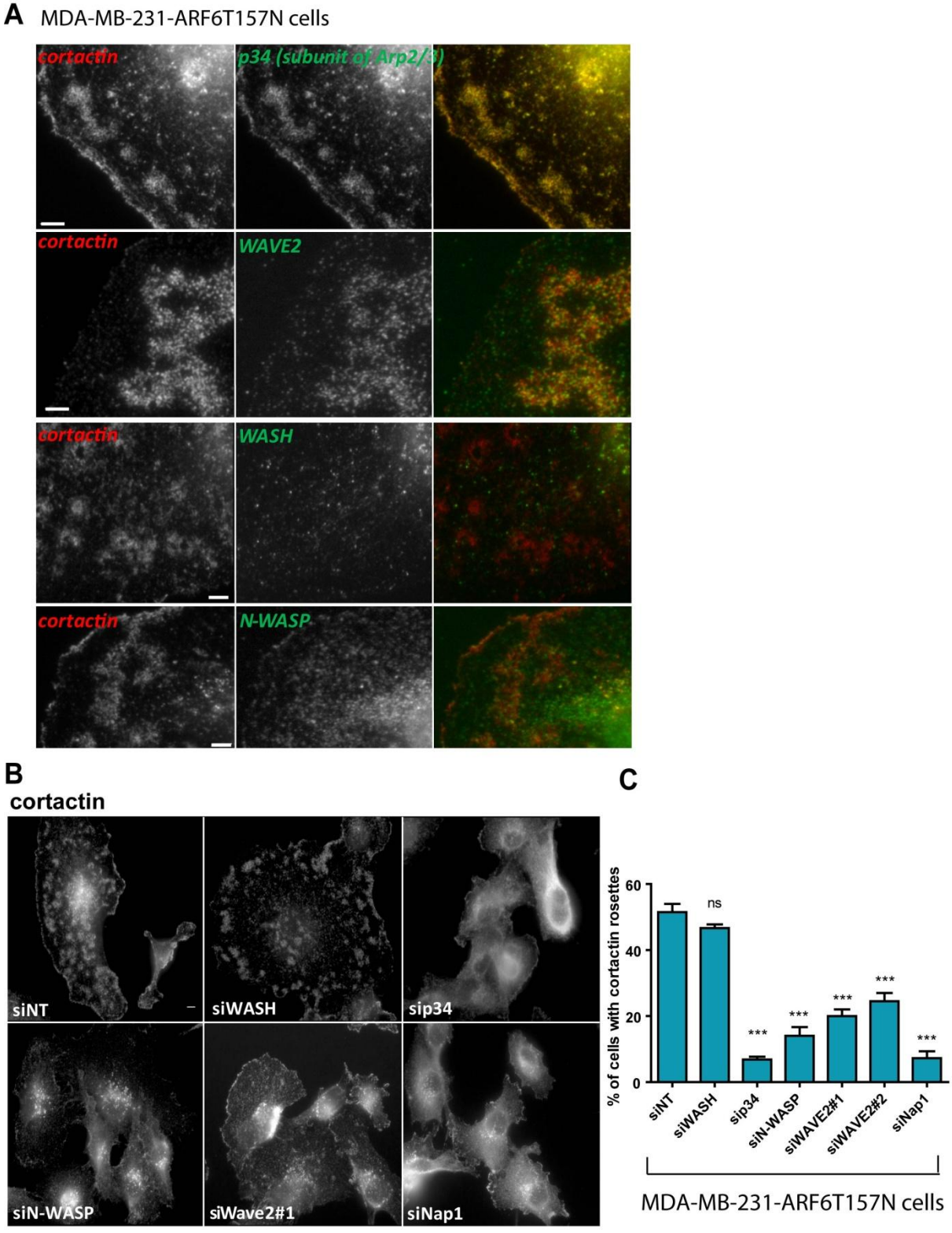
A
MDA-MB-231-ARF6T157N cells
cortactin
p34 (subunit of Arp2/3)
cortactin
WAVE2
cortactin
WASH
cortactin
N-WASP
B
cortactin
siNT
siWASH
sip34
siN-WASP
siWave2#1
siNap1
C
% of cells with cortactin rosettes
60
40
20
0
ns
***
***
***
***
***
siNT
siWASH
sip34
siN-WASP
siWAVE2#1
siWAVE2#2
siNap1
MDA-MB-231-ARF6T157N cells

Fig.2

Figure 2: Cortactin ventral structures formation depend on the Arp2/3 and SCAR/WAVE complexes. **(A)** Cells stably expressing ARF6T157N were plated on cross-linked unlabeled gelatin, fixed and stained for cortactin and the indicated markers. Images were acquired with epifluorescence microscopy. Scale bar, 5 µm. **(B-C)** Cells stably expressing ARF6T157N, treated with the indicated siRNAs for 72 hours. Cells were then plated on cross-linked unlabeled gelatin, fixed and stained for cortactin. **(B)** Images were acquired with epifluorescence microscopy. Scale bar, 5 µm. **(C)** Quantification of cells was done by scoring the percentage of cells displaying rosettes. Values are mean ± SEM from at least four independent experiments, scoring about 200 cells for each cell population. Comparisons were made with a Student t- test. ns, non significant, ***, $P < 0.001$ (compared with siNT-treated cells).

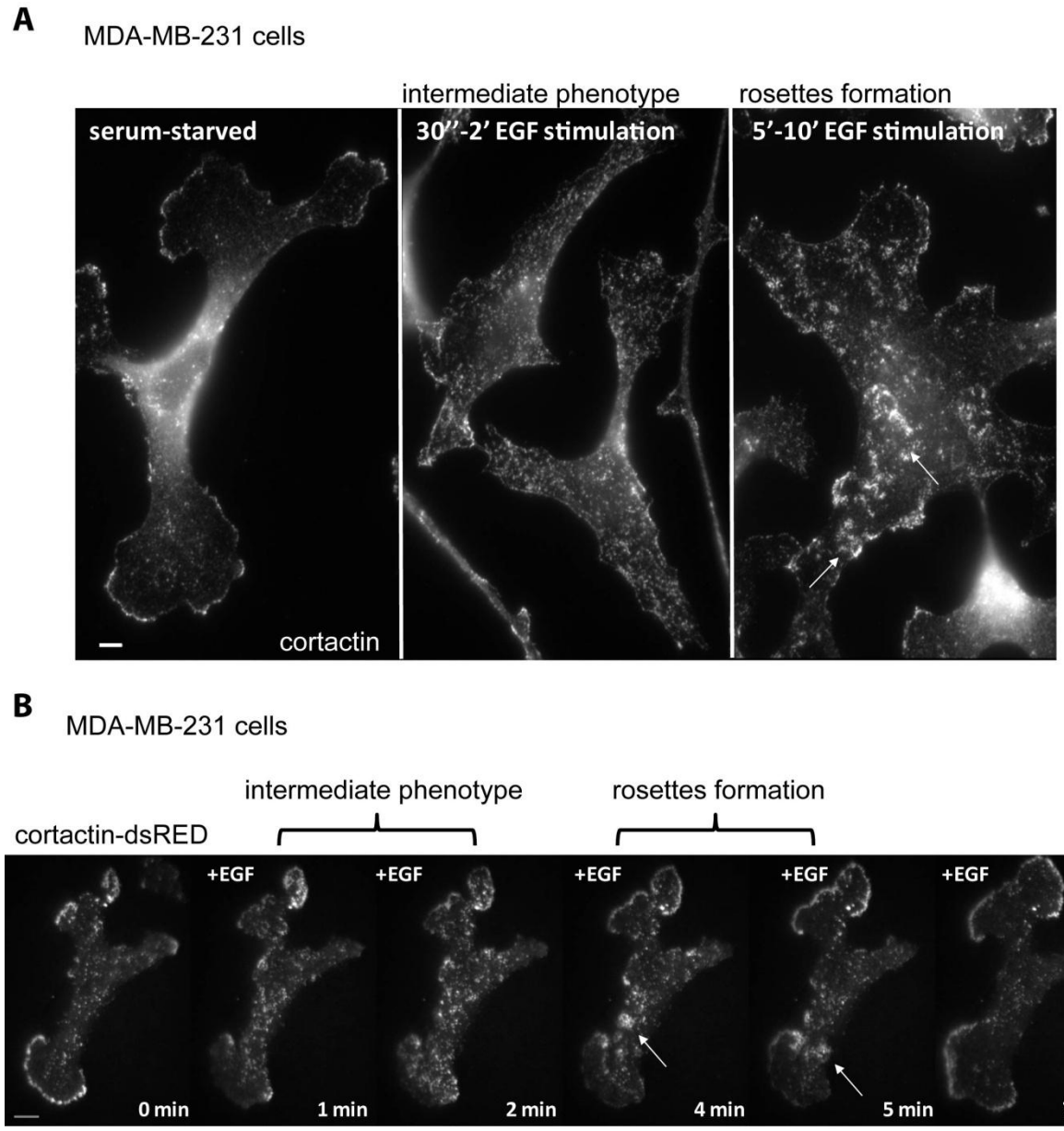
A
MDA-MB-231 cells
intermediate phenotype
rosettes formation
serum-starved
30''-2' EGF stimulation
5'-10' EGF stimulation
cortactin
B
MDA-MB-231 cells
intermediate phenotype
rosettes formation
cortactin-dsRED
+EGF
+EGF
+EGF
+EGF
+EGF
0 min
1 min
2 min
4 min
5 min
7 min

Fig.3

Figure 3: EGF stimulation triggers the formation of ventral actin structures in MDA-MB-231 cells. (A) MDA-MB-231 cells were plated on cross-linked unlabeled gelatin and serum starved over-night and stimulated with EGF for 30'', 2', 5' and 10'. Then they were fixed and stained for cortactin. Images were acquired with epifluorescence microscopy. Arrows point to forming cortactin-positive structures. Scale bar, 5 μm. **(B)** Still images of a TIRF microscopy time-lapse sequence of MDA-MB-231 cells transiently transfected with dsRed-cortactin (left panels). Cells were plated on cross-linked unlabeled gelatin, serum-starved over night prior imaging acquisition. EGF was added directly on the medium after 1 min of acquisition. Arrows point to forming cortactin-positive structures. Time is in min. Scale bar, 8 μm.

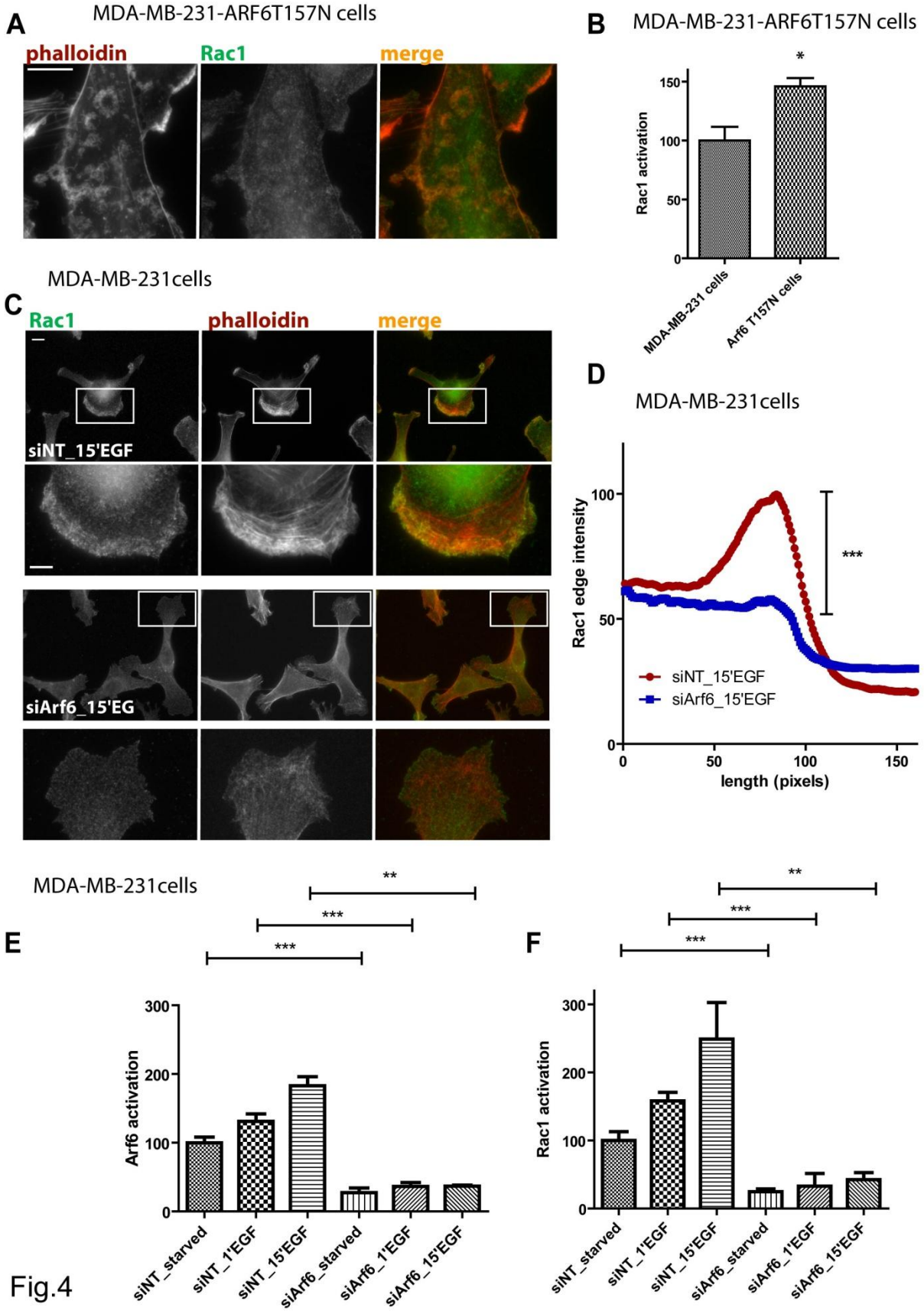
A
MDA-MB-231-ARF6T157N cells
phalloidin
Rac1
merge
B
MDA-MB-231-ARF6T157N cells
Rac1 activation
150
100
50
0
*
MDA-MB-231 cells
Arf6 T157N cells
MDA-MB-231cells
C
Rac1
phalloidin
merge
siNT_15'EGF
siArf6_15'EG
D
MDA-MB-231cells
Rac1 edge intensity
100
50
0
***
siNT_15'EGF
siArf6_15'EGF
0
50
100
150
length (pixels)
MDA-MB-231cells
E
**
***
***
Arf6 activation
300
200
100
0
siNT_starved
siNT_1'EGF
siNT_15'EGF
siArf6_starved
siArf6_1'EGF
siArf6_15'EGF
F
**
***
***
Rac1 activation
300
200
100
0
siNT_starved
siNT_1'EGF
siNT_15'EGF
siArf6_starved
siArf6_1'EGF
siArf6_15'EGF

Fig.4

Figure 4: Rac1 localizes on ventral actin structures and ARF6 is required for Rac1 activation and recruitment at the plasma membrane. (A) MDA-MB-231 cells stably expressing ARF6T157N were plated on cross-linked unlabeled gelatin, fixed and stained for actin and Rac1. Scale bars, 10 µm. **(B)** Rac1 activation levels in MDA-MB-231 cells versus cells stably expressing ARF6T157N were measured with a G-LISA Rac1 activation kit (Cytoskeleton Inc). Values are normalized mean ± SEM from replicates measurements from one experiment. Comparisons were made with a Student t-test. *, $P < 0.05$ (compared with MDA-MB-231 cells). **(C-D)** MDA-MB-231 cells were treated with the indicated siRNAs for 72 hours, plated on gelatin, serum-starved and treated with EGF for 15 minutes. Then fixed and stained for actin and Rac1. **(C)** Images were acquired by epifluorescence microscopy. Scale bar, 10 µm. Insets are magnification of the boxed regions. Scale bar, 5 µm. **(D)** Quantification of Rac1 edge intensity profile along a line of 160 pixels drawn perpendicularly to the cell leading edge. Values are normalized fluorescence intensities for each pixel, averaged for at least 50 cells per condition. Values derive from two independent experiments. Comparisons were made with a one-way ANOVA (Kruskall-Wallis) test. ***, $P < 0.001$ (compared with siNT-treated cells). **(E-F)** MDA-MB-231 cells were treated with the indicated siRNAs for 72 hours, plated on gelatin, serum-starved and treated with EGF for 1 and 15 minutes. ARF6 **(E)** and Rac1 **(F)** activation levels in the different conditions were measured with G-LISA ARF6 **(E)** and G-LISA Rac1 **(F)** activation kits (Cytoskeleton, Inc). Values are normalized mean ± SEM from replicates measurements from two independent experiments. Comparisons were made with a Student t-test. **, $P < 0.01$, ***, $P < 0.001$ (compared with siNT-treated cells).

SUPPLEMENTAL INFORMATION

ARF6 implication in ventral actin organization in breast cancer cells

Valentina Marchesin and Philippe Chavrier

SUPPLEMENTAL FIGURES

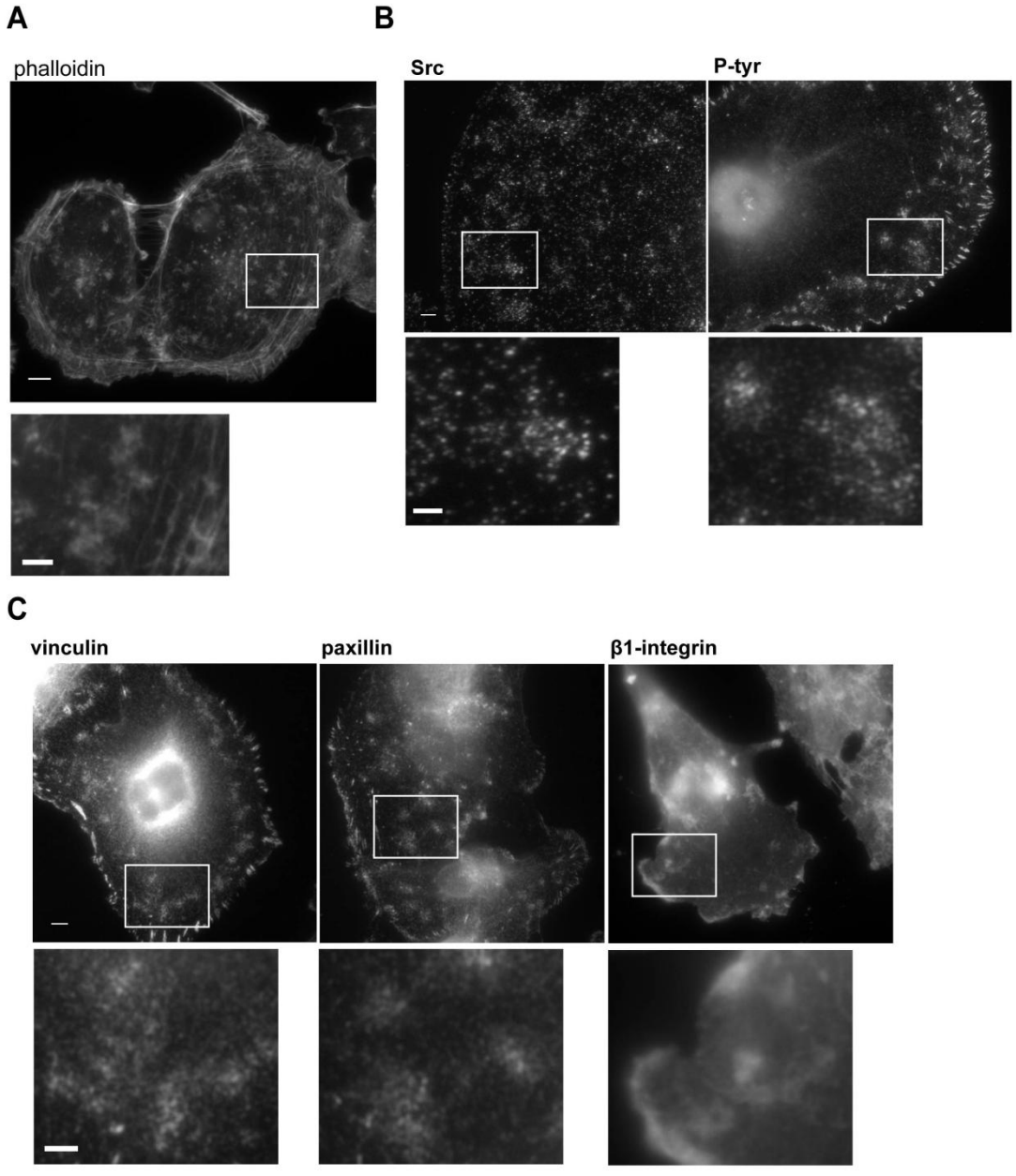

Fig.S1

Supplemental Figure S1 accompanying Figure 1: Cortactin ventral structures are positive for invadopodial/podosomal markers and ECM adhesion proteins. (A-B-C) MDA-MB-231 cells stably expressing ARF6T157N were plated on cross-linked unlabeled gelatin, fixed and stained for the indicated markers. Images were acquired with epifluorescence microscopy. Insets are magnification of the boxed regions. Scale bars, 5 μm.

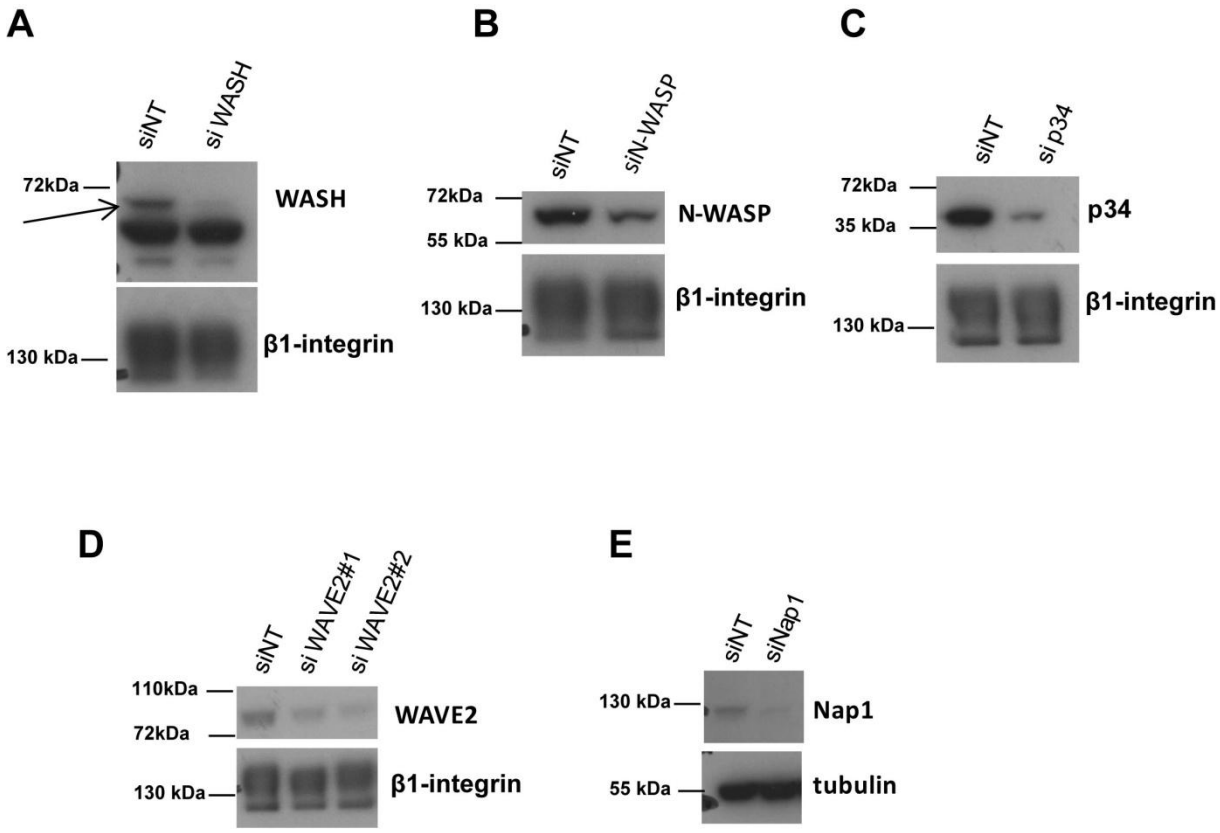

Fig.S2

Supplemental Figure S2 accompanying Figure 2: Immunoblotting analysis of siRNA-treated cells. (A-E) Immunoblotting analysis of lysates of MDA-MB-231 cells stably expressing ARF6T157N treated with indicated siRNAs for 72 hrs. Antibodies are indicated on the right. Immunoblotting analysis with anti-α tubulin and anti β1-integrin was used as loading control.

SUPPLEMENTAL MATERIAL AND METHOD:

Table S1: Antibodies used for this study.

Cortactin	Monoclonal (Mouse)	Millipore	IF
Alexa Fluor–conjugated phalloidin		Invitrogen	IF
SRC	Polyclonal (Rabbit)	Upstate Biotechnology	IF
P-tyrosines	Monoclonal (Mouse)	Upstate Biotechnology	IF
paxillin	Monoclonal (Mouse)	Transduction laboratories	IF
vinculin	Monoclonal (Mouse)	M.Glukhova (Institut Curie, Paris, France)	IF
β1-integrin	Monoclonal (Mouse)	Beckman Coulter	IF
β1-integrin	Polyclonal (Rabbit)	C. Albiges-Rizo, Institut Albert Bonniot, Grenoble, France	WB
WAVE2	Monoclonal (Mouse)	G.Scita (IFOM,Milan, Italy)	IF
WAVE2	Polyclonal (Rabbit)	A. Gautreau (CNRS, Gif-sur-Yvette, France)	WB
p34-Arc (ARPC2)	Polyclonal (Rabbit)	Millipore	IF/WB
WASH	Polyclonal (Rabbit)	Derivery et al., 2009	IF/WB
N-WASP	Polyclonal (Rabbit)	Cell Signaling Technology	IF/WB
Rac1	Monoclonal (Mouse)	BD Transduction Laboratories	IF
α-tubulin	Monoclonal (Mouse)	Sigma	WB
Nap1	Polyclonal (Rabbit)	Upstate Biotechnology	WB
Secondary antibodies		Jackson ImmunoResearch Laboratories, Inc	IF
HRP-conjugated anti-rabbit IgG		Sigma	WB
HRP-conjugated anti-mouse IgG		Jackson ImmunoResearch Laboratories, Inc	WB

Table S2: siRNAs used for this study.

siRNA Gene	Sequence (Sens)	Company
ARF6	5'-CGGCAUUACUACACUGGGA-3'	Thermo Fisher Scientific
WASH	5'- UGUCGGAUCUCUUCAACAA-3'	Thermo Fisher Scientific
NCKAP1 (Nap1)	5'-GGUCGUAGCUCUUUCUUCA-3', 5'-GGAGAAUGUUGAUGUGUUA-3', 5'-GCAGACGACUUUAUAGAUA-3', 5'-CAUCCUAUCUUAUCGACAA-3'	Thermo Fisher Scientific
ARPC2 (p34)	5'-GUACGGGAGUUUCUUGGUA-3'	Thermo Fisher Scientific
WASF2 (WAVE2#1)	5'- GGGCAGAGCUUUCUCAGUU-3'	Thermo Fisher Scientific
WASF2 (WAVE2#2)	5'-GGAUUUGGGUCUCCAGGGA-3’	Thermo Fisher Scientific
(WASL) N-WASP	5’-CAGCAGAUCGGAACUGUAU-3’ 5’-UAGAGAGGGUGCUCAGCUA-3’ 5’-GGUGUUGCUUGUCUUGUUA-3’ 5’-CCAGAAAUCACAACAAAUA-3’	Thermo Fisher Scientific
Non targeting		Thermo Fisher Scientific

Chapter 7: Discussion and conclusions

The main purpose of my PhD work was to bring novel insights at the mechanism of polarized recycling and exocytosis regulated by ARF6, a process that is essential for several cellular functions including cell migration and invasion.

In a minor study, I addressed the contribution of ARF6 to actin cytoskeleton remodeling in breast cancer cells. By expressing a hyper-activated mutant of ARF6 (ARF6T157N) in MDA-MB-231 cells, a breast cancer-derived cell line, I observed the formation of actin ventral structures, highly dynamic and positive for markers such as cortactin, the Arp2/3 complex, the SCAR/WAVE complex and its most prominent regulator Rac1. The observation that similar structures form in normal condition upon EGF stimulation brought us to hypothesize a role for ARF6 and for ARF6-dependent ventral structures in lamellipodia formation and possibly breast cancer cell directed migration. In addition, we showed that ARF6 depletion inhibits Rac1 activation and its targeting to the plasma membrane in response to EGF treatment, suggesting a role for ARF6 in linking EGFR signaling to Rac1 activation and redirection to the leading edge, where it presumably activates the SCAR/WAVE complex and regulates ventral actin polymerization during lamellipodia extension. We hypothesize that this process could be important for efficient breast cancer cell chemotactic migration. To confirm our hypothesis, it would be interesting in the future to perform migration assays in which MDA-MB-231 cells would be cultured under a gradient of cytokine and monitored for their capacity to respond to this gradient and to form persistent lamellipodia in presence or absence of ARF6. Such an assay has been described by Montagnac and colleagues that consists in generating two overlapping collagen layers, an inner gel containing fluorescently-labeled EGF and an outer one containing cells and measuring the persistence migration of the cells towards the gradient (Montagnac et al., 2013). This assay could also allow to image cortactin waves possibly forming at the leading edge towards the directional cues.

Another interesting issue to address in the future is the spatio-temporal activation and localization of Rac1 at different subcellular locations in control cells compared to ARF6 depleted cells or to cells over-expressing ARF6T157N. For instance by making use of genetically-encoded biosensors based on Förster resonance energy transfer (FRET) interaction as a report of Rac1 activity, such as Rac1Raichiu (Hodgson et al., 2010), it could be possible not only to visualize how ARF6 affects Rac1 active pool in the different conditions but also to follow the possible Rac1 activation at the level of the cortactin waves in order to prove the function of these structures in lamellipodia extension and cell migration.

Several studies in the years have shown that ARF6 regulates the formation of actin protrusion and membrane ruffling and promotes the acquisition of migratory phenotypes in cells of epithelial origin likely through activation of Rac1 (Nishiya et al., 2005; Palacios and D'Souza-Schorey, 2003; Radhakrishna et al., 1996; Santy and Casanova, 2001). A recent study has described the formation of motile actin structures at the ventral surface of HeLa and Beas-2b cells, a lung bronchial epithelial cell line, upon acute activation of protein kinase C (PKC) induced by the phorbol ester PMA (Caviston et al., 2014). For both cell types, formation of the ventral actin structures was enhanced by expression of active mutants of either ARF1 or ARF6 and of ARFGEFs such as ARNO. By contrast, formation of these structures was blocked by inhibitors of PKC and SRC and required $PI(4,5)P_2$, Rac, ARF6, and ARF1 (Caviston et al., 2014). The authors propose that ARF1 and, although to a minor extent, ARF6 can form these structures independently probably sharing common effectors and activation of PKC and SRC can guide the shared activities of ARF1 and ARF6 to reorganize the cortical actin cytoskeleton (Caviston et al., 2014).

In this study I showed how ARF6 activation induces the formation of similar ventral cortactin structures in a highly aggressive breast cancer cell line in response to EGF and point to the possibility that this process could be important for breast cancer cell motility. I showed that the SCAR/WAVE complex, NPF known to be involved in lamellipodia formation, is absolutely required for their formation and I provided evidences that ARF6 could activate upstream SCAR/WAVE by mediating Rac1 recruitment and activation at the plasma membrane. Future studies are however required to prove whether this pathway is important for breast cancer cell migration and to better characterize the mechanism through which ARF6 regulates the targeting of Rac1 at the surface.

In my main study, I have worked on the previously untested hypothesis of ARF6 controlling the trafficking of MT1-MMP and I have delineated a possible mechanism through which ARF6 could control MT1-MMP endosomes exocytosis for efficient targeting of the protease to invadopodia and for promoting pericellular matrix remodeling. This mechanism is summarized in the scheme in figure 36.

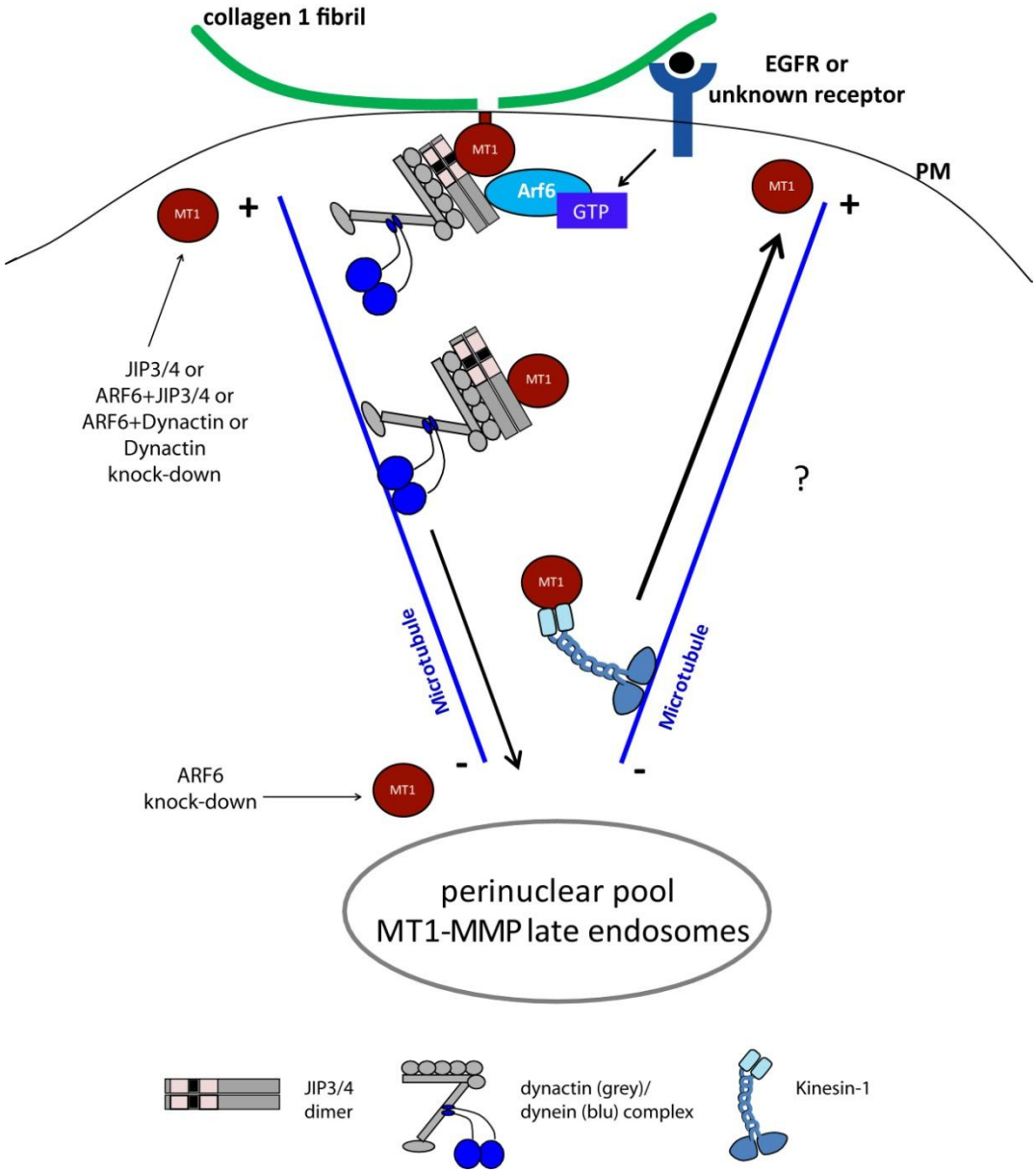

Figure 36: Model for ARF6-JIP3/JIP4 pathway controlling MT1-MMP exocytosis and ECM invasion during breast cancer progression

In MDA-MB-231 cells MT1-MMP is enriched in late endocytic compartments (Steffen et al., 2008) that require the microtubule plus-end-directed kinesin-family motor proteins for exocytosis at the surface (Wiesner et al., 2010) (Castro-Castro et al., unpublished data). A study published by Pedro Monteiro from my host lab recently proposed that formation of long-lasting (over several minutes) LE-to-plasma membrane connections ensure MT1-MMP targeting at invadopodia plasma membrane (Monteiro et al., 2013). Here I showed by immunohistochemistry analysis of human breast cancer samples that ARF6 is enriched at the plasma membrane of cells in highly aggressive carcinomas. It is likely that peripheral ARF6 correspond to an activated pool based on various evidence from the literature (D'Souza-Schorey and Chavrier, 2006; Donaldson and Jackson, 2011) and by recent findings showing that the ARF6-GEF GEP100/BRAG2, known to

link EGFR signaling to ARF6 activation, was over-expressed in a cohort of IDCs (Morishige et al., 2008). We believe that one function of ARF6 is to control negatively the clearance and inward movement of MT1-MMP endosomes from the cell periphery by negatively controlling the activity of the minus-end-directed motor dynactin/dynein. This assumption is based on the fact that loss of ARF6 function results in mispositioning of MT1-MMP-LEs in the perinuclear region and knockdown of the p150Glued dynactin complex subunit rescues MT1-MMP endosome positioning in ARF6-depleted cells, strongly supporting the implication of dynactin/dynein activity in MT1-MMP endosome clearance. As a consequence silencing of ARF6 leads to a decrease in MT1-MMP exocytosis and MT1-MMP-dependent pericellular collagen degradation, as well as to a general decrease in the capacity of cells to invade in a 3D collagen environment.

We also believe that ARF6 does so by interacting with JIP3 and JIP4, two dimeric coiled-coil proteins recently identified as ARF6 effectors (Montagnac et al., 2009) and known to interact with kinesin-1 and dynactin (Bowman et al., 2000; Cavalli et al., 2005; Montagnac et al., 2009). Based on the fact that knock-down of JIP3/4 leads to an accumulation of MT1-MMP at the periphery, we suggest that JIP3/4 may function as adaptor proteins for MT1-MMP containing vesicles that would then bind to dynactin and activate the dynactin/dynein complex. ARF6, activated (i.e. GTP-bound) at the plasma membrane either by EGFR or by other stimuli, would bind to JIP3/4 and exert a negative regulation on the JIP3/4/dynactin/dynein complex.

Along this line, it was recently shown that the mammalian dynein motor is largely inactive in the cytoplasm and that activation of its motility requires the simultaneous binding of dynein to adaptor proteins, defining a particular cargo for transport, and dynactin, which in absence of an adaptor would have very low affinity for dynein (McKenney et al., 2014). These cargo adaptors include several coiled coil proteins such as the dimeric Bicaudal D2 (BicD2) that links dynein to Rab6-membrane organelles and Rab11-FIP3 that links dynein to Rab11-positive recycling endosomes (McKenney et al., 2014). Similarly, JIP3/4 may link dynein to MT1-MMP-positive endosomes in an ARF-controlled manner.

In an earlier study in our lab, Montagnac et al. showed by *in vitro* experiments that upon binding of GTP-ARF6 to their LZII domain, JIP3/JIP4 switched from kinesin-1 to dynactin interaction. These observations were interpreted as ARF6 favoring the minus-end directed transport of vesicles (Montagnac et al., 2009). Based on my data, I propose that active ARF6 favoring interaction of JIP3/4 with dynactin may rather inhibit dynactin/dynein-mediated transport. This assumption could be further tested in future experiments. For instance, activation of ARF6 could be induced (for example by EGF stimulation) and the distribution of MT1-MMP endosomes analyzed; according to my model, they should accumulate at the periphery.

In addition, based on the crystal structure of the complex of the LZII domain of JIP4 with GTP-ARF6 in solution it has been proposed that when GTP-ARF6 is associated with the membrane, a dimer of JIP4 (or JIP3) can interact only with one membrane-bound GTP-ARF6 molecule (Isabet

et al., 2009) (Fig.37A), favoring dynactin/dynein binding to this face of the JIP dimer (Fig.37B). The other LZII domain of the dimer is free (of ARF6) and available for binding either to kinesin-1 or dynactin (Fig.37B). The LZII domain of JIP3/4, indeed, is known to bind also to the light chain of kinesin-1 (KLC) (Bowman et al., 2000; Montagnac et al., 2009) and JIP3 in particular was shown to function as an adaptor protein for kinesin-1 in the neurons and also to enhance kinesin-1 motor activity (Sun et al., 2011). Thus the role of ARF6 in the regulation of JIPs' interaction with motors and MT1-MMP-vesicles trafficking may be more complex and may also involve the participation of kinesin-1. The contribution of ARF6-JIP3/4 pathway in the regulation of plus-directed, kinesin-1-dependent transport of MT1-MMP would also be an interesting issue to address in the future.

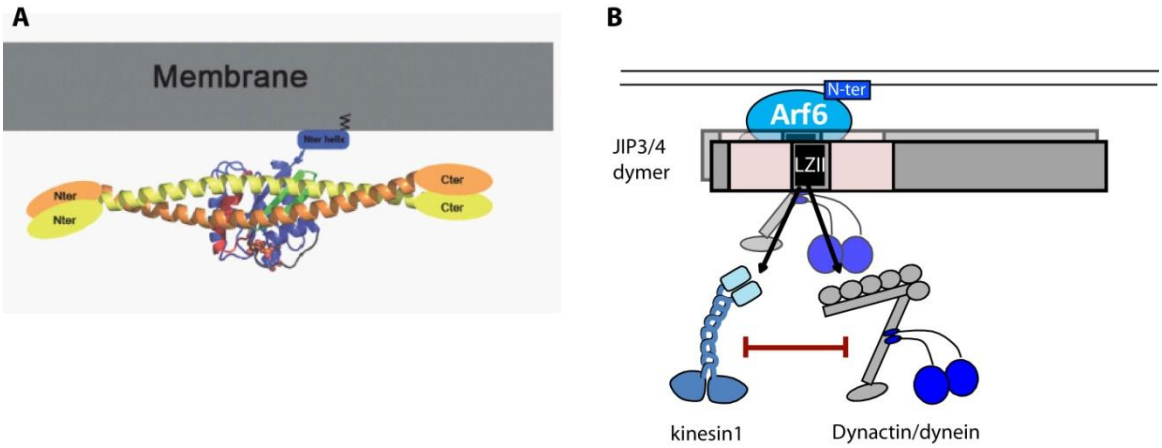

Figure 37: Model for ARF6-JIP3/JIP4-motors interaction at the plasma membrane. (A) Structural model of the ARF6–$(JIP4)_2$ heterotrimer at the membrane. ARF6 is shown in blue and the two monomers of JIP4-LZII are drawn in yellow and orange. The myristoylated amphipatic N-terminal helix of ARF6 that is critical for interaction with membrane is indicated as a blue cylinder lying against the membrane. Picture from Isabet et al., 2009. **(B)** Schematic representation of the ARF6–JIP3/4-motors interaction at the membrane. KLC and dynactin can both bind to the LZII domain of JIP3/4 in a way that is mutually exclusive (Bowman et al., 2000; Cavalli et al., 2005; Montagnac et al., 2009). The JIP dimer bound to ARF6 (in transparence) is favored in binding dynactin/dynein (in transparence). The other LZII domain of the dimer is free (of ARF6) and available for binding either to kinesin-1 or dynactin.

Of particular interest is a recent study that identified a mechanism involving Arl8, another small GTP-binding protein of the ARF family localized on mature lysosomes, and SKIP, an adaptor protein that binds to the light chain of kinesin-1 (Rosa-Ferreira and Munro, 2011). The interaction between Arl8 and SKIP recruits kinesin-1 to lysosomes and hence direct their movement towards the microtubules plus-ends (Rosa-Ferreira and Munro, 2011). There could be then a conserved mechanism in which different ARF family proteins in different locations of the cell bind to adaptor proteins for the motors and regulate the movement of different organelles and cargos.

The resolution of molecular and structural interactions between all these different actors (ARF6, JIP3/4, dynactin/dynein) would probably help to better understand these regulation mechanisms.

Indeed, if the crystal structure of the interaction between ARF6-GTP and JIP3/4 has been solved (Isabet et al., 2009), the interactions sites between JIP3/4 and the dynactin subunits are not known yet. However, this will be complicated by the fact that the dynactin subunit(s) interacting directly with JIP3/4 have not been identified yet.

Another issue that remains to be explained is how JIP3 and JIP4 may associate to MT1-MMP-containing vesicles. Although JIP3 can be peripherically associated to membranes (Cavalli et al., 2005) and JIP3 and JIP4 are capable to interact with some trans-membrane receptors such us TrkB and Cdo (Huang et al., 2011; Takaesu et al., 2006), to date how JIP3 and JIP4 associate to membrane and can recognize their specific cargo vesicles still remains elusive. In addition, the lack of good antibodies for JIP3/4 and the fact that the overexpressed proteins are mainly cytosolic make it difficult to determine their localization and association to MT1-MMP endosomes.

Despite the accumulation of MT1-MMP-positive endosomes at the periphery of JIP3/4-depleted cells possibly due to defect in the clearance of MT1-MMP vesicles from the surface, silencing of JIP3/4 leads to a decrease in MT1-MMP exocytosis at the surface and MT1-MMP-dependent pericellular collagen degradation and consequently in the capacity of cells to invade collagen matrices. This suggests that in normal condition breast cancers cells requires MT1-MMP endosomes to move and switch direction dynamically to adapt to changing in ECM microenvironments and this process might be tightly regulated by the continuous GTP-GDP cycling of ARF6 that would regulate JIP3/4-dependent transport of MT1-MMP. Moreover several studies also from the lab have described how MT1-MMP target to the membrane requires a complex machinery involving the SNARE membrane fusion protein VAMP7, the exocyst vesicle-docking complex and several other players of the actin cytoskeleton and each of them is tightly regulated for targeting of MT1-MMP to invadopodia (Monteiro et al., 2013; Sakurai-Yageta et al., 2008; Steffen et al., 2008; Yu et al., 2012). Therefore, in cells depleted for JIP3/4, despite a massive accumulation of MT1-MMP endosomes at the cell periphery, these endosomes cannot engage in a productive exocytic reaction.

Some evidences in literature link JIP3/4 with cancer cell invasion. JIP3 mRNA levels, for instance, were shown to be significantly higher in highly aggressive glioblastoma tumors rather than in samples derived from normal brain tissues or low-grade brain tumors (Takino et al., 2005), while the JIP4 splice variant SPAG9 was shown by RT-PCR and immunohistochemestry to be elevated in a variety of human cancers including renal, breast, cervical, thyroid, colon and lung carcinoma and it has been proposed to be used as a marker for early cancer detection (Garg et al., 2009a; Garg et al., 2009b; Garg et al., 2009c; Kanojia et al., 2009; Kanojia et al., 2011; Wang et al., 2013). Moreover SPAG9 silencing led to a decrease in lung carcinoma-derived cells invasion and proliferation (Wang et al., 2013). However, no mechanism either for JIP3 or JIP4/SPAG9 role

in invasion had been identified. In this study I further support an implication for JIP3/4 in cancer cell invasion and I propose a possible role for JIP3/4 in MT1-MMP trafficking. It would be interesting for the future to perform immunohistochemestry and/or RT-PCR experiments in order to analyze JIP3/4 expression and/or localization in human breast cancer samples and to correlate them with those of ARF6 and MT1-MMP.

In conclusion, although several issues remains to be understood, we have delineated a possible mechanism in which ARF6 through JIP3/4 could control intracellular trafficking of MT1-MMP-positive endosomes and exocytosis for efficient targeting of the protease to invadopodia and to promote pericellular matrix remodeling.

Another subject of interest for future studies is represented by the regulation of ARF6/JIP3/4 pathway in the context of JNK signaling and cancer cell invasion. JIP3/4 indeed are well known to be scaffold proteins for JNK signaling pathway since they can bind to JNK and its upstream regulatory kinases (see chapter 3.1.). JIP3/4 have been proposed to favor the transport of JNK and its associated MAPKKs and MAPKKKs bidirectionally along microtubules in neuronal cells (Abe et al., 2009; Cavalli et al., 2005). JNK was also shown to phosphorylate paxillin (a focal adhesion and invadopodial component) and to be required for cell migration of tumor cells (Huang et al., 2003). Therefore a tempting hypothesis would be that the ARF6/JIP3/4 mechanism we have identified could also control the delivery and localization of JNK to invadopodia sites of degradation and then influence the activity of these structures in invasive cells. It is also possible that JNK may affect the motor adaptor function of JIP3/4 through some phosphorylation events as was demonstrated in neurons (Cavalli et al., 2005) and thus JNK signaling may regulate invasion by controlling the trafficking of JIP3/4-dependent cargoes such as MT1-MMP.

Based on the fact that our *in vitro* data strongly point to a role for ARF6 in MT1-MMP-dependent breast cancer cell invasion and our human samples analysis revealed an accumulation of ARF6 and MT1-MMP at the plasma membrane of cells in aggressive tumor types, we wanted to check whether ARF6 is also required *in vivo* for cells to breach the BM and for the *in situ* to invasive transition of breast cancer. Results obtained with an intraductal human in mouse xenograft suggested that ARF6 is required for the formation of tumor foci in the fat pad of the mammary gland upon injection of human breast cancer cells in the mammary duct. However, these data present several limitations and further control experiments should be done (see chapter 5.3). It would be however interesting for the future to use the intraductal model to inject cells stably depleted for JIP3 and/or JIP4 in order to confirm JIP3/4 implication in the breaching of the BM *in vivo* and in breast cancer progression.

In conclusion my PhD work has provided novel insights into how ARF6 exerts its pro-invasive role in breast cancer and on the mechanism of transport and delivery of MT1-MMP to

invadopodia. A better understanding of invadopodia formation and the underlying signalling pathways is important to find out new ways of inhibiting the invasive proprieties in tumours. Targeting invadopodia-associated proteins, however, is still in its infancy.

ARF6 pathways had been associated with EMT through disruption of E-cadherin-based cell-cell contacts and increased β1-integrin recycling in tumor epithelial cells (Onodera et al., 2012; Palacios et al., 2001). Moreover the group of Dr. H. Sabe has shown how ARF6 contribute to invadopodia assembly by recruiting cortactin and paxillin through the effector AMAP1 (Hashimoto et al., 2005; Onodera et al., 2005) and that ARF6-GEF GEP100/BRAG2 links EGFR signaling to ARF6 activation because of its ability to bind to ligand-activated EGFR (Morishige et al., 2008). They also showed that the EGFR-GEP100-ARF6-AMAP1 pathway is up-regulated in breast cancer and they proposed AMAP1 or AMAP1 interaction with cortactin as possible targets for breast cancer therapeutics especially for the treatment of patients with cancer that has become resistant to the currently available EGFR inhibitors (Sabe et al., 2009).

In this study we showed by IHC that ARF6 is overexpressed in carcinoma cells as compared to normal epithelial cells and a striking plasma membrane accumulation of ARF6 signal was observed in hormone receptor-negative invasive breast tumors. This distribution of ARF6 was higher in infiltrating components of IDCs as compared to in situ tumor regions and in higher-grade tumors. Therefore ARF6 could be studied in the future as a possible prognostic marker for breast cancer progression. We also showed that ARF6 could contribute to breast cancer cell invasion by regulating MT1-MMP transport to invadopodia sites of degradation and the molecular pathway ARF6-JIP3/4-MT1-MMP we identified could also provide future novel therapeutics targets. ARF6 itself probably does not represent a potential target due to its ubiquitous expression in different types of cells, organs and tissues and its implication in housekeeping roles such as cytokinesis. However, disruption of ARF6 interaction with JIP3/4 or JIP3/4 interaction with the motors through pharmacological inhibitors could be studied in the future a possible strategy for targeted therapy.

BIBLIOGRAPHY

Abe, N., A. Almenar-Queralt, C. Lillo, Z. Shen, J. Lozach, S.P. Briggs, D.S. Williams, L.S. Goldstein, and V. Cavalli. 2009. Sunday driver interacts with two distinct classes of axonal organelles. *The Journal of biological chemistry*. 284:34628-34639.

Allaire, P.D., M. Seyed Sadr, M. Chaineau, E. Seyed Sadr, S. Konefal, M. Fotouhi, D. Maret, B. Ritter, R.F. Del Maestro, and P.S. McPherson. 2013. Interplay between Rab35 and Arf6 controls cargo recycling to coordinate cell adhesion and migration. *Journal of cell science*. 126:722-731.

Allan, V.J. 2011. Cytoplasmic dynein. *Biochemical Society transactions*. 39:1169-1178.

Almeida, E.A., D. Ilic, Q. Han, C.R. Hauck, F. Jin, H. Kawakatsu, D.D. Schlaepfer, and C.H. Damsky. 2000. Matrix survival signaling: from fibronectin via focal adhesion kinase to c-Jun NH(2)-terminal kinase. *The Journal of cell biology*. 149:741-754.

Annabi, B., M. Lachambre, N. Bousquet-Gagnon, M. Page, D. Gingras, and R. Beliveau. 2001. Localization of membrane-type 1 matrix metalloproteinase in caveolae membrane domains. *The Biochemical journal*. 353:547-553.

Arimoto, M., S.P. Koushika, B.C. Choudhary, C. Li, K. Matsumoto, and N. Hisamoto. 2011. The Caenorhabditis elegans JIP3 protein UNC-16 functions as an adaptor to link kinesin-1 with cytoplasmic dynein. *The Journal of neuroscience : the official journal of the Society for Neuroscience*. 31:2216-2224.

Arjonen, A., J. Alanko, S. Veltel, and J. Ivaska. 2012. Distinct recycling of active and inactive beta1 integrins. *Traffic*. 13:610-625.

Artym, V.V., Y. Zhang, F. Seillier-Moiseiwitsch, K.M. Yamada, and S.C. Mueller. 2006. Dynamic interactions of cortactin and membrane type 1 matrix metalloproteinase at invadopodia: defining the stages of invadopodia formation and function. *Cancer research*. 66:3034-3043.

Ayala, I., M. Baldassarre, G. Giacchetti, G. Caldieri, S. Tete, A. Luini, and R. Buccione. 2008. Multiple regulatory inputs converge on cortactin to control invadopodia biogenesis and extracellular matrix degradation. *Journal of cell science*. 121:369-378.

Baietti, M.F., Z. Zhang, E. Mortier, A. Melchior, G. Degeest, A. Geeraerts, Y. Ivarsson, F. Depoortere, C. Coomans, E. Vermeiren, P. Zimmermann, and G. David. 2012. Syndecan-syntenin-ALIX regulates the biogenesis of exosomes. *Nature cell biology*. 14:677-685.

Balasubramanian, N., D.W. Scott, J.D. Castle, J.E. Casanova, and M.A. Schwartz. 2007. Arf6 and microtubules in adhesion-dependent trafficking of lipid rafts. *Nature cell biology*. 9:1381-1391.

Baldassarre, M., A. Pompeo, G. Beznoussenko, C. Castaldi, S. Cortellino, M.A. McNiven, A. Luini, and R. Buccione. 2003. Dynamin participates in focal extracellular matrix degradation by invasive cells. *Molecular biology of the cell*. 14:1074-1084.

Beaty, B.T., V.P. Sharma, J.J. Bravo-Cordero, M.A. Simpson, R.J. Eddy, A.J. Koleske, and J. Condeelis. 2013. beta1 integrin regulates Arg to promote invadopodial maturation and matrix degradation. *Molecular biology of the cell*. 24:1661-1675, S1661-1611.

Behbod, F., F.S. Kittrell, H. LaMarca, D. Edwards, S. Kerbawy, J.C. Heestand, E. Young, P. Mukhopadhyay, H.W. Yeh, D.C. Allred, M. Hu, K. Polyak, J.M. Rosen, and D. Medina. 2009. An intraductal human-in-mouse transplantation model mimics the subtypes of ductal carcinoma in situ. *Breast Cancer Res*. 11:R66.

Blasius, T.L., D. Cai, G.T. Jih, C.P. Toret, and K.J. Verhey. 2007. Two binding partners cooperate to activate the molecular motor Kinesin-1. *The Journal of cell biology*. 176:11-17.

Bloom, H.J., and W.W. Richardson. 1957. Histological grading and prognosis in breast cancer; a study of 1409 cases of which 359 have been followed for 15 years. *Br J Cancer*. 11:359-377.

Bowden, E.T., M. Barth, D. Thomas, R.I. Glazer, and S.C. Mueller. 1999. An invasion-related complex of cortactin, paxillin and PKCmu associates with invadopodia at sites of extracellular matrix degradation. *Oncogene*. 18:4440-4449.

Bowden, E.T., E. Onikoyi, R. Slack, A. Myoui, T. Yoneda, K.M. Yamada, and S.C. Mueller. 2006. Co-localization of cortactin and phosphotyrosine identifies active invadopodia in human breast cancer cells. *Experimental cell research*. 312:1240-1253.

Bowman, A.B., A. Kamal, B.W. Ritchings, A.V. Philp, M. McGrail, J.G. Gindhart, and L.S. Goldstein. 2000. Kinesin-dependent axonal transport is mediated by the sunday driver (SYD) protein. *Cell*. 103:583-594.

Bravo-Cordero, J.J., M.A. Magalhaes, R.J. Eddy, L. Hodgson, and J. Condeelis. 2013. Functions of cofilin in cell locomotion and invasion. *Nature reviews. Molecular cell biology*. 14:405-415.

Bravo-Cordero, J.J., R. Marrero-Diaz, D. Megias, L. Genis, A. Garcia-Grande, M.A. Garcia, A.G. Arroyo, and M.C. Montoya. 2007. MT1-MMP proinvasive activity is regulated by a novel Rab8-dependent exocytic pathway. *The EMBO journal*. 26:1499-1510.

Bromann, P.A., H. Korkaya, and S.A. Courtneidge. 2004. The interplay between Src family kinases and receptor tyrosine kinases. *Oncogene*. 23:7957-7968.

Brown, F.D., A.L. Rozelle, H.L. Yin, T. Balla, and J.G. Donaldson. 2001. Phosphatidylinositol 4,5-bisphosphate and Arf6-regulated membrane traffic. *The Journal of cell biology*. 154:1007-1017.

Brown, H.M., H.A. Van Epps, A. Goncharov, B.D. Grant, and Y. Jin. 2009. The JIP3 scaffold protein UNC-16 regulates RAB-5 dependent membrane trafficking at C. elegans synapses. *Developmental neurobiology*. 69:174-190.

Buccione, R., J.D. Orth, and M.A. McNiven. 2004. Foot and mouth: podosomes, invadopodia and circular dorsal ruffles. *Nature reviews. Molecular cell biology*. 5:647-657.

Buchsbaum, R.J., B.A. Connolly, and L.A. Feig. 2002. Interaction of Rac exchange factors Tiam1 and Ras-GRF1 with a scaffold for the p38 mitogen-activated protein kinase cascade. *Molecular and cellular biology*. 22:4073-4085.

Butler, G.S., M.J. Butler, S.J. Atkinson, H. Will, T. Tamura, S. Schade van Westrum, T. Crabbe, J. Clements, M.P. d'Ortho, and G. Murphy. 1998. The TIMP2 membrane type 1 metalloproteinase "receptor" regulates the concentration and efficient activation of progelatinase A. A kinetic study. *The Journal of biological chemistry*. 273:871-880.

Byrd, D.T., M. Kawasaki, M. Walcoff, N. Hisamoto, K. Matsumoto, and Y. Jin. 2001. UNC-16, a JNK-signaling scaffold protein, regulates vesicle transport in C. elegans. *Neuron*. 32:787-800.

Campellone, K.G., and M.D. Welch. 2010. A nucleator arms race: cellular control of actin assembly. *Nature reviews. Molecular cell biology*. 11:237-251.

Caswell, P.T., S. Vadrevu, and J.C. Norman. 2009. Integrins: masters and slaves of endocytic transport. *Nature reviews. Molecular cell biology*. 10:843-853.

Cavalli, V., P. Kujala, J. Klumperman, and L.S. Goldstein. 2005. Sunday Driver links axonal transport to damage signaling. *The Journal of cell biology*. 168:775-787.

Caviston, J.P., L.A. Cohen, and J.G. Donaldson. 2014. Arf1 and Arf6 promote ventral actin structures formed by acute activation of protein kinase C and Src. *Cytoskeleton*. 71:380-394.

Chambers, A.F., A.C. Groom, and I.C. MacDonald. 2002. Dissemination and growth of cancer cells in metastatic sites. *Nature reviews. Cancer*. 2:563-572.

Chen, W.T. 1989. Proteolytic activity of specialized surface protrusions formed at rosette contact sites of transformed cells. *The Journal of experimental zoology*. 251:167-185.

Chen, W.T., J.M. Chen, S.J. Parsons, and J.T. Parsons. 1985. Local degradation of fibronectin at sites of expression of the transforming gene product pp60src. *Nature*. 316:156-158.

Chen, Z., D. Borek, S.B. Padrick, T.S. Gomez, Z. Metlagel, A.M. Ismail, J. Umetani, D.D. Billadeau, Z. Otwinowski, and M.K. Rosen. 2010. Structure and control of the actin regulatory WAVE complex. *Nature*. 468:533-538.

Chesneau, L., D. Dambournet, M. Machicoane, I. Kouranti, M. Fukuda, B. Goud, and A. Echard. 2012. An ARF6/Rab35 GTPase cascade for endocytic recycling and successful cytokinesis. *Current biology : CB*. 22:147-153.

Claing, A., W. Chen, W.E. Miller, N. Vitale, J. Moss, R.T. Premont, and R.J. Lefkowitz. 2001. beta-Arrestin-mediated ADP-ribosylation factor 6 activation and beta 2-adrenergic receptor endocytosis. *The Journal of biological chemistry*. 276:42509-42513.

Clark, E.S., A.S. Whigham, W.G. Yarbrough, and A.M. Weaver. 2007. Cortactin is an essential regulator of matrix metalloproteinase secretion and extracellular matrix degradation in invadopodia. *Cancer research*. 67:4227-4235.

Cocucci, E., G. Racchetti, P. Podini, M. Rupnik, and J. Meldolesi. 2004. Enlargeosome, an exocytic vesicle resistant to nonionic detergents, undergoes endocytosis via a nonacidic route. *Molecular biology of the cell*. 15:5356-5368.

Cohen, L.A., A. Honda, P. Varnai, F.D. Brown, T. Balla, and J.G. Donaldson. 2007. Active Arf6 recruits ARNO/cytohesin GEFs to the PM by binding their PH domains. *Molecular biology of the cell*. 18:2244-2253.

Cowell, C.F., B. Weigelt, R.A. Sakr, C.K. Ng, J. Hicks, T.A. King, and J.S. Reis-Filho. 2013. Progression from ductal carcinoma in situ to invasive breast cancer: revisited. *Molecular oncology*. 7:859-869.

d'Ortho, M.P., H. Will, S. Atkinson, G. Butler, A. Messent, J. Gavrilovic, B. Smith, R. Timpl, L. Zardi, and G. Murphy. 1997. Membrane-type matrix metalloproteinases 1 and 2 exhibit broad-spectrum proteolytic capacities comparable to many matrix metalloproteinases. *European journal of biochemistry / FEBS*. 250:751-757.

D'Souza-Schorey, C., R.L. Boshans, M. McDonough, P.D. Stahl, and L. Van Aelst. 1997. A role for POR1, a Rac1-interacting protein, in ARF6-mediated cytoskeletal rearrangements. *The EMBO journal*. 16:5445-5454.

D'Souza-Schorey, C., and P. Chavrier. 2006. ARF proteins: roles in membrane traffic and beyond. *Nature reviews. Molecular cell biology*. 7:347-358.

D'Souza-Schorey, C., G. Li, M.I. Colombo, and P.D. Stahl. 1995. A regulatory role for ARF6 in receptor-mediated endocytosis. *Science*. 267:1175-1178.

D'Souza-Schorey, C., E. van Donselaar, V.W. Hsu, C. Yang, P.D. Stahl, and P.J. Peters. 1998. ARF6 targets recycling vesicles to the plasma membrane: insights from an ultrastructural investigation. *The Journal of cell biology*. 140:603-616.

Dai, J., J. Li, E. Bos, M. Porcionatto, R.T. Premont, S. Bourgoin, P.J. Peters, and V.W. Hsu. 2004. ACAP1 promotes endocytic recycling by recognizing recycling sorting signals. *Developmental cell*. 7:771-776.

Desmarais, V., H. Yamaguchi, M. Oser, L. Soon, G. Mouneimne, C. Sarmiento, R. Eddy, and J. Condeelis. 2009. N-WASP and cortactin are involved in invadopodium-dependent chemotaxis to EGF in breast tumor cells. *Cell motility and the cytoskeleton*. 66:303-316.

Destaing, O., E. Planus, D. Bouvard, C. Oddou, C. Badowski, V. Bossy, A. Raducanu, B. Fourcade, C. Albiges-Rizo, and M.R. Block. 2010. beta1A integrin is a master regulator of invadosome organization and function. *Molecular biology of the cell*. 21:4108-4119.

Dickens, M., J.S. Rogers, J. Cavanagh, A. Raitano, Z. Xia, J.R. Halpern, M.E. Greenberg, C.L. Sawyers, and R.J. Davis. 1997. A cytoplasmic inhibitor of the JNK signal transduction pathway. *Science*. 277:693-696.

Dietrich, K.A., C.V. Sindelar, P.D. Brewer, K.H. Downing, C.R. Cremo, and S.E. Rice. 2008. The kinesin-1 motor protein is regulated by a direct interaction of its head and tail.

Proceedings of the National Academy of Sciences of the United States of America. 105:8938-8943.
Dodding, M.P., and M. Way. 2011. Coupling viruses to dynein and kinesin-1. *The EMBO journal*. 30:3527-3539.
Doherty, G.J., and H.T. McMahon. 2009. Mechanisms of endocytosis. *Annual review of biochemistry*. 78:857-902.
Donaldson, J.G., and C.L. Jackson. 2011. ARF family G proteins and their regulators: roles in membrane transport, development and disease. *Nature reviews. Molecular cell biology*. 12:362-375.
Drerup, C.M., and A.V. Nechiporuk. 2013. JNK-interacting protein 3 mediates the retrograde transport of activated c-Jun N-terminal kinase and lysosomes. *PLoS genetics*. 9:e1003303.
Dunphy, J.L., R. Moravec, K. Ly, T.K. Lasell, P. Melancon, and J.E. Casanova. 2006. The Arf6 GEF GEP100/BRAG2 regulates cell adhesion by controlling endocytosis of beta1 integrins. *Current biology : CB*. 16:315-320.
Dyer, N., E. Rebollo, P. Dominguez, N. Elkhatib, P. Chavrier, L. Daviet, C. Gonzalez, and M. Gonzalez-Gaitan. 2007. Spermatocyte cytokinesis requires rapid membrane addition mediated by ARF6 on central spindle recycling endosomes. *Development*. 134:4437-4447.
Eckert, M.A., T.M. Lwin, A.T. Chang, J. Kim, E. Danis, L. Ohno-Machado, and J. Yang. 2011. Twist1-induced invadopodia formation promotes tumor metastasis. *Cancer cell*. 19:372-386.
Egeblad, M., and Z. Werb. 2002. New functions for the matrix metalloproteinases in cancer progression. *Nature reviews. Cancer*. 2:161-174.
Elston, E.W., and I.O. Ellis. 1993. Method for grading breast cancer. *J Clin Pathol*. 46:189-190.
Fielding, A.B., E. Schonteich, J. Matheson, G. Wilson, X. Yu, G.R. Hickson, S. Srivastava, S.A. Baldwin, R. Prekeris, and G.W. Gould. 2005. Rab11-FIP3 and FIP4 interact with Arf6 and the exocyst to control membrane traffic in cytokinesis. *The EMBO journal*. 24:3389-3399.
Franco, M., P. Chardin, M. Chabre, and S. Paris. 1993. Myristoylation is not required for GTP-dependent binding of ADP-ribosylation factor ARF1 to phospholipids. *The Journal of biological chemistry*. 268:24531-24534.
Franco, M., P.J. Peters, J. Boretto, E. van Donselaar, A. Neri, C. D'Souza-Schorey, and P. Chavrier. 1999. EFA6, a sec7 domain-containing exchange factor for ARF6, coordinates membrane recycling and actin cytoskeleton organization. *The EMBO journal*. 18:1480-1491.
Friedl, P., and S. Alexander. 2011. Cancer invasion and the microenvironment: plasticity and reciprocity. *Cell*. 147:992-1009.
Friedl, P., and D. Gilmour. 2009. Collective cell migration in morphogenesis, regeneration and cancer. *Nature reviews. Molecular cell biology*. 10:445-457.
Friedl, P., and K. Wolf. 2003. Proteolytic and non-proteolytic migration of tumour cells and leucocytes. *Biochemical Society symposium*:277-285.
Friedl, P., and K. Wolf. 2009. Proteolytic interstitial cell migration: a five-step process. *Cancer metastasis reviews*. 28:129-135.
Friedl, P., and K. Wolf. 2010. Plasticity of cell migration: a multiscale tuning model. *The Journal of cell biology*. 188:11-19.
Fukata, M., T. Watanabe, J. Noritake, M. Nakagawa, M. Yamaga, S. Kuroda, Y. Matsuura, A. Iwamatsu, F. Perez, and K. Kaibuchi. 2002. Rac1 and Cdc42 capture microtubules through IQGAP1 and CLIP-170. *Cell*. 109:873-885.
Gallo, K.A., and G.L. Johnson. 2002. Mixed-lineage kinase control of JNK and p38 MAPK pathways. *Nature reviews. Molecular cell biology*. 3:663-672.
Garg, M., D. Kanojia, S. Salhan, S. Suri, A. Gupta, N.K. Lohiya, and A. Suri. 2009a. Sperm-associated antigen 9 is a biomarker for early cervical carcinoma. *Cancer*. 115:2671-2683.

Garg, M., D. Kanojia, S. Suri, S. Gupta, A. Gupta, and A. Suri. 2009b. Sperm-associated antigen 9: a novel diagnostic marker for thyroid cancer. *The Journal of clinical endocrinology and metabolism*. 94:4613-4618.

Garg, M., D. Kanojia, S. Suri, and A. Suri. 2009c. Small interfering RNA-mediated down-regulation of SPAG9 inhibits cervical tumor growth. *Cancer*. 115:5688-5699.

Ghossoub, R., F. Lembo, A. Rubio, C.B. Gaillard, J. Bouchet, N. Vitale, J. Slavik, M. Machala, and P. Zimmermann. 2014. Syntenin-ALIX exosome biogenesis and budding into multivesicular bodies are controlled by ARF6 and PLD2. *Nature communications*. 5:3477.

Goldberg, J. 1998. Structural basis for activation of ARF GTPase: mechanisms of guanine nucleotide exchange and GTP-myristoyl switching. *Cell*. 95:237-248.

Goley, E.D., and M.D. Welch. 2006. The ARP2/3 complex: an actin nucleator comes of age. *Nature reviews. Molecular cell biology*. 7:713-726.

Gould, G.W., and J. Lippincott-Schwartz. 2009. New roles for endosomes: from vesicular carriers to multi-purpose platforms. *Nature reviews. Molecular cell biology*. 10:287-292.

Granger, E., G. McNee, V. Allan, and P. Woodman. 2014. The role of the cytoskeleton and molecular motors in endosomal dynamics. *Seminars in cell & developmental biology*. 31:20-29.

Grant, B.D., and J.G. Donaldson. 2009. Pathways and mechanisms of endocytic recycling. *Nature reviews. Molecular cell biology*. 10:597-608.

Gupton, S.L., and F.B. Gertler. 2007. Filopodia: the fingers that do the walking. *Science's STKE : signal transduction knowledge environment*. 2007:re5.

Ha, H.Y., H.B. Moon, M.S. Nam, J.W. Lee, Z.Y. Ryoo, T.H. Lee, K.K. Lee, B.J. So, H. Sato, M. Seiki, and D.Y. Yu. 2001. Overexpression of membrane-type matrix metalloproteinase-1 gene induces mammary gland abnormalities and adenocarcinoma in transgenic mice. *Cancer research*. 61:984-990.

Hammond, J.W., K. Griffin, G.T. Jih, J. Stuckey, and K.J. Verhey. 2008. Co-operative versus independent transport of different cargoes by Kinesin-1. *Traffic*. 9:725-741.

Hashimoto, A., S. Hashimoto, R. Ando, K. Noda, E. Ogawa, H. Kotani, M. Hirose, T. Menju, M. Morishige, T. Manabe, Y. Toda, S. Ishida, and H. Sabe. 2011. GEP100-Arf6-AMAP1-cortactin pathway frequently used in cancer invasion is activated by VEGFR2 to promote angiogenesis. *PloS one*. 6:e23359.

Hashimoto, S., A. Hashimoto, A. Yamada, Y. Onodera, and H. Sabe. 2005. Assays and properties of the ArfGAPs, AMAP1 and AMAP2, in Arf6 function. *Methods in enzymology*. 404:216-231.

Hashimoto, S., Y. Onodera, A. Hashimoto, M. Tanaka, M. Hamaguchi, A. Yamada, and H. Sabe. 2004. Requirement for Arf6 in breast cancer invasive activities. *Proceedings of the National Academy of Sciences of the United States of America*. 101:6647-6652.

Hauck, C.R., D.A. Hsia, D. Ilic, and D.D. Schlaepfer. 2002. v-Src SH3-enhanced interaction with focal adhesion kinase at beta 1 integrin-containing invadopodia promotes cell invasion. *The Journal of biological chemistry*. 277:12487-12490.

Heasman, S.J., and A.J. Ridley. 2008. Mammalian Rho GTPases: new insights into their functions from in vivo studies. *Nature reviews. Molecular cell biology*. 9:690-701.

Hertzog, M., and P. Chavrier. 2011. Cell polarity during motile processes: keeping on track with the exocyst complex. *The Biochemical journal*. 433:403-409.

Hilpela, P., M.K. Vartiainen, and P. Lappalainen. 2004. Regulation of the actin cytoskeleton by PI(4,5)P2 and PI(3,4,5)P3. *Current topics in microbiology and immunology*. 282:117-163.

Hirai, S., A. Kawaguchi, R. Hirasawa, M. Baba, T. Ohnishi, and S. Ohno. 2002. MAPK-upstream protein kinase (MUK) regulates the radial migration of immature neurons in telencephalon of mouse embryo. *Development*. 129:4483-4495.

Hirokawa, N., Y. Noda, Y. Tanaka, and S. Niwa. 2009. Kinesin superfamily motor proteins and intracellular transport. *Nature reviews. Molecular cell biology*. 10:682-696.

Hodgson, L., F. Shen, and K. Hahn. 2010. Biosensors for characterizing the dynamics of rho family GTPases in living cells. *Current protocols in cell biology / editorial board, Juan S. Bonifacino ... [et al.]*. Chapter 14:Unit 14 11 11-26.

Holmbeck, K., P. Bianco, J. Caterina, S. Yamada, M. Kromer, S.A. Kuznetsov, M. Mankani, P.G. Robey, A.R. Poole, I. Pidoux, J.M. Ward, and H. Birkedal-Hansen. 1999. MT1-MMP-deficient mice develop dwarfism, osteopenia, arthritis, and connective tissue disease due to inadequate collagen turnover. *Cell*. 99:81-92.

Honda, A., M. Nogami, T. Yokozeki, M. Yamazaki, H. Nakamura, H. Watanabe, K. Kawamoto, K. Nakayama, A.J. Morris, M.A. Frohman, and Y. Kanaho. 1999. Phosphatidylinositol 4-phosphate 5-kinase alpha is a downstream effector of the small G protein ARF6 in membrane ruffle formation. *Cell*. 99:521-532.

Horiuchi, D., C.A. Collins, P. Bhat, R.V. Barkus, A. Diantonio, and W.M. Saxton. 2007. Control of a kinesin-cargo linkage mechanism by JNK pathway kinases. *Current biology : CB*. 17:1313-1317.

Hotary, K., X.Y. Li, E. Allen, S.L. Stevens, and S.J. Weiss. 2006. A cancer cell metalloprotease triad regulates the basement membrane transmigration program. *Genes & development*. 20:2673-2686.

Hotary, K.B., E.D. Allen, P.C. Brooks, N.S. Datta, M.W. Long, and S.J. Weiss. 2003. Membrane type I matrix metalloproteinase usurps tumor growth control imposed by the three-dimensional extracellular matrix. *Cell*. 114:33-45.

Houndolo, T., P.L. Boulay, and A. Claing. 2005. G protein-coupled receptor endocytosis in ADP-ribosylation factor 6-depleted cells. *The Journal of biological chemistry*. 280:5598-5604.

Hu, B., B. Shi, M.J. Jarzynka, J.J. Yiin, C. D'Souza-Schorey, and S.Y. Cheng. 2009. ADP-ribosylation factor 6 regulates glioma cell invasion through the IQ-domain GTPase-activating protein 1-Rac1-mediated pathway. *Cancer research*. 69:794-801.

Hu, J., A. Mukhopadhyay, P. Truesdell, H. Chander, U.K. Mukhopadhyay, A.S. Mak, and A.W. Craig. 2011. Cdc42-interacting protein 4 is a Src substrate that regulates invadopodia and invasiveness of breast tumors by promoting MT1-MMP endocytosis. *Journal of cell science*. 124:1739-1751.

Huang, C., Z. Rajfur, C. Borchers, M.D. Schaller, and K. Jacobson. 2003. JNK phosphorylates paxillin and regulates cell migration. *Nature*. 424:219-223.

Huang, P., Y.M. Altshuller, J.C. Hou, J.E. Pessin, and M.A. Frohman. 2005. Insulin-stimulated plasma membrane fusion of Glut4 glucose transporter-containing vesicles is regulated by phospholipase D1. *Molecular biology of the cell*. 16:2614-2623.

Huang, S.H., S. Duan, T. Sun, J. Wang, L. Zhao, Z. Geng, J. Yan, H.J. Sun, and Z.Y. Chen. 2011. JIP3 mediates TrkB axonal anterograde transport and enhances BDNF signaling by directly bridging TrkB with kinesin-1. *The Journal of neuroscience : the official journal of the Society for Neuroscience*. 31:10602-10614.

Humphreys, D., A. Davidson, P.J. Hume, and V. Koronakis. 2012. Salmonella virulence effector SopE and Host GEF ARNO cooperate to recruit and activate WAVE to trigger bacterial invasion. *Cell host & microbe*. 11:129-139.

Humphreys, D., A.C. Davidson, P.J. Hume, L.E. Makin, and V. Koronakis. 2013. Arf6 coordinates actin assembly through the WAVE complex, a mechanism usurped by Salmonella to invade host cells. *Proceedings of the National Academy of Sciences of the United States of America*. 110:16880-16885.

Huttner, W.B., and J. Zimmerberg. 2001. Implications of lipid microdomains for membrane curvature, budding and fission. *Current opinion in cell biology*. 13:478-484.

Hynes, R.O. 2002. Integrins: bidirectional, allosteric signaling machines. *Cell*. 110:673-687.

Ichetovkin, I., W. Grant, and J. Condeelis. 2002. Cofilin produces newly polymerized actin filaments that are preferred for dendritic nucleation by the Arp2/3 complex. *Current biology : CB*. 12:79-84.

Ikenouchi, J., and M. Umeda. 2010. FRMD4A regulates epithelial polarity by connecting Arf6 activation with the PAR complex. *Proceedings of the National Academy of Sciences of the United States of America*. 107:748-753.

Isabet, T., G. Montagnac, K. Regazzoni, B. Raynal, F. El Khadali, P. England, M. Franco, P. Chavrier, A. Houdusse, and J. Menetrey. 2009. The structural basis of Arf effector specificity: the crystal structure of ARF6 in a complex with JIP4. *The EMBO journal*. 28:2835-2845.

Ito, M., M. Akechi, R. Hirose, M. Ichimura, N. Takamatsu, P. Xu, Y. Nakabeppu, S. Tadayoshi, K. Yamamoto, and K. Yoshioka. 2000. Isoforms of JSAP1 scaffold protein generated through alternative splicing. *Gene*. 255:229-234.

Ito, M., K. Yoshioka, M. Akechi, S. Yamashita, N. Takamatsu, K. Sugiyama, M. Hibi, Y. Nakabeppu, T. Shiba, and K.I. Yamamoto. 1999. JSAP1, a novel jun N-terminal protein kinase (JNK)-binding protein that functions as a Scaffold factor in the JNK signaling pathway. *Molecular and cellular biology*. 19:7539-7548.

Itoh, T., M. Tanioka, H. Matsuda, H. Nishimoto, T. Yoshioka, R. Suzuki, and M. Uehira. 1999. Experimental metastasis is suppressed in MMP-9-deficient mice. *Clinical & experimental metastasis*. 17:177-181.

Itoh, T., M. Tanioka, H. Yoshida, T. Yoshioka, H. Nishimoto, and S. Itohara. 1998. Reduced angiogenesis and tumor progression in gelatinase A-deficient mice. *Cancer research*. 58:1048-1051.

Itoh, Y., and M. Seiki. 2006. MT1-MMP: a potent modifier of pericellular microenvironment. *Journal of cellular physiology*. 206:1-8.

Itoh, Y., A. Takamura, N. Ito, Y. Maru, H. Sato, N. Suenaga, T. Aoki, and M. Seiki. 2001. Homophilic complex formation of MT1-MMP facilitates proMMP-2 activation on the cell surface and promotes tumor cell invasion. *The EMBO journal*. 20:4782-4793.

Iwanaga, A., G. Wang, D. Gantulga, T. Sato, T. Baljinnyam, K. Shimizu, K. Takumi, M. Hayashi, T. Akashi, H. Fuse, K. Sugihara, M. Asano, and K. Yoshioka. 2008. Ablation of the scaffold protein JLP causes reduced fertility in male mice. *Transgenic research*. 17:1045-1058.

Jagadish, N., R. Rana, D. Mishra, M. Kumar, and A. Suri. 2005. Sperm associated antigen 9 (SPAG9): a new member of c-Jun NH2 -terminal kinase (JNK) interacting protein exclusively expressed in testis. *The Keio journal of medicine*. 54:66-71.

Jiang, A., K. Lehti, X. Wang, S.J. Weiss, J. Keski-Oja, and D. Pei. 2001. Regulation of membrane-type matrix metalloproteinase 1 activity by dynamin-mediated endocytosis. *Proceedings of the National Academy of Sciences of the United States of America*. 98:13693-13698.

Jiang, W.G., G. Davies, T.A. Martin, C. Parr, G. Watkins, M.D. Mason, and R.E. Mansel. 2006. Expression of membrane type-1 matrix metalloproteinase, MT1-MMP in human breast cancer and its impact on invasiveness of breast cancer cells. *International journal of molecular medicine*. 17:583-590.

Johansson, M., N. Rocha, W. Zwart, I. Jordens, L. Janssen, C. Kuijl, V.M. Olkkonen, and J. Neefjes. 2007. Activation of endosomal dynein motors by stepwise assembly of Rab7-RILP-p150Glued, ORP1L, and the receptor betalll spectrin. *The Journal of cell biology*. 176:459-471.

Jovanovic, O.A., F.D. Brown, and J.G. Donaldson. 2006. An effector domain mutant of Arf6 implicates phospholipase D in endosomal membrane recycling. *Molecular biology of the cell*. 17:327-335.

Jovic, M., M. Sharma, J. Rahajeng, and S. Caplan. 2010. The early endosome: a busy sorting station for proteins at the crossroads. *Histology and histopathology*. 25:99-112.

Kahn, R.A., and A.G. Gilman. 1984. Purification of a protein cofactor required for ADP-ribosylation of the stimulatory regulatory component of adenylate cyclase by cholera toxin. *The Journal of biological chemistry*. 259:6228-6234.

Kahn, R.A., and A.G. Gilman. 1986. The protein cofactor necessary for ADP-ribosylation of Gs by cholera toxin is itself a GTP binding protein. *The Journal of biological chemistry*. 261:7906-7911.

Kalluri, R. 2003. Basement membranes: structure, assembly and role in tumour angiogenesis. *Nature reviews. Cancer*. 3:422-433.

Kang, J.S., G.U. Bae, M.J. Yi, Y.J. Yang, J.E. Oh, G. Takaesu, Y.T. Zhou, B.C. Low, and R.S. Krauss. 2008. A Cdo-Bnip-2-Cdc42 signaling pathway regulates p38alpha/beta MAPK activity and myogenic differentiation. *The Journal of cell biology*. 182:497-507.

Kanojia, D., M. Garg, S. Gupta, A. Gupta, and A. Suri. 2009. Sperm-associated antigen 9, a novel biomarker for early detection of breast cancer. *Cancer epidemiology, biomarkers & prevention : a publication of the American Association for Cancer Research, cosponsored by the American Society of Preventive Oncology*. 18:630-639.

Kanojia, D., M. Garg, S. Gupta, A. Gupta, and A. Suri. 2011. Sperm-associated antigen 9 is a novel biomarker for colorectal cancer and is involved in tumor growth and tumorigenicity. *The American journal of pathology*. 178:1009-1020.

Kardon, J.R., S.L. Reck-Peterson, and R.D. Vale. 2009. Regulation of the processivity and intracellular localization of Saccharomyces cerevisiae dynein by dynactin. *Proceedings of the National Academy of Sciences of the United States of America*. 106:5669-5674.

Kardon, J.R., and R.D. Vale. 2009. Regulators of the cytoplasmic dynein motor. *Nature reviews. Molecular cell biology*. 10:854-865.

Kean, M.J., K.C. Williams, M. Skalski, D. Myers, A. Burtnik, D. Foster, and M.G. Coppolino. 2009. VAMP3, syntaxin-13 and SNAP23 are involved in secretion of matrix metalloproteinases, degradation of the extracellular matrix and cell invasion. *Journal of cell science*. 122:4089-4098.

Kelkar, N., M.H. Delmotte, C.R. Weston, T. Barrett, B.J. Sheppard, R.A. Flavell, and R.J. Davis. 2003. Morphogenesis of the telencephalic commissure requires scaffold protein JNK-interacting protein 3 (JIP3). *Proceedings of the National Academy of Sciences of the United States of America*. 100:9843-9848.

Kelkar, N., S. Gupta, M. Dickens, and R.J. Davis. 2000. Interaction of a mitogen-activated protein kinase signaling module with the neuronal protein JIP3. *Molecular and cellular biology*. 20:1030-1043.

Kelkar, N., C.L. Standen, and R.J. Davis. 2005. Role of the JIP4 scaffold protein in the regulation of mitogen-activated protein kinase signaling pathways. *Molecular and cellular biology*. 25:2733-2743.

Kessenbrock, K., V. Plaks, and Z. Werb. 2010. Matrix metalloproteinases: regulators of the tumor microenvironment. *Cell*. 141:52-67.

Khokha, R., A. Murthy, and A. Weiss. 2013. Metalloproteinases and their natural inhibitors in inflammation and immunity. *Nature reviews. Immunology*. 13:649-665.

Kim, D.J., L.A. Martinez-Lemus, and G.E. Davis. 2013. EB1, p150Glued, and Clasp1 control endothelial tubulogenesis through microtubule assembly, acetylation, and apical polarization. *Blood*. 121:3521-3530.

Kinoshita, T., H. Sato, A. Okada, E. Ohuchi, K. Imai, Y. Okada, and M. Seiki. 1998. TIMP-2 promotes activation of progelatinase A by membrane-type 1 matrix metalloproteinase immobilized on agarose beads. *The Journal of biological chemistry*. 273:16098-16103.

Klein, S., M. Franco, P. Chardin, and F. Luton. 2006. Role of the Arf6 GDP/GTP cycle and Arf6 GTPase-activating proteins in actin remodeling and intracellular transport. *The Journal of biological chemistry*. 281:12352-12361.

Knauper, V., H. Will, C. Lopez-Otin, B. Smith, S.J. Atkinson, H. Stanton, R.M. Hembry, and G. Murphy. 1996. Cellular mechanisms for human procollagenase-3 (MMP-13) activation. Evidence that MT1-MMP (MMP-14) and gelatinase a (MMP-2) are able to generate active enzyme. *The Journal of biological chemistry*. 271:17124-17131.

Kobayashi, H., and M. Fukuda. 2012. Rab35 regulates Arf6 activity through centaurin-beta2 (ACAP2) during neurite outgrowth. *Journal of cell science*. 125:2235-2243.

Koo, T.H., B.A. Eipper, and J.G. Donaldson. 2007. Arf6 recruits the Rac GEF Kalirin to the plasma membrane facilitating Rac activation. *BMC cell biology*. 8:29.

Koronakis, V., P.J. Hume, D. Humphreys, T. Liu, O. Horning, O.N. Jensen, and E.J. McGhie. 2011. WAVE regulatory complex activation by cooperating GTPases Arf and Rac1. *Proceedings of the National Academy of Sciences of the United States of America*. 108:14449-14454.

Kowalski, J.R., C. Egile, S. Gil, S.B. Snapper, R. Li, and S.M. Thomas. 2005. Cortactin regulates cell migration through activation of N-WASP. *Journal of cell science*. 118:79-87.

Krauss, M., M. Kinuta, M.R. Wenk, P. De Camilli, K. Takei, and V. Haucke. 2003. ARF6 stimulates clathrin/AP-2 recruitment to synaptic membranes by activating phosphatidylinositol phosphate kinase type Igamma. *The Journal of cell biology*. 162:113-124.

Krauss, R.S., F. Cole, U. Gaio, G. Takaesu, W. Zhang, and J.S. Kang. 2005. Close encounters: regulation of vertebrate skeletal myogenesis by cell-cell contact. *Journal of cell science*. 118:2355-2362.

Labrecque, L., C. Nyalendo, S. Langlois, Y. Durocher, C. Roghi, G. Murphy, D. Gingras, and R. Beliveau. 2004. Src-mediated tyrosine phosphorylation of caveolin-1 induces its association with membrane type 1 matrix metalloproteinase. *The Journal of biological chemistry*. 279:52132-52140.

Lafleur, M.A., F.A. Mercuri, N. Ruangpanit, M. Seiki, H. Sato, and E.W. Thompson. 2006. Type I collagen abrogates the clathrin-mediated internalization of membrane type 1 matrix metalloproteinase (MT1-MMP) via the MT1-MMP hemopexin domain. *The Journal of biological chemistry*. 281:6826-6840.

Le, T.L., A.S. Yap, and J.L. Stow. 1999. Recycling of E-cadherin: a potential mechanism for regulating cadherin dynamics. *The Journal of cell biology*. 146:219-232.

Lebensohn, A.M., and M.W. Kirschner. 2009. Activation of the WAVE complex by coincident signals controls actin assembly. *Molecular cell*. 36:512-524.

Lee, C.M., D. Onesime, C.D. Reddy, N. Dhanasekaran, and E.P. Reddy. 2002. JLP: A scaffolding protein that tethers JNK/p38MAPK signaling modules and transcription factors. *Proceedings of the National Academy of Sciences of the United States of America*. 99:14189-14194.

Li, A., J.C. Dawson, M. Forero-Vargas, H.J. Spence, X. Yu, I. Konig, K. Anderson, and L.M. Machesky. 2010. The actin-bundling protein fascin stabilizes actin in invadopodia and potentiates protrusive invasion. *Current biology : CB*. 20:339-345.

Li, J., B.A. Ballif, A.M. Powelka, J. Dai, S.P. Gygi, and V.W. Hsu. 2005. Phosphorylation of ACAP1 by Akt regulates the stimulation-dependent recycling of integrin beta1 to control cell migration. *Developmental cell*. 9:663-673.

Li, J., P.J. Peters, M. Bai, J. Dai, E. Bos, T. Kirchhausen, K.V. Kandror, and V.W. Hsu. 2007. An ACAP1-containing clathrin coat complex for endocytic recycling. *The Journal of cell biology*. 178:453-464.

Li, M., S.S. Ng, J. Wang, L. Lai, S.Y. Leung, M. Franco, Y. Peng, M.L. He, H.F. Kung, and M.C. Lin. 2006. EFA6A enhances glioma cell invasion through ADP ribosylation factor 6/extracellular signal-regulated kinase signaling. *Cancer research*. 66:1583-1590.

Li, M., J. Wang, S.S. Ng, C.Y. Chan, M.L. He, F. Yu, L. Lai, C. Shi, Y. Chen, D.T. Yew, H.F. Kung, and M.C. Lin. 2009. Adenosine diphosphate-ribosylation factor 6 is required for epidermal growth factor-induced glioblastoma cell proliferation. *Cancer*. 115:4959-4972.

Li, X.Y., I. Ota, I. Yana, F. Sabeh, and S.J. Weiss. 2008. Molecular dissection of the structural machinery underlying the tissue-invasive activity of membrane type-1 matrix metalloproteinase. *Molecular biology of the cell*. 19:3221-3233.

Linder, S. 2009. Invadosomes at a glance. *Journal of cell science*. 122:3009-3013.

Lizarraga, F., R. Poincloux, M. Romao, G. Montagnac, G. Le Dez, I. Bonne, G. Rigaill, G. Raposo, and P. Chavrier. 2009. Diaphanous-related formins are required for invadopodia formation and invasion of breast tumor cells. *Cancer research*. 69:2792-2800.

Lorenz, M., H. Yamaguchi, Y. Wang, R.H. Singer, and J. Condeelis. 2004. Imaging sites of N-wasp activity in lamellipodia and invadopodia of carcinoma cells. *Current biology : CB*. 14:697-703.

Lundmark, R., G.J. Doherty, Y. Vallis, B.J. Peter, and H.T. McMahon. 2008. Arf family GTP loading is activated by, and generates, positive membrane curvature. *The Biochemical journal*. 414:189-194.

Lupas, A. 1996. Coiled coils: new structures and new functions. *Trends in biochemical sciences*. 21:375-382.

Machesky, L.M., and A. Li. 2010. Fascin: Invasive filopodia promoting metastasis. *Communicative & integrative biology*. 3:263-270.

Macia, E., M. Partisani, O. Paleotti, F. Luton, and M. Franco. 2012. Arf6 negatively controls the rapid recycling of the beta2 adrenergic receptor. *Journal of cell science*. 125:4026-4035.

Mader, C.C., M. Oser, M.A. Magalhaes, J.J. Bravo-Cordero, J. Condeelis, A.J. Koleske, and H. Gil-Henn. 2011. An EGFR-Src-Arg-cortactin pathway mediates functional maturation of invadopodia and breast cancer cell invasion. *Cancer research*. 71:1730-1741.

Magkou, C., L. Nakopoulou, C. Zoubouli, K. Karali, I. Theohari, P. Bakarakos, and I. Giannopoulou. 2008. Expression of the epidermal growth factor receptor (EGFR) and the phosphorylated EGFR in invasive breast carcinomas. *Breast cancer research : BCR*. 10:R49.

Massenburg, D., J.S. Han, M. Liyanage, W.A. Patton, S.G. Rhee, J. Moss, and M. Vaughan. 1994. Activation of rat brain phospholipase D by ADP-ribosylation factors 1,5, and 6: separation of ADP-ribosylation factor-dependent and oleate-dependent enzymes. *Proceedings of the National Academy of Sciences of the United States of America*. 91:11718-11722.

Mazzone, M., M. Baldassarre, G. Beznoussenko, G. Giacchetti, J. Cao, S. Zucker, A. Luini, and R. Buccione. 2004. Intracellular processing and activation of membrane type 1 matrix metalloprotease depends on its partitioning into lipid domains. *Journal of cell science*. 117:6275-6287.

McKenney, R.J., W. Huynh, M.E. Tanenbaum, G. Bhabha, and R.D. Vale. 2014. Activation of cytoplasmic dynein motility by dynactin-cargo adapter complexes. *Science*. 345:337-341.

McMahon, H.T., and E. Boucrot. 2011. Molecular mechanism and physiological functions of clathrin-mediated endocytosis. *Nature reviews. Molecular cell biology*. 12:517-533.

Menetrey, J., E. Macia, S. Pasqualato, M. Franco, and J. Cherfils. 2000. Structure of Arf6-GDP suggests a basis for guanine nucleotide exchange factors specificity. *Nature structural biology*. 7:466-469.

Meyer, D., A. Liu, and B. Margolis. 1999. Interaction of c-Jun amino-terminal kinase interacting protein-1 with p190 rhoGEF and its localization in differentiated neurons. *The Journal of biological chemistry*. 274:35113-35118.

Miki, H., K. Miura, and T. Takenawa. 1996. N-WASP, a novel actin-depolymerizing protein, regulates the cortical cytoskeletal rearrangement in a PIP2-dependent manner downstream of tyrosine kinases. *The EMBO journal*. 15:5326-5335.

Mitra, S.K., and D.D. Schlaepfer. 2006. Integrin-regulated FAK-Src signaling in normal and cancer cells. *Current opinion in cell biology*. 18:516-523.

Miyata, T., H. Ohnishi, J. Suzuki, Y. Yoshikumi, H. Ohno, H. Mashima, H. Yasuda, T. Ishijima, H. Osawa, K. Satoh, K. Sunada, H. Kita, H. Yamamoto, and K. Sugano. 2004. Involvement of syntaxin 4 in the transport of membrane-type 1 matrix metalloproteinase to the plasma membrane in human gastric epithelial cells. *Biochemical and biophysical research communications*. 323:118-124.

Montagnac, G., H. de Forges, E. Smythe, C. Gueudry, M. Romao, J. Salamero, and P. Chavrier. 2011. Decoupling of activation and effector binding underlies ARF6 priming of fast endocytic recycling. *Current biology : CB*. 21:574-579.

Montagnac, G., A. Echard, and P. Chavrier. 2008. Endocytic traffic in animal cell cytokinesis. *Current opinion in cell biology*. 20:454-461.

Montagnac, G., V. Meas-Yedid, M. Irondelle, A. Castro-Castro, M. Franco, T. Shida, M.V. Nachury, A. Benmerah, J.C. Olivo-Marin, and P. Chavrier. 2013. alphaTAT1 catalyses microtubule acetylation at clathrin-coated pits. *Nature*. 502:567-570.

Montagnac, G., J.B. Sibarita, S. Loubery, L. Daviet, M. Romao, G. Raposo, and P. Chavrier. 2009. ARF6 Interacts with JIP4 to control a motor switch mechanism regulating endosome traffic in cytokinesis. *Current biology : CB*. 19:184-195.

Monteiro, P., C. Rosse, A. Castro-Castro, M. Irondelle, E. Lagoutte, P. Paul-Gilloteaux, C. Desnos, E. Formstecher, F. Darchen, D. Perrais, A. Gautreau, M. Hertzog, and P. Chavrier. 2013. Endosomal WASH and exocyst complexes control exocytosis of MT1-MMP at invadopodia. *The Journal of cell biology*. 203:1063-1079.

Moore, C.A., S.K. Milano, and J.L. Benovic. 2007. Regulation of receptor trafficking by GRKs and arrestins. *Annual review of physiology*. 69:451-482.

Morgan, M.R., H. Hamidi, M.D. Bass, S. Warwood, C. Ballestrem, and M.J. Humphries. 2013. Syndecan-4 phosphorylation is a control point for integrin recycling. *Developmental cell*. 24:472-485.

Morgan, M.R., M.J. Humphries, and M.D. Bass. 2007. Synergistic control of cell adhesion by integrins and syndecans. *Nature reviews. Molecular cell biology*. 8:957-969.

Morishige, M., S. Hashimoto, E. Ogawa, Y. Toda, H. Kotani, M. Hirose, S. Wei, A. Hashimoto, A. Yamada, H. Yano, Y. Mazaki, H. Kodama, Y. Nio, T. Manabe, H. Wada, H. Kobayashi, and H. Sabe. 2008. GEP100 links epidermal growth factor receptor signalling to Arf6 activation to induce breast cancer invasion. *Nature cell biology*. 10:85-92.

Mueller, S.C., and W.T. Chen. 1991. Cellular invasion into matrix beads: localization of beta 1 integrins and fibronectin to the invadopodia. *Journal of cell science*. 99 (Pt 2):213-225.

Mukherjee, S., V.V. Gurevich, J.C. Jones, J.E. Casanova, S.R. Frank, E.T. Maizels, M.F. Bader, R.A. Kahn, K. Palczewski, K. Aktories, and M. Hunzicker-Dunn. 2000. The ADP ribosylation factor nucleotide exchange factor ARNO promotes beta-arrestin release necessary for luteinizing hormone/choriogonadotropin receptor desensitization. *Proceedings of the National Academy of Sciences of the United States of America*. 97:5901-5906.

Muller, P.A., P.T. Caswell, B. Doyle, M.P. Iwanicki, E.H. Tan, S. Karim, N. Lukashchuk, D.A. Gillespie, R.L. Ludwig, P. Gosselin, A. Cromer, J.S. Brugge, O.J. Sansom, J.C. Norman, and K.H. Vousden. 2009. Mutant p53 drives invasion by promoting integrin recycling. *Cell*. 139:1327-1341.

Muralidharan-Chari, V., J. Clancy, C. Plou, M. Romao, P. Chavrier, G. Raposo, and C. D'Souza-Schorey. 2009a. ARF6-regulated shedding of tumor cell-derived plasma membrane microvesicles. *Current biology : CB*. 19:1875-1885.

Muralidharan-Chari, V., H. Hoover, J. Clancy, J. Schweitzer, M.A. Suckow, V. Schroeder, F.J. Castellino, J.S. Schorey, and C. D'Souza-Schorey. 2009b. ADP-ribosylation factor 6 regulates tumorigenic and invasive properties in vivo. *Cancer research*. 69:2201-2209.

Muresan, V., M.C. Stankewich, W. Steffen, J.S. Morrow, E.L. Holzbaur, and B.J. Schnapp. 2001. Dynactin-dependent, dynein-driven vesicle transport in the absence of membrane proteins: a role for spectrin and acidic phospholipids. *Molecular cell*. 7:173-183.

Murphy, D.A., and S.A. Courtneidge. 2011. The 'ins' and 'outs' of podosomes and invadopodia: characteristics, formation and function. *Nature reviews. Molecular cell biology*. 12:413-426.

Murtagh, J.J., Jr., M.R. Mowatt, C.M. Lee, F.J. Lee, K. Mishima, T.E. Nash, J. Moss, and M. Vaughan. 1992. Guanine nucleotide-binding proteins in the intestinal parasite Giardia

lamblia. Isolation of a gene encoding an approximately 20-kDa ADP-ribosylation factor. *The Journal of biological chemistry*. 267:9654-9662.
Nakahara, H., S.C. Mueller, M. Nomizu, Y. Yamada, Y. Yeh, and W.T. Chen. 1998. Activation of beta1 integrin signaling stimulates tyrosine phosphorylation of p190RhoGAP and membrane-protrusive activities at invadopodia. *The Journal of biological chemistry*. 273:9-12.
Naslavsky, N., R. Weigert, and J.G. Donaldson. 2003. Convergence of non-clathrin- and clathrin-derived endosomes involves Arf6 inactivation and changes in phosphoinositides. *Molecular biology of the cell*. 14:417-431.
Naslavsky, N., R. Weigert, and J.G. Donaldson. 2004. Characterization of a nonclathrin endocytic pathway: membrane cargo and lipid requirements. *Molecular biology of the cell*. 15:3542-3552.
Nguyen, Q., C.M. Lee, A. Le, and E.P. Reddy. 2005. JLP associates with kinesin light chain 1 through a novel leucine zipper-like domain. *The Journal of biological chemistry*. 280:30185-30191.
Nishiya, N., W.B. Kiosses, J. Han, and M.H. Ginsberg. 2005. An alpha4 integrin-paxillin-Arf-GAP complex restricts Rac activation to the leading edge of migrating cells. *Nature cell biology*. 7:343-352.
Noritake, J., T. Watanabe, K. Sato, S. Wang, and K. Kaibuchi. 2005. IQGAP1: a key regulator of adhesion and migration. *Journal of cell science*. 118:2085-2092.
Nurnberg, A., T. Kitzing, and R. Grosse. 2011. Nucleating actin for invasion. *Nature reviews. Cancer*. 11:177-187.
Nyalendo, C., E. Beaulieu, H. Sartelet, M. Michaud, N. Fontaine, D. Gingras, and R. Beliveau. 2008. Impaired tyrosine phosphorylation of membrane type 1-matrix metalloproteinase reduces tumor cell proliferation in three-dimensional matrices and abrogates tumor growth in mice. *Carcinogenesis*. 29:1655-1664.
Nyalendo, C., M. Michaud, E. Beaulieu, C. Roghi, G. Murphy, D. Gingras, and R. Beliveau. 2007. Src-dependent phosphorylation of membrane type I matrix metalloproteinase on cytoplasmic tyrosine 573: role in endothelial and tumor cell migration. *The Journal of biological chemistry*. 282:15690-15699.
Nyalendo, C., H. Sartelet, D. Gingras, and R. Beliveau. 2010. Inhibition of membrane-type 1 matrix metalloproteinase tyrosine phosphorylation blocks tumor progression in mice. *Anticancer research*. 30:1887-1895.
Ohuchi, E., K. Imai, Y. Fujii, H. Sato, M. Seiki, and Y. Okada. 1997. Membrane type 1 matrix metalloproteinase digests interstitial collagens and other extracellular matrix macromolecules. *The Journal of biological chemistry*. 272:2446-2451.
Oikawa, T., T. Itoh, and T. Takenawa. 2008. Sequential signals toward podosome formation in NIH-src cells. *The Journal of cell biology*. 182:157-169.
Onodera, Y., S. Hashimoto, A. Hashimoto, M. Morishige, Y. Mazaki, A. Yamada, E. Ogawa, M. Adachi, T. Sakurai, T. Manabe, H. Wada, N. Matsuura, and H. Sabe. 2005. Expression of AMAP1, an ArfGAP, provides novel targets to inhibit breast cancer invasive activities. *The EMBO journal*. 24:963-973.
Onodera, Y., J.M. Nam, A. Hashimoto, J.C. Norman, H. Shirato, S. Hashimoto, and H. Sabe. 2012. Rab5c promotes AMAP1-PRKD2 complex formation to enhance beta1 integrin recycling in EGF-induced cancer invasion. *The Journal of cell biology*. 197:983-996.
Oser, M., C.C. Mader, H. Gil-Henn, M. Magalhaes, J.J. Bravo-Cordero, A.J. Koleske, and J. Condeelis. 2010. Specific tyrosine phosphorylation sites on cortactin regulate Nck1-dependent actin polymerization in invadopodia. *Journal of cell science*. 123:3662-3673.
Oser, M., H. Yamaguchi, C.C. Mader, J.J. Bravo-Cordero, M. Arias, X. Chen, V. Desmarais, J. van Rheenen, A.J. Koleske, and J. Condeelis. 2009. Cortactin regulates cofilin and N-WASp

activities to control the stages of invadopodium assembly and maturation. *The Journal of cell biology*. 186:571-587.
Osmani, N., F. Peglion, P. Chavrier, and S. Etienne-Manneville. 2010. Cdc42 localization and cell polarity depend on membrane traffic. *The Journal of cell biology*. 191:1261-1269.
Padron, D., R.D. Tall, and M.G. Roth. 2006. Phospholipase D2 is required for efficient endocytic recycling of transferrin receptors. *Molecular biology of the cell*. 17:598-606.
Page-McCaw, A., A.J. Ewald, and Z. Werb. 2007. Matrix metalloproteinases and the regulation of tissue remodelling. *Nature reviews. Molecular cell biology*. 8:221-233.
Palacios, F., and C. D'Souza-Schorey. 2003. Modulation of Rac1 and ARF6 activation during epithelial cell scattering. *The Journal of biological chemistry*. 278:17395-17400.
Palacios, F., L. Price, J. Schweitzer, J.G. Collard, and C. D'Souza-Schorey. 2001. An essential role for ARF6-regulated membrane traffic in adherens junction turnover and epithelial cell migration. *The EMBO journal*. 20:4973-4986.
Palacios, F., J.K. Schweitzer, R.L. Boshans, and C. D'Souza-Schorey. 2002. ARF6-GTP recruits Nm23-H1 to facilitate dynamin-mediated endocytosis during adherens junctions disassembly. *Nature cell biology*. 4:929-936.
Palacios, F., J.S. Tushir, Y. Fujita, and C. D'Souza-Schorey. 2005. Lysosomal targeting of E-cadherin: a unique mechanism for the down-regulation of cell-cell adhesion during epithelial to mesenchymal transitions. *Molecular and cellular biology*. 25:389-402.
Palamidessi, A., E. Frittoli, M. Garre, M. Faretta, M. Mione, I. Testa, A. Diaspro, L. Lanzetti, G. Scita, and P.P. Di Fiore. 2008. Endocytic trafficking of Rac is required for the spatial restriction of signaling in cell migration. *Cell*. 134:135-147.
Paleotti, O., E. Macia, F. Luton, S. Klein, M. Partisani, P. Chardin, T. Kirchhausen, and M. Franco. 2005. The small G-protein Arf6GTP recruits the AP-2 adaptor complex to membranes. *The Journal of biological chemistry*. 280:21661-21666.
Pandey, P.R., J. Saidou, and K. Watabe. 2010. Role of myoepithelial cells in breast tumor progression. *Front Biosci (Landmark Ed)*. 15:226-236.
Parachoniak, C.A., Y. Luo, J.V. Abella, J.H. Keen, and M. Park. 2011. GGA3 functions as a switch to promote Met receptor recycling, essential for sustained ERK and cell migration. *Developmental cell*. 20:751-763.
Parton, R.G., and K. Simons. 2007. The multiple faces of caveolae. *Nature reviews. Molecular cell biology*. 8:185-194.
Pasqualato, S., J. Menetrey, M. Franco, and J. Cherfils. 2001. The structural GDP/GTP cycle of human Arf6. *EMBO reports*. 2:234-238.
Pasqualato, S., L. Renault, and J. Cherfils. 2002. Arf, Arl, Arp and Sar proteins: a family of GTP-binding proteins with a structural device for 'front-back' communication. *EMBO reports*. 3:1035-1041.
Perentes, J.Y., N.D. Kirkpatrick, S. Nagano, E.Y. Smith, C.M. Shaver, D. Sgroi, I. Garkavtsev, L.L. Munn, R.K. Jain, and Y. Boucher. 2011. Cancer cell-associated MT1-MMP promotes blood vessel invasion and distant metastasis in triple-negative mammary tumors. *Cancer research*. 71:4527-4538.
Peschard, P., and M. Park. 2007. From Tpr-Met to Met, tumorigenesis and tubes. *Oncogene*. 26:1276-1285.
Peters, P.J., V.W. Hsu, C.E. Ooi, D. Finazzi, S.B. Teal, V. Oorschot, J.G. Donaldson, and R.D. Klausner. 1995. Overexpression of wild-type and mutant ARF1 and ARF6: distinct perturbations of nonoverlapping membrane compartments. *The Journal of cell biology*. 128:1003-1017.
Philippar, U., E.T. Roussos, M. Oser, H. Yamaguchi, H.D. Kim, S. Giampieri, Y. Wang, S. Goswami, J.B. Wyckoff, D.A. Lauffenburger, E. Sahai, J.S. Condeelis, and F.B. Gertler. 2008. A Mena invasion isoform potentiates EGF-induced carcinoma cell invasion and metastasis. *Developmental cell*. 15:813-828.

Piper, R.C., and D.J. Katzmann. 2007. Biogenesis and function of multivesicular bodies. *Annual review of cell and developmental biology*. 23:519-547.

Poincloux, R., F. Lizarraga, and P. Chavrier. 2009. Matrix invasion by tumour cells: a focus on MT1-MMP trafficking to invadopodia. *Journal of cell science*. 122:3015-3024.

Powelka, A.M., J. Sun, J. Li, M. Gao, L.M. Shaw, A. Sonnenberg, and V.W. Hsu. 2004. Stimulation-dependent recycling of integrin beta1 regulated by ARF6 and Rab11. *Traffic*. 5:20-36.

Prat, A., M.C. Cheang, M. Martin, J.S. Parker, E. Carrasco, R. Caballero, S. Tyldesley, K. Gelmon, P.S. Bernard, T.O. Nielsen, and C.M. Perou. 2013. Prognostic significance of progesterone receptor-positive tumor cells within immunohistochemically defined luminal A breast cancer. *J Clin Oncol*. 31:203-209.

Premont, R.T., A. Claing, N. Vitale, J.L. Freeman, J.A. Pitcher, W.A. Patton, J. Moss, M. Vaughan, and R.J. Lefkowitz. 1998. beta2-Adrenergic receptor regulation by GIT1, a G protein-coupled receptor kinase-associated ADP ribosylation factor GTPase-activating protein. *Proceedings of the National Academy of Sciences of the United States of America*. 95:14082-14087.

Prigent, M., T. Dubois, G. Raposo, V. Derrien, D. Tenza, C. Rosse, J. Camonis, and P. Chavrier. 2003. ARF6 controls post-endocytic recycling through its downstream exocyst complex effector. *The Journal of cell biology*. 163:1111-1121.

Proux-Gillardeaux, V., R. Rudge, and T. Galli. 2005. The tetanus neurotoxin-sensitive and insensitive routes to and from the plasma membrane: fast and slow pathways? *Traffic*. 6:366-373.

Puyraimond, A., R. Fridman, M. Lemesle, B. Arbeille, and S. Menashi. 2001. MMP-2 colocalizes with caveolae on the surface of endothelial cells. *Experimental cell research*. 262:28-36.

Radhakrishna, H., O. Al-Awar, Z. Khachikian, and J.G. Donaldson. 1999. ARF6 requirement for Rac ruffling suggests a role for membrane trafficking in cortical actin rearrangements. *Journal of cell science*. 112 (Pt 6):855-866.

Radhakrishna, H., and J.G. Donaldson. 1997. ADP-ribosylation factor 6 regulates a novel plasma membrane recycling pathway. *The Journal of cell biology*. 139:49-61.

Radhakrishna, H., R.D. Klausner, and J.G. Donaldson. 1996. Aluminum fluoride stimulates surface protrusions in cells overexpressing the ARF6 GTPase. *The Journal of cell biology*. 134:935-947.

Remacle, A., G. Murphy, and C. Roghi. 2003. Membrane type I-matrix metalloproteinase (MT1-MMP) is internalised by two different pathways and is recycled to the cell surface. *Journal of cell science*. 116:3905-3916.

Remacle, A.G., D.V. Rozanov, P.C. Baciu, A.V. Chekanov, V.S. Golubkov, and A.Y. Strongin. 2005. The transmembrane domain is essential for the microtubular trafficking of membrane type-1 matrix metalloproteinase (MT1-MMP). *Journal of cell science*. 118:4975-4984.

Ridley, A.J. 2006. Rho GTPases and actin dynamics in membrane protrusions and vesicle trafficking. *Trends in cell biology*. 16:522-529.

Ridley, A.J. 2011. Life at the leading edge. *Cell*. 145:1012-1022.

Ridley, A.J., M.A. Schwartz, K. Burridge, R.A. Firtel, M.H. Ginsberg, G. Borisy, J.T. Parsons, and A.R. Horwitz. 2003. Cell migration: integrating signals from front to back. *Science*. 302:1704-1709.

Roberts, A.J., T. Kon, P.J. Knight, K. Sutoh, and S.A. Burgess. 2013. Functions and mechanics of dynein motor proteins. *Nature reviews. Molecular cell biology*. 14:713-726.

Rohatgi, R., H.Y. Ho, and M.W. Kirschner. 2000. Mechanism of N-WASP activation by CDC42 and phosphatidylinositol 4, 5-bisphosphate. *The Journal of cell biology*. 150:1299-1310.

Rohde, G., D. Wenzel, and V. Haucke. 2002. A phosphatidylinositol (4,5)-bisphosphate binding site within mu2-adaptin regulates clathrin-mediated endocytosis. *The Journal of cell biology*. 158:209-214.

Rosa-Ferreira, C., and S. Munro. 2011. Arl8 and SKIP act together to link lysosomes to kinesin-1. *Developmental cell*. 21:1171-1178.

Rosse, C., C. Lodillinsky, L. Fuhrmann, M. Nourieh, P. Monteiro, M. Irondelle, E. Lagoutte, S. Vacher, F. Waharte, P. Paul-Gilloteaux, M. Romao, L. Sengmanivong, M. Linch, J. van Lint, G. Raposo, A. Vincent-Salomon, I. Bieche, P.J. Parker, and P. Chavrier. 2014. Control of MT1-MMP transport by atypical PKC during breast-cancer progression. *Proceedings of the National Academy of Sciences of the United States of America*. 111:E1872-1879.

Sabe, H., S. Hashimoto, M. Morishige, E. Ogawa, A. Hashimoto, J.M. Nam, K. Miura, H. Yano, and Y. Onodera. 2009. The EGFR-GEP100-Arf6-AMAP1 signaling pathway specific to breast cancer invasion and metastasis. *Traffic*. 10:982-993.

Sabeh, F., I. Ota, K. Holmbeck, H. Birkedal-Hansen, P. Soloway, M. Balbin, C. Lopez-Otin, S. Shapiro, M. Inada, S. Krane, E. Allen, D. Chung, and S.J. Weiss. 2004. Tumor cell traffic through the extracellular matrix is controlled by the membrane-anchored collagenase MT1-MMP. *The Journal of cell biology*. 167:769-781.

Sabeh, F., R. Shimizu-Hirota, and S.J. Weiss. 2009. Protease-dependent versus -independent cancer cell invasion programs: three-dimensional amoeboid movement revisited. *The Journal of cell biology*. 185:11-19.

Sakamoto, R., D.T. Byrd, H.M. Brown, N. Hisamoto, K. Matsumoto, and Y. Jin. 2005. The Caenorhabditis elegans UNC-14 RUN domain protein binds to the kinesin-1 and UNC-16 complex and regulates synaptic vesicle localization. *Molecular biology of the cell*. 16:483-496.

Sakurai-Yageta, M., C. Recchi, G. Le Dez, J.B. Sibarita, L. Daviet, J. Camonis, C. D'Souza-Schorey, and P. Chavrier. 2008. The interaction of IQGAP1 with the exocyst complex is required for tumor cell invasion downstream of Cdc42 and RhoA. *The Journal of cell biology*. 181:985-998.

Santy, L.C. 2002. Characterization of a fast cycling ADP-ribosylation factor 6 mutant. *The Journal of biological chemistry*. 277:40185-40188.

Santy, L.C., and J.E. Casanova. 2001. Activation of ARF6 by ARNO stimulates epithelial cell migration through downstream activation of both Rac1 and phospholipase D. *The Journal of cell biology*. 154:599-610.

Santy, L.C., K.S. Ravichandran, and J.E. Casanova. 2005. The DOCK180/Elmo complex couples ARNO-mediated Arf6 activation to the downstream activation of Rac1. *Current biology : CB*. 15:1749-1754.

Sato, H., T. Takino, Y. Okada, J. Cao, A. Shinagawa, E. Yamamoto, and M. Seiki. 1994. A matrix metalloproteinase expressed on the surface of invasive tumour cells. *Nature*. 370:61-65.

Schoumacher, M., R.D. Goldman, D. Louvard, and D.M. Vignjevic. 2010. Actin, microtubules, and vimentin intermediate filaments cooperate for elongation of invadopodia. *The Journal of cell biology*. 189:541-556.

Schweitzer, J.K., and C. D'Souza-Schorey. 2002. Localization and activation of the ARF6 GTPase during cleavage furrow ingression and cytokinesis. *The Journal of biological chemistry*. 277:27210-27216.

Seals, D.F., E.F. Azucena, Jr., I. Pass, L. Tesfay, R. Gordon, M. Woodrow, J.H. Resau, and S.A. Courtneidge. 2005. The adaptor protein Tks5/Fish is required for podosome formation and function, and for the protease-driven invasion of cancer cells. *Cancer cell*. 7:155-165.

Shankar, S., B. Mohapatra, S. Verma, R. Selvi, N. Jagadish, and A. Suri. 2004. Isolation and characterization of a haploid germ cell specific sperm associated antigen 9 (SPAG9) from the baboon. *Molecular reproduction and development*. 69:186-193.

Sigismund, S., S. Confalonieri, A. Ciliberto, S. Polo, G. Scita, and P.P. Di Fiore. 2012. Endocytosis and signaling: cell logistics shape the eukaryotic cell plan. *Physiological reviews*. 92:273-366.

Singletary, S.E., C. Allred, P. Ashley, L.W. Bassett, D. Berry, K.I. Bland, P.I. Borgen, G.M. Clark, S.B. Edge, D.F. Hayes, L.L. Hughes, R.V. Hutter, M. Morrow, D.L. Page, A. Recht, R.L. Theriault, A. Thor, D.L. Weaver, H.S. Wieand, and F.L. Greene. 2003. Staging system for breast cancer: revisions for the 6th edition of the AJCC Cancer Staging Manual. *The Surgical clinics of North America*. 83:803-819.

Sodek, K.L., M.J. Ringuette, and T.J. Brown. 2007. MT1-MMP is the critical determinant of matrix degradation and invasion by ovarian cancer cells. *British journal of cancer*. 97:358-367.

Sorlie, T., C.M. Perou, R. Tibshirani, T. Aas, S. Geisler, H. Johnsen, T. Hastie, M.B. Eisen, M. van de Rijn, S.S. Jeffrey, T. Thorsen, H. Quist, J.C. Matese, P.O. Brown, D. Botstein, P.E. Lonning, and A.L. Borresen-Dale. 2001. Gene expression patterns of breast carcinomas distinguish tumor subclasses with clinical implications. *Proceedings of the National Academy of Sciences of the United States of America*. 98:10869-10874.

Sorlie, T., R. Tibshirani, J. Parker, T. Hastie, J.S. Marron, A. Nobel, S. Deng, H. Johnsen, R. Pesich, S. Geisler, J. Demeter, C.M. Perou, P.E. Lonning, P.O. Brown, A.L. Borresen-Dale, and D. Botstein. 2003. Repeated observation of breast tumor subtypes in independent gene expression data sets. *Proceedings of the National Academy of Sciences of the United States of America*. 100:8418-8423.

Spinardi, L., J. Rietdorf, L. Nitsch, M. Bono, C. Tacchetti, M. Way, and P.C. Marchisio. 2004. A dynamic podosome-like structure of epithelial cells. *Experimental cell research*. 295:360-374.

Steffen, A., G. Le Dez, R. Poincloux, C. Recchi, P. Nassoy, K. Rottner, T. Galli, and P. Chavrier. 2008. MT1-MMP-dependent invasion is regulated by TI-VAMP/VAMP7. *Current biology : CB*. 18:926-931.

Stenmark, H. 2009. Rab GTPases as coordinators of vesicle traffic. *Nature reviews. Molecular cell biology*. 10:513-525.

Strongin, A.Y., I. Collier, G. Bannikov, B.L. Marmer, G.A. Grant, and G.I. Goldberg. 1995. Mechanism of cell surface activation of 72-kDa type IV collagenase. Isolation of the activated form of the membrane metalloprotease. *The Journal of biological chemistry*. 270:5331-5338.

Stylli, S.S., A.H. Kaye, and P. Lock. 2008. Invadopodia: at the cutting edge of tumour invasion. *Journal of clinical neuroscience : official journal of the Neurosurgical Society of Australasia*. 15:725-737.

Stylli, S.S., T.T. Stacey, A.M. Verhagen, S.S. Xu, I. Pass, S.A. Courtneidge, and P. Lock. 2009. Nck adaptor proteins link Tks5 to invadopodia actin regulation and ECM degradation. *Journal of cell science*. 122:2727-2740.

Sun, F., C. Zhu, R. Dixit, and V. Cavalli. 2011. Sunday Driver/JIP3 binds kinesin heavy chain directly and enhances its motility. *The EMBO journal*. 30:3416-3429.

Suzuki, A., C. Arikawa, Y. Kuwahara, K. Itoh, M. Watanabe, H. Watanabe, T. Suzuki, Y. Funakoshi, H. Hasegawa, and Y. Kanaho. 2010. The scaffold protein JIP3 functions as a downstream effector of the small GTPase ARF6 to regulate neurite morphogenesis of cortical neurons. *FEBS letters*. 584:2801-2806.

Suzuki, T., Y. Kanai, T. Hara, J. Sasaki, T. Sasaki, M. Kohara, T. Maehama, C. Taya, H. Shitara, H. Yonekawa, M.A. Frohman, T. Yokozeki, and Y. Kanaho. 2006. Crucial role of the small GTPase ARF6 in hepatic cord formation during liver development. *Molecular and cellular biology*. 26:6149-6156.

Tague, S.E., V. Muralidharan, and C. D'Souza-Schorey. 2004. ADP-ribosylation factor 6 regulates tumor cell invasion through the activation of the MEK/ERK signaling pathway. *Proceedings of the National Academy of Sciences of the United States of America*. 101:9671-9676.

Takaesu, G., J.S. Kang, G.U. Bae, M.J. Yi, C.M. Lee, E.P. Reddy, and R.S. Krauss. 2006. Activation of p38alpha/beta MAPK in myogenesis via binding of the scaffold protein JLP to the cell surface protein Cdo. *The Journal of cell biology*. 175:383-388.

Takino, T., M. Nakada, H. Miyamori, Y. Watanabe, T. Sato, D. Gantulga, K. Yoshioka, K.M. Yamada, and H. Sato. 2005. JSAP1/JIP3 cooperates with focal adhesion kinase to regulate c-Jun N-terminal kinase and cell migration. *The Journal of biological chemistry*. 280:37772-37781.

Takino, T., K. Yoshioka, H. Miyamori, K.M. Yamada, and H. Sato. 2002. A scaffold protein in the c-Jun N-terminal kinase signaling pathway is associated with focal adhesion kinase and tyrosine-phosphorylated. *Oncogene*. 21:6488-6497.

Tarone, G., D. Cirillo, F.G. Giancotti, P.M. Comoglio, and P.C. Marchisio. 1985. Rous sarcoma virus-transformed fibroblasts adhere primarily at discrete protrusions of the ventral membrane called podosomes. *Experimental cell research*. 159:141-157.

Tehrani, S., N. Tomasevic, S. Weed, R. Sakowicz, and J.A. Cooper. 2007. Src phosphorylation of cortactin enhances actin assembly. *Proceedings of the National Academy of Sciences of the United States of America*. 104:11933-11938.

Teuliere, J., M.M. Faraldo, M.A. Deugnier, M. Shtutman, A. Ben-Ze'ev, J.P. Thiery, and M.A. Glukhova. 2005. Targeted activation of beta-catenin signaling in basal mammary epithelial cells affects mammary development and leads to hyperplasia. *Development*. 132:267-277.

Tolde, O., D. Rosel, P. Vesely, P. Folk, and J. Brabek. 2010. The structure of invadopodia in a complex 3D environment. *European journal of cell biology*. 89:674-680.

Tsuchiya, M., S.R. Price, S.C. Tsai, J. Moss, and M. Vaughan. 1991. Molecular identification of ADP-ribosylation factor mRNAs and their expression in mammalian cells. *The Journal of biological chemistry*. 266:2772-2777.

Tushir, J.S., J. Clancy, A. Warren, C. Wrobel, J.S. Brugge, and C. D'Souza-Schorey. 2010. Unregulated ARF6 activation in epithelial cysts generates hyperactive signaling endosomes and disrupts morphogenesis. *Molecular biology of the cell*. 21:2355-2366.

Tushir, J.S., and C. D'Souza-Schorey. 2007. ARF6-dependent activation of ERK and Rac1 modulates epithelial tubule development. *The EMBO journal*. 26:1806-1819.

Uekita, T., Y. Itoh, I. Yana, H. Ohno, and M. Seiki. 2001. Cytoplasmic tail-dependent internalization of membrane-type 1 matrix metalloproteinase is important for its invasion-promoting activity. *The Journal of cell biology*. 155:1345-1356.

Uruno, T., J. Liu, P. Zhang, Y. Fan, C. Egile, R. Li, S.C. Mueller, and X. Zhan. 2001. Activation of Arp2/3 complex-mediated actin polymerization by cortactin. *Nature cell biology*. 3:259-266.

Valastyan, S., and R.A. Weinberg. 2011. Tumor metastasis: molecular insights and evolving paradigms. *Cell*. 147:275-292.

Vallee, R.B., R.J. McKenney, and K.M. Ori-McKenney. 2012. Multiple modes of cytoplasmic dynein regulation. *Nature cell biology*. 14:224-230.

Verhey, K.J., and J.W. Hammond. 2009. Traffic control: regulation of kinesin motors. *Nature reviews. Molecular cell biology*. 10:765-777.

Verhey, K.J., D.L. Lizotte, T. Abramson, L. Barenboim, B.J. Schnapp, and T.A. Rapoport. 1998. Light chain-dependent regulation of Kinesin's interaction with microtubules. *The Journal of cell biology*. 143:1053-1066.

Verhey, K.J., D. Meyer, R. Deehan, J. Blenis, B.J. Schnapp, T.A. Rapoport, and B. Margolis. 2001. Cargo of kinesin identified as JIP scaffolding proteins and associated signaling molecules. *The Journal of cell biology*. 152:959-970.

Vitale, N., S. Chasserot-Golaz, Y. Bailly, N. Morinaga, M.A. Frohman, and M.F. Bader. 2002. Calcium-regulated exocytosis of dense-core vesicles requires the activation of ADP-

ribosylation factor (ARF)6 by ARF nucleotide binding site opener at the plasma membrane. *The Journal of cell biology*. 159:79-89.
Volpicelli-Daley, L.A., Y. Li, C.J. Zhang, and R.A. Kahn. 2005. Isoform-selective effects of the depletion of ADP-ribosylation factors 1-5 on membrane traffic. *Molecular biology of the cell*. 16:4495-4508.
Wagner, E.F., and A.R. Nebreda. 2009. Signal integration by JNK and p38 MAPK pathways in cancer development. *Nature reviews. Cancer*. 9:537-549.
Wang, X., D. Ma, J. Keski-Oja, and D. Pei. 2004. Co-recycling of MT1-MMP and MT3-MMP through the trans-Golgi network. Identification of DKV582 as a recycling signal. *The Journal of biological chemistry*. 279:9331-9336.
Wang, Y., Q. Dong, Y. Miao, L. Fu, X. Lin, and E. Wang. 2013. Clinical significance and biological roles of SPAG9 overexpression in non-small cell lung cancer. *Lung cancer*. 81:266-272.
Watanabe, T., S. Wang, J. Noritake, K. Sato, M. Fukata, M. Takefuji, M. Nakagawa, N. Izumi, T. Akiyama, and K. Kaibuchi. 2004. Interaction with IQGAP1 links APC to Rac1, Cdc42, and actin filaments during cell polarization and migration. *Developmental cell*. 7:871-883.
Watson, P., and D.J. Stephens. 2005. ER-to-Golgi transport: form and formation of vesicular and tubular carriers. *Biochimica et biophysica acta*. 1744:304-315.
Weaver, A.M., A.V. Karginov, A.W. Kinley, S.A. Weed, Y. Li, J.T. Parsons, and J.A. Cooper. 2001. Cortactin promotes and stabilizes Arp2/3-induced actin filament network formation. *Current biology : CB*. 11:370-374.
Weed, S.A., A.V. Karginov, D.A. Schafer, A.M. Weaver, A.W. Kinley, J.A. Cooper, and J.T. Parsons. 2000. Cortactin localization to sites of actin assembly in lamellipodia requires interactions with F-actin and the Arp2/3 complex. *The Journal of cell biology*. 151:29-40.
Wennerberg, K., K.L. Rossman, and C.J. Der. 2005. The Ras superfamily at a glance. *Journal of cell science*. 118:843-846.
Wertheimer, E., A. Gutierrez-Uzquiza, C. Rosemblit, C. Lopez-Haber, M.S. Sosa, and M.G. Kazanietz. 2012. Rac signaling in breast cancer: a tale of GEFs and GAPs. *Cellular signalling*. 24:353-362.
Whale, A., F.N. Hashim, S. Fram, G.E. Jones, and C.M. Wells. 2011. Signalling to cancer cell invasion through PAK family kinases. *Front Biosci (Landmark Ed)*. 16:849-864.
White, C.D., M.D. Brown, and D.B. Sacks. 2009. IQGAPs in cancer: a family of scaffold proteins underlying tumorigenesis. *FEBS letters*. 583:1817-1824.
Whitmarsh, A.J., J. Cavanagh, C. Tournier, J. Yasuda, and R.J. Davis. 1998. A mammalian scaffold complex that selectively mediates MAP kinase activation. *Science*. 281:1671-1674.
Wiesner, C., J. Faix, M. Himmel, F. Bentzien, and S. Linder. 2010. KIF5B and KIF3A/KIF3B kinesins drive MT1-MMP surface exposure, CD44 shedding, and extracellular matrix degradation in primary macrophages. *Blood*. 116:1559-1569.
Williams, K.C., and M.G. Coppolino. 2011. Phosphorylation of membrane type 1-matrix metalloproteinase (MT1-MMP) and its vesicle-associated membrane protein 7 (VAMP7)-dependent trafficking facilitate cell invasion and migration. *The Journal of biological chemistry*. 286:43405-43416.
Williams, K.C., R.E. McNeilly, and M.G. Coppolino. 2014. SNAP23, Syntaxin4, and vesicle-associated membrane protein 7 (VAMP7) mediate trafficking of membrane type 1-matrix metalloproteinase (MT1-MMP) during invadopodium formation and tumor cell invasion. *Molecular biology of the cell*. 25:2061-2070.
Willoughby, E.A., G.R. Perkins, M.K. Collins, and A.J. Whitmarsh. 2003. The JNK-interacting protein-1 scaffold protein targets MAPK phosphatase-7 to dephosphorylate JNK. *The Journal of biological chemistry*. 278:10731-10736.
Wilson, G.M., A.B. Fielding, G.C. Simon, X. Yu, P.D. Andrews, R.S. Hames, A.M. Frey, A.A. Peden, G.W. Gould, and R. Prekeris. 2005. The FIP3-Rab11 protein complex regulates recycling

endosome targeting to the cleavage furrow during late cytokinesis. *Molecular biology of the cell*. 16:849-860.

Wolf, K., I. Mazo, H. Leung, K. Engelke, U.H. von Andrian, E.I. Deryugina, A.Y. Strongin, E.B. Brocker, and P. Friedl. 2003. Compensation mechanism in tumor cell migration: mesenchymal-amoeboid transition after blocking of pericellular proteolysis. *The Journal of cell biology*. 160:267-277.

Wolf, K., M. Te Lindert, M. Krause, S. Alexander, J. Te Riet, A.L. Willis, R.M. Hoffman, C.G. Figdor, S.J. Weiss, and P. Friedl. 2013. Physical limits of cell migration: control by ECM space and nuclear deformation and tuning by proteolysis and traction force. *The Journal of cell biology*. 201:1069-1084.

Wolf, K., Y.I. Wu, Y. Liu, J. Geiger, E. Tam, C. Overall, M.S. Stack, and P. Friedl. 2007. Multi-step pericellular proteolysis controls the transition from individual to collective cancer cell invasion. *Nature cell biology*. 9:893-904.

Wolff, A.C., M.E. Hammond, J.N. Schwartz, K.L. Hagerty, D.C. Allred, R.J. Cote, M. Dowsett, P.L. Fitzgibbons, W.M. Hanna, A. Langer, L.M. McShane, S. Paik, M.D. Pegram, E.A. Perez, M.F. Press, A. Rhodes, C. Sturgeon, S.E. Taube, R. Tubbs, G.H. Vance, M. van de Vijver, T.M. Wheeler, and D.F. Hayes. 2007. American Society of Clinical Oncology/College of American Pathologists guideline recommendations for human epidermal growth factor receptor 2 testing in breast cancer. *Journal of clinical oncology : official journal of the American Society of Clinical Oncology*. 25:118-145.

Workman, P., E.O. Aboagye, F. Balkwill, A. Balmain, G. Bruder, D.J. Chaplin, J.A. Double, J. Everitt, D.A. Farningham, M.J. Glennie, L.R. Kelland, V. Robinson, I.J. Stratford, G.M. Tozer, S. Watson, S.R. Wedge, S.A. Eccles, and I. Committee of the National Cancer Research. 2010. Guidelines for the welfare and use of animals in cancer research. *Br J Cancer*. 102:1555-1577.

Wu, H., A.B. Reynolds, S.B. Kanner, R.R. Vines, and J.T. Parsons. 1991. Identification and characterization of a novel cytoskeleton-associated pp60src substrate. *Molecular and cellular biology*. 11:5113-5124.

Wu, X., B. Gan, Y. Yoo, and J.L. Guan. 2005. FAK-mediated src phosphorylation of endophilin A2 inhibits endocytosis of MT1-MMP and promotes ECM degradation. *Developmental cell*. 9:185-196.

Yamaguchi, H., and J. Condeelis. 2007. Regulation of the actin cytoskeleton in cancer cell migration and invasion. *Biochimica et biophysica acta*. 1773:642-652.

Yamaguchi, H., M. Lorenz, S. Kempiak, C. Sarmiento, S. Coniglio, M. Symons, J. Segall, R. Eddy, H. Miki, T. Takenawa, and J. Condeelis. 2005. Molecular mechanisms of invadopodium formation: the role of the N-WASP-Arp2/3 complex pathway and cofilin. *The Journal of cell biology*. 168:441-452.

Yang, C.Z., H. Heimberg, C. D'Souza-Schorey, M.M. Mueckler, and P.D. Stahl. 1998. Subcellular distribution and differential expression of endogenous ADP-ribosylation factor 6 in mammalian cells. *The Journal of biological chemistry*. 273:4006-4011.

Yasuda, J., A.J. Whitmarsh, J. Cavanagh, M. Sharma, and R.J. Davis. 1999. The JIP group of mitogen-activated protein kinase scaffold proteins. *Molecular and cellular biology*. 19:7245-7254.

Yu, X., T. Zech, L. McDonald, E.G. Gonzalez, A. Li, I. Macpherson, J.P. Schwarz, H. Spence, K. Futo, P. Timpson, C. Nixon, Y. Ma, I.M. Anton, B. Visegrady, R.H. Insall, K. Oien, K. Blyth, J.C. Norman, and L.M. Machesky. 2012. N-WASP coordinates the delivery and F-actin-mediated capture of MT1-MMP at invasive pseudopods. *The Journal of cell biology*. 199:527-544.

Zambonin-Zallone, A., A. Teti, M. Grano, A. Rubinacci, M. Abbadini, M. Gaboli, and P.C. Marchisio. 1989. Immunocytochemical distribution of extracellular matrix receptors in

human osteoclasts: a beta 3 integrin is colocalized with vinculin and talin in the podosomes of osteoclastoma giant cells. *Experimental cell research*. 182:645-652.
Zhao, Y., and J.H. Keen. 2008. Gyrating clathrin: highly dynamic clathrin structures involved in rapid receptor recycling. *Traffic*. 9:2253-2264.
Zimmermann, P., K. Meerschaert, G. Reekmans, I. Leenaerts, J.V. Small, J. Vandekerckhove, G. David, and J. Gettemans. 2002. PIP(2)-PDZ domain binding controls the association of syntenin with the plasma membrane. *Molecular cell*. 9:1215-1225.
Zimmermann, P., Z. Zhang, G. Degeest, E. Mortier, I. Leenaerts, C. Coomans, J. Schulz, F. N'Kuli, P.J. Courtoy, and G. David. 2005. Syndecan recycling [corrected] is controlled by syntenin-PIP2 interaction and Arf6. *Developmental cell*. 9:377-388.